Investigating the Genetics of Primary Open-Angle Glaucoma in Tasmania

by

Jac Claire Charlesworth, BSc (Hons)

Submitted in fulfilment of the requirements for the Degree of

Doctor of Philosophy

University of Tasmania

(September 2006)

Statement of originality

This thesis contains no material accepted for a degree or diploma by the university or any other institution, except by way of background information and duly acknowledged in the thesis, and to the best of my knowledge and belief, contains no material previously published or written by another person, except where due acknowledgement is made in the text of the thesis.

Jac Charlesworth

Authority of access statement

This thesis may be made available for loan and limited copying in accordance with the *Copyright Act 1968*.

Jac Charlesworth

Statement of co-authorship

Jac Charlesworth has incorporated a version of the published paper Charlesworth *et al.* (2006) into Chapter 5 of her dissertation. This work was co-authored with Dr Jim Stankovich, Dr David A. Mackey, Dr Jamie E. Craig, Dr Michael Haybittel, Dr Rodney Westmore and Dr Michèle Sale, with the majority of the research, analyses, text and figures generated and prepared by Jac herself. The contribution of the other authors to the publication was primarily in the revision and proofreading of the final paper.

Charlesworth JC, Stankovich JM, Mackey DA, Craig JE, Haybittel M, Westmore RN and Sale MM (2006). Confirmation of the adult-onset primary open angle glaucoma locus GLC1B at 2cen-q13 in an Australian family. *Ophthalmologica* 220(1): 23-30.

Approximate proportionate of authorship contributed by Jac Charlesworth: 85%

Additional contributions from co-authors: Input on text for initial submission (all); Recruitment and clinical examination (DAM, JEC, MH, RNW); Advice with regard to statistical analyses (JMS); Revisions and assistance with responses to reviewers (MMS, JMS).

Jac Charlesworth has also incorporated a version of the published paper Charlesworth *et al.* (2005) into Chapter 6 of her dissertation. This work was co-authored with Dr Thomas Dyer, Dr Jim Stankovich, Dr John Blangero, Dr David Mackey, Dr Jamie Craig, Dr Catherine Green, Dr Simon Foote, Dr Paul Baird and Dr Michèle Sale, with the majority of the research, analyses, text and figures generated and prepared by Jac herself. The contribution of the other authors to the publication was primarily in methodological support and the revision and proofreading of the final paper.

Charlesworth JC, Dyer TD, Stankovich JM, Blangero J, Mackey DA, Craig JE, Green CM, Foote SJ, Baird PN and Sale MM (2005). Linkage to 10q22 for maximum intraocular pressure and 1p32 for maximum cup-to-disc ratio in an extended primary open-angle glaucoma pedigree. *Invest Ophthalmol Vis Sci* 46(10): 3723-9.

Approximate proportionate of authorship contributed by Jac Charlesworth: 85%

Additional contributions from co-authors: Input on text for initial submission (all); Recruitment and clinical examination (DAM, JEC, CMG,); Genome-wide scan (PNB, SJF) Advice with regard to statistical analyses (TDD, JB, JMS); Revisions and assistance with responses to reviewers (MMS, JMS, TDD, JB).

Jac Charlesworth

Abstract

Glaucoma is a major cause of visual impairment and the second leading cause of blindness worldwide. The most common form is adult-onset, primary open-angle glaucoma (POAG), which has a strong genetic component, with family history an established risk factor. This dissertation explores several different approaches to the analysis of extended POAG pedigrees to dissect the genetic aetiology of this phenotypically and genetically heterogeneous disease. The families were collected as part of the Glaucoma Inheritance Study in Tasmania (GIST), a study of glaucoma in Tasmania, representing almost complete population ascertainment of POAG patients.

One aim of this study was to investigate linkage to the POAG loci known at the time in a selection of 10 extended pedigrees from the GIST. These pedigrees were genotyped at POAG loci GLC1A, GLC1B, GLC1C, GLC1D, GLC1E and GLC1F, at an average marker spacing of 4 cM within each locus. Initial Markov chain Monte Carlo based linkage analyses revealed several suggestive results, and two families were subsequently selected for fine-mapping and follow-up analyses. One of these, family GTas15, produced p-values of 0.01 or less at five markers flanked by D2S1897 and D2S2269 in the follow-up nonparametric linkage analysis, with a minimum p-value of 0.005 at D2S1897. A 9 cM haplotype of interest was identified, overlapping the original GLC1B locus. These findings provided supportive evidence for the GLC1B locus on chromosome 2cen-q13, and verified the existence of a POAG susceptibility gene in this region.

This study also aimed to identify genetic contributions to POAG by investigating quantitative components of the disease phenotype. Genome-wide multipoint variance-components linkage analyses of maximum recorded intraocular pressure (IOP) and

maximum vertical cup-to-disc ratio were conducted on data from a single, extended POAG pedigree from the GIST, previously found to segregate the myocilin Q368X mutation in some individuals. Multipoint linkage analysis of maximum recorded IOP produced a significant peak LOD score of 3.3 (p=0.00015) near marker D10S537 on chromosome 10q22, whereas maximum cup-to-disc ratio produced a suggestive peak LOD score of 2.3 (p=0.00056) near markers D1S197 to D1S220 on chromosome 1p32. Inclusion of the myocilin Q368X mutation as a covariate provided evidence of an interaction between this mutation and the IOP and cup-to-disc ratio loci. Identification of genes contributing to the variance of the quantitative phenotype components of this disease will enhance understanding of the pathophysiology of POAG as a whole.

Acknowledgements

I owe a huge debt of gratitude to so many people who have helped me through my PhD, both professionally and socially. First and foremost I would like to thank my supervisors. In particular, Michèle Sale, for introducing me to the wonderful world of genetics, for your dedication and your faith in me, and for always challenging me - you've changed my life and I'll never look back. To Jim Stankovich, for your never-ending enthusiasm and you ability to make statistics not only intelligible, but also interesting. And to Alison Venn, for helping in my moment of need - if this really was a birth I couldn't have asked for a better midwife.

I wish to thank all the clinicians involved with this project, especially Associate Professor David Mackey and Dr Jamie Craig for the original patient ascertainment, your invaluable clinical knowledge and the constant stream of new ideas - thankyou both for allowing me to run with some of mine. Dr Paul Baird, for taking risks and for sharing data, your generosity is greatly appreciated. To Tim Albion, for developing the Genetic Research System database that made my life so much easier, and for modifying it at every request. To Dr John Blangero and Dr Thomas Dyer, for your inspiration, your technical support and for showing me life after the PhD. Thank you for being so generous with your time and your resources (but perhaps not for the karaoke). To Dr Eric Sobel, for sharing your enthusiasm and for answering my many questions. To Maree Ring, for your genealogical expertise and for cheerfully searching proformas whenever I has the slightest query. Thanks also to Shelly Brown for your assistance in the laboratory, especially for the blood extractions– you saved this needlephobe from having to think too hard about sample collection. To Dr Carey Denholm, the wisest Owl – thankyou for helping me find my way through the 'Hundred Acre Wood'. Particular thanks go to Lucy Frost, for your generosity and your unwavering faith in my technological abilities. Thank you for broadening my thinking and for forcing me to keep learning – you've taught me so much about myself. I'd especially like to thank Jean and Alastair Richardson, and Jenna and Philip Mead for their unwavering support and understanding. I'd like to thank my lab-mates Liesel Fitzgerald, James McKay and in particular Kathryn Burdon. Kath, the best thing that came out of this PhD was my friendship with you and I will treasure it always. Finally wish to thank my dearest friend and companion Jo – you bring light in. I look forward to embarking on our next (hopefully less stressful) adventure!

Particular acknowledgement needs to be made of the following individuals who have contributed to this project:

The GIST clinicians: **Dr David Mackey, Dr Jamie Craig, Dr Paul McCartney, Dr Richard Cooper, Dr Michael Haybittel** and **Dr Rodney Westmore** for setting up the GIST with such forethought. In particular, Dr David Mackey and Dr Jamie Craig for allowing me access to the GIST and for working so hard and giving up so much time to be involved in all stages of this project – your input was invaluable.

The GIST genealogist **Maree Ring** for her meticulous research in constructing and linking the original GIST pedigrees.

Research Assistant **Shelly Brown** for helping with the blood extractions.

Dr John Blangero and **Dr Thomas Dyer** for their generous advice regarding the ascertainment correction and variance components analysis using SOLAR.

Dr Eric Sobel for his advice on using SimWalk2.

Mr Tim Albion for his technical support and for producing and managing the Genetic Research System database.

The **University of Tasmania** for my PhD scholarship.

The **Menzies Research Institute** for supporting me throughout my candidature.

Finally, **Dr Michèle Sale** for her supervision throughout the project and **Dr Jim Stankovich** for his supervision and statistical support.

This project was primarily supported by the **Glaucoma Research Foundation.**

Abbreviation List

ASP: Affected sibling pair

BMES: Blue Mountains Eye Study

CCT: central corneal thickness

CEPH: Centre d'Etude du Polymorphisme Humain

cM: centiMorgan

DNA: Deoxyribonucleic acid

EDTA: Ethylene-diamine-tetra-acetic acid

GAW: Genetic Analysis Workshop

GDB: Genome Database

GIST: Glaucoma Inheritance Study in Tasmania

GWS: Genome-wide scan

HUGO: Human Genome Organisation

IBD: Identity by descent

IOP: Intraocular pressure

JOAG: Juvenile-onset open angle glaucoma

kb: Kilobase

kDa: Kilodalton

LOD: Logarithm of the odds

MCMC: Markov chain Monte Carlo

mmHg: Millimetres of mercury

MVIP: Melbourne Visual Impairment Project

NHMRC: National Health and Medical Research Council of Australia

NTG: Normal-tension glaucoma

OH: Ocular hypertensive

PACG: Primary acute closed-angle glaucoma

PCG: Primary congenital glaucoma (Buphthalmos)

PCR: Polymerase chain reaction

PEP: Primer extension preamplification

POAG: Primary open-angle glaucoma

QTL: Quantitative trait locus

SNP: Single nucleotide polymorphism

SSCP: Single-strand conformational polymorphism

Table of Contents

Figures and Tables

Chapter 1

Chapter 2

Chapter 3

Chapter 4

Chapter 5

Chapter 6

Appendices

Chapter 1 – Introduction

1.1 Introduction to glaucoma

Glaucoma is a term used to describe a heterogeneous group of eye disorders involving damage to the optic nerve and loss of vision, resulting in irreversible blindness if left untreated. The varying types of glaucoma are classified according to aetiology (primary vs. secondary), anatomy of the anterior chamber (open angle vs. closed angle) and age of onset (congenital vs. juvenile vs. adult). There are three major types of glaucoma: primary open-angle glaucoma (POAG), primary angle closure glaucoma (PACG) and primary congenital glaucoma (PCG or Buphthalmos), as well as several secondary forms associated with a wide range of ocular pathologies and developmental abnormalities such as aniridia and Rieger syndrome. Adult-onset, primary open-angle glaucoma is the most common form of glaucoma and is the focus of this dissertation.

1.2 Prevalence

Glaucoma is a major cause of visual impairment and blindness in developed countries and is the second leading cause of blindness worldwide (Quigley 1996; Resnikoff *et al.* 2004). Glaucoma was responsible for 12.3% of global blindness (4.5 million people) in 2002 (Resnikoff *et al.* 2004). Primary open-angle glaucoma is the most common form, accounting for approximately 67-75% of glaucoma cases (Leske and Rosenthal 1979; Buhrmann *et al.* 2000; Bourne *et al.* 2003). Within Australia, POAG affects 2-3% of the population over the age of 40 (Mitchell *et al.* 1996), with up to half of those affected being undiagnosed (Coffey *et al.* 1993; Dielemans *et al.* 1994; Mitchell *et al.* 1996; Wensor *et al.* 1998; Leske *et al.* 2001; Weih *et al.* 2001b; Mukesh *et al.* 2002). Onset of POAG typically occurs after the fourth decade of life, and prevalence rises with age, reaching as high as 10% of those over 85 years of age (Mitchell *et al.* 1996; Weih *et al.*

2001b). The number of Australians affected by the disease is expected to double over the next 30 years as the population ages (Rochtchina and Mitchell 2000).

Prevalence of POAG varies between ethnic groups. The prevalence of POAG in the urban population of Thailand appears to resemble Caucasian prevalence rates (Bourne *et al.* 2003). In the United States, POAG is three to six times more common in African Americans than Caucasians (Tielsch *et al.* 1991b). The higher prevalence and earlier age of onset of POAG in black populations has been confirmed in several studies including those based in the West Indies (Mason *et al.* 1989), Barbados (Leske *et al.* 1994), Britain (Wormald *et al.* 1994), East Africa (Buhrmann *et al.* 2000) and West Africa (Ntim-Amponsah *et al.* 2004). The prevalence of POAG has been shown to be higher in Afro-Caribbean individuals than African Americans (Leske *et al.* 1994), while the prevalence of POAG in rural East Africa was shown to be less than in Afro-Caribbean populations but similar to African American prevalence rates (Buhrmann *et al.* 2000).

1.3 Primary open-angle glaucoma

Primary open-angle glaucoma is the most common form of glaucoma, accounting for 67-75% of glaucoma cases (Leske and Rosenthal 1979; Buhrmann *et al.* 2000; Bourne *et al.* 2003). It is divided into adult onset (after 40 years) and the juvenile onset form (JOAG) with age of onset between 3 and 40 years. The underlying pathogenesis of POAG is not fully understood, however the loss of vision in all subtypes is due to a final common pathway of retinal ganglion cell death by apoptosis, leading to atrophy of the optic nerve and a cupped appearance.

The adult-onset form of POAG has a milder presentation and more moderate elevation of intraocular pressure (IOP), compared with the juvenile-onset form. Current medical and surgical treatments can delay progression with a satisfactory outcome in the majority of cases, provided the disease is detected early. The greatest clinical issue for POAG is the painless progression of the disease, often resulting in late diagnosis by which time irreversible optic nerve damage may have occurred, which in some cases is advanced at the time of diagnosis. Glaucoma of all forms is treatable by lowering IOP. This is achieved by either topical therapy (eye-drops), laser treatment, or surgery in more severe cases. Glaucoma treatment has been shown to slow loss of vision in randomised control trials (Kass *et al.* 2002; Leske *et al.* 2003; Leske *et al.* 2004), and thus glaucoma blindness may be largely preventable if early diagnosis was achievable in all cases.

Estimates suggest JOAG is far less common than typical adult onset POAG (Sarfarazi 1997) and is in fact a rare presentation, with some prevalence estimates as low as 1 in 50,000; however there are no reliable, published prevalence studies. JOAG also tends to be more severe than adult-onset POAG, involving higher IOP and a poor response to drug treatments, often requiring surgical intervention (Craig and Mackey 1999). JOAG is a useful sub-classification in which to search for genetic contributions to glaucoma as it often exhibits an autosomal dominant inheritance pattern, occurs at an early age, demonstrates a well defined phenotype and is likely to be found in multiple living generations of a pedigree. However, the rarity of the disease hinders attempts to collect large, informative datasets. Also, while one JOAG gene (*MYOC*) has been shown to also account for approximately 3% of adult-onset POAG (Stone *et al.* 1997; Alward *et al.* 2002), the wider relevance of other JOAG genes to adult-onset POAG is not yet clear.

1.4 Clinical definition of POAG

There is no universally accepted definition of POAG, a phenotypically complex and subtle disease (Kahn and Milton 1980; Wolfs *et al.* 2000; Kroese and Burton 2003). The clinical diagnosis is based on a combination of several main characteristics: specific changes to the appearance of the optic nerve head, characteristic visual field loss and a slow and generally asymptomatic progression (Khaw *et al.* 2004). Diagnosis is made when all principal features are present, but is less certain when one or more of the key features are absent. POAG is usually bilateral, although sometimes asymmetric (American Academy of Ophthalmology 2003). Elevated intraocular pressure (IOP) is a major contributing factor to POAG, but this elevation is neither necessary nor sufficient for onset or progression of the disease, and is no longer typically included in the modern clinical *definition* of POAG (American Academy of Ophthalmology 2003; Khaw *et al.* 2004), although its monitoring and treatment remains a fundamental cornerstone of glaucoma management (European Glaucoma Society 1998; Van Veldhuisen *et al.* 2000; Goldberg *et al.* 2002).

Diagnosis of POAG additionally relies on the absence of any secondary explanations for progressive glaucomatous optic nerve change, such as pseudoexfoliation or pigment dispersion syndrome, as well as evidence of open, normal-appearing anterior-chamber angles (American Academy of Ophthalmology 2003). Open and closed-angle glaucoma are differentiated by gonioscopy, a procedure involving examination of the width of the iridocorneal angle (between the iris and the cornea at their junction). The angle is the area of outflow of aqueous humor and contains the trabecular meshwork (Figure 1.1).

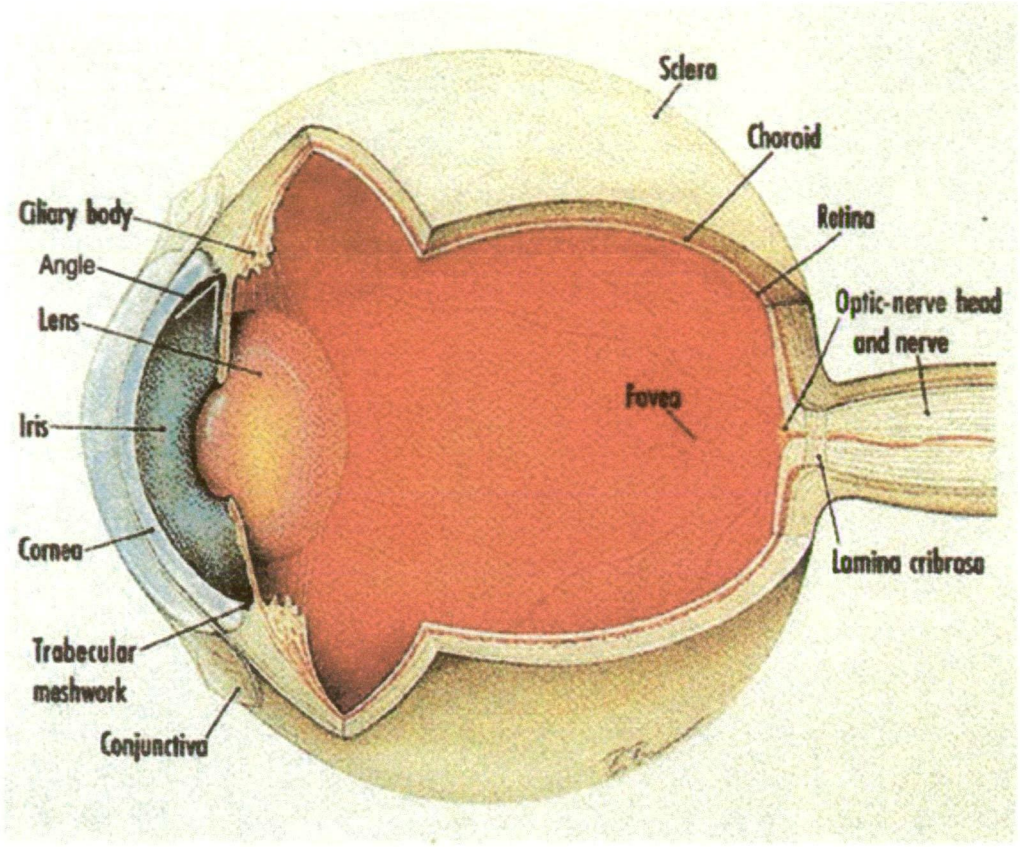

Figure 1.1 - Anatomy of the eye

This schematic representation of the eye shows all the major structures relevant to glaucoma. The anterior segment or front portion of the eye includes the angle of the eye; the point where the iris meets the cornea. The trabecular meshwork is located within the angle.

Figure taken from Quigley HA (1993). Open-angle glaucoma. N Engl J Med *328(15): 1097-106.*

There is still much debate over a suitable and universal clinical definition of POAG and a lack of consistency in the clinical definition of POAG in published studies (Bathija *et al.* 1998; Foster *et al.* 2002; Kroese and Burton 2003). Bathija *et al.* (1998) conducted a literature review of 182 papers between 1980 and 1990 to determine the criteria used to define glaucoma, revealing that the definition used was clearly reported in only 66% of papers, and even in these there was much variability, with raised IOP the only criterion in 20% of described definitions.

1.4.1 Intraocular pressure

Pressure within the eye is dependent on the production rate of fluid (aqueous humor) from the ciliary body and rate of fluid drainage through the trabecular meshwork and diffusion through the uvea and sclera (Figure 1.2). The consistent volume of the adult eye necessitates that aqueous humor production and outflow are almost equal. In most instances, elevated IOP is the result of impaired drainage of aqueous humor through the trabecular meshwork outflow pathways (Quigley 1993). Prolonged increased IOP may exert physical force on the structural framework of the lamina cribrosa in the optic nerve, leading to axonal injury, and this process has been suggested as one mechanism leading to neuronal damage in glaucoma. Diurnal (daily) variation in IOP has been well documented (Drance 1963; Asrani et al. 2000; Liu 2001; Hughes et al. 2003; Liu et al. 2003), with a larger range of IOP fluctuation in untreated POAG cases than normal individuals (Sacca et al. 1998; Asrani et al. 2000; Hughes et al. 2003; Liu et al. 2003).

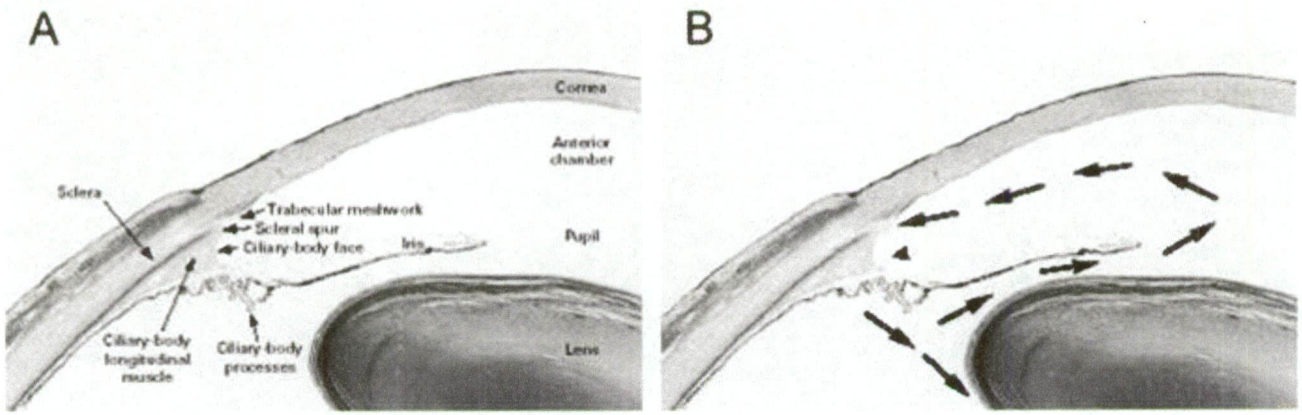

Figure 1.2 - The anterior segment of the eye, aqueous humor production, and outflow

Panel A is a transverse section of the anterior segment or front portion of the eye. The major structures are labelled. The scleral spur is the posterior boundary of the trabecular meshwork and the point of attachment of the longitudinal muscle of the ciliary body. Contraction of the longitudinal muscle can open the trabecular meshwork and increase aqueous outflow.

Panel B shows the flow of aqueous humor through the anterior segment. Aqueous humor is produced by the ciliary-body processes. It flows around the lens, then passes through the pupil and into the anterior chamber, where it nourishes the cornea before leaving the eye through the trabecular meshwork into the venous system. A small amount of aqueous humor exits by way of uveoscleral channels through the iris root and ciliary body.

Figure taken from Alward WL, Fingert JH, Coote MA, et al. *(1998). Clinical features associated with mutations in the chromosome 1 open- angle glaucoma gene (GLC1A).* N Engl J Med *338(15): 1022-7.*

Elevated intraocular pressure is a major risk factor for POAG, but this elevation is neither necessary nor sufficient for onset or progression of the disease. POAG that includes optic nerve damage and visual field loss, but with IOP below 22mmHg (a somewhat arbitrary cut-off for normal IOP, approximately 2 standard deviations above the European population mean of 16mmHg) is sometimes referred to as normal-tension glaucoma (NTG). Initially thought to be a rare sub-form of POAG, NTG has now been shown to account for 20-50% of the disease (Tielsch *et al.* 1991a; Werner 1996). Whether NTG constitutes a pathological entity distinct from POAG is debated (Kamal and Hitchings 1998); it may simply be part of a spectrum of phenotypes extending from patients with ocular hypertension and no evidence of optic neuropathy, to those with optic nerve damage without significantly elevated IOP. The Baltimore Eye Study found no support for the distinction between 'low-tension' and 'high-tension' glaucoma (Sommer *et al.* 1991). Similarities have been found between the optic nerve heads of low and high tension glaucoma patients, suggesting both phenotypes may belong to a spectrum of the same disease (Tomita 2000). It is important to note that several studies have shown that glaucomatous optic nerve damage occurs even at low pressures as a result of abnormal pressure sensitivity in some individuals (Anderson *et al.* 1998; Van Veldhuisen *et al.* 2000). IOP is no longer included in most definitions of POAG (American Academy of Ophthalmology 2003; Khaw *et al.* 2004), yet it remains the primary target of POAG treatment and monitoring (European Glaucoma Society 1998; Van Veldhuisen *et al.* 2000; Goldberg *et al.* 2002). It has been clearly shown in several prospective randomised control trials that lowering IOP reduces the progression of optic nerve damage, with an approximate 10% decrease in risk per mmHg decrease in IOP (Gordon *et al.* 2002; Leske *et al.* 2003; Leske *et al.* 2004), supporting IOP targeting as an effective treatment for many forms of POAG, including NTG.

Individuals with raised IOP (greater than or equal to 22mmHg) but no evidence of glaucomatous optic nerve damage or visual field loss are referred to as having ocular hypertension (OH).

While not an essential component for a clinical diagnosis of POAG, IOP still functions as an important risk factor for the disease. The Baltimore Eye Survey identified an increased prevalence of POAG associated with increasing IOP (Sommer *et al.* 1991), later confirmed in the Barbados Eye Study (Leske *et al.* 1995) and the Rotterdam Study in the Netherlands (Dielemans *et al.* 1994). Sommer (1996) suggests that, while the relationship between IOP and POAG is not strictly linear, it is nevertheless monotonic: the higher the IOP the greater the risk of POAG, similar to the relationship between blood pressure and stroke. In the Ocular Hypertension Treatment Study and the Early Manifest Glaucoma Trail the risk of POAG increased by 10% for each 1mmHg increase in IOP (Gordon *et al.* 2002; Leske *et al.* 2003). The continuous nature of the glaucoma-IOP relationship, originally described in the Baltimore Eye Survey (Sommer *et al.* 1991), was confirmed in an Australian population (Mitchell *et al.* 1996), highlighting the arbitrary nature of using a single threshold IOP value to distinguish the commonly used categories of low and high tension glaucomas. This taxonomic dilemma has been further complicated by the recent widespread acceptance that Goldman applanation tonometry errors in IOP measurement based on inter-individual variation in corneal thickness would result in patients with borderline IOP values being potentially misclassified as NTG (see section 1.5).

A relatively low proportion (25%) of POAG cases in the Blue Mountains Eye Study had elevated IOP, suggesting approximately 75% of cases had low IOP, however the measurements were taken in a cross-sectional study, giving no information about peak

or mean IOP or the duration of elevation (Mitchell *et al.* 1996). Prospective studies reveal lower rates of normal IOP; almost 40% of previously undiagnosed cases in the Rotterdam Study had pressure below 21mmHg (Dielemans *et al.* 1994), with similar results in the Baltimore Eye Survey (50%) (Sommer *et al.* 1991).

The Blue Mountains Eye Study also found a modest but statistically significant association between increasing iris colour and IOP. After adjustment for variables associated with IOP the mean measurements were 15.92mmHg for blue iris colour, 16.04mmHg for hazel or green, 16.11mmHg for tan-brown and 16.49mmHg for dark brown ($p=0.001$ for trend) suggesting iris colour may be associated with IOP (Mitchell *et al.* 2003). The Melbourne Visual Impairment Project identified a similar relationship between iris colour and IOP and determined that the association did not appear to be confounded by ethnicity (Weih *et al.* 2001a).

1.4.2 Optic disc abnormalities

The normal optic disc is the site of passage, from the eye, of more than 1 million axons that make up the optic nerve. Within the optic disc is the lamina cribrosa, composed of fenestrated connective tissue, through which the bundles of axons pass. The diameter of a normal optic disc, as well as the number of axons within the disc, varies from eye to eye (Jonas *et al.* 1988b; Jonas *et al.* 1990; Quigley *et al.* 1990). Generally the axons do not completely fill the disc, leaving a depression in its centre known as the cup (Figure 1.3).

The characteristic changes in the optic nerve head associated with POAG include increased cupping or excavation, notching or thinning of the neuroretinal rim, disc haemorrhages, asymmetry of cupping between the two eyes and loss of the retinal nerve

fibre layer (European Glaucoma Society 1998; American Academy of Ophthalmology 2003). The optic nerve head is best examined using a slit lamp with a binocular view. A standard way to describe the appearance of the optic nerve head is by the vertical cup-to-disc ratio, which expresses the size of the cup in relation to the optic nerve head size (Figure 1.3). The vertical cup-to-disc ratio is a simple, robust indicator of glaucomatous loss of the neuroretinal rim (Foster *et al.* 2002). A normal cup-to-disc ratio is approximately 0.3 (Jonas *et al.* 1988b), which may increase to between 0.7 and 1.0 (Jonas *et al.* 1988a) with mild to end-stage glaucomatous injury. Eyes with a cup-to-disc ratio greater than or equal to 0.55 are at increased risk of developing glaucomatous visual field loss compared with eyes having a cup-to-disc ratio less than 0.55 (Quigley *et al.* 1992). In the Ocular Hypertension Treatment Study the risk of POAG increased 1.3 times for each 0.1 increase of horizontal or vertical cup-to-disc ratio (Gordon *et al.* 2002). Accurate assessment of the cup-to-disc ratio remains one of the main indicators used in the clinical assessment of POAG (Jonas *et al.* 1999).

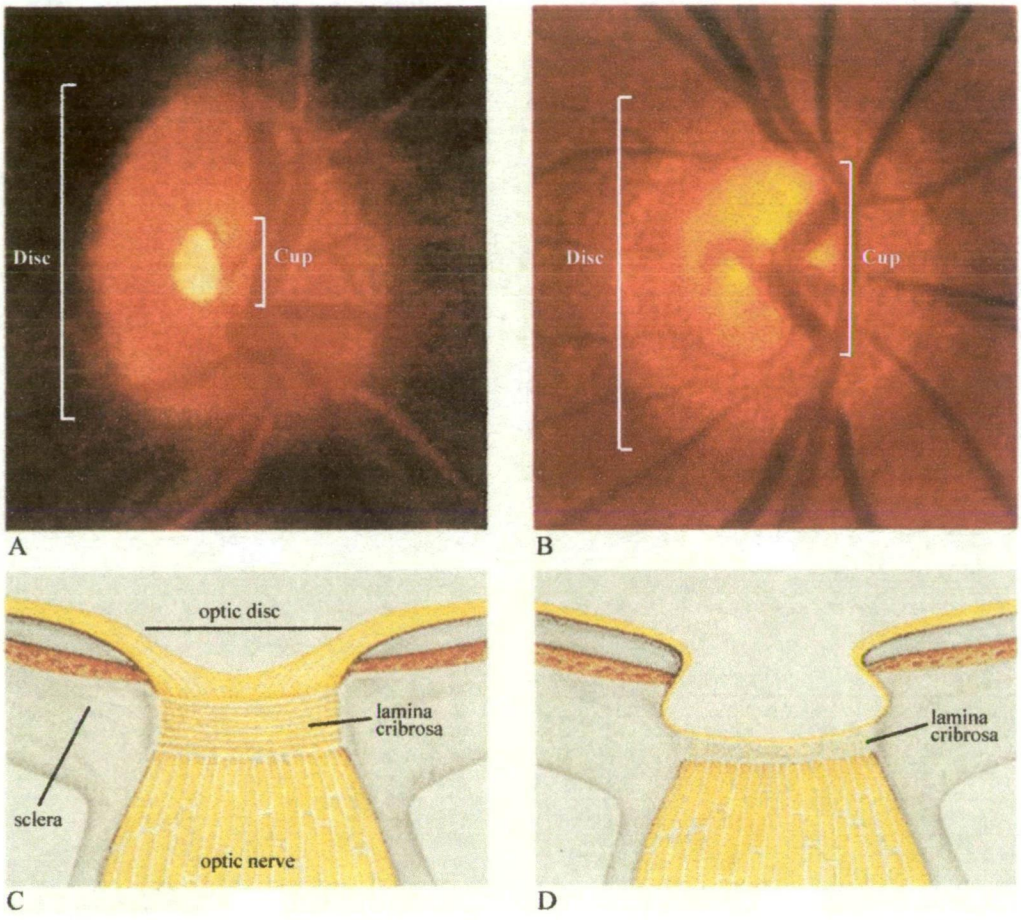

Figure 1.3 - Normal and glaucomatous optic discs

Panel A shows a normal optic disc with a small cup-to-disc ratio, indicated by the tiny pale central area (cup) within the larger orange disc.

Panel B shows a glaucomatous optic disc with a large cup-to-disc ratio. The cup is much larger than in Panel A and shows signs of excavation, indicated by the sharp and undermined edge of the cup.

Panel C and **Panel D** are schematic diagrams of the features of normal and glaucomatous discs, respectively. The internal structure of the lamina cribrosa is compressed and rotates backward on its insertion into the sclera in patients with glaucoma.

Figure adapted from Quigley HA (1993). Open-angle glaucoma. N Engl J Med *328(15): 1097-106.*

The Baltimore Eye Study confirmed that African American individuals have, on average, larger optic discs than white European Americans (Varma *et al.* 1994; Varma *et al.* 1995). They suggest the same number of optic nerve axons are splayed over a larger disc perimeter, resulting in African American individuals having larger cups but the same neuroretinal nerve area when compared with European American individuals (Varma *et al.* 1995). Similar results have also been obtained from the Australian Aboriginal population (Dr Jamie Craig 2005, personal communication)

1.4.3 Visual field abnormalities

Specific patterns of peripheral and central vision loss characteristic of POAG are the result of optic nerve fibre damage during the course of disease progression (Figure 1.4). Vision loss is first manifest in the mid-peripheral field, with central visual function involved much later in disease progression (Khaw *et al.* 2004). Computer assisted visual field testing is the most common way to estimate optic nerve function. The procedure assesses the ability of the eye to detect the brightness of small points of light both centrally and peripherally. Visual field loss characteristic of POAG includes nasal-field loss, superior or inferior arcuate-field loss, generalised depression, and paracentral visual field loss (American Academy of Ophthalmology 2003). Eventually, in the end stages of POAG, all vision may be lost leading to total blindness.

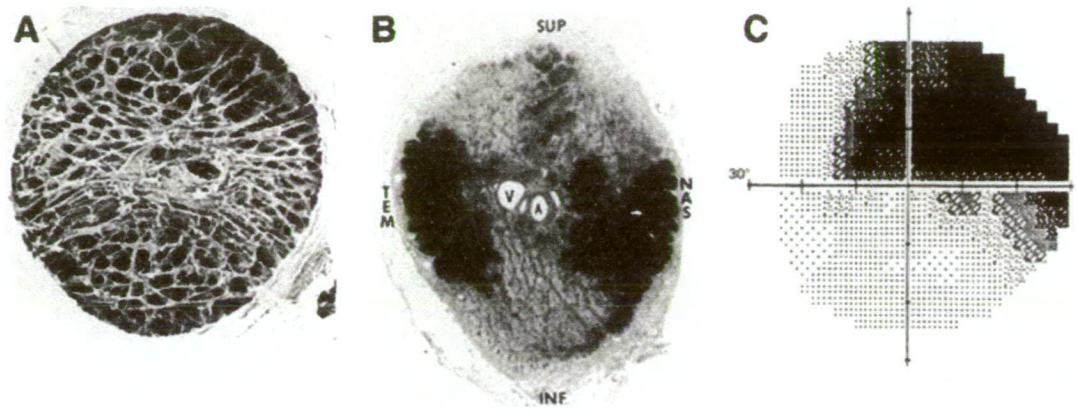

Figure 1.4 - Loss of visual field in POAG

Panel A depicts an optic disc with the neural tissue digested by enzymes to show the connective tissue alone. The larger pores and lower density of the supportive tissue at the top and bottom of the disc are clearly evident.

Panel B is a cross-section of the optic nerve showing the hourglass pattern of the preferential loss of nerve fibres (seen as a decrease of the dark, myelinated tissue) in the polar regions of lower density supportive tissue. These selectively susceptible zones of the nerve serve the mid-peripheral visual field.

Panel C shows the resulting characteristic loss of side vision, revealed by the automated visual-field test, shown as a dark area in the schematic diagram.

V denotes vein, **A** artery, **TEM** temporal, **NAS** nasal, **SUP** superior, and **INF** inferior.

Figure taken from Quigley HA (1993). Open-angle glaucoma. N Engl J Med *328(15): 1097-106.*

1.5 Risk factors for POAG

Factors associated with increased risk of progression to glaucoma but more likely to be an early manifestation of POAG, such as nerve fibre layer defects, asymmetric cupping of the optic disc and raised IOP, are not specifically included as risk factors in this section and have been discussed previously. It is unclear whether IOP is a component of the POAG phenotype or a risk factor for POAG, however there is a clear link between increased IOP and risk of POAG, as described in section 1.4.1.

Central corneal thickness (CCT) has been suggested as a risk factor for POAG. Applanation tomometry measurements of IOP are known to be influenced by CCT (Hansen and Ehlers 1971; Stodtmeister 1998): CCT has a positive and apparently linear correlation with IOP (Wolfs *et al.* 1997), thus thick corneas increase the *measured* IOP in contrast to the *actual* true IOP. CCT is now known to be strongly genetically determined (Toh *et al.* 2005), with familial thick corneas shown to segregate in a family with apparent ocular hypertension (Dohadwala and Damji 2000). In the Ocular Hypertension Treatment Study it was determined that thinner CCT measurements appeared to increase the risk of developing POAG, with a CCT of 555μm or less conferring a three-fold increase in risk compared with CCT measurements of 588μm or more (Gordon *et al.* 2002). Reanalysis of this data determined that a 40μm decrease in CCT produced a 1.8 times increase in the risk of developing POAG (Coleman *et al.* 2004). The mean CCT measurement was 23.5μm thinner in African Americans than other participants in the Ocular Hypertension Treatment Study (Gordon *et al.* 2002), possibly accounting for a component of their increased risk of POAG.

1.5.1 Demographic risk factors

Family history, age, gender and ethnicity are the common demographic risk factors associated with POAG.

Family history is an established risk factor for POAG (Rosenthal and Perkins 1985; Tielsch *et al.* 1994; Wolfs *et al.* 1998; Budde and Jonas 1999; Nemesure *et al.* 2001; Weih *et al.* 2001b; Le *et al.* 2003; Fan *et al.* 2004). Many of the population-based studies report a three to four-fold increase in risk of POAG for first degree relatives of affected cases (Tielsch *et al.* 1994; Leske *et al.* 1995; Nemesure *et al.* 1996; Mitchell *et al.* 2002). Moreover, results from the Rotterdam Eye Study, in the most carefully controlled study of its kind, suggest relatives of POAG patients have a ten-fold increase in risk of the disease (Wolfs *et al.* 1998). The variation in risk between various studies may be due to many factors, including the late age of onset of the disease and high rate of undiagnosed cases (up to 50% as described in section 1.2), as well as a lack of disclosure within families. Studies on the under-reporting of family history suggest the risk attributable to family history may be even greater than previously suggested; for example the Glaucoma Inheritance Study in Tasmania (GIST) determined that 27% of previously diagnosed POAG cases were unaware of their positive family history (McNaught *et al.* 2000).

Several studies have shown an increase in risk of POAG with increasing age, including the Visual Impairment Project (Le *et al.* 2003), Barbados Eye Study (Leske *et al.* 2001), and many others (Dielemans *et al.* 1994; Leske *et al.* 1995; Mitchell *et al.* 1996; Voogd *et al.* 2005). The Visual Impairment Project found a significant increase in risk of POAG over 60 years of age, increasing rapidly with every additional decade of life (Le *et al.* 2003). While older age appears to predispose individuals to POAG, it is not clear

whether older eyes are themselves more susceptible to damage, or if the increase in risk is the result of cumulative exposure to other risk factors, making the optic nerve head more vulnerable to damage.

The relationship between gender and the risk of developing POAG is unclear. The Barbados Eye Study (Leske *et al.* 2001) and the Rotterdam Study (Dielemans *et al.* 1994) showed a trend towards a higher risk of POAG in men than women, while the Dalby Sweden Study showed a higher incidence in women (Bengtsson 1989). Most other studies have shown little or no relationship between the risk of POAG and gender (Viggosson *et al.* 1986; Tielsch *et al.* 1991b; Klein *et al.* 1992; Mitchell *et al.* 1996; Weih *et al.* 2001b; Gordon *et al.* 2002; Landers *et al.* 2002; Le *et al.* 2003).

As mentioned in Section 1.2, the prevalence of POAG varies between ethnic groups, suggesting an underlying genetic susceptibility to the disease. In the Baltimore Eye Survey, African Americans had a three to six-fold increase in risk of POAG compared with Caucasians (Tielsch *et al.* 1991b). A similar increase in risk has also been demonstrated in other populations of African descent (Mason *et al.* 1989; Leske *et al.* 1994; Wormald *et al.* 1994).

1.5.2 Cardiovascular risk factors

Several cardiovascular-related risk factors have been postulated for POAG, including smoking, alcohol consumption, cardiovascular disease, hypertension and diabetes.

While one small Chinese study has recently identified a strong (ten-fold) increase in risk of POAG associated with cigarette smoking (Fan *et al.* 2004), most large studies have shown little or no increase in risk associated with smoking (Klein *et al.* 1993; Leske *et*

al. 1995; Kang *et al.* 2003; Le *et al.* 2003). However, a weak correlation between smoking and increased IOP has been shown (Carel *et al.* 1984; Wu and Leske 1997), suggesting smoking may have an indirect link to POAG risk (Cheng *et al.* 2000).

Cardiovascular disease has been associated with the senile sclerotic subgroup of glaucomatous optic disc appearance (Broadway and Drance 1998), but not necessarily with risk of POAG (Leske *et al.* 1995; Bonomi *et al.* 2000; Weih *et al.* 2001b; Le *et al.* 2003).

Hypertension has been shown to be associated with the risk of POAG in some studies (Dielemans *et al.* 1995; Tielsch *et al.* 1995b; Bonomi *et al.* 2000; Mitchell *et al.* 2004), but not in others (Leske *et al.* 1995; Weih *et al.* 2001b; Le *et al.* 2003). Ocular perfusion pressure (blood pressure minus IOP) has been shown to be associated with POAG (Leske *et al.* 1995; Tielsch *et al.* 1995b; Bonomi *et al.* 2000) and may be a more appropriate risk factor for optic nerve head ischemia and POAG than hypertension. The Baltimore Eye Survey, including 2500 African American and 2500 Caucasian individuals, identified an inverse relationship between perfusion pressure and risk of POAG (Tielsch *et al.* 1995b).

There is no convincing association between diabetes and POAG (Leske *et al.* 1995; Tielsch *et al.* 1995a; Ellis *et al.* 2000; Landers *et al.* 2002; Le *et al.* 2003). The association between diabetes and POAG identified in some studies (Klein *et al.* 1994; Dielemans *et al.* 1996) may in part be the result of inherent selection bias. Individuals diagnosed with diabetes are more likely to have frequent ophthalmological investigations than individuals from the general population, decreasing their chances of having undiagnosed POAG.

1.6 Mode of transmission

Primary open-angle glaucoma is thought to be a complex trait resulting from the interaction of multiple genes in conjunction with environmental influences. In general, most familial POAG *appears* to segregate as an autosomal dominant trait with somewhat reduced penetrance (Stoilova *et al.* 1996; Wirtz *et al.* 1997; Sarfarazi *et al.* 1998; Trifan *et al.* 1998; Wirtz *et al.* 1999; Charlesworth *et al.* 2006), although on further investigation these inheritance patterns do not reflect a simple mode of inheritance or a single underlying genetic cause. While genetic susceptibility is clearly involved in the pathophysiology of POAG, the late age of onset and generally painless progression, coupled with variations in definition and clinical diagnosis and the potential for phenocopies, often make it difficult to discern the exact mode of inheritance from family data.

1.7 Nomenclature of POAG loci

The glaucoma loci have been named according to the Human Genome Organisation (HUGO) guidelines for human gene nomenclature (Wain *et al.* 2002). The first part of the locus name, GLC, indicates glaucoma. Following this is a number indicating the type of glaucoma; 1 for primary open-angle, 2 for angle closure and 3 for primary congenital glaucoma. A letter is then added to indicate each new locus. Thus, the first POAG locus is named GLC1A, and the first primary congenital glaucoma locus is GLC3A.

1.8 Summary of POAG genetics

The Rotterdam Study reported a ten fold increase in risk of POAG for first degree relatives of patients compared with the general population, suggesting a strong genetic

component to the disease (Wolfs *et al.* 1998), although, as mentioned in section 1.5.1, studies investigating the under-reporting of family history suggest that even this may be an underestimation (McNaught *et al.* 2000). Many extended POAG pedigrees have been reported (Morissette *et al.* 1995; Stoilova *et al.* 1996; Wirtz *et al.* 1997; Sarfarazi *et al.* 1998; Trifan *et al.* 1998; Baird *et al.* 2003; Charlesworth *et al.* 2006), consistent with a high disease heritability. The ethnic differences in the risk of POAG, described in section 1.5.1, also support an underlying genetic component to the disease.

There have been few twin studies of POAG (Teikari 1987; Gottfredsdottir *et al.* 1999) and some reports of twin pairs within the context of wider family studies (Teikari *et al.* 1987; Wiggs *et al.* 1995), yet while the results of these few studies are highly variable, they do suggest a strong genetic component to the disease. The heritability of POAG was estimated at 13% in one study of 29 monozygotic twins and 79 dizygotic pairs (Teikari 1987) and 98% in another study of 50 monozygotic twin pairs (Gottfredsdottir *et al.* 1999). However, as mentioned in section 1.4, the clinical diagnosis and stringency of the phenotype definition of POAG varies and is not defined according to strict guidelines, confounding the interpretation of heritability estimates from these few published studies. POAG phenotype components, such as IOP and vertical cup-to-disc ratio, may have more simple genetic architectures than an overall diagnosis of POAG, and may offer more insight into the genetic composition of the disease. The heritabilities of IOP and vertical cup-to-disc ratio have been estimated at 0.29-0.36 and 0.48-0.56 respectively (Klein *et al.* 2004; Chang *et al.* 2005), both strongly consistent with a genetic component to these parameters.

POAG is clearly genetically heterogeneous; three genes for adult onset POAG have been identified; *MYOC* (MIM: 601652) encoding myocilin (Stone *et al.* 1997), *OPTN*

(MIM: 602432) encoding optineurin (Rezaie *et al.* 2002), and *WDR36* (MIM:609669) encoding WD40-repeat 36 (Monemi *et al.* 2005), however mutations in these genes account for only a fraction of familial POAG. In addition, five other loci for POAG have been mapped: GLC1B (Stoilova *et al.* 1996), GLC1C (Wirtz *et al.* 1997), GLC1D (Trifan *et al.* 1998), GLC1F (Wirtz *et al.* 1999) and GLC1I (Allingham *et al.* 2005), however the genes at these loci remain to be identified (Table 1.1). GLC1B was localised using six pedigrees with 3-7 affected individuals per family and GLC1I was localised in a subset of 15 out of 81 pedigrees with an average of 2-3 affected individuals per family, while the remaining POAG loci have been localised using single pedigrees containing 10-16 affected individuals. Although four of these loci were originally identified between 1996 and 1998, only two have been replicated in published studies; GLC1B (Raymond *et al.* 1999 [abstract], Charlesworth *et al.* 2006) and GLC1C (Kitsos *et al.* 2001); one of these as a result of this dissertation (Charlesworth *et al.* 2006). The results of several additional studies using an affected sib pair strategy and genome-wide approach suggest several additional chromosomal regions may be involved in POAG susceptibility (Wiggs *et al.* 2000; Nemesure *et al.* 2003).

Locus	Maximum LOD	Location	Original Reference	Region width (cM)	Gene	Gene reference
GLC1A	6.5	1q21-31	Sheffield *et al.* 1993	20	*MYOC* (myocilin)	Stone *et al.* 1997
GLC1B	6.48	2cen-q13	Stoilova *et al.* 1996	11.2	Not identified	nil
GLC1C	3.02	3q21-24	Wirtz *et al.* 1997	11.1	Not identified	nil
GLC1D	3.61	8q23	Trifan *et al.* 1998	6.3	Not identified	nil
GLC1E	10	10p15-14	Sarfarazi *et al.* 1998	21	*OPTN* (optineurin)	Rezaie *et al.* 2002
GLC1F	4.06	7q35-36	Wirtz *et al.* 1999	5.3	Not identified	nil
GLC1G	5.41	5q22.1	Monemi *et al.* 2005	2	*WDR36* (WD40 repeat 36)	Monemi et al. 2005
GLC1I	3.24	15q11-13	Allingham *et al.* 2005	11	Not identified	nil

Table 1.1 - Summary of the known POAG loci and original references

The recent identification of GLC1G and the responsible gene *WDR36* on chromosome 5q22.1 (Monemi *et al.* 2005) and GLC1I on chromosome 5q11-13 (Allingham *et al.* 2005) occurred after completion of the analysis phase of this investigation, hence these loci are not described in the remaining chapters of this dissertation.

1.8.1 GLC1A and Myocilin

Sheffield *et al.* (1993) identified the first genetic locus for juvenile onset open-angle glaucoma in a single North American family of 67 individuals, 37 of whom participated in the study, including 22 affected with JOAG. Affected individuals were characterised clinically by an early age of onset (often during the second decade of life), apparently normal trabecular meshwork, very high IOP (often greater than 50mmHg) and relatively pressure-resistant optic nerves. The locus was refined to a 20 cM region of chromosome 1q21-31, flanked by D1S191 and D1S194 (Sheffield *et al.* 1993), and subsequently assigned the name GLC1A by the Human Genome Organisation (HUGO).

Linkage of this locus to JOAG was confirmed and refined in several families (Richards *et al.* 1994; Wiggs *et al.* 1994; Graff 1995; Morissette *et al.* 1995; Wiggs *et al.* 1995; Lichter *et al.* 1996; Meyer *et al.* 1996). Most of the confirmation studies included families with similar characteristics to the JOAG family used in the initial localisation of GLC1A (Richards *et al.* 1994; Wiggs *et al.* 1994; Graff 1995; Lichter *et al.* 1996). Two of these confirmation studies identified linkage to GLC1A in pedigrees containing individuals with juvenile and adult-onset POAG (Morissette *et al.* 1995; Meyer *et al.* 1996). These findings provided the first suggestion that the phenotype determined by the GLC1A locus may be more heterogeneous than originally thought; potentially influencing both JOAG and adult-onset POAG.

Stone *et al.* (1997) discovered that the causative gene at the GLC1A locus encoded the trabecular-meshwork induced glucocorticoid response (TIGR) protein (GenBank accession number NM_000261) (Stone *et al.* 1997). The TIGR protein was originally cloned as a steroid response protein from cultured trabecular meshwork cells (Polansky *et al.* 1997). Kubota *et al.* (1997) independently isolated a gene from retinal cDNA and showed it localised to cilium connecting the inner and outer segments of photoreceptor cells. They named the protein product myocilin due to its sequence homology to *Dictyostelium discoideum* myosin (Kubota *et al.* 1997). Myocilin and the TIGR protein were later determined to be the same protein, and the official HUGO nomenclature for the gene became *MYOC* (MIM: 601652) with protein product myocilin.

MYOC is a three exon gene spanning approximately 17kb of genomic DNA on chromosome 1q24.3 (Figure 1.5). Myocilin is expressed as a 2.3kb transcript encoding a 504 amino acid (57kDa) protein (Fingert *et al.* 1999). The *MYOC* gene has two major domains: a 5′ (proximal) myosin-like domain, encoded by exon 1, that shows similarities to *Dictyostelium discoideum* (slime mould) non-muscle myosin heavy chain and the 3′ (distal) olfactomedin-like domain (Kubota *et al.* 1997), encoded by exon 3. Olfactomedins are olfactory epithelium-specific extracellular proteins found predominantly in nasal mucus. Upstream of the coding sequence, the promoter contains a TATA box, a Sac box, an AP-1 like sequence, an AP-2 site, an NF-Kβ-related site and an E-box (Kirstein *et al.* 2000; Fingert *et al.* 2002) (Figure 1.5). The transcription factor USF binds to the myocilin promoter at the E-box site and is essential for myocilin transcription (Kirstein *et al.* 2000).

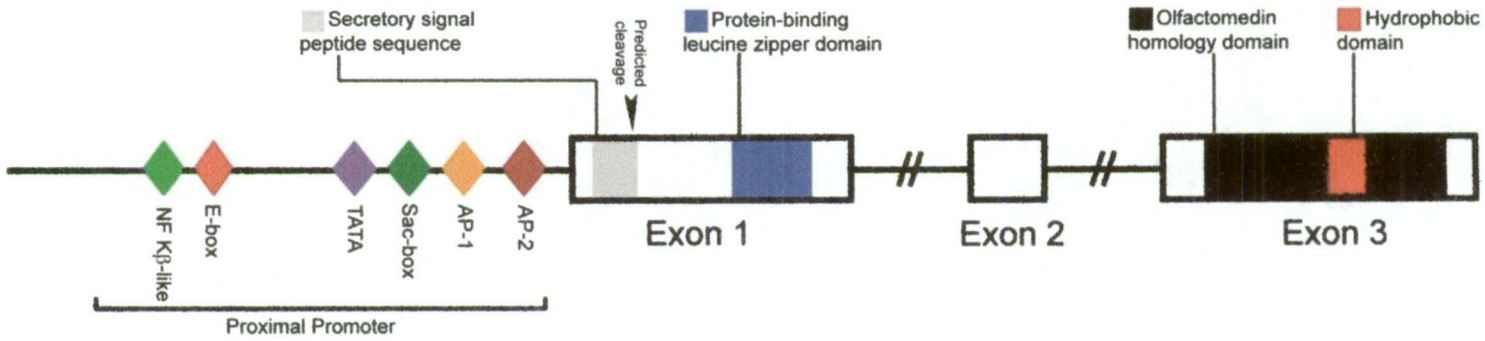

Figure 1.5 - Putative functional motifs of the *MYOC* gene and myocilin protein

Proximal promoter elements are denoted by coloured diamonds. Exon 1 contains both the cleavage site of the putative signal peptide, predicted from analysis of the myocilin protein sequence, and the leucine zipper protein binding domain. Exon 3 contains the region of homology with olfactomedin, including the hydrophobic domain.

Adapted from Fingert JH, Stone EM, Sheffield VC and Alward WL (2002). Myocilin glaucoma. Surv Ophthalmol *47(6): 547-61.*

The myocilin protein contains a leucine zipper motif (eight leucine residues evenly spaced every seven residues between amino acids 117 and 166) that form a coiled-coiled structure able to facilitate interactions between proteins (Nguyen *et al.* 1998). It remains unknown which proteins, if any, bind to the leucine zipper of myocilin, however there is evidence that myocilin is able to form homodimers via this domain (Fautsch and Johnson 2001).

Myocilin is a glycoprotein, existing in both glycosylated and non-glycosylated forms, and has been detected in both intra- and extra-cellular locations (Polansky *et al.* 1997; Nguyen *et al.* 1998). Expression of myocilin has been demonstrated in most tissues, ranging from bone marrow to cardiac muscle (Fingert *et al.* 1998). In the eye, myocilin expression is high in the trabecular meshwork, sclera, ciliary body and iris and considerably lower in the optic nerve head and retina (Tamm 2002). Secreted myocilin is also present in the aqueous humor (Fautsch and Johnson 2001).

In the original study by Stone *et al.* (1997), mutations in the *MYOC* gene were found to segregate in five out of eight JOAG families linked to GLC1A on chromosome 1q (Stone *et al.* 1997). Although many *MYOC* mutations were subsequently identified in a range of JOAG pedigrees, disease causing variants of this gene are not the exclusive cause of JOAG. Wiggs *et al.* (1998) found identifiable *MYOC* mutations in only two of 25 JOAG pedigrees (8%); while Alward *et al.* (2002) detected *MYOC* mutations in three of 47 (6.4%) unrelated JOAG patients.

Although initially identified in JOAG pedigrees, mutations in the *MYOC* gene have now been shown to account for approximately 3% of adult-onset POAG (Fingert *et al.* 1999; Alward *et al.* 2002). Fingert *et al.* (1999) screened 1,703 POAG patients from five

populations representing three racial groups for mutations in *MYOC*. These populations included Caucasians from the United States, Australia, and Canada, African Americans from the United States and Asians from Japan. These diverse populations revealed similar frequencies of *MYOC* mutations in POAG patients, ranging from 2.6 to 4.3% (Fingert *et al.* 1999). The majority (90%) of mutations were located in exon 3, which contains the olfactomedin domain. Similar *MYOC* mutation prevalence rates in POAG patients were obtained by other investigators: 4.0% in a Japanese population (Suzuki *et al.* 1997), 4.6% in predominantly Caucasian populations from the United States and Australia (Alward *et al.* 1998) and 4% in a predominantly Caucasian population from the United States (Shimizu *et al.* 2000). More than 50 different myocilin mutations have been reported in POAG and, consistent with earlier findings, the majority of the disease causing *MYOC* variants for POAG occur in the third exon of the gene (Alward *et al.* 2002).

The most common *MYOC* mutation is Q368X, which is associated with a late onset POAG phenotype (Alward *et al.* 1998). The Q368X *MYOC* mutation was identified in 1.6% of 1,703 unrelated POAG patients from Australia, Canada, Japan and the United States; and found in all populations except the Japanese (Fingert *et al.* 1999). This mutation results in a truncated protein missing 135 amino acids from the C terminus of myocilin, which represents approximately half the olfactomedin domain. Fingert *et al.* (1999) detected Q368X in 27 POAG pedigrees, thought to be unrelated, from Australia, Canada and the United States, including both African American and Caucasian individuals. The authors typed microsatellite markers closely flanking *MYOC* in all 27 pedigrees, and the amount of DNA sharing at these sites was found to be significantly higher than in normal controls ($p<0.05$), suggesting a common ancestor for the mutation (Fingert *et al.* 1999). Evidence of a founder effect has since been identified in 15

Australian POAG pedigrees, with a common origin prior to European settlement (Baird *et al.* 2003).

Patients with the Q368X mutation generally present with normal to elevated IOP (Allingham *et al.* 1998; Alward *et al.* 1998; Wiggs *et al.* 1998; Angius *et al.* 2000; Craig *et al.* 2001) that is often well controlled by medical therapy (Allingham *et al.* 1998; Angius *et al.* 2000). Q368X carriers generally present with a late age of onset of between 50–60 years of age (Allingham *et al.* 1998; Alward *et al.* 1998; Wiggs *et al.* 1998; Craig *et al.* 2001); later than most other, generally missense, *MYOC* mutations in the olfactomedin domain (Allingham *et al.* 1998). However, Shimizu *et al.* (2000) reported two mixed age of onset POAG families (including both JOAG and adult onset POAG) where carriers of the Q368X mutation were diagnosed by 40 years of age. The generally observed delayed age of onset may indicate rapid elimination of the obviously truncated protein by control mechanisms in the endoplasmic reticulum, while more subtly mutated forms might escape these processes.

Although extensive analysis of the myocilin gene and protein sequences has been conducted, the normal physiological role of myocilin and the mechanisms by which mutations lead to glaucoma have yet to be fully elucidated. It is postulated that mutant myocilin accumulates in the secretory compartments of trabecular meshwork cells, thereby interfering with the normal functions of these cells such as scavenging the debris that may obstruct aqueous humor outflow (Fingert *et al.* 2002). It is less clear whether wild-type myocilin plays a role in aqueous humor outflow under normal conditions.

1.8.2 GLC1B

The second POAG locus, designated GLC1B and located on chromosome 2cen-q13, was identified in 1996 (Stoilova *et al.* 1996). Seventeen Caucasian families, including 203 subjects and 90 affected individuals, were genotyped with 215 microsatellite markers across the genome. Families consisted of at least two to three affected offspring and one available parent. Six families showed linkage to D2S436, while eight other families were not linked and three produced ambiguous results. Additional markers, genotyped only in the linked families, were used to localise GLC1B to an 11.2 cM region flanked by D2S2161 and D2S176. This locus was replicated in an American Society of Human Genetics conference abstract (Raymond *et al.* 1999) and in studies undertaken as part of this Ph.D. research project (Charlesworth *et al.* 2006; see Chapter 5).

1.8.3 GLC1C

Wirtz *et al.* (1997) identified a third POAG locus using a single 76-member North American family including 9 POAG patients and seven glaucoma suspect individuals. A 15 cM genome-wide scan mapped the disease locus to an 11.1 cM region flanked by D3S3637 and D3S1744 on chromosome 3q21-24. This linkage was confirmed by Kitsos *et al.* (2001) in a Greek family of 34 individuals, including 10 affected with POAG, however the authors were unable to refine the region of interest.

1.8.4 GLC1D

Trifan *et al.* (1998) identified the fourth POAG locus using a single 23-member North American family spanning four generations, 20 of whom were available and eight affected with POAG. Haplotype reconstruction and recombination analysis placed the

new locus within a 6.3 cM region, flanked by D8S1830 and D8S592, on 8q23 (Trifan *et al.* 1998).

1.8.5 GLC1E and Optineurin

Sarfarazi *et al.* (1998) identified the fifth POAG locus using a single British family with the normal tension form of POAG. The family used in the study consisted of 60 individuals over four generations, 46 of whom were available to participate in the study including 15 classified as affected. Random selections of microsatellite markers from across the genome were typed until suggestive evidence of linkage was identified at D10S1172. An additional 23 markers localised GLC1E to a 21 cM region on 10p15-14 flanked by D10S1729 and D10S1664 (Sarfarazi *et al.* 1998).

The susceptibility gene at GLC1E on chromosome 10p14 was identified by Rezaie *et al.* (2002) in a study of 54 POAG families. The gene identified at this locus, designated *OPTN* (MIM: 602432) for its protein product optineurin ('optic neuropathy inducing' protein), was previously known as *FIP*-2 (Li *et al.* 1998) or *NRP* (Schwamborn *et al.* 2000). *OPTN* spans approximately 37kb of genomic DNA, including three non-coding exons in the 5′ untranslated region and 13 translated exons (Figure 1.6), producing a 577 amino acid protein of unknown function. Alternative splicing in the 5′-UTR generates at least three different isoforms, all with the same reading frame (Genbank accession numbers AF420371 to AF420373) (Rezaie *et al.* 2002).

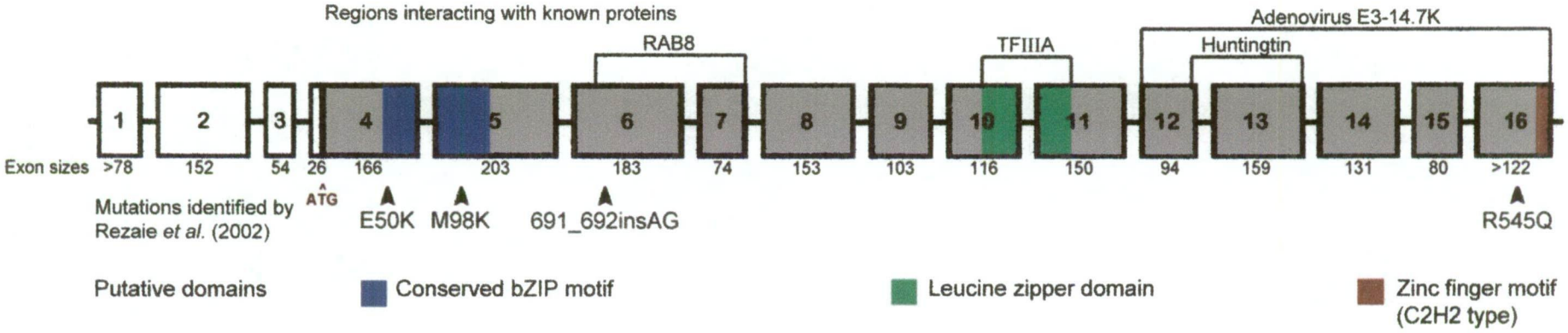

Figure 1.6 - Putative structure of the optineurin gene

Putative functional motifs and regions interacting with known proteins are shown. The approximate locations of the mutations identified by Rezaie *et al.* (2002) are also displayed. Exons 1-3 are non-coding, with the ATG start site marked in exon 4.

Adapted from Rezaie T, Child A, Hitchings R, et al. *(2002). Adult-onset primary open-angle glaucoma caused by mutations in optineurin.* Science *295(5557): 1077-9. Online supplementary material (http://www.sciencemag.org/)*

After originally mapping GLC1E to 10p14-p15 in a normal-tension glaucoma family, Sarfarazi *et al.* (1998) reduced the critical region to 5 cM and began screening candidate genes. Four genes were excluded before *OPTN* was sequenced and a segregating E50K missense mutation identified in the original kindred (Rezaie *et al.* 2002). The authors then screened a set of 54 POAG families, each including at least one member with NTG, revealing four additional *OPTN* mutations. As a result of these findings the authors suggest mutations in *OPTN* may be responsible for 16.7% of hereditary normal-tension glaucoma (Rezaie *et al.* 2002).

Funayama *et al.* (2004) identified a possible disease causing mutation (H26D) in the Japanese population, although this change was found in only 1 of 411 (0.24%) POAG patients and 0 of 218 controls (Funayama *et al.* 2004). Several other sequence changes, predicted to be disease causing, have been described in Chinese open-angle glaucoma cases (Leung *et al.* 2003). However, recent studies involving Caucasian, African American and Japanese POAG patients and controls have shown little to no association between the four previously identified *OPTN* sequence variants and POAG or the normal to low tension subtypes (Alward *et al.* 2003; Wiggs *et al.* 2003). No mutations were detected in the 13 coding exons of *OPTN* in a study of 8 POAG families from Finland (Forsman *et al.* 2003). The majority of reports therefore conclude that, with the exception of E50K which appears to cause severe autosomal dominant NTG, most *OPTN* sequence variants may be susceptibility alleles or risk factors for POAG, rather than disease causing variants, or at most rare causes of NTG (Alward *et al.* 2003; Leung *et al.* 2003; Wiggs *et al.* 2003; Baird *et al.* 2004; Toda *et al.* 2004; Jansson *et al.* 2005; Mukhopadhyay *et al.* 2005a; Weisschuh *et al.* 2005). The contribution of *OPTN* to NTG, and to POAG as a whole, remains to be fully elucidated.

Optineurin is expressed in the trabecular meshwork, non-pigmented ciliary epithelium, retina and brain (Rezaie *et al.* 2002), and interacts with many proteins including Huntingtin (Faber *et al.* 1998), Ras-associated protein RAB8 (Hattula and Peranen 2000), adenovirus E3-14.7K (Li *et al.* 1998), transcription factor IIIA (Moreland *et al.* 2000) and two unknown kinases (Schwamborn *et al.* 2000) as shown in Figure 1.6.

Optineurin has been suggested as a component of the tumour necrosis factor-alpha (TNF-α) signalling pathway; able to shift the equilibrium towards induction of apoptosis (Li *et al.* 1998). TNF-α may be able to induce retinal ganglion cell apoptosis in patients with POAG (Yan *et al.* 2000; Yuan and Neufeld 2000). Rezaie *et al.* (2002) speculated that wild-type optineurin plays a neuroprotective role in the eye and optic nerve through the TNF-α pathway, resulting in vision loss and optic neuropathy typical of glaucoma when defective (Rezaie *et al.* 2002). Sustained elevated IOP, TNF-α exposure, and prolonged dexamethasone treatment all significantly up-regulate *OPTN* expression, suggesting that *OPTN* is part of the transcriptome activated in response to glaucomatous insult, which also supports the protective role of optineurin in the trabecular meshwork (Vittitow and Borras 2002).

1.8.6 GLC1F

Wirtz *et al.* (1999) localised GLC1F using a 36 person family, including 25 individuals available to participate in the study, 10 of whom were affected with POAG. A 5-10 cM genome-wide scan detected linkage to D7S2439. Haplotype analysis refined GLC1F to a 5.3 cM region on chromosome 7q35-36, flanked by markers D7S2442 and D7S483 (Wirtz *et al.* 1999).

1.8.7 GLC1G and WD40-Repeat 36

There were several initial indications of linkage to chromosome 5q reported between 2003 and 2004 (Monemi *et al.* 2003; Kramer *et al.* 2004; Samples *et al.* 2004). Follow-up saturation mapping in a total of seven POAG families allowed Monemi *et al.* (2005) to refine the GLC1G locus to a region of approximately 2 cM, flanked by markers D5S1466 and D5S2051 on chromosome 5q21.3-22.1.

The GLC1G region of interest contained several predicted and seven known genes, including *MAN2A1, TSLP, WDR36* and *CAMK4*. Monemi *et al.* (2005) directly sequenced the known genes and identified *WDR36* (MIM:609669) as the gene of interest at GLC1G, after detecting a mutation in exon 17 of *WDR36* (D658G) in all seven affected individuals. The change was also present in nine asymptomatic 'carriers' but was absent in another nine unaffected family members and the six married in unaffected spouses (Monemi *et al.* 2005). This mutation was absent in 476 normal control chromosomes. The authors sequenced a total of 130 unrelated POAG cases and identified 24 sequence alterations, four of which were predicted to be disease causing and 12 which were intronic alterations (Monemi *et al.* 2005). The most common disease causing mutation identified (D658G) was identified in 13 of 670 unrelated familial probands and sporadic cases of POAG (1.9%), six with high- and seven with low-tension glaucoma. The three other predicted disease causing mutations were identified in a combined total of four out of 130 (3%) unrelated POAG cases. None of these mutations were detected in (at least 200) control chromosomes. The authors concluded that *WDR36* accounted for at least 5% of both familial and sporadic POAG in their study population (Monemi *et al.* 2005). The impact of this gene on the wider population of POAG patients has yet to be determined.

WDR36 is a 23 exon gene that encodes a 951 amino acid protein containing a G-protein beta WD-40 repeat, which consists of eight tandem repeats of approximately 40 residues each containing a central Trp-Asp dipeptide. These repeat motifs are also present in a wide variety of other proteins of diverse functionality, and are involved in protein-protein interactions. *WDR36* was also identified by Mao *et al.* (2004) as one of the genes uniquely involved in T cell activation and highly co-regulated with interleukin 2 (*IL2*). The gene is therefore also known as *TA-WDRP* after the T-cell activation WD repeat protein (Mao *et al.* 2004).

Monemi *et al.* (2005) observed expression of two distinct mRNA transcripts in human heart, placenta, liver, skeletal muscle, kidney and pancreas. Expression was also observed in ocular tissues, including the lens, iris, ciliary body, trabecular meshwork, retina, and optic nerve (Monemi *et al.* 2005). The *in vivo* functions of *WDR36* and its involvement in POAG pathogenesis are yet to be elucidated.

1.8.8 GLC1I

Allingham *et al.* (2005) used a stratification technique known as ordered subset analysis (Hauser *et al.* 2004) to identify linkage to an 11 cM region of chromosome 15q11-13, with a peak LOD of 3.24, in a subset of 15 early adult-onset POAG families. This region was originally identified as an area of interest in a genome-wide scan, although the original detection did not reach significance, with a LOD of 1.27 at D15S165 (Wiggs *et al.* 2000). The collection of 81 multiplex POAG families (*MYOC* and *OPTN* mutation free), including an average of 2-3 affected individuals, was stratified based on mean age at diagnosis per family, as a surrogate for age of onset. Maximal evidence for linkage was found with a subset of 15 pedigrees with a mean family-specific age at diagnosis of 44.1 ± 9.1 years, much lower than the 61.3 ± 10.4 years in the

complimentary set of 70 families (Allingham *et al.* 2005). The 15 pedigree subset consisted of 10 Caucasian families including a total of 35 affected individuals and 4 African American families including 12 affected individuals. The peak LOD of 3.24 (without correction for multiple testing) was identified at the *GABRB3* locus, with LOD-1 interval boundaries at the centromere and marker D15S822 (Allingham *et al.* 2005).

1.8.9 Other POAG loci

The results of Wiggs *et al.* (2000) using a 7 cM genome-wide scan of affected sib pairs (ASP) suggest several additional chromosomal regions may be involved in POAG susceptibility. The study initially used a set of 113 ASP from 41 multiplex families, including 126 affected individuals. Regions of interest (defined by a LOD score greater than 1) were followed up in a second set of 69 ASP from 33 multiplex families, including 81 affected individuals. The majority of pedigrees consisted of two to four affected siblings in a generation; however several larger families were included in the dataset, one of these with nine affected individuals. Five regions produced LOD scores greater than 2.0: chromosomes 2p14, 14q11, 17p13, 17q25 and 19q13 (Wiggs *et al.* 2000).

Nemesure *et al.* (2003) conducted a genome-wide scan for POAG loci on Afro-Caribbean individuals from the Barbados Family Study of open-angle glaucoma. This study was designed to evaluate the genetic component of POAG in a population of African descent. A 10 cM genome-wide scan was conducted on 662 individuals, 256 of whom were classified as affected, from 146 families. Two-point LOD scores greater than one were identified on chromosomes 1q43, 2q31-33, 9q34, 10q24-p12, 11q14 and 14q11-21 (Nemesure *et al.* 2003). Multipoint analyses reduced the regions of interest,

with LOD scores greater than two obtained for chromosomes 2q, 10p and 14q. The region of interest on chromosome 14q11.2-21.2, spanning D14S283 and D14S288 overlaps the region identified by Wiggs *et al.* (2000), however this peak did not reach significance (Lander and Kruglyak 1995) (maximum LOD=2.02), nor could it be excluded (Nemesure *et al.* 2003). The authors concluded this result may provide weak support for the suggestion of a glaucoma locus near D14S283. The regions of interest on chromosomes 2q31.1-34 (spanning D2S2314 and D2S2178) and 10p13-12.1 (spanning D10S1477 and D10S601 but not including *OPTN*) produced multipoint LOD scores greater than 3 and empirical p-values <0.002 (Nemesure *et al.* 2003).

A recent genome-wide scan revealed evidence for two novel loci at 9q22 and 20p12 involved in JOAG (Wiggs *et al.* 2004), although the relevance of these loci to POAG as a whole remains to be seen.

1.9 Complexity of POAG genetics

There appears to be much complexity in the genetics of POAG; made apparent by the variable impact of the susceptibility genes *MYOC* and *OPTN* following their initial identification, and the existence of many additional susceptibility loci where the genes of interest remain to be discovered. Dissecting the genetics of POAG is further complicated by evidence of interaction and additional genes acting as phenotypic modifiers of the disease.

1.9.1 CYP1B1

One of the genes causing autosomal recessive primary congenital glaucoma is *CYP1B1* (MIM:601771), encoding a 543 amino acid member of the cytochrome p450 gene superfamily, subfamily 1 (Stoilov *et al.* 1997). A mutation in the *CYP1B1* gene was

shown by Vincent *et al.* (2002) to modify the phenotype of POAG when inherited together with a *MYOC* mutation, decreasing the age of onset from 51 years (range 48-64 years; *MYOC* alone) to 27 years (range 23-38 years). The authors concluded that digenic inheritance with a *CYP1B1* mutation modifies the *MYOC* glaucoma phenotype (Vincent *et al.* 2002).

1.9.2 APOE

Apolipoprotein E is an essential protein in lipid transport and variants of the *APOE* gene (MIM:107741) have been associated with cholesterol related myocardial infarction (Mahley and Huang 1999; Lambert *et al.* 2000) and predisposition to Alzheimer's disease (Roses 1996; Bullido *et al.* 1998; Lambert *et al.* 1998). *APOE* is up-regulated in response to oxidative stress (Miyata and Smith 1996) and is involved in neuronal degeneration and stress-induced injury. Variants of *APOE* appear able to influence the phenotype components of POAG through several pathways, including interaction with *MYOC*.

Copin *et al.* (2002) determined that the G allele of the *APOE* -219 SNP was associated with both visual field loss and increased cup-to-disc ratio ($p=0.0012$ and 0.015 respectively) in a study of 191 unrelated Caucasian POAG patients and 102 control subjects. The authors suggest that optic nerve degeneration may be influenced by genetic factors, independent of IOP (Copin *et al.* 2002). A highly significant interaction between the *APOE* -491T allele and a *MYOC* promoter SNP -1000G, associated with increased IOP and limited effectiveness of IOP lowering treatment in POAG patients, was also identified. The involvement of *APOE* variants with POAG may account for the previously identified linkage to 19q (Wiggs *et al.* 2000), and for the reported increased frequency of Alzheimer's disease in glaucoma patients (Bayer *et al.* 2002).

Vickers *et al.* (2002) examined the *APOE* ε2, ε3 and ε4 alleles in a sample of 70 NTG patients, 72 POAG patients and 51 control subjects from the Tasmanian population. The study indicated that approximately twice as many NTG (38.0%) and POAG (34.2%) patients carried an ε4 allele compared with control subjects (18.9%). The authors suggest inheritance of the ε4 allele in this population is associated with elevated risk of glaucomatous changes that are not necessarily related to IOP (Vickers *et al.* 2002).

There is, however, still some debate as to the extent of the involvement between *APOE* and POAG. One study recently examined the frequency of APOE alleles ε2, ε3 and ε4 in 137 POAG patients (no NTG) and 75 controls and detected no association with POAG (Ressiniotis *et al.* 2004). The original investigation of Copin *et al.* (2002) has been criticised by suggestions that some of the results associating *APOE* with POAG may be invalid due to the methods used to analyse visual field loss and cup-to-disc ratio (Bunce *et al.* 2003), and case/control studies to date have been based on small sample sizes.

1.9.3 Genetic contributions to IOP

Duggal *et al.* (2005) recently conducted a segregation analysis on 2337 individuals from 620 Beaver Dam Eye Study families to determine the genetic contribution to IOP as a component of the POAG phenotype. The segregation analysis determined the best model of IOP consisted of an unmeasured environmental effect in combination with a polygenic genetic component (Duggal *et al.* 2005). A genome-wide scan of 218 sib-pairs confirmed the heterogeneity of IOP, identifying two novel loci for the trait. Peak evidence for linkage was obtained on chromosome 6 with marker D6S1027 (p=0.008)

and on chromosome 13 with marker D13S317 (p=0.00071). However, multipoint linkage analysis weakened any suggestion of linkage in both regions and neither reached genome-wide significance (Duggal *et al.* 2005). While this study lacked power and would benefit from the inclusion of additional pedigrees and/or fine mapping, it does suggest that investigating the genetic contributions to each of the phenotype components of POAG, such as IOP or cup-to-disc ratio, may be a valuable approach to investigating the genetics of this complex disease.

1.10 Impact of gene identification

POAG is clearly a complex disease with much overlap within the clinical phenotypes (such as POAG and JOAG) and the genetics of the disease. *MYOC* for example was identified as a causative gene for the rare disease JOAG, and now appears to also be responsible for 3% of adult onset POAG (Stone *et al.* 1997; Alward *et al.* 2002). Results obtained following the identification of *OPTN*, the second POAG susceptibility gene, have been variable across populations; for example the original study by Rezaie *et al.* (2002) suggested *OPTN* could be responsible for 16.7% of familial POAG and NTG; while Alward *et al.* (2003) identified a low prevalence of *OPTN* mutations (less than 0.1%) in unselected cases of both POAG and NTG. Variants of other genes such as *APOE* and *CYP1B1* further complicate genetic studies of glaucoma by apparently modifying the POAG phenotype (Copin *et al.* 2002; Vincent *et al.* 2002). The findings for *MYOC* suggest the identification of additional glaucoma genes may be relevant to a wider population of POAG patients than the rare pedigrees in which they were initially identified, although the studies of *OPTN* are less supportive of this claim. Identifying genes involved in the normal tension subtype of glaucoma may offer insights that are relevant to elucidating the pathogenesis of POAG as a whole, such as the genetic mechanisms of optic nerve susceptibility and damage in the absence of elevated IOP.

There is also considerable clinical overlap between the sub-classifications of the various forms of glaucoma. Arbitrary threshold values for age of onset and IOP are used to classify subtypes of POAG, whereas these different forms are likely to be part of a spectrum of disease. Determining the molecular pathogenesis and contributing risk factors of POAG may provide more accurate classification of the disease.

The isolation and characterisation of glaucoma genes will allow a better understanding of the pathogenesis of the disease, and may lead to the development of more suitable treatment strategies. It is anticipated that the identification of novel POAG genes could be translated into direct health outcomes via predictive testing. Once a disease causing variant is identified, at-risk unaffected individuals can be screened for the mutation and counselled about the implications of results. Management strategies, including increased frequency of ophthalmic examination in those carrying a mutation, could then be implemented to provide the best possible chance of disease detection prior to permanent visual loss. These strategies have been implemented in some situations, such as determining an appropriate frequency of clinical screening for individuals within a pedigree segregating a disease causing *MYOC* mutation based on mutation status (Mackey and Craig 2003).

1.11 Aims of the study

Several genes for POAG have been identified (Fingert *et al.* 1999; Rezaie *et al.* 2002; Monemi *et al.* 2005), yet mutations in these genes appear to account for only a small portion of familial POAG. The disease is clearly genetically heterogeneous, and while five additional loci have been mapped (Stoilova *et al.* 1996; Wirtz *et al.* 1997; Trifan *et al.* 1998; Wirtz *et al.* 1999; Allingham *et al.* 2005), the genes within these regions

remain to be elucidated. Genome-wide scan data also suggest that several additional chromosomal regions may be involved in POAG susceptibility (Wiggs *et al.* 2000; Nemesure *et al.* 2003). Follow-up analyses of POAG susceptibility loci and subsequent gene identification has been hindered by the late age of onset (in most cases), unclear mode of inheritance and penetrance, the asymptomatic progression of the disease that results in approximately half of cases remaining undiagnosed, the phenotypic uncertainty and often poor disease classification and the potential for phenocopies.

This dissertation explores different approaches to the genetic analysis of POAG, taking into consideration the complex nature of the disease and the size and structure of available pedigrees, to dissect the genetic aetiology of this phenotypically and genetically heterogeneous disease in extended pedigrees from the Tasmanian population.

One of the principal objectives of this study was to investigate the primary open-angle glaucoma loci known at the time of inception (GLC1A, -B, -C,-D, -E and -F) in 10 extended pedigrees from the Glaucoma Inheritance Study in Tasmania (GIST), a population-based study of glaucoma genetics in Tasmania representing almost complete population ascertainment. This dataset, including pedigree structure and clinical information, is described in Chapter 2, while the molecular methodology is described in Chapter 3. Initial and exploratory linkage analyses, including marker selection, simulations, Markov chain Monte Carlo based analyses and exact parametric and nonparametric analyses are described in Chapter 4. Follow-up analyses of suggestive results are described in Chapter 5.

Genome-wide scan data were also available for an additional extended POAG pedigree from Tasmania, previously investigated using nonparametric dichotomous trait analysis approaches. A second aim of this dissertation was to use variance components analyses (also nonparametric) on quantitative trait data, derived from phenotypic information collected as part of the routine clinical examination of POAG patients, to identify loci contributing to these traits. These analyses are described in Chapter 6.

Chapter 2 - Extended Pedigrees from the Glaucoma Inheritance Study in Tasmania

2.1 Background

2.1.1 Genetic studies in Tasmania

Tasmania, the 'island state of Australia', is an island population which is not significantly inbred (Lafranchi *et al.* 1988), but displays many of the benefits for studies of the genetic aetiology of complex disease. Island populations with a high standard of health care, but a limited number of facilities and specialists, support the easy identification and follow-up of disease cases; while the preservation of comprehensive and accurate genealogical records facilitates the reconstruction of extended pedigrees and increases the likelihood of identifying and linking additional disease cases into pre-identified pedigrees.

Tasmania has a population of approximately 474,000 (Australian Bureau of Statistics 2002), and was colonized as a penal settlement of the British empire in 1803. Free settlers were also encouraged to migrate to the colony through the early to mid 19th Century. Convict transportation ceased in 1853, coinciding with reduced immigration of free settlers.

Tasmania's early history and genealogy has been well documented, including extensive convict records of transportation, military records, records of free passage, and land grants provided for assisted immigrants. In 1838 Tasmania was the first Australian state to pass an Act requiring the civil registration of births, deaths and marriages, not long after England (July 1837). Previously, baptism, marriage and burial records were primarily recorded by the church and the actual number was understated.

Furthermore, this population is a relatively homogenous one whose ancestry is principally from the British Isles. Census data from 2001 indicates that 84.9% of Tasmania's current 472,000 residents were born in Australia (compared with 71.1% for Victoria, the nearest Australian state), while almost 90% of Tasmanians were born in Australia or the United Kingdom (compared with 75.6% for Victoria; Australian Bureau of Statistics 2001). A further indicator of relative population homogeneity is given by ancestry, where 88.7% of the Tasmanian population is of North-West European ancestry (based on parental origin), compared with 69.4% for Victoria (Australian Bureau of Statistics 2001).

A founder effect has been observed for a small number of Mendelian diseases in Tasmania. For example, a large kindred segregating Huntington disease has been traced back nine generations to the father of a female migrant who came to Tasmania in 1842 and gave rise to 765 living descendents (Pridmore 1990). Founder effects have been observed in Tasmanian families with multiple endocrine neoplasia type 1 (MEN1) (Shepherd 1985; Teh *et al.* 1995), Leber hereditary optic neuropathy (LHON) (Mackey and Howell 1992), and also in 15 Australian (primarily Tasmanian) POAG families segregating a common haplotype around the *MYOC* Q368X mutation (Baird *et al.* 2003).

2.1.2 The Glaucoma Inheritance Study in Tasmania

This study was conducted as a part of the Glaucoma Inheritance Study in Tasmania (GIST) (Mackey and Craig 2002), a large population study of glaucoma genetics based in Tasmania, Australia. Through the collaborative involvement of Tasmanian

ophthalmologists, the aim of the GIST was to identify and involve all diagnosed glaucoma patients in Tasmania. The study represents almost complete population ascertainment based on population prevalence predictions derived from the Blue Mountains Eye Study (Mitchell *et al.* 1996).

The study identified adult-onset POAG families by first attempting to recruit all diagnosed glaucoma patients and then using genealogical data provided by participants, combined with Tasmania's comprehensive genealogical records, to determine familial relationships between patients. Once initial pedigrees were identified and expanded, all available family members over 40 years of age were invited to participate in the study.

To date, blood has been collected from over 1,353 individuals from 116 Tasmanian families containing at least two first-degree relatives, 435 (32%) of whom are affected. All were examined by specialised ophthalmologists and have had IOP measured, Humphrey visual fields and stereo disc photographs taken, and clinical history documented (methodology used by the examining clinicians is described in Appendix 1). Many individuals have been examined sequentially since the inception of the study. The GIST dataset contains several large families with five or more affected individuals that compare favourably with pedigrees used to localise the known POAG loci in the published literature.

For this dissertation 10 extended pedigrees, with a total of 457 individuals, were selected from the GIST dataset for linkage analysis with the known POAG loci. Blood or buccal mucosa swabs for DNA isolation were collected from 237 of these individuals as part of the GIST.

2.1.3 Definition of glaucoma affection status

Clinical examination and diagnosis of patients involved in the GIST is well documented (Coote *et al.* 1996). In brief, POAG was defined as an optic neuropathy which has present at least two of the following features: (1) optic nerve head excavation with thinning of the neuroretinal rim (generally measured by an enlarged vertical cup-to-disc ratio≥0.7), often but not necessarily including significant focal or generalised loss of retinal nerve fibre layer, notching, pitting, or 'Drance' type nerve fibre layer haemorrhages; (2) elevation of the IOP over a population-based normal range, or over the average of the unaffected individuals within a pedigree (generally IOP>21mmHg or 2 standard deviations from the population mean); and (3) reproducible visual field defects consistent with the disc changes and with common descriptions of glaucomatous field loss (Coote *et al.* 1996). An individual with only one of the previously mentioned clinical features was classified as being 'glaucoma suspect'. Glaucomatous changes secondary to rubeosis or trauma were excluded, as were cases of anterior segment dysgenesis. More detail on the clinical methodology of the GIST is provided in Appendix 1.

2.2 Methods

2.2.1 Ethics approval

Ethics approval for this study was obtained from the Human Research Ethics Committees of the Royal Children's Hospital, Victoria, the Royal Victorian Eye and Ear Hospital, the Royal Hobart Hospital and the University of Tasmania. This study was conducted in accordance with the Declaration of Helsinki (revised in 1989) and the statement of the National Health and Medical Research Council of Australia on ethical conduct in research involving humans (NHMRC 1999). Written informed consent was obtained from all participants.

2.2.2 Extended pedigrees for linkage analysis (Chapters 4 and 5)

POAG pedigrees for linkage analysis were selected from the GIST database on the basis of size, number of clinically diagnosed POAG cases, lack of spouses also diagnosed with POAG (to avoid, where possible, multiple sources of inheritance), and lack of any previously identified myocilin mutations in the pedigree. Several individuals from each POAG pedigree in the GIST had been previously screened for mutations in the *MYOC* gene in collaboration with Dr Edwin Stone in Iowa (see Fingert *et al.* 1999). At least five affected individuals from each pedigree selected for use in this study had been screened for mutations in all three exons of *MYOC* in Dr Stone's Laboratory. Although these individuals may not be indicative of the entire pedigree, they offered a guide to selecting pedigrees without known *MYOC* involvement, where possible. The aim, for this study, was to select large but compact pedigrees from the GIST, with five or more closely related POAG cases. The existence of loops, both marriage and consanguineous, within the pedigrees was not a consideration for exclusion.

2.2.3 Family GTas02 for variance components linkage analysis (Chapter 6)

GTas02, the largest of the GIST pedigrees, had been under investigation by Dr Paul Baird and collaborators at the Walter and Eliza Hall Institute (Victoria) for several years prior to the inception of this study. These investigations included single-stranded conformational polymorphism (SSCP) screening of *MYOC* mutations (Craig *et al.* 2001; Baird *et al.* 2003) and a 10 cM genome-wide scan (Baird *et al.* 2005). The resulting data provided an opportunity to apply the method of variance components linkage analysis to the problem of POAG genetics, and were made available to this investigation for that purpose.

The details of family GTas02 are provided in Chapter 6; hence the remainder of this chapter describes the extended pedigree dataset selected for the linkage analyses described in Chapters 4 and 5.

2.2.4 Control individuals for population frequency information

DNA was collected from 156 elderly Tasmanian nursing home residents who were ophthalmically examined. A subset of 72 of these individuals, entirely free of glaucoma or glaucoma suspect status, was used a control dataset for population-specific allele frequencies and mutation detection.

These individuals were ascertained using a restricted sampling method, selected only from participating nursing homes, which could in theory lead to sample bias by selecting for individuals who have survived to old age. However, these individuals were recruited from Tasmania, the same source population as the POAG patients, and while not entirely representative of the population at large they provide more appropriate allele frequency data than most publicly available databases, such as the Centre d'Etude du Polymorphisme Humain (CEPH; http://www.cephb.fr/cephdb).

2.2.5 Genetic material extraction

Blood samples, or in some cases buccal mucosal swabs, were collected as part of the GIST (Mackey and Craig 2002). Genetic material was extracted from these sources using a variety of methods, depending on the age, condition and type of sample available, as described in Chapter 3.1.

2.3 Description of the pedigrees

2.3.1 Dataset overview

The final dataset selected for power calculations and linkage analyses, contained 10 large POAG pedigrees including a total of 457 people. Of these individuals there were 237 with both DNA and clinical information available. This dataset included 87 individuals diagnosed with POAG according to the criteria in Chapter 2.1.3. In order to be conservative, individuals classified as 'glaucoma suspects' (see Chapter 2.1.3) were classed as unknown, rather than unaffected, for the purposes of the linkage analyses. Table 2.1 describes these pedigrees, including the number of individuals with both clinical information and genetic material available for use in the investigation, and the number of individuals with clinically diagnosed POAG.

Family ID	Total	Available	Affected
GTas03	123	59	15
*GTas03a**	*76*	*39*	*9*
*GTas03b**	*41*	*19*	*6*
GTas04	45	25	9
GTas35	32	15	6
GTas37a	51	29	8
GTas37b	37	24	15
GTas54	33	17	7
GTas11	15	10	5
Gtas15	31	14	6
GTas17	45	26	9
GTas121	45	18	7
Total†	**457**	**237**	**87**

Table 2.1 - Size of the selected GIST pedigrees

*GTas3a and GTas3b represent two branches of family GTas03.

†The 'Total' is derived from the 10 main pedigrees with GTas03 considered as one pedigree (not including GTas3a and GTas3b).

2.3.2 Description of selected GIST pedigrees

A system of symbols is used throughout the pedigree diagrams to describe the clinical features of each individual. In this system the pedigree symbol is broken down into quadrants with each quadrant denoting a component of the clinical phenotype (Figure 2.1). A brief description of the clinical thresholds used for each component is given in section 2.1.3, while more detail on the clinical methodology is provided in Appendix 1. Four unfilled quadrants denote unexamined family members with unknown POAG status, or ophthalmically examined participants that had no evidence of any of the clinical characteristics of POAG at the time of their most recent examination. The latter have hyphenated ID numbers below their pedigree symbol.

The 10 extended pedigrees selected for linkage analysis are described below, including figures showing pedigree structure and clinical features of POAG (Figures 2.2 – 2.11).

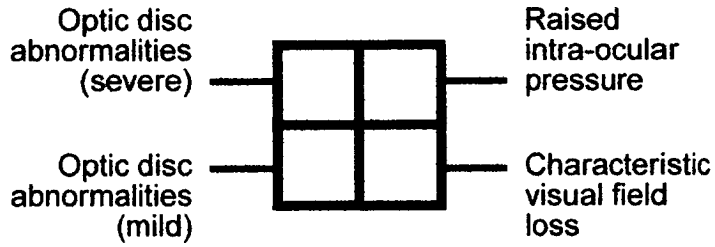

Figure 2.1 - Pedigree symbol key

A filled quadrant in the upper right indicates the individual has raised IOP; the lower right indicates characteristic visual field loss; the left top and bottom quadrants indicate optic disc abnormalities characteristic of POAG and are filled from bottom (mild) to bottom plus top (severe).

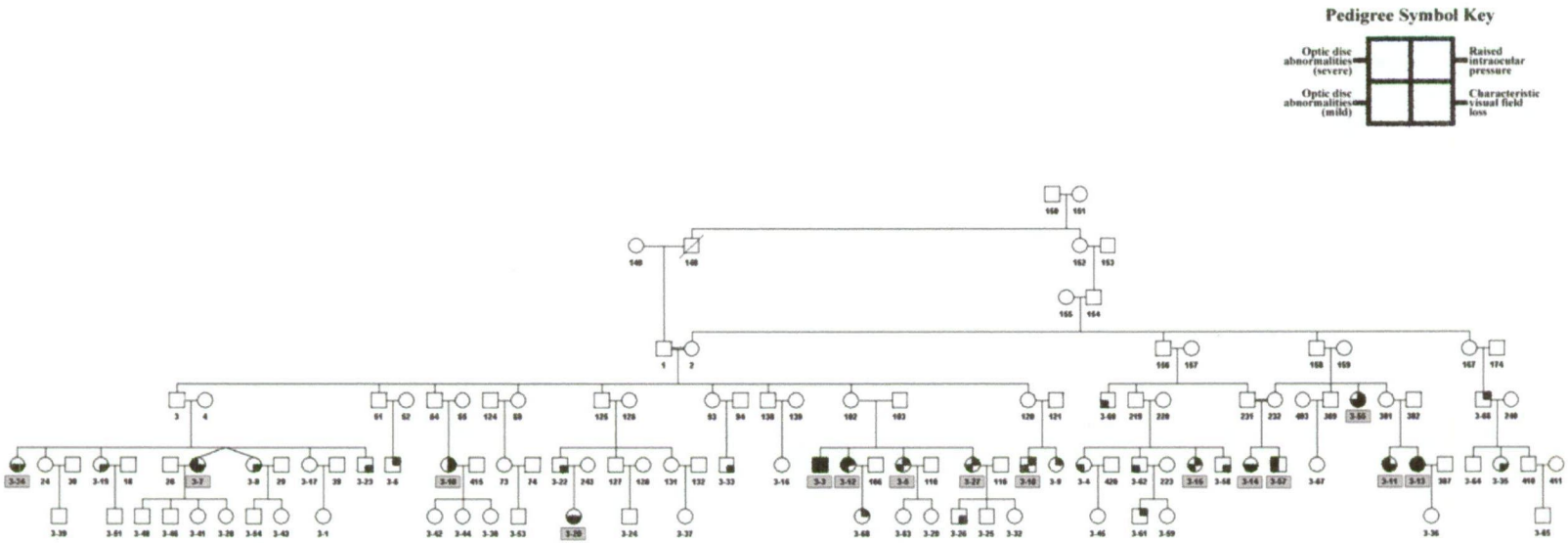

Figure 2.2 Family GTas03

The original 123 member pedigree GTas03 is shown. Individuals are labelled with their ID number. Individuals with available clinical and genetic data have hyphenated ID numbers. Clinically diagnosed POAG cases are highlighted. The consanguineous marriage loops can be seen between individuals 1 and 2, and individuals 231 and 232. Dizygotic twins 3-7 and 3-8 are also shown.

Pedigree Symbol Key

The pedigree symbol is broken down into quadrants with each quadrant denoting a component of the clinical phenotype. A filled quadrant in the upper right indicates the individual has raised IOP; the lower right indicates characteristic visual field loss; the left top and bottom quadrants indicate optic disc abnormalities characteristic of POAG and are filled from bottom (mild) to top (severe).

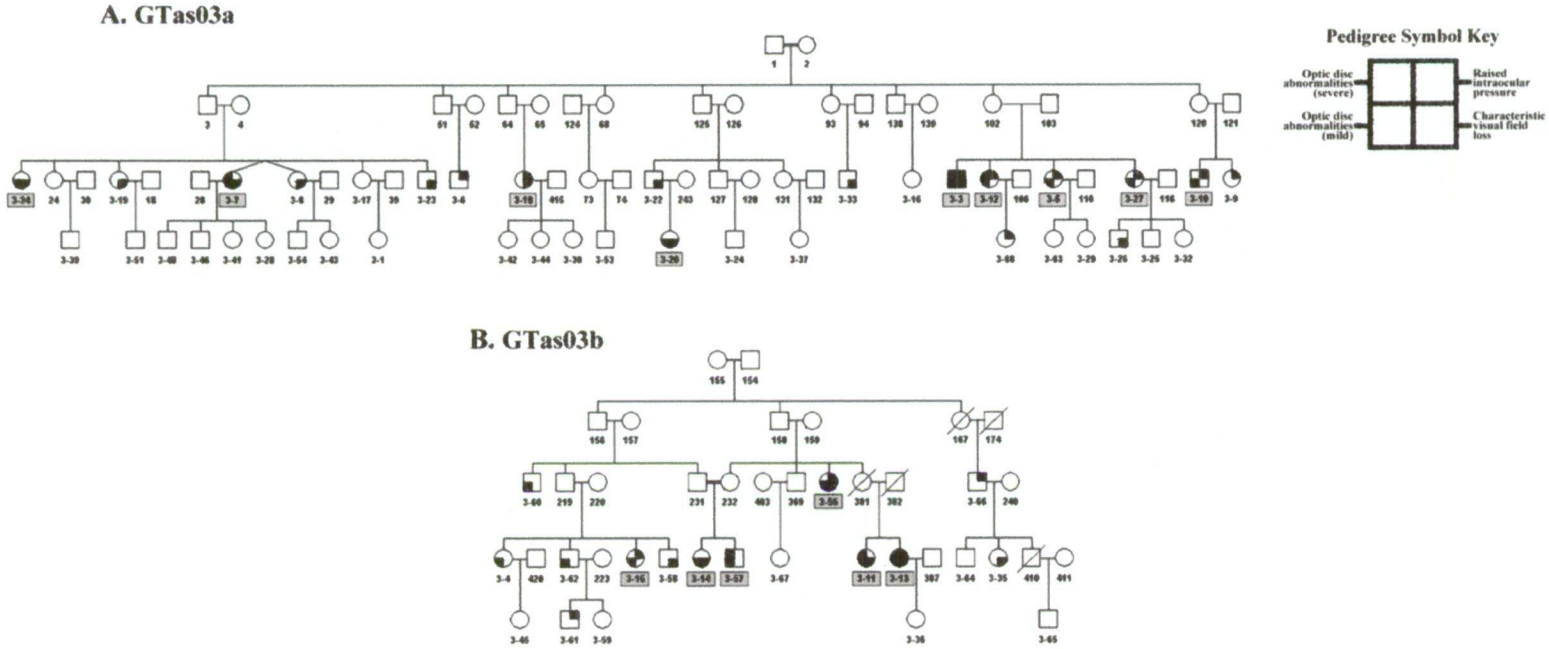

Figure 2.3 Family GTas03 subdivided into GTas03a and GTas03b

The original 123 member pedigree GTas03 (shown in Figure 2.2) was divided into sub-pedigrees GTas3a and GTas3b are shown in Panels A and B respectively. Individuals are labelled with their ID number. Individuals with available clinical and genetic data have hyphenated ID numbers. Clinically diagnosed POAG cases are highlighted. The consanguineous marriage loop can be seen in GTas3b (Panel B), while the dizygotic twins can be seen in GTas3a (Panel A).

Pedigree Symbol Key

The pedigree symbol is broken down into quadrants with each quadrant denoting a component of the clinical phenotype. A filled quadrant in the upper right indicates the individual has raised IOP; the lower right indicates characteristic visual field loss; the left top and bottom quadrants indicate optic disc abnormalities characteristic of POAG and are filled from bottom (mild) to top (severe).

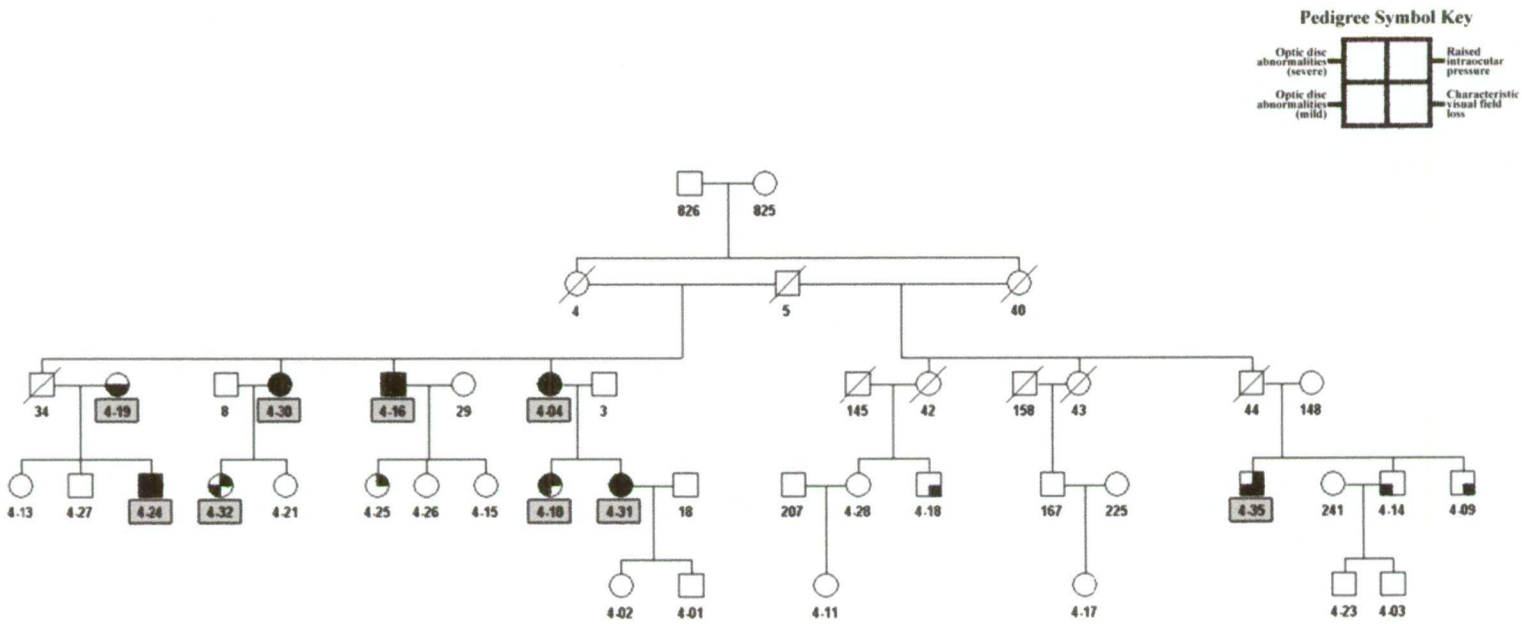

Figure 2.4 Family GTas04

Individuals are labelled with their ID number. Individuals with available clinical and genetic data have hyphenated ID numbers. Clinically diagnosed POAG cases are highlighted. The marriage loop can be seen between individual 5 and sisters 4 and 40.

Pedigree Symbol Key

The pedigree symbol is broken down into quadrants with each quadrant denoting a component of the clinical phenotype. A filled quadrant in the upper right indicates the individual has raised IOP; the lower right indicates characteristic visual field loss; the left top and bottom quadrants indicate optic disc abnormalities characteristic of POAG and are filled from bottom (mild) to top (severe).

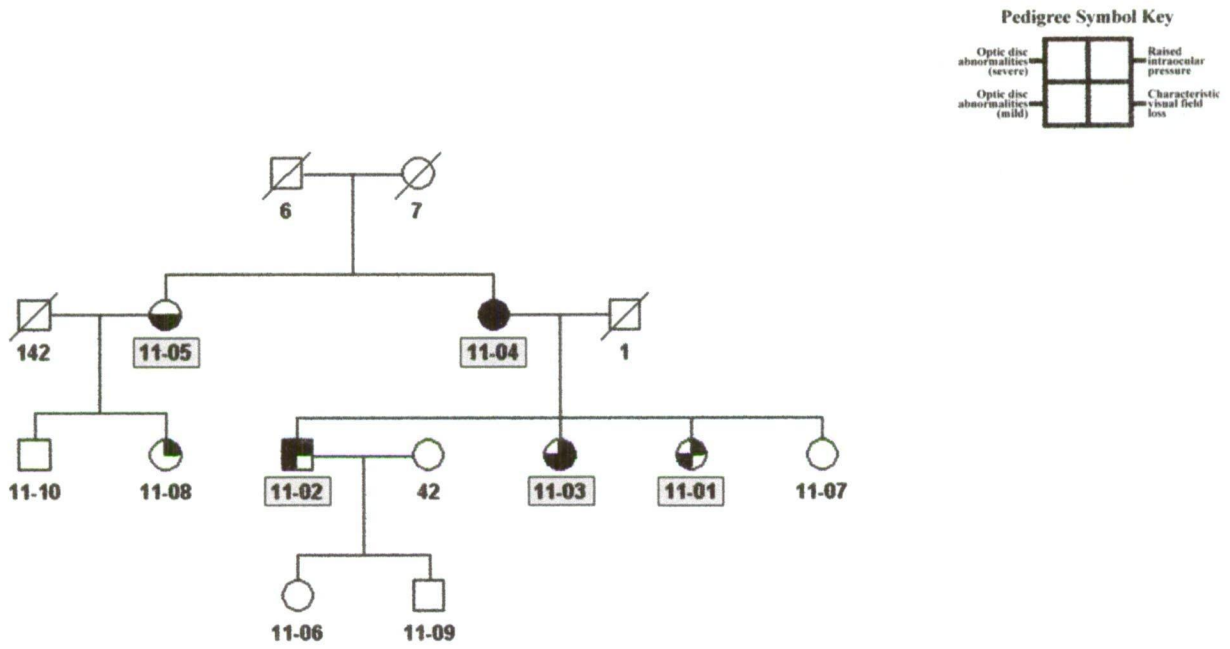

Figure 2.5 Family GTas11

Individuals are labelled with their ID number. Individuals with available clinical and genetic data have hyphenated ID numbers. *Clinically diagnosed POAG cases are highlighted.*

Pedigree Symbol Key

The pedigree symbol is broken down into quadrants with each quadrant denoting a component of the clinical phenotype. A filled quadrant in the upper right indicates the individual has raised IOP; the lower right indicates characteristic visual field loss; the left top and bottom quadrants indicate optic disc abnormalities characteristic of POAG and are filled from bottom (mild) to top (severe).

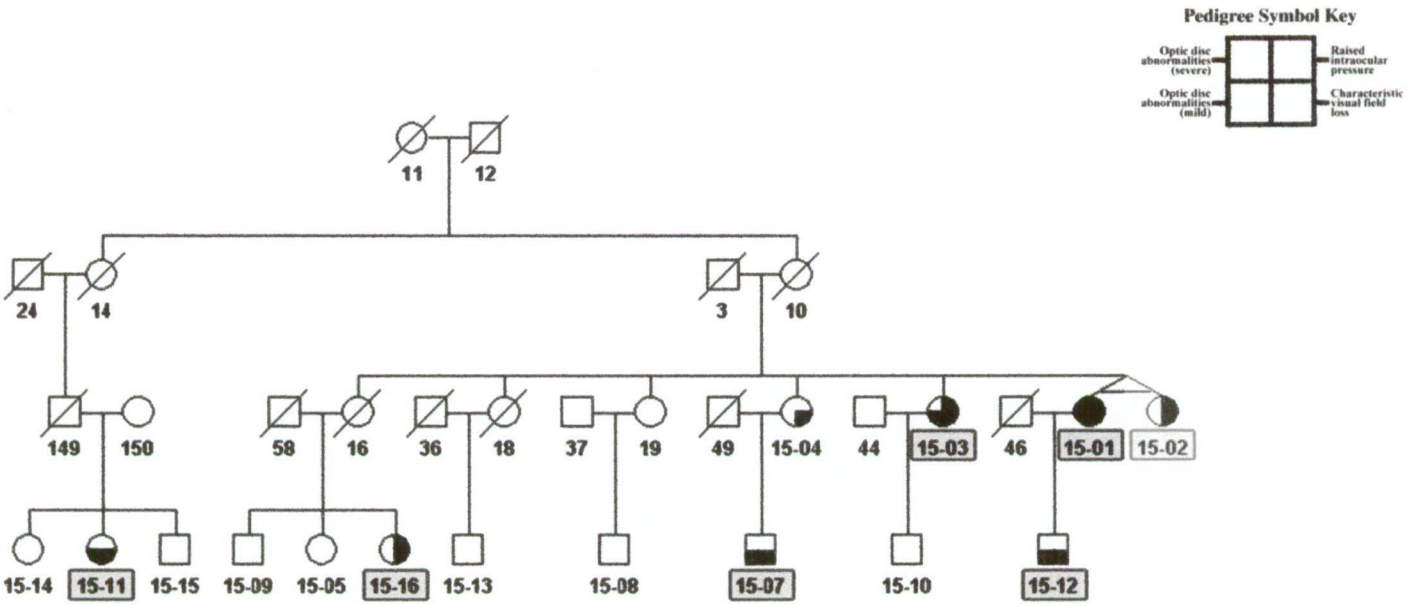

Figure 2.6 Family GTas15

Individuals are labelled with their ID number. Individuals with available clinical and genetic data have hyphenated ID numbers. Clinically diagnosed POAG cases are highlighted. Individual 15-02 was removed from all analyses since she was the monozygotic twin of 15-01.

Pedigree Symbol Key

The pedigree symbol is broken down into quadrants with each quadrant denoting a component of the clinical phenotype. A filled quadrant in the upper right indicates the individual has raised IOP; the lower right indicates characteristic visual field loss; the left top and bottom quadrants indicate optic disc abnormalities characteristic of POAG and are filled from bottom (mild) to top (severe).

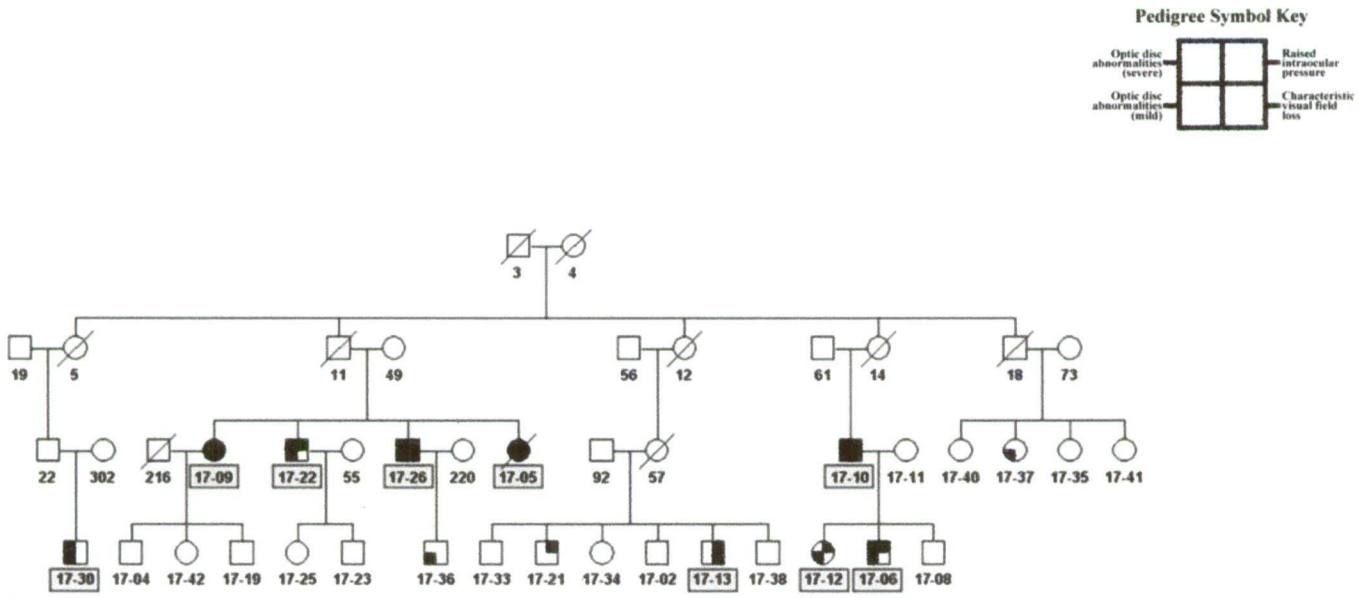

Figure 2.7 Family GTas17

Individuals are labelled with their ID number. Individuals with available clinical and genetic data have hyphenated ID numbers. *Clinically diagnosed POAG cases are highlighted.*

Pedigree Symbol Key

The pedigree symbol is broken down into quadrants with each quadrant denoting a component of the clinical phenotype. A filled quadrant in the upper right indicates the individual has raised IOP; the lower right indicates characteristic visual field loss; the left top and bottom quadrants indicate optic disc abnormalities characteristic of POAG and are filled from bottom (mild) to top (severe).

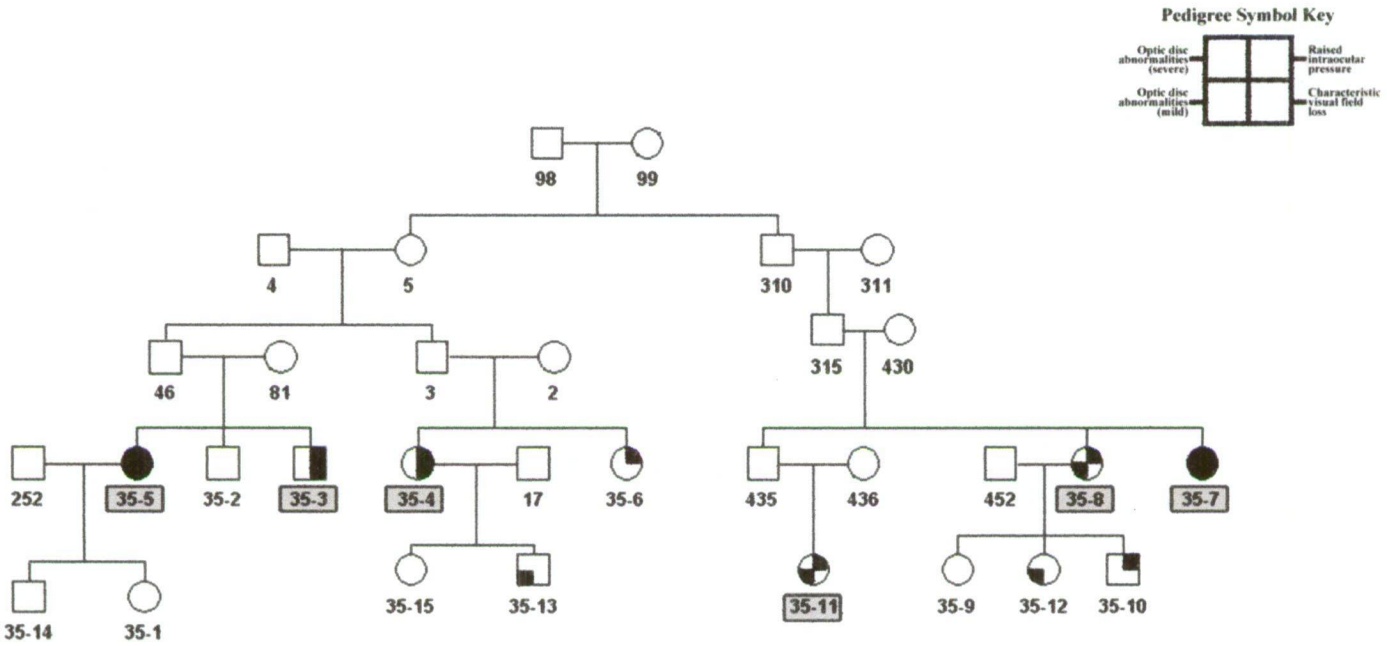

Figure 2.8 Family GTas35

Individuals are labelled with their ID number. Individuals with available clinical and genetic data have hyphenated ID numbers. *Clinically diagnosed POAG cases are highlighted.*

Pedigree Symbol Key

The pedigree symbol is broken down into quadrants with each quadrant denoting a component of the clinical phenotype. A filled quadrant in the upper right indicates the individual has raised IOP; the lower right indicates characteristic visual field loss; the left top and bottom quadrants indicate optic disc abnormalities characteristic of POAG and are filled from bottom (mild) to top (severe).

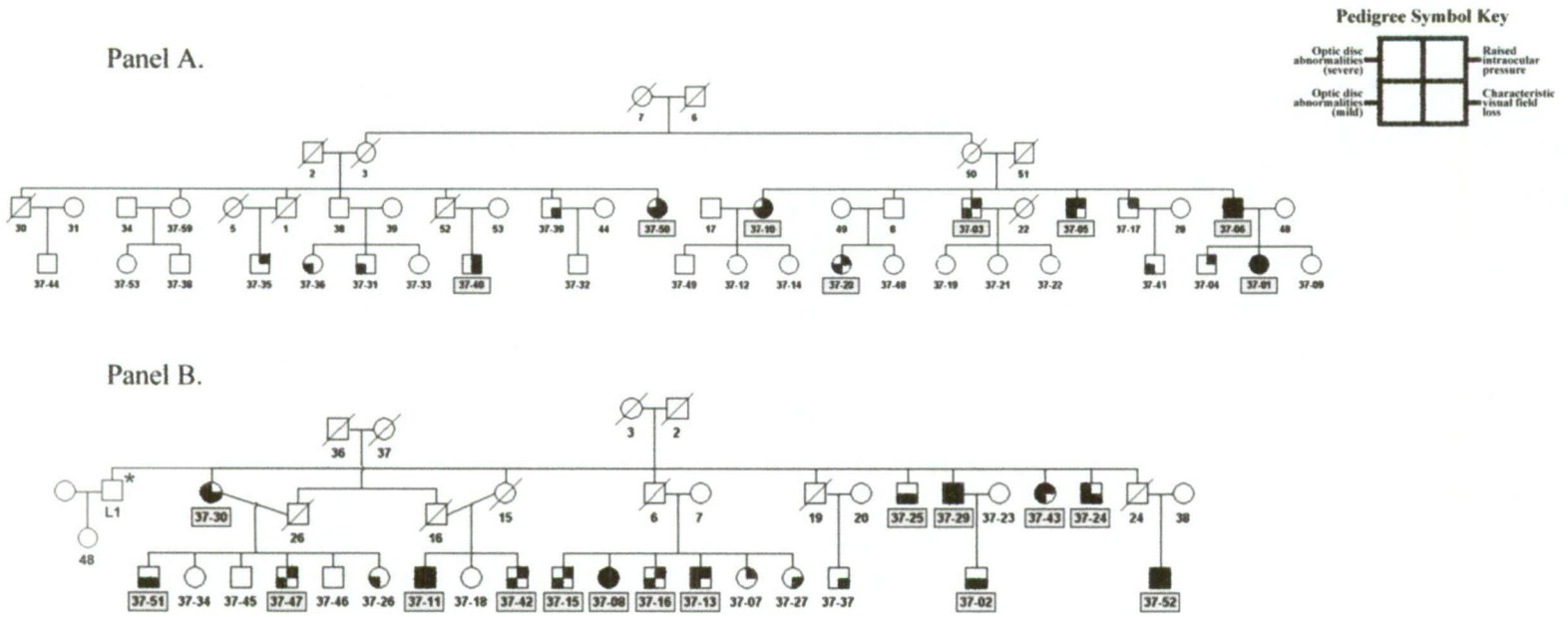

Figure 2.9 Families GTas37a and GTas37b

Individual 48 in family GTas37a (Panel A) is the daughter of individual L1 (shown with asterisk next to pedigree symbol) from family GTas37b (Panel B). Individual L1 was not included in the study. The marraige loop in family GTas37b can be seen between brothers 16 and 26 and sisters 15 and 37-30 (Panel B).

Individuals are labelled with their ID number. Individuals with available clinical and genetic data have hyphenated ID numbers. Clinically diagnosed POAG cases are highlighted.

Pedigree Symbol Key

The pedigree symbol is broken down into quadrants with each quadrant denoting a component of the clinical phenotype. A filled quadrant in the upper right indicates the individual has raised IOP; the lower right indicates characteristic visual field loss; the left top and bottom quadrants indicate optic disc abnormalities characteristic of POAG and are filled from bottom (mild) to top (severe).

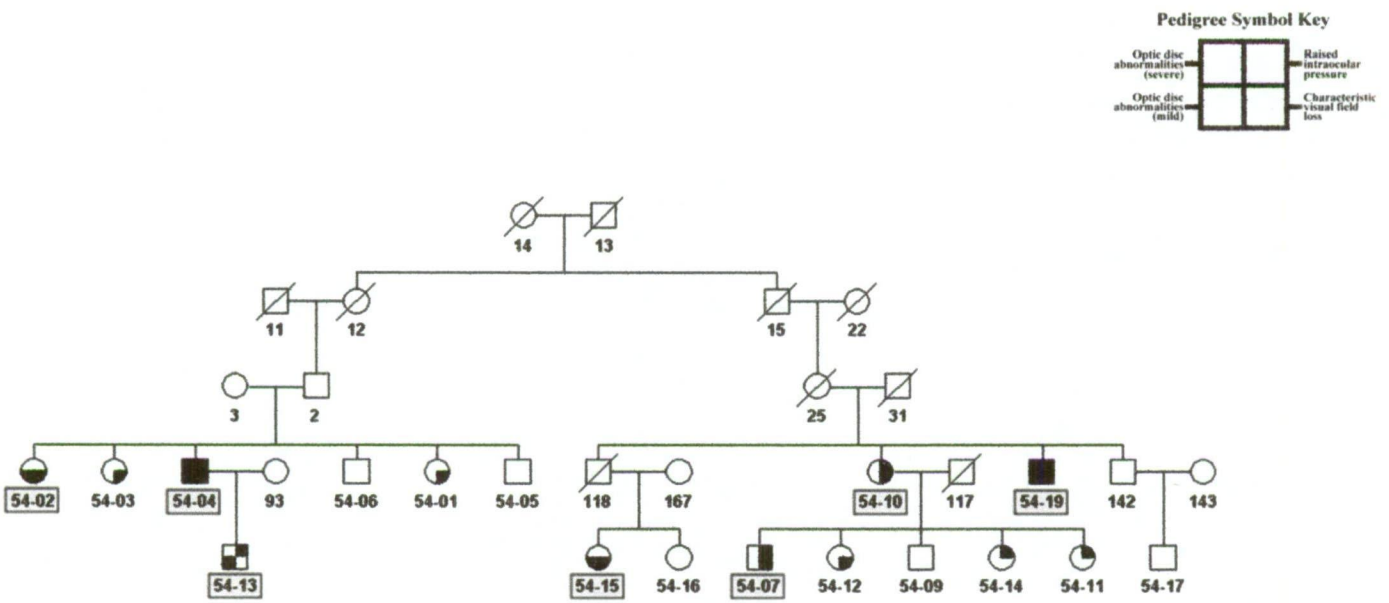

Figure 2.10 Family GTas54

Individuals are labelled with their ID number. Individuals with available clinical and genetic data have hyphenated ID numbers. *Clinically diagnosed POAG cases are highlighted.*

Pedigree Symbol Key

The pedigree symbol is broken down into quadrants with each quadrant denoting a component of the clinical phenotype. A filled quadrant in the upper right indicates the individual has raised IOP; the lower right indicates characteristic visual field loss; the left top and bottom quadrants indicate optic disc abnormalities characteristic of POAG and are filled from bottom (mild) to top (severe).

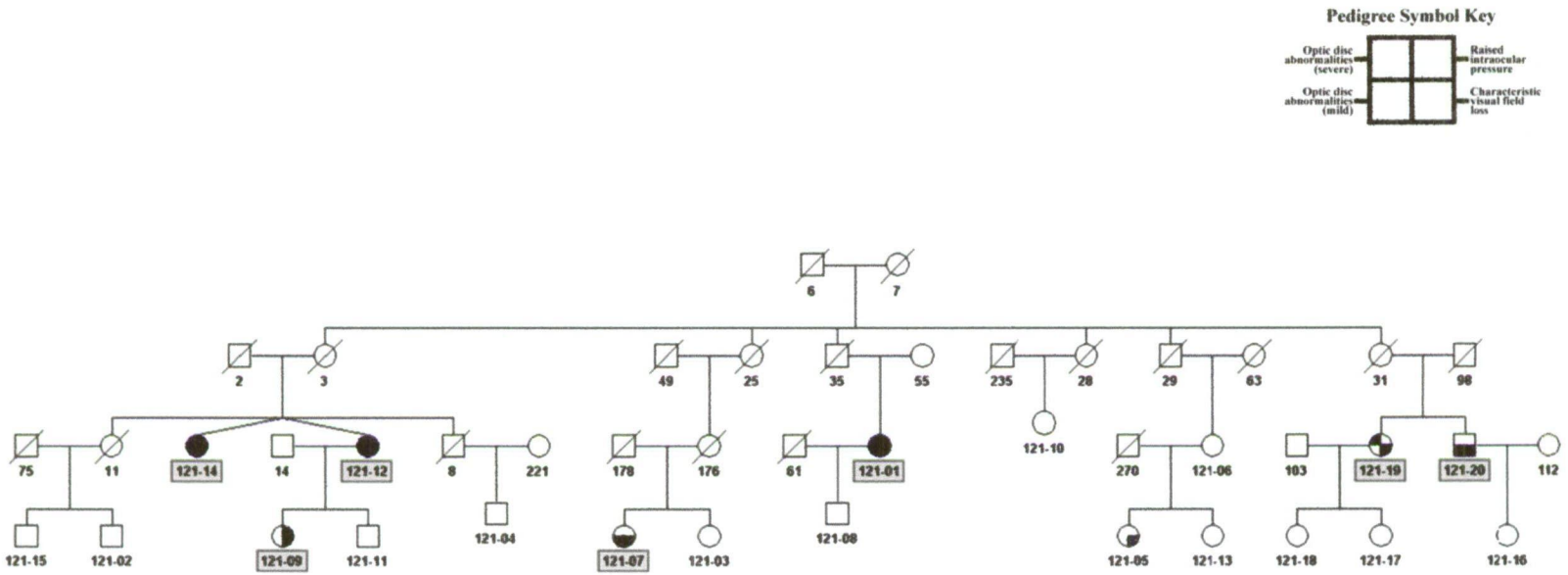

Figure 2.11 Family GTas121

Individuals are labelled with their ID number. Individuals with available clinical and genetic data have hyphenated ID numbers. Clinically diagnosed POAG cases are highlighted. Dizygotic twins 121-12 and 121-14 are shown.

Pedigree Symbol Key

The pedigree symbol is broken down into quadrants with each quadrant denoting a component of the clinical phenotype. A filled quadrant in the upper right indicates the individual has raised IOP; the lower right indicates characteristic visual field loss; the left top and bottom quadrants indicate optic disc abnormalities characteristic of POAG and are filled from bottom (mild) to top (severe).

2.3.3 Multiple sources of inheritance and subdivided pedigrees

Family GTas03, the largest of the selected GIST pedigrees, has two apparent branches (Figure 2.2); however the origin of POAG within each branch may either have come from a single source (individuals 150 to 155) or from two different founders (for example individual 149 or 153). As a result of both size and the possibility of digenic inheritance, GTas03 was split into two sub-pedigrees at individual 2 (as shown in Figure 2.3). One sub-pedigree, named GTas3a (Figure 2.3, Panel A), was founded by individuals 1 and 2 while the second, GTas3b (Figure 2.3, Panel B), was founded by individuals 154 and 155. This was not considered a permanent division of GTas03, but an option for analyses depending on the method used.

Pedigrees GTas37a and GTas37b (Figure 2.9, Panel A and B respectively) are separate branches of an originally larger pedigree. The two branches of the pedigree were linked by marriage. Individual 48, the spouse of 37-06 in family GTas37a (Figure 2.9, Panel A) is the daughter of individual L1 in family GTas37b (Figure 2.9, Panel B). Individual L1 was not available for this study, but is another child of the founding couple of family GTas37b, individuals 3 and 4. The presence of POAG within each branch clearly originated from different sources, thus the larger pedigree was permanently divided, allowing the branches to be analysed separately.

2.3.4 Consanguinity and marriage loops

Several of the GIST pedigrees contained loops, both consanguineous and marriage loops. The existence of loops can result in computational problems with likelihood calculations, and analysis approaches based on the Elston-Stewart algorithm (Elston and Stewart 1971), such as LINKAGE, require these loops be broken prior to analysis. The MAKEPED component of the LINKAGE software package (Lathrop and Lalouel 1984;

Lathrop *et al.* 1984; Lathrop *et al.* 1986) was used to break each loop at a specified individual, and reconstruct the pedigrees prior to analysis, as described in Chapter 4.4.1.

Family GTas03 contains two consanguineous loops (Figure 2.2); the first links the two branches of the pedigree with a marriage between individual 1 and his second-cousin once removed (individual 2); the second is a first cousin marriage (individuals 231 and 232). This second loop is also present in GTas03b (Figure 2.3, Panel B). When required by the analysis approach, these loops were broken at individual 2 and 232 respectively.

Family GTas04 (Figure 2.4) contains a marriage loop at individuals 4, 5 and 40 (Figure 2.4), with individual 5 marrying two sisters, individuals 4 and 40. For some analysis approaches this loop was broken at individual 4.

Family GTas37b (Figure 2.9, Panel B) includes a marriage loop, with sisters 15 and 37-30 marrying brothers 16 and 26 respectively. For some analysis approaches this loop was broken at individual 16.

2.3.5 Monozygotic and dizygotic twins

Several of the GIST pedigrees included either monozygotic or dizygotic twins. The nature of the twin relationship was confirmed by comparing genotypes across the entire set of microsatellite markers used in this study (see Chapter 4.3.1 for marker information).

Family GTas03 (or pedigree GTas3b when subdivided) includes a set of dizygotic twins (individuals 3-7 and 3-8; see Figure 2.2), of whom only individual 3-7 was clinically

classified as affected (individual 3-8 is a glaucoma suspect, presenting with some characteristic loss of visual field which may indicate the presence of as yet unclassifiable optic disc damage). Both individuals were included in all analyses.

Family GTas15 includes a set of monozygotic twins (individuals 15-01 and 15-02; see Figure 2.6). Both individuals have clinically diagnosed POAG, although at last examination individual 15-02 was less severely affected in terms of optic nerve degeneration compared with individual 15-01. While this phenotype difference would not have influenced the results, as analyses were based on 'affected' or 'unknown' glaucoma status, individual 15-02 was removed from all analyses to prevent error due to the apparent doubling of genetically identical individuals within the pedigree.

Family GTas121 also includes a set of dizygotic twins (individuals 121-12 and 121-14; see Figure 2.11), both of whom have been diagnosed with severe POAG, including raised IOP, characteristic visual field loss and severe optic nerve degeneration as manifested by vertical cup-to-disc ratios of greater than 0.8. Both individuals were included in all analyses.

Chapter 3 - Molecular Methodology

3.1 Genetic material

Whole blood was collected in 10ml EDTA tubes from consenting individuals during the initial stages of the GIST and at several follow-up stages, hence storage time for the blood samples varied from 6 months to more than 5 years old. The bulk of the DNA extraction was conducted as part of the GIST, however extraction of additional samples using the methods described below was required and conducted as part of this dissertation.

3.1.1 DNA extraction from whole blood - resin method

DNA was extracted using the Nucleon BACC3 kit (Amersham Pharmacia Biotech). Four times the volume of the sample of Reagent A was added and mixed for 4 minutes at room temperature. The samples were centrifuged at 1300g for 5 minutes and the supernatant discarded. The pellet was resuspended in 2ml of Reagent B and transferred to a clean tube before adding 15µl of 50 µg/ml RNase and incubating at 37°C for 30 minutes. Protein was precipitated by the addition of 500µl of sodium perchlorate solution and the samples mixed by inversion. Two ml of chloroform was added and mixed by inversion before the addition of 300µl of Nucleon resin without remixing the phases. The samples were centrifuged at 1300g for 3 minutes. The upper phase was transferred to a clean tube and 2 volumes of cold absolute ethanol added. The sample was mixed by inversion until the precipitate appeared, followed by centrifuging at 4000g for 5 minutes. The supernatant was discarded. The pellet was washed with cold 70% ethanol and centrifuged again at 4000g for 5 minutes. The pellets were air dried and resuspended in 100µl of TE buffer. DNA was stored in screw-capped tubes at 4°C. Typical yields were 180 to 350µg of DNA per 10ml of blood.

3.1.2 DNA extraction from whole blood - salting out method

This method was used for blood samples that has been stored for 5 years or more, or samples producing low yields with the resin method (3.1.1). Any frozen blood samples were thawed on ice. 10ml of whole blood was transferred to a 50ml tube and 35ml lysis buffer [10mM Tris-HCl (pH 7.5); 400mM NaCl; 2mM EDTA (pH 8.0)] added. The sample was inverted several times, cooled on ice for 15 minutes then centrifuged at 1300g for 10 minutes. The supernatant was then discarded and another 30ml of lysis buffer added. The red-white nuclei pellet was disrupted by inversion of the sample and kept on ice for 15 minutes. The sample was then centrifuged at 1300g for 10 minutes and the supernatant discarded. The nuclei pellet was placed on ice and 3ml of lysis buffer added. The sample was shaken but not fully resuspended, removed from the ice and 400µl of 10% SDS and 65µl of 20mg/ml proteinase K (Sigma-Aldrich) added. The pellet was digested at 50°C for a minimum 4 hours and 1.5ml of saturated NaCl [6M; Millipore filtered] added, followed by vigorous shaking for 15 seconds. The sample was then centrifuged at 1300g for 15 minutes. The supernatant was transferred to a fresh 50ml tube avoiding transfer of any salt contamination and 10ml of cold 100% ethanol added to the sample. The sample was swirled gently and precipitated DNA transferred by pipette to an Eppendorf tube containing 1ml of cold 70% ethanol. The sample was spun in a microcentrifuge at 15,000g for 5 minutes. The supernatant was gently discarded and 1ml of cold 70% ethanol added to the pellet. The sample was again centrifuged at 15,000g for 5 minutes, the ethanol removed and the pellet allowed to air dry. The DNA pellet was resuspended slowly overnight in 125µl TE buffer [10mM Tris-HCl; 1mM Na_2EDTA (pH 8.0)]. DNA was stored in screw-capped tubes at 4°C. Typical yields were 50 to 150µg of DNA per 10ml of blood.

3.1.3 DNA extraction from buccal mucosa swabs

DNA was extracted from the buccal mucosa swabs using the PureGene DNA isolation kit (Gentra Systems). All reagents were supplied in the kit unless otherwise indicated. The buccal mucosa of participants was scraped with a cytology brush, which was then immersed in 300µl of cell lysis solution in a screw-cap tube. Brushes were transported in this state then stored at 4°C until required for extraction. Samples were incubated overnight at 55°C with 1.5µl of 20 mg/ml Proteinase K (Sigma-Aldrich). After cooling to room temperature, 1.5µl of 5 mg/ml RNaseA was added, the tube inverted several times to mix, and the sample incubated at 37°C for 15 minutes. The sample was again allowed to cool to room temperature before the addition of 100µl of Protein Precipitation Solution (Gentra Systems), mixing by inversion and incubation on ice for 5 minutes. The sample was centrifuged at 15,000g for 3 minutes and the supernatant added to a clean tube containing 200µl of isopropanol (Sigma-Aldrich) and 0.5µl of 20mg/ml glycogen (Sigma-Aldrich). The tube was again mixed by inversion and incubated at room temperature for 5 minutes before centrifuging at 15,000g for 5 minutes. The supernatant layer was then discarded and 300µl of 70% molecular grade ethanol (Sigma-Aldrich) added to the pellet. The sample was again centrifuged at 15,000g for 1 minute, the supernatant discarded and the pellet allowed to air dry. Once completely dry, the pellets were resuspended in 20µl of TE buffer with heating to 65°C for 1 hour. All DNA samples were stored in screw-capped tubes at 4°C. Typical yields were 10 to 20µg of DNA per swab. Family GTas121 (Figure 2.11) was the only GIST pedigree included in this study containing individuals whose genetic material was *only* available from buccal mucosa swabs (individuals 121-18 and 121-19). Buccal samples were occasionally provided to augment diminished stocks of DNA for other individuals in the study, although these swabs were generally extracted and stored to protect against complete exhaustion of the samples.

3.1.4 DNA quantitation and quality control

For all collections, we determined the total DNA yield by measuring the A260 absorbance and diluted aliquots for use to approximately 50μg/ml. The quality of genomic DNA was also ascertained by electrophoresing 1μl of 50μg/ml DNA on 0.8% (w/v) agarose (Gibco BRL) gels in 1xTBE buffer [0.5M Tris base, 0.5M Boric acid 10mM EDTA (pH 8.0)] with 0.3ng/ml ethidium bromide. Samples were electrophoresed at 80 volts for 45 minutes and photographed under 100% UV light (Figure 3.1). High molecular weight smears are visible in lanes 2 to 9 (containing 1ul of 50μg/ml DNA), and the bulk of product is generally larger than 500bp (Figure 3.1).

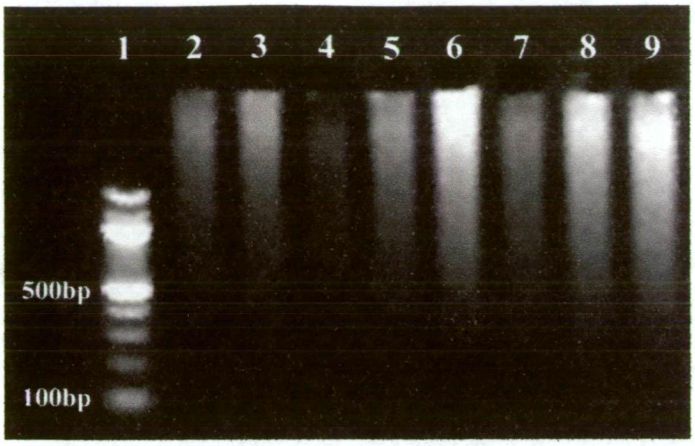

Figure 3.1 - Visualisation of genomic DNA by agarose gel electrophoresis

Electrophoresis of genomic DNA samples on a 0.8% agarose gel stained with ethidium bromide and photographed under 100% UV light. Lane 1 contains a 100bp ladder (Promega). Lanes 2-9 contain 1µl of 50µg/ml genomic DNA samples from individuals 35-08 to 35-15.

3.2 General PCR conditions

All PCR reactions were conducted using Corbett Research 960C cooled thermal cyclers, unless otherwise noted. 10x PCR buffer was prepared, containing 100mM Tris HCl, 500mM KCl, and variable concentrations of $MgCl_2$ (see below). PCR reactions were carried out in a total volume of either 10 or 30µl and contained between 1.0 and 3.5mM final Mg^{2+} concentration, 0.2mM dNTP (Promega), 0.8µM of each primer and 0.005 U/µl *Taq* DNA polymerase (Qiagen). Reactions underwent 30 cycles of denaturing at 94°C for 30 seconds, primer pair specific annealing temperature for 30 seconds and extension at 72°C for 30 seconds followed by a final extension at 72°C for 15 minutes. Annealing temperatures and optimal Mg^{2+} concentrations were determined empirically for each primer pair by cycling over a range of temperatures and Mg^{2+} concentrations in a PC-690G gradient thermal cycler (Corbett Research) and assessment of the optimal conditions made by visualisation on 1.5% agarose gels containing 0.3ng/ml ethidium bromide. Actual primer conditions and temperatures are listed in Appendix 2. Results of a typical microsatellite optimisation experiment are shown in Figure 3.2; whereby optimum conditions for marker D10S1713 were determined to be a magnesium concentration of 1.5mM with an annealing temperature between 53 and 58°C, with 55°C used for amplification of DNA from study subjects for analyses in Chapter 4.

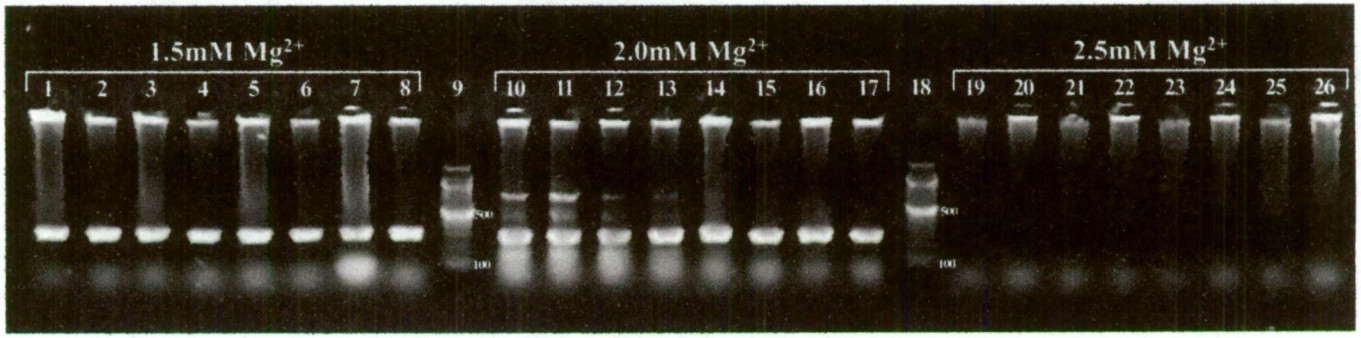

Figure 3.2 - Gradient Optimisation of the Primer Pair for marker D10S1713

Electrophoresis of optimisation PCR samples for marker D10S1713 on a 1.5% agarose gel stained with ethidium bromide and photographed under 100% UV light. Lanes 1 to 8 contain optimisation samples with a magnesium concentration of 1.5mM and graduate in temperature from 53°C (lane 1) to 60°C (lane 8) in 1 degree increments. Lanes 10 to 17 contain optimisation samples with a magnesium concentration of 2.0mM and graduate in temperature from 53°C (lane 10) to 60°C (lane 17) in 1 degree increments. Lanes 19 to 26 contain optimisation samples with a magnesium concentration of 2.5mM and graduate in temperature from 53°C (lane 19) to 60°C (lane 26) in 1 degree increments. Lanes 9 and 18 contain 100bp ladder (Promega) sizing reference. The sizes of the expected alleles for microsatellite repeat D10S1713 are between 245 and 255bp.

3.3 Whole genome amplification by Primer Extension Preamplification

Primer Extension Preamplification (PEP), a PCR-based technique of whole genome amplification originally developed by Zhang *et al.* (1992), was modified and used to provide sufficient DNA for multiple PCR-based analyses from buccal mucosa swabs or diminished blood samples. Each reaction contained 50ng genomic DNA, 2.0mM Mg2+, 0.2mM dNTP (Promega), 20pmol/μl polyN 15mer primer (Operon technologies) and 5U Taq DNA polymerase (Qiagen). Reactions underwent 50 cycles of 94°C for 1 minute, 37°C for 2 minutes and 55°C for 4 minutes followed by a final extension of 72°C for 10 minutes. Products were electrophoresed on 1% agarose gels containing 0.3ng/ml ethidium bromide to confirm the presence of high molecular weight product (Figure 3.3). High molecular weight smears are visible in lanes 2 to 15 of Figure 3.3, showing that most of the PEP product is greater than 500bp, although a large proportion of the product is smaller that the genomic DNA samples shown in Figure 3.1. PEP DNA samples were diluted 1:8 with distilled water for use in PCR.

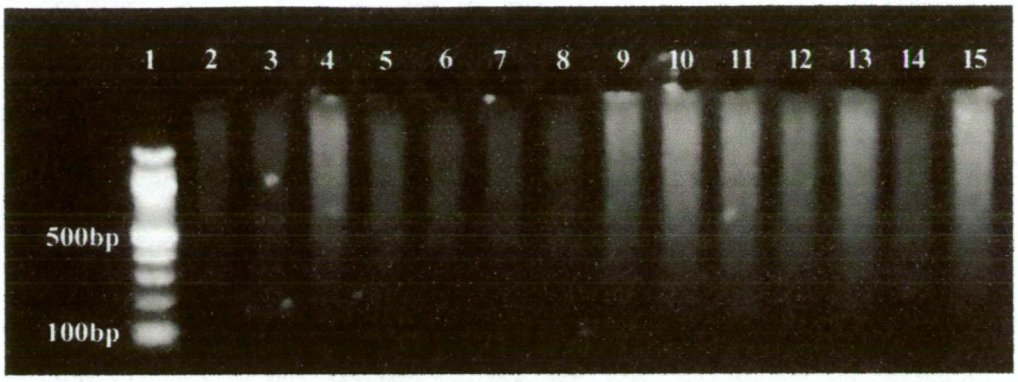

Figure 3.3 - Agarose gel electrophoresis visualisation of DNA amplified by Primer Extension Preamplification (PEP)

Electrophoresis of PEP product on a 1% agarose gel stained with ethidium bromide and photographed under 100% UV light. Lane 1 contains the 100bp ladder (Promega) size reference. Lanes 2 to 15 contain 5µl of LNH control samples amplified by the Primer Extension Preamplification protocol.

3.4 Fluorescent genotyping of microsatellites

The forward PCR primer for each marker was labeled at the 5' end with either 6-FAM or HEX (Sigma-Aldrich). PCR reactions were carried out in 10μl reaction volumes as described in 3.3, with the following exception. Fragments labeled with 6-FAM underwent 25 amplification cycles, while those with HEX underwent 35 cycles. The optimum primer annealing temperature and magnesium concentration for each marker was determined according to section 3.2. One microlitre of each PCR reaction was pooled into an 8μl final volume, with between 5 and 8 markers per pool, with a minimum of 20bp between the maximum and minimum expected allele sizes of markers labeled with the same dye. Primer sequence, pool and fluorescent label information is provided in Appendix 2. Pooled samples were electrophoresed using an ABI PRISM 310 Genetic Analyzer (Applied Biosystems) with POP4 polymer (Applied Biosystems). Data were analysed with Genescan® (version 3.7) and Genotyper® (version 3.7) software (Applied Biosystems). Example electropherograms from pedigree GTas03 are shown in Figure 3.4.

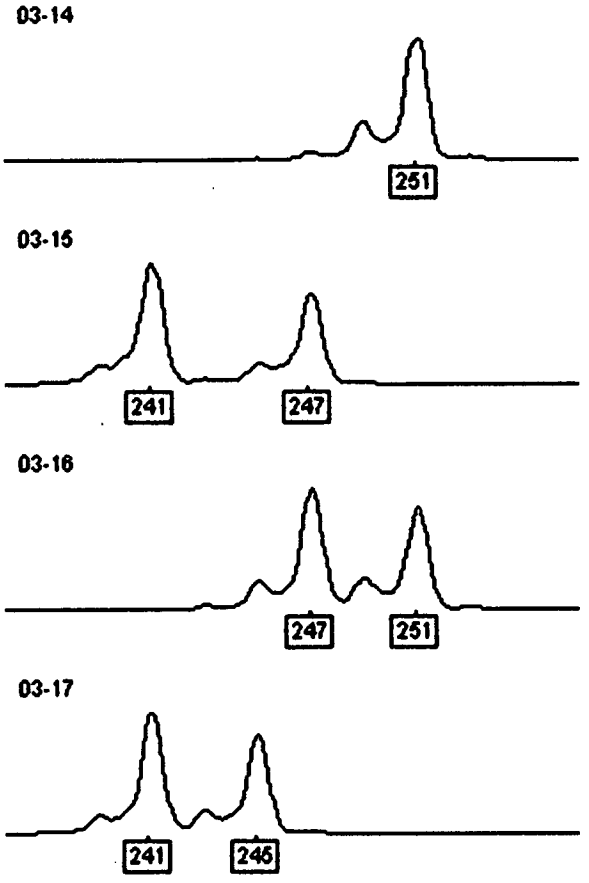

Figure 3.4 - Genotyping Data for 6-FAM labeled marker D10S1713

The four panels represent electropherograms generated by genotyping D10S1713 and electrophoresed using an ABI PRISM 310 Genetic Analyzer (Applied Biosystems). Individual ID numbers are shown in the top right of each trace. The electropherogram peaks have been labeled with their representative size in base pairs. Individual 03-14 is homozygous for the 251bp allele.

3.5 DNA sequencing

Amplified fragments for sequencing were PCR amplified in 30µl volumes, purified with Ultra Clean PCR clean up kit spin columns (MoBio) and cycle sequenced with Big Dye Terminator Ready Reaction Mix (Applied Biosystems) over 25 cycles. Products were precipitated with 2µl of 3M sodium acetate (pH 4.2) and 50µl of 100% molecular grade ethanol (Sigma-Aldrich). Following a 15 minute incubation at room temperature, samples were centrifuged at 13,000rpm for 20 minutes. The supernatant was discarded and the pellet washed with 200µl of 70% molecular grade ethanol. Samples were then centrifuged at 13,000rpm for 5 minutes and the supernatant discarded. The pellet was dried by a one minute incubation at 95°C with the lid open and was resuspended in 15µl of Template Suppression Reagent (Applied Biosystems). Samples were electrophoresed on an ABI PRISM 310 Genetic Analyzer (Applied Biosystems) with POP6 polymer (Applied Biosystems). Data were analysed using Sequence Analysis® (Applied Biosystems) and Sequencher® (GeneCodes) software.

Chapter 4 – Investigating the Known POAG loci GLC1A-F in 10 Extended Pedigrees from the Glaucoma Inheritance Study in Tasmania

4.1 Background

Only the first six named POAG loci (GLC1A-F) and the studies involved in their detection and replication are considered in this dissertation. The loci GLC1G (Monemi *et al.* 2005) and GLC1I (Allingham *et al.* 2005) as well as the genes *OPTN* (Rezaie *et al.* 2002) at GLC1E and *WDR36* (Monemi *et al.* 2005) at GLC1G were identified after completion of the initial linkage analysis phase of this investigation.

Since the analysis phase of this investigation was initiated prior to the identification of *OPTN* as the gene at GLC1E (Rezaie *et al.* 2002), markers were selected within the GLC1E locus for linkage analysis, rather than mutation screening of the *OPTN* gene. Following the identification of *OPTN* we decided to continue with the linkage analysis and consider mutation screening of the *OPTN* gene in pedigrees showing linkage to the GLC1E region on chromosome 10p15-p14. *OPTN* consists of three non-coding and 13 translated exons, hence initial linkage analysis of the region may also be a more economic (although less powerful) screening method.

As mentioned in Chapter 1.3.1, the lack of consistency in the clinical definition of POAG in published studies may have contributed to the lack of success in gene identification and replication studies. There is no universally accepted definition of this phenotypically complex and subtle disease (Kahn and Milton 1980; Wolfs *et al.* 2000; Kroese and Burton 2003), and there is still much debate as to an appropriate definition of POAG diagnosis to be used by published studies (Bathija *et al.* 1998; Foster *et al.* 2002; Kroese and Burton 2003).

In the original identification of GLC1B (Stoilova *et al.* 1996), GLC1C (Wirtz *et al.* 1997), and GLC1D (Trifan *et al.* 1998), POAG affection status was based on the presence of at least two of the triad of key clinical features: raised IOP, characteristic visual field loss and characteristic optic disc abnormalities. In the case of GLC1E (Sarfarazi *et al.* 1998), and GLC1F (Wirtz *et al.* 1999), IOP was not a major consideration in the classification of affection status, contributing only as an auxiliary measure to visual field defects and vertical cup-to-disc ratio.

The 10 extended pedigrees selected from the GIST for use in this study compare favourably with pedigrees used in previous studies to localise the named POAG loci. Only the original GLC1B study (Stoilova *et al.* 1996) used a dataset containing multiple POAG pedigrees. The remaining studies were based on single, large POAG pedigrees.

In the identification of GLC1C Wirtz *et al.* (1997) used a single 76 member pedigree from North America containing 44 available individuals, including nine affected individuals. This linkage was confirmed in a Greek family of 34 individuals, including 10 affected individuals (Kitsos *et al.* 2001). Similarly, Trifan *et al.* (1998) used a single 23 member North American family spanning four generations, 20 of whom were available and eight affected with POAG in the identification of GLC1D. The fifth POAG locus (GLC1E) was identified in a family of 60 individuals over four generations, 46 of whom were available to participate in the study including 15 classified as affected (Sarfarazi *et al.* 1998). GLC1F was identified in a 36 person family including 25 individuals who were available to participate in the study, 10 of whom were affected with POAG (Wirtz *et al.* 1999). Stoilova *et al.* (1996) used 17 Caucasian families, including 203 subjects and 90 affecteds, in their initial identification

of GLC1B. The pedigrees consisted of at least two to three affected offspring and one available parent. While several of the pedigrees in the current study (described in Chapter 2) are smaller than those in the aforementioned datasets, pedigrees such as GTas03 and GTas37b are equivalent in size to previous studies of POAG genetics, and the collection as a whole is more substantial.

The POAG loci GLC1A-F were originally identified using two-point and/or multipoint parametric linkage analysis (Sheffield *et al.* 1993; Stoilova *et al.* 1996; Wirtz *et al.* 1997; Sarfarazi *et al.* 1998; Trifan *et al.* 1998; Wirtz *et al.* 1999). While not all studies provided full details of the parametric model used (for example Stoilova *et al.* 1996), the majority of studies assumed autosomal dominant inheritance, with a disease gene frequency of 0.0001. In most cases complete penetrance was assumed, although Wirtz *et al.* (1997) used an age-dependent penetrance for GLC1C, and the same group used a fixed penetrance of 0.75 for the detection of GLC1F (Wirtz *et al.* 1999). The data available suggests most studies did not include phenocopies in the model, although a phenocopy rate of 2% was employed in the study where GLC1F was identified (Wirtz *et al.* 1999). The GLC1C replication study of Kitsos *et al.* (2001) used an initial penetrance of 0.75, and then examined the effect on the peak LOD of varying the penetrance between 0.6 and 0.8. Most of these studies appeared to use equal allele frequencies rather than population generated frequencies. The two-point parametric linkage results from the original identification of the known POAG loci are shown in Table 4.1. The decreased LOD scores obtained by affected only analysis are also shown.

Locus	Maximum LOD	Marker	Max. LOD affected only	Reference
GLC1A	6.50	D1S212	Not assessed	Sheffield *et al.* 1993
GLC1B	6.48	D2S113	3.40*	Stoilova *et al.* 1996
GLC1C	3.02	D3S1535	2.12	Wirtz *et al.* 1997
GLC1D	3.61	D8S1471	Not shown	Sarfarazi *et al.* 1998
GLC1E	10.0	D10S1216	3.43	Trifan *et al.* 1998
GLC1F	4.01	D7S2439	2.96	Wirtz *et al.* 1999

Table 4.1 - Two-point parametric linkage results from the original identification of the POAG loci GLC1A-F

* Affected only peak LOD was distal to the original peak, at marker D2S373.

4.2 Aims

The aims of this study were: to genotype the 10 extended POAG pedigrees from the GIST (described in Chapter 2) with microsatellite markers at the previously identified loci GLC1A-F, at an average marker spacing of 3 to 4 cM; extract comprehensive allele frequency information from a similar control population source; check the dataset for genotyping errors; and use Markov chain Monte Carlo (MCMC) estimation based parametric and nonparametric linkage analyses as a first pass approach to identify any pedigrees showing suggestive linkage to any of the known POAG loci. Families showing suggestive results in these initial analyses were to be retained for additional genotyping and follow-up analysis (described in Chapter 5).

A secondary aim was to utilise exact parametric and nonparametric linkage analyses, based on previously published investigations into the genetic contribution to POAG, with the remaining dataset. The dataset for this secondary aim was to be derived from pedigrees exhibiting regions of interest from the initial MCMC based analyses, excluding those selected for the additional genotyping and follow-up analyses described in Chapter 5.

4.3 General Methods

4.3.1 Microsatellite marker selection

Microsatellite markers were selected to cover the six known regions of linkage to POAG, GLC1A-F (Sheffield *et al.* 1993; Stoilova *et al.* 1996; Wirtz *et al.* 1997; Sarfarazi *et al.* 1998; Trifan *et al.* 1998; Wirtz *et al.* 1999). As this project was initiated prior to the online release of the Human Genome Project sequence maps (Lander *et al.* 2001), gene and marker maps from the 1996 Genetic Location Database (Collins *et al.* 1996) were used for marker selection. Heterogeneity information from the Genome

Database (http://www.gdb.org/), availability of typed genotyping controls from the Centre d'Etude du Polymorphisme Humain (http://www.cephb.fr/cephdb), marker location and spacing were used to weight marker choice.

The final set of markers used to investigate linkage to the known POAG loci GLC1A-F are shown in Table 4.2. The table shows the POAG locus and chromosomal region, as well as marker location and heterozygosity. A total of 25 markers were selected, at an approximate density of one marker per 4 cM for each region.

Locus	Region	Marker	Distance (cM)*	Heterozygosity†
GLC1A	1q21-q31	D1S2635	176.5	0.87
		D1S2707	181.3	0.82
		D1S2675	182.0	0.73
GLC1B	2cen-q13	D2S2161	97.3	0.77
		D2S113	99.0	0.77
		D2S2264	102.6	0.77
		D2S1897	105.8	0.89
		D2S1892	107.8	0.80
GLC1C	3q21-q24	D3S3637	146.4	0.90
		D3S1301	151.7	0.77
		D3S3694	153.5	0.84
		D3S1569	158.1	0.80
		D3S1608	160.3	0.61
GLC1D	8q23	D8S1749	113.0	0.74
		D8S556	120.4	0.80
		D8S198	133.1	0.83
GLC1E	10p15-p14	D10S1729	3.6	0.72
		D10S1713	6.7	0.60
		D10S1691	9.3	0.67
		D10S547	12.6	0.74
		D10S1664	16.1	0.75
GLC1F	7q35-q36	D7S2511	158.1	0.79
		D7S505	160.3	0.69
		D7S2439	163.0	0.80
		D7S2546	166.9	0.75

Table 4.2 - The 25 microsatellite markers used to investigate linkage to the known POAG loci GLC1A-F

*Marker location in centiMorgans, based on the 1996 Genetic Location Database (Collins *et al.* 1996).

†Heterozygosity based on CEPH data (http://www.cephb.fr/cephdb).

4.3.2 Genotyping methods

The PCR conditions for each of the microsatellite markers were optimised as described in Chapter 3.2. The final collection of 237 individuals from 10 extended pedigrees was genotyped with the 25 selected microsatellite markers, using the methods described in Chapter 3.4. Forward primers were labelled with fluorescent dyes and organised into four pools for optimum analysis on the ABI310 Genetic Analyzer (Applied Biosystems), as shown in Appendix 2. DNAs from CEPH families 884 and 1331 (http://www.cephb.fr/cephdb) were genotyped as allele sizing controls.

4.3.3 Genotype error checking

Mendelian inconsistent genotyping errors were detected using PedCheck version 1.1 (O'Connell and Weeks 1998) at levels 1-4. Level 1 detects inconsistencies between parent child relationships, such as allele incompatibility or more than 4 alleles in a sibship. Level 2 uses genotype elimination to detect inconsistencies across wider pedigree relationships and multiple generations. Level 3 identifies critical erroneous genotypes by sequentially untyping individuals. Level 4 uses an odds-ratio algorithm to pinpoint the most likely source of error (O'Connell and Weeks 1998). In general, most errors were detected at level 1; and level 4 was rarely employed since level 3 checking often returned only one critical genotype. Genotypes flagged by these inheritance checks were double checked and rescored (blind) by a second individual. Any remaining discrepancies were flagged and the genotyping repeated. Any unresolved errors following repeat genotyping were removed from the dataset and the error checking program rerun with the updated data until no more errors were detected.

The mistyping analysis component of SimWalk2 version 2.86 (Sobel and Lange 1996) was used to identify possible Mendelian consistent genotyping errors and unlikely

double-recombinants (Sobel *et al.* 2002). SimWalk2 determines the posterior mistyping probability for each allele based on the marker map and an *a priori* error model. In this study the empirical error model (Sobel *et al.* 2002) was used to flag possible problem genotypes. This model incorporates common errors such as false homozygosity and recognises that mistyping of one allele is more common than two. The empirical model is comprised of five default error rates: (ε_1) 0.0125 for false homozygosity; (ε_2) 0.0075 for misreading one allele; (ε_3) 0.005 for misreading both alleles; (ε_4) 0.01 for misreading a homozygote as a heterozygote; and (ε_5) 0.0025 for random mistyping; which translates to an overall error rate of 0.0175 ($\varepsilon_3 + \varepsilon_4 + \varepsilon_5$) for a true homozygous genotype and to 0.0275 ($\varepsilon_1 + \varepsilon_2 + \varepsilon_3 + \varepsilon_5$) for a true heterozygous genotype (Sobel *et al.* 2002). The program output consists of the sample identification number, marker name, and the genotype purported to be erroneous, along with the probability of mistyping for the first, second, both, and either allele(s) when any probability is greater than a chosen significance threshold. In this study a stringent significance threshold of 0.25 for the probability of mistyping was used to flag potentially erroneous data.

As with Mendelian inconsistent errors, genotypes were double checked and rescored blind by a second individual, and only altered where errors were obvious on reanalysis of the data. For example, where repeat genotyping revealed a case of false homozygosity due to allele dropout in the initial sample, data was updated to include both alleles. Any remaining errors, discrepancies or areas of uncertainty were removed from the dataset.

In the case of all genotypes flagged as potentially erroneous, the data were never changed based only on statistical inference, but always on regenotyping.

4.3.4 Allele frequency generation

Marker allele frequencies for linkage analysis were derived from a set of 72 elderly glaucoma-free individuals (described in Chapter 2.2.4) genotyped with each of the 25 selected microsatellite markers.

4.3.5 Data storage and file generation

All individual, family, genotype, phenotype and genetic map data were stored in a dedicated database program developed by Tim Albion (Menzies Research Institute, unpublished). This program not only provided data storage and an interface for data manipulation, but also could be interrogated to produce input files for various software packages. The linkage utility program MEGA2 (Mukhopadhyay *et al.* 2005b) was also used to generate program specific input files for the majority of the analysis programs used in this dissertation.

4.4 Statistical methods

4.4.1 Maximum LOD simulation analyses

Linkage simulations were conducted using FASTSLINK (Ott 1989; Weeks *et al.* 1990), to provide a sense of the power of each pedigree to produce a significant or suggestive LOD score. Simulations were conducted using a marker with 6 alleles: one common (frequency=0.299), four less common (frequency=0.175) and one rare allele (frequency=0.001). For each pedigree, 1000 simulations were conducted assuming 90% penetrance, a 2% phenocopy rate and a disease allele frequency of 0.0001. Simulated genotypic data was analysed using the MSIM component of FASTSLINK to approximate the expected maximum LOD score.

Several of the pedigrees contained both marriage and inbreeding loops (described in Chapter 2.3.4), all of which were broken using the LINKAGE utility program MAKEPED (Lathrop and Lalouel 1984; Lathrop *et al.* 1984; Lathrop *et al.* 1986) by duplicating a selected individual with both parents and children in the pedigree.

4.4.2 Markov chain Monte Carlo algorithm for inheritance information extraction

A Markov chain Monte Carlo (MCMC) algorithm based approach was employed to obtain multipoint inheritance information from the entire dataset, using SimWalk2 version 2.86-2.91 (Sobel and Lange 1996). Starting with an estimate of the most likely genetic descent graph (the path of gene flow within a pedigree) as the initial position, SimWalk2 uses the MCMC algorithm to traverse the space of genetic descent graphs consistent with the available data for each pedigree, using the Metropolis acceptance criterion (Metropolis *et al.* 1953) to move to the next configuration (Sobel and Lange 1996). During this process, the MCMC 'random walk' samples the configurations in proportion to their likelihood, given the available genotype data. A sample average is then used to provide estimated results for the original pedigree (Sobel and Lange 1996). It is important to note that this is an estimation based method, as configurations that are possible, but highly unlikely, will not be sampled. It is also important to note that this method is able to extract multipoint inheritance information from the entire pedigree, including even the largest of the GIST pedigrees, without trimming the pedigree or analysing markers individually. This inheritance information can be used for a range of analysis purposes, including parametric linkage analysis (determining if the inheritance pattern fits a specific model for a trait causing gene) or nonparametric linkage analyses (determining whether the inheritance information deviates from the expectation under independent assortment). These two analysis approaches were applied, as described below.

4.4.3 MCMC based nonparametric linkage analysis

Nonparametric linkage analysis was conducted using the MCMC based estimation method employed in SimWalk2 version 2.86-2.91 (Sobel and Lange 1996). While intrinsically estimation based, this method increases the power of the clustering statistics by using information from all genotyped individuals, unaffected as well as affected, to sample the identity by descent (IBD) configurations proportional to their likelihood. Alleles are identical by descent if they are copies of the same ancestral allele, thus IBD configurations are a measure of the sharing of genetic material. The nonparametric statistics D and E were evaluated for all pedigrees and for the combined dataset. Statistic D calculates the extent of allele sharing among affected relative pairs (Sobel and Lange 1996) and is similar to the NPL_{pairs} statistic used in GeneHunter and Merlin (Whittemore and Halpern 1994; Kruglyak et al. 1996), while statistic E, equivalent to NPL_{all}, measures the degree of allele sharing in all subsets of affected individuals at once (Whittemore and Halpern 1994; Kruglyak et al. 1996). SimWalk2 uses gene-dropping to calculate empirical p-values for each statistic by comparing the observed value of the statistic to that found under the null hypothesis, which is generated by repeated sampling of fully informative marker data simulated with a gene-dropping algorithm, without linkage to the phenotype. In the absence of complete IBD-inheritance information, for example when individuals in the pedigree are unavailable for genotyping, the p-values from this procedure are potentially conservative (Sobel and Lange 1996), possibly understating the statistical significance. Approximate MCMC inference of IBD probabilities may also be more conservative than exact Lander-Green inference, further understating the significance.

4.4.4 MCMC based parametric linkage analysis

Multipoint parametric linkage analysis was conducted using the MCMC estimation based approach employed in SimWalk2 version 2.86-2.91 (Sobel and Lange 1996). SimWalk2 utilises the method of location scores to indicate the likelihood of the trait loci at various locations within the marker map. Location scores indicate the relative likelihood of several positions among the marker loci for the trait locus, given the pedigree data and the marker map. These pedigrees are then used to estimate the location score curve for the original pedigree. The location scores are directly comparable to multipoint LOD scores and are presented in $\log_{10}$ units.

The initial model used was based on previous studies of POAG genetics (Sheffield *et al.* 1993; Stoilova *et al.* 1996; Sarfarazi *et al.* 1998; Trifan *et al.* 1998), including an assumption of autosomal dominant inheritance, a disease gene frequency of 0.0001, penetrance of 0.9 and a 2% phenocopy rate. An alternative low penetrance model (0.75) was also included, based on the studies of Wirtz *et al.* (1999) and Kitsos *et al.* (2001).

Given the variable late age of onset, combined with the complexities of defining affection status for POAG, all parametric analyses were affected only, where all individuals were scored as either affected or unknown for the purposes of the analysis. This approach is far more conservative than including trait information from unaffected individuals, but prevents errors due to misclassification of affection status.

4.4.5 Haplotype analysis

The most likely haplotypes for regions of interest within the GIST pedigree dataset, including information from individuals classed as POAG status unknown, were

estimated using the haplotyping component of SimWalk2 version 2.86-2.91 (Sobel and Lange 1996). SimWalk2 employs the MCMC algorithm combined with simulated annealing to determine the most likely haplotype configuration for each pedigree. A slight modification to the criteria for moving between configurations during the MCMC random walk produces the simulated annealing procedure, which samples from the configuration space in search of the single most likely configuration (Sobel and Lange 1996). The process was repeated (up to eight times) with different random seeds until a stable configuration was obtained.

Haplotypes were displayed using Pedigree/Draw 5.1 (SFBR; http://www.sfbr.org/sfbr/public/software/pedraw/peddrw.html now available from http://www.pedigree-draw.com). The size and complexity of the GIST pedigrees, combined with a lack of complete information (due to deceased linking individuals and unascertained spouses) complicated the haplotype reconstruction process by reducing the phase information. As a result, the final haplotype output must be considered the most likely configuration, but not necessarily an exact result.

4.4.6 Selection of pedigrees for follow-up analysis

Pedigrees displaying 'interesting' results in the SimWalk2 nonparametric and parametric analyses were considered for follow-up analysis including additional genotyping within the region of interest. The criteria for consideration was a p-value for a nonparametric statistic of less than 0.1 combined with a location score of at least 1.0 within the same pedigree and region of interest. Depending on the number of results flagged as interesting, not all pedigrees fulfilling the criteria for consideration would necessarily be accepted for follow-up analysis.

4.4.7 Exact nonparametric linkage analysis of selected pedigrees

Exact nonparametric linkage analyses were conducted on select pedigrees and regions of interest using GeneHunter-Plus version 1.2 (Kruglyak *et al.* 1996; Kong and Cox 1997). This analysis is an affecteds-only approach based on the Lander-Green algorithm (Lander and Green 1987), which is restricted by pedigree size. GeneHunter can analyse a maximum pedigree size of 20 bits ($2n-f \leq 20$; where n=number of founders, f=number of non-founders); hence pedigrees were manually trimmed to 20 bits prior to analysis. Pedigrees were analysed individually, due to the expectation of high genetic heterogeneity across the dataset, using the NPL_{all} statistic (Whittemore and Halpern 1994).

4.4.8 Exact two-point parametric linkage analysis of selected pedigrees

Exact two-point parametric analyses were conducted only on regions of interest in select pedigrees using FASTLINK (Cottingham *et al.* 1993; Schaffer *et al.* 1994), a modified version of LINKAGE (Lathrop and Lalouel 1984; Lathrop *et al.* 1984; Lathrop *et al.* 1986). As in section 4.4.4, the initial model including an assumption of autosomal dominant inheritance, a disease gene frequency of 0.0001, penetrance of 0.9 and a 2% phenocopy rate, with an alternative 0.75 penetrance model included also. All FASTLINK parametric analyses were also affected only, where all individuals were scored as either affected or unknown for the purposes of the analysis. This analysis method is the most similar to the methodology used in previous studies of POAG loci (Sheffield *et al.* 1993; Stoilova *et al.* 1996; Wirtz *et al.* 1997; Sarfarazi *et al.* 1998; Trifan *et al.* 1998; Wirtz *et al.* 1999).

4.5 Results

4.5.1 Maximum LOD simulation

The linkage simulation results are shown in Table 4.3. The maximum and average LOD scores simulated under the model of one marker with six alleles, including one common and one rare allele, are shown along with the percentage of the total simulated LOD scores greater than 1, 2 and 3. Seven of the families produced maximum simulated LOD scores greater than 3, with the largest at 4.17 for family GTas37b. The smallest family (GTas11) produced a simulated maximum LOD of 1.19, and while not large enough to enable the identification of significant linkage alone, this family was retained as a valuable component of the overall dataset. The subdivided pedigrees GTas3a and GTas3b are included in Table 4.3 and shown in italics. These pedigrees were analysed in place of GTas03 when required.

Family ID	Total individuals	Available individuals	Affected individuals	Max LOD	Average LOD	% > 1	% > 2	% > 3
GTas03#	123	59	15	**5.88**	2.38	86.5	62.5	30.0
GTas03a	*76*	*39*	*9*	***3.73***	*1.42*	*61.0*	*27.5*	*5.5*
GTas03b#	*41*	*19*	*6*	*1.86*	*0.66*	*26.5*	*0.0*	*0.0*
GTas04#	45	25	9	2.59	0.99	49.0	8.5	0.0
GTas35	32	15	6	1.71	0.73	40.0	0.0	0.0
GTas37a	51	29	8	**3.29**	1.22	56.0	20.0	1.5
GTas37b#	37	24	15	**4.17**	1.73	71.5	38.5	10.5
GTas54	33	17	7	**3.75**	1.13	53.5	16.5	1.0
GTas11	15	10	5	1.19	0.59	29.0	0.0	0.0
GTas15	31	14	6	**3.14**	1.12	50.0	16.0	0.5
GTas17	45	26	9	**3.34**	1.26	57.0	17.0	1.0
GTas121	45	18	7	2.57	0.98	47.0	6.0	0.0

Table 4.3 - Maximum LOD simulations for the GIST pedigrees

# indicates the pedigree has had at least one loop broken prior to simulation analyses.

Italics: subdivided pedigrees GTas03a and GTas03b, branches of family GTas03

Bold: LOD>3

4.5.2 Genotype error checking

Mendelian inconsistent genotyping errors were detected at a frequency of 2.6% in the first pass of genotyping (157 genotypes), and at approximately 0.8% during the repeat genotyping process (seven genotypes).

Possible Mendelian consistent errors were flagged by SimWalk2 in approximately 3% of genotypes (181 samples), and approximately a third of these (63) were considered true errors following repeat genotyping and scoring (overall Mendelian consistent error rate of 1.1%). The high level of flagged errors was due to the stringent significance threshold used (0.25) which required more genotypes be checked than the default threshold of 0.5.

4.5.3 MCMC based nonparametric linkage analysis

The SimWalk2 nonparametric linkage analysis results for each of the investigated POAG loci GLC1A-F, including the value for the statistics D and E and corresponding empirical p-values, are shown in Tables 4.4 to 4.9. Nonparametric linkage statistics and p-values are also given for the combined dataset. Empirical p-values less than or equal to 0.1 were highlighted for follow-up consideration.

There were 5 pedigrees/regions highlighted for potential follow-up in the initial nonparametric linkage analysis. Family GTas15 produced p-values between 0.05 and 0.07 for the last three markers on chromosome 2 (D2S2264 to D2S1892) with a peak value of 1.13 (p=0.05) for Statistic E at marker D2S1897 (Table 4.5). Families GTas03 and GTas11 both produced interesting results for markers D3S3694 to D3S1608 on chromosome 3, with peak scores of 1.54 (p=0.03) for Statistic E at marker D3S3694 for family GTas03 and 1.35 (p=0.04) for Statistic E also at marker D3S3694 for family GTas11 (Table 4.6). GTas121 also showed some interesting signs of linkage to

chromosome 3, at the two most distal markers D3S1569 and D3S1608 with a peak score of 1.39 (p=0.04) with Statistic E at marker D3S1569 (Table 4.6). Family GTas35 showed signs of interesting results with both statistics on chromosome 10 at markers D10S1691 to D10S1664, with peak scores of 1.30 (p=0.05) for the distal markers D10S547 and D10S1664 with Statistic D (Table 4.8). There were no highlighted nonparametric linkage results for the investigated regions of interest on chromosomes 1 (GLC1A; Table 4.4), chromosome 8 (GLC1D; Table 4.7) and chromosome 7 (GLC1F; Table 4.9) with this set of 10 pedigrees from the GIST.

Family ID	Marker	Haldane cM	Statistic D	p-value	Statistic E	p-value
All	D1S2635	0.00	0.08	0.84	0.21	0.62
	D1S2707	4.95	0.02	0.95	0.08	0.83
	D1S2675	5.70	0.03	0.92	0.09	0.81
GTas03	D1S2635	0.00	0.09	0.81	0.07	0.85
	D1S2707	4.95	0.07	0.86	0.05	0.90
	D1S2675	5.70	0.08	0.84	0.06	0.88
GTas04	D1S2635	0.00	0.17	0.67	0.19	0.64
	D1S2707	4.95	0.17	0.68	0.19	0.65
	D1S2675	5.70	0.17	0.68	0.19	0.65
GTas11	D1S2635	0.00	0.64	0.23	0.71	0.20
	D1S2707	4.95	0.60	0.25	0.67	0.22
	D1S2675	5.70	0.59	0.26	0.65	0.23
GTas15	D1S2635	0.00	0.20	0.63	0.26	0.54
	D1S2707	4.95	0.12	0.77	0.17	0.68
	D1S2675	5.70	0.13	0.75	0.17	0.67
GTas17	D1S2635	0.00	0.26	0.55	0.27	0.53
	D1S2707	4.95	0.23	0.59	0.25	0.56
	D1S2675	5.70	0.32	0.48	0.30	0.50
GTas35	D1S2635	0.00	0.09	0.81	0.07	0.85
	D1S2707	4.95	0.05	0.90	0.03	0.94
	D1S2675	5.70	0.07	0.85	0.05	0.89
GTas37a	D1S2635	0.00	0.39	0.40	0.35	0.45
	D1S2707	4.95	0.38	0.41	0.34	0.46
	D1S2675	5.70	0.39	0.41	0.34	0.45
GTas37b	D1S2635	0.00	0.25	0.56	0.26	0.56
	D1S2707	4.95	0.39	0.40	0.34	0.46
	D1S2675	5.70	0.31	0.49	0.26	0.55
GTas54	D1S2635	0.00	0.20	0.64	0.22	0.61
	D1S2707	4.95	0.08	0.83	0.11	0.78
	D1S2675	5.70	0.15	0.72	0.17	0.68
GTas121	D1S2635	0.00	0.12	0.76	0.12	0.76
	D1S2707	4.95	0.03	0.93	0.03	0.94
	D1S2675	5.70	0.04	0.91	0.04	0.92

Table 4.4 - Simwalk2 MCMC based nonparametric linkage results for chromosome 1 (GLC1A)

Family ID	Marker	Haldane cM	Statistic D	p-value	Statistic E	p-value
All	D2S2161	0.00	0.29	0.52	0.31	0.50
	D2S113	1.77	0.36	0.43	0.39	0.41
	D2S2264	5.45	0.19	0.65	0.21	0.62
	D2S1897	8.76	0.24	0.58	0.32	0.48
	D2S1892	10.76	0.18	0.66	0.22	0.60
GTas03	D2S2161	0.00	0.57	0.27	0.52	0.30
	D2S113	1.77	0.58	0.26	0.54	0.29
	D2S2264	5.45	0.50	0.32	0.49	0.32
	D2S1897	8.76	0.28	0.53	0.27	0.54
	D2S1892	10.76	0.16	0.70	0.17	0.67
GTas04	D2S2161	0.00	0.77	0.17	0.77	0.17
	D2S113	1.77	0.80	0.16	0.80	0.16
	D2S2264	5.45	0.15	0.71	0.17	0.67
	D2S1897	8.76	0.30	0.50	0.29	0.51
	D2S1892	10.76	0.30	0.50	0.29	0.51
GTas11	D2S2161	0.00	0.25	0.56	0.22	0.60
	D2S113	1.77	0.38	0.41	0.39	0.41
	D2S2264	5.45	0.11	0.77	0.13	0.74
	D2S1897	8.76	0.11	0.77	0.13	0.74
	D2S1892	10.76	0.04	0.91	0.04	0.91
GTas15	D2S2161	0.00	0.42	0.38	0.47	0.34
	D2S113	1.77	**1.11**	**0.08**	**1.27**	**0.05**
	D2S2264	5.45	**1.27**	**0.05**	**1.44**	**0.04**
	D2S1897	8.76	**1.47**	**0.03**	**1.68**	**0.02**
	D2S1892	10.76	**1.26**	**0.06**	**1.40**	**0.04**
GTas17	D2S2161	0.00	0.35	0.44	0.39	0.41
	D2S113	1.77	0.35	0.44	0.39	0.41
	D2S2264	5.45	0.36	0.44	0.39	0.40
	D2S1897	8.76	0.36	0.44	0.40	0.40
	D2S1892	10.76	0.36	0.44	0.39	0.41
GTas35	D2S2161	0.00	0.06	0.86	0.04	0.91
	D2S113	1.77	0.07	0.86	0.04	0.91
	D2S2264	5.45	0.06	0.88	0.03	0.93
	D2S1897	8.76	0.06	0.87	0.03	0.94
	D2S1892	10.76	0.17	0.67	0.16	0.69
GTas37a	D2S2161	0.00	0.06	0.88	0.04	0.90
	D2S113	1.77	0.08	0.83	0.07	0.85
	D2S2264	5.45	0.50	0.31	0.47	0.34
	D2S1897	8.76	0.39	0.41	0.36	0.44
	D2S1892	10.76	0.38	0.41	0.35	0.45
GTas37b	D2S2161	0.00	0.22	0.60	0.16	0.70
	D2S113	1.77	0.21	0.62	0.14	0.72
	D2S2264	5.45	0.15	0.71	0.08	0.83
	D2S1897	8.76	0.22	0.61	0.15	0.70
	D2S1892	10.76	0.22	0.61	0.16	0.69
GTas54	D2S2161	0.00	0.24	0.58	0.27	0.54
	D2S113	1.77	0.23	0.59	0.26	0.55
	D2S2264	5.45	0.23	0.59	0.26	0.55
	D2S1897	8.76	0.27	0.54	0.30	0.50
	D2S1892	10.76	0.27	0.53	0.30	0.51
GTas121	D2S2161	0.00	0.18	0.66	0.19	0.65
	D2S113	1.77	0.19	0.65	0.19	0.64
	D2S2264	5.45	0.20	0.63	0.21	0.62
	D2S1897	8.76	0.35	0.44	0.35	0.44
	D2S1892	10.76	0.39	0.41	0.38	0.42

Table 4.5 - Simwalk2 MCMC based nonparametric linkage results for chromosome 2 (GLC1B)

Bold: Statistics D or E p-value≤0.1.

Family ID	Marker	Haldane cM	Statistic D	p-value	Statistic E	p-value
All	D3S3637	0.00	0.76	0.17	**1.04**	**0.09**
	D3S1301	5.54	0.48	0.33	0.92	0.12
	D3S3694	7.38	0.58	0.27	0.95	0.11
	D3S1569	12.19	0.61	0.25	0.62	0.24
	D3S1608	14.52	0.59	0.26	0.60	0.25
GTas03	D3S3637	0.00	**1.43**	**0.04**	**1.54**	**0.03**
	D3S1301	5.54	**1.07**	**0.09**	**1.10**	**0.08**
	D3S3694	7.38	**1.02**	**0.10**	**1.04**	**0.09**
	D3S1569	12.19	0.43	0.37	0.44	0.36
	D3S1608	14.52	0.42	0.38	0.43	0.38
GTas04	D3S3637	0.00	0.17	0.68	0.15	0.71
	D3S1301	5.54	0.23	0.59	0.19	0.64
	D3S3694	7.38	0.27	0.53	0.23	0.60
	D3S1569	12.19	0.30	0.50	0.24	0.57
	D3S1608	14.52	0.29	0.52	0.23	0.59
GTas11	D3S3637	0.00	**1.21**	**0.06**	**1.35**	**0.04**
	D3S1301	5.54	**1.09**	**0.08**	**1.24**	**0.06**
	D3S3694	7.38	**1.11**	**0.08**	**1.27**	**0.05**
	D3S1569	12.19	0.55	0.28	0.56	0.27
	D3S1608	14.52	0.55	0.28	0.56	0.28
GTas15	D3S3637	0.00	0.43	0.37	0.38	0.42
	D3S1301	5.54	0.24	0.58	0.21	0.62
	D3S3694	7.38	0.26	0.55	0.25	0.56
	D3S1569	12.19	0.26	0.55	0.25	0.56
	D3S1608	14.52	0.26	0.55	0.26	0.56
GTas17	D3S3637	0.00	0.31	0.49	0.31	0.50
	D3S1301	5.54	0.35	0.44	0.34	0.46
	D3S3694	7.38	0.34	0.46	0.33	0.47
	D3S1569	12.19	0.23	0.59	0.24	0.58
	D3S1608	14.52	0.21	0.62	0.22	0.60
GTas35	D3S3637	0.00	0.29	0.51	0.31	0.49
	D3S1301	5.54	0.12	0.76	0.13	0.75
	D3S3694	7.38	0.10	0.79	0.11	0.78
	D3S1569	12.19	0.20	0.63	0.21	0.62
	D3S1608	14.52	0.19	0.65	0.20	0.64
GTas37a	D3S3637	0.00	0.09	0.81	0.14	0.73
	D3S1301	5.54	0.07	0.86	0.08	0.84
	D3S3694	7.38	0.28	0.52	0.30	0.50
	D3S1569	12.19	0.34	0.46	0.34	0.46
	D3S1608	14.52	0.33	0.47	0.32	0.47
GTas37b	D3S3637	0.00	0.18	0.66	0.19	0.64
	D3S1301	5.54	0.06	0.87	0.12	0.77
	D3S3694	7.38	0.11	0.78	0.15	0.71
	D3S1569	12.19	0.20	0.63	0.23	0.59
	D3S1608	14.52	0.21	0.61	0.24	0.58
GTas54	D3S3637	0.00	0.26	0.55	0.31	0.49
	D3S1301	5.54	0.55	0.28	0.63	0.23
	D3S3694	7.38	0.52	0.30	0.62	0.24
	D3S1569	12.19	0.70	0.20	0.70	0.20
	D3S1608	14.52	0.78	0.17	0.72	0.19
GTas121	D3S3637	0.00	0.64	0.23	0.68	0.21
	D3S1301	5.54	0.65	0.22	0.70	0.20
	D3S3694	7.38	0.55	0.28	0.57	0.27
	D3S1569	12.19	**1.32**	**0.05**	**1.39**	**0.04**
	D3S1608	14.52	**1.23**	**0.06**	**1.31**	**0.05**

Table 4.6 - SimWalk2 MCMC based nonparametric linkage results for chromosome 3 (GLC1C)

Bold: Statistics D or E p-value≤0.1.

Family ID	Marker	Haldane cM	Statistic D	p-value	Statistic E	p-value
All peds	D8S1749	0.00	0.135	0.73	0.225	0.60
	D8S556	7.95	0.071	0.85	0.106	0.78
	D8S198	22.24	0.330	0.47	0.463	0.34
GTas03	D8S1749	0.00	0.14	0.73	0.14	0.72
	D8S556	7.95	0.12	0.76	0.14	0.73
	D8S198	22.24	0.08	0.83	0.09	0.82
GTas04	D8S1749	0.00	0.28	0.53	0.32	0.48
	D8S556	7.95	0.32	0.48	0.39	0.41
	D8S198	22.24	0.47	0.34	0.51	0.31
GTas11	D8S1749	0.00	0.25	0.57	0.30	0.50
	D8S556	7.95	0.13	0.74	0.19	0.65
	D8S198	22.24	0.43	0.37	0.46	0.35
GTas15	D8S1749	0.00	0.29	0.51	0.26	0.56
	D8S556	7.95	0.29	0.51	0.25	0.56
	D8S198	22.24	0.34	0.45	0.29	0.51
GTas17	D8S1749	0.00	0.30	0.51	0.30	0.50
	D8S556	7.95	0.22	0.60	0.22	0.60
	D8S198	22.24	0.26	0.55	0.26	0.55
GTas35	D8S1749	0.00	0.49	0.33	0.46	0.35
	D8S556	7.95	0.37	0.42	0.36	0.44
	D8S198	22.24	0.33	0.47	0.32	0.48
GTas37a	D8S1749	0.00	0.12	0.76	0.11	0.77
	D8S556	7.95	0.05	0.89	0.05	0.90
	D8S198	22.24	0.25	0.56	0.27	0.54
GTas37b	D8S1749	0.00	0.37	0.43	0.42	0.38
	D8S556	7.95	0.39	0.41	0.45	0.35
	D8S198	22.24	0.43	0.37	0.49	0.32
GTas54	D8S1749	0.00	0.37	0.42	0.43	0.37
	D8S556	7.95	0.39	0.41	0.43	0.37
	D8S198	22.24	0.51	0.31	0.59	0.26
GTas121	D8S1749	0.00	0.15	0.71	0.16	0.70
	D8S556	7.95	0.15	0.71	0.16	0.69
	D8S198	22.24	0.23	0.59	0.23	0.59

Table 4.7 - SimWalk2 MCMC based nonparametric linkage results for chromosome 8 (GLC1D)

Family ID	Marker	Haldane cM	Statistic D	p-value	Statistic E	p-value
All	D10S1729	0.00	0.22	0.61	0.25	0.56
	D10S1713	3.24	0.20	0.64	0.23	0.59
	D10S1691	5.88	0.35	0.45	0.34	0.45
	D10S547	9.37	0.39	0.41	0.33	0.47
	D10S1664	12.94	0.33	0.47	0.30	0.51
GTas03	D10S1729	0.00	0.08	0.84	0.12	0.76
	D10S1713	3.24	0.04	0.91	0.07	0.86
	D10S1691	5.88	0.22	0.60	0.28	0.53
	D10S547	9.37	0.36	0.44	0.40	0.40
	D10S1664	12.94	0.62	0.24	0.65	0.23
GTas04	D10S1729	0.00	0.30	0.50	0.30	0.50
	D10S1713	3.24	0.30	0.50	0.29	0.51
	D10S1691	5.88	0.30	0.51	0.29	0.51
	D10S547	9.37	0.30	0.50	0.30	0.51
	D10S1664	12.94	0.18	0.66	0.16	0.69
GTas11	D10S1729	0.00	0.30	0.50	0.23	0.59
	D10S1713	3.24	0.27	0.53	0.21	0.62
	D10S1691	5.88	0.26	0.55	0.19	0.64
	D10S547	9.37	0.21	0.62	0.15	0.70
	D10S1664	12.94	0.12	0.76	0.08	0.83
GTas15	D10S1729	0.00	0.62	0.24	0.65	0.22
	D10S1713	3.24	0.63	0.24	0.66	0.22
	D10S1691	5.88	0.62	0.24	0.65	0.22
	D10S547	9.37	0.52	0.30	0.53	0.30
	D10S1664	12.94	0.47	0.34	0.48	0.33
GTas17	D10S1729	0.00	0.36	0.43	0.39	0.41
	D10S1713	3.24	0.35	0.44	0.38	0.42
	D10S1691	5.88	0.21	0.62	0.23	0.59
	D10S547	9.37	0.27	0.54	0.27	0.53
	D10S1664	12.94	0.11	0.77	0.13	0.74
GTas35	D10S1729	0.00	0.64	0.23	0.66	0.22
	D10S1713	3.24	0.70	0.20	0.74	0.18
	D10S1691	5.88	**1.18**	**0.07**	**1.19**	**0.06**
	D10S547	9.37	**1.30**	**0.05**	**1.31**	**0.05**
	D10S1664	12.94	**1.30**	**0.05**	**1.31**	**0.05**
GTas37a	D10S1729	0.00	0.24	0.58	0.20	0.63
	D10S1713	3.24	0.32	0.48	0.27	0.54
	D10S1691	5.88	0.40	0.39	0.33	0.46
	D10S547	9.37	0.49	0.33	0.39	0.41
	D10S1664	12.94	0.59	0.26	0.49	0.32
GTas37b	D10S1729	0.00	0.36	0.43	0.54	0.29
	D10S1713	3.24	0.33	0.47	0.42	0.38
	D10S1691	5.88	0.31	0.49	0.35	0.45
	D10S547	9.37	0.22	0.61	0.28	0.53
	D10S1664	12.94	0.10	0.79	0.21	0.62
GTas54	D10S1729	0.00	0.37	0.42	0.36	0.44
	D10S1713	3.24	0.38	0.42	0.35	0.45
	D10S1691	5.88	0.40	0.40	0.34	0.46
	D10S547	9.37	0.26	0.55	0.21	0.62
	D10S1664	12.94	0.27	0.54	0.22	0.60
GTas121	D10S1729	0.00	0.07	0.85	0.07	0.85
	D10S1713	3.24	0.05	0.89	0.05	0.89
	D10S1691	5.88	0.05	0.90	0.04	0.91
	D10S547	9.37	0.06	0.86	0.06	0.87
	D10S1664	12.94	0.09	0.82	0.08	0.83

Table 4.8 - SimWalk2 MCMC based nonparametric linkage results for chromosome 10 (GLC1E)

Bold: Statistics D or E p-value≤0.1.

Family ID	Marker	Haldane cM	Statistic D	p-value	Statistic E	p-value
All	D7S2511	0.00	0.15	0.70	0.14	0.73
	D7S505	2.29	0.20	0.63	0.10	0.80
	D7S2439	5.01	0.22	0.60	0.12	0.77
	D7S2546	9.12	0.15	0.71	0.09	0.81
GTas03	D7S2511	0.00	0.29	0.52	0.27	0.54
	D7S505	2.29	0.34	0.46	0.31	0.49
	D7S2439	5.01	0.25	0.56	0.22	0.61
	D7S2546	9.12	0.26	0.54	0.24	0.58
GTas04	D7S2511	0.00	0.51	0.31	0.45	0.35
	D7S505	2.29	0.54	0.29	0.49	0.32
	D7S2439	5.01	0.59	0.26	0.55	0.28
	D7S2546	9.12	0.23	0.59	0.20	0.63
GTas11	D7S2511	0.00	0.04	0.90	0.04	0.91
	D7S505	2.29	0.03	0.93	0.03	0.93
	D7S2439	5.01	0.03	0.93	0.03	0.93
	D7S2546	9.12	0.03	0.93	0.03	0.93
GTas15	D7S2511	0.00	0.45	0.36	0.38	0.42
	D7S505	2.29	0.44	0.37	0.36	0.44
	D7S2439	5.01	0.37	0.42	0.30	0.50
	D7S2546	9.12	0.52	0.31	0.46	0.35
GTas17	D7S2511	0.00	0.14	0.73	0.13	0.74
	D7S505	2.29	0.20	0.63	0.19	0.64
	D7S2439	5.01	0.25	0.56	0.24	0.58
	D7S2546	9.12	0.30	0.51	0.28	0.52
GTas35	D7S2511	0.00	0.23	0.58	0.26	0.55
	D7S505	2.29	0.33	0.47	0.36	0.44
	D7S2439	5.01	0.37	0.43	0.39	0.41
	D7S2546	9.12	0.38	0.42	0.41	0.39
GTas37a	D7S2511	0.00	0.53	0.30	0.63	0.24
	D7S505	2.29	0.29	0.51	0.39	0.41
	D7S2439	5.01	0.31	0.50	0.41	0.39
	D7S2546	9.12	0.09	0.82	0.09	0.81
GTas37b	D7S2511	0.00	0.13	0.73	0.22	0.60
	D7S505	2.29	0.35	0.45	0.42	0.38
	D7S2439	5.01	0.35	0.44	0.43	0.37
	D7S2546	9.12	0.37	0.43	0.44	0.36
GTas54	D7S2511	0.00	0.36	0.44	0.37	0.43
	D7S505	2.29	0.41	0.39	0.42	0.38
	D7S2439	5.01	0.45	0.36	0.47	0.34
	D7S2546	9.12	0.57	0.27	0.62	0.24
GTas121	D7S2511	0.00	0.25	0.56	0.28	0.53
	D7S505	2.29	0.25	0.57	0.28	0.53
	D7S2439	5.01	0.25	0.57	0.27	0.53
	D7S2546	9.12	0.21	0.62	0.23	0.59

Table 4.9 - SimWalk2 MCMC based nonparametric linkage results for chromosome 7 (GLC1F)

4.5.4 MCMC based parametric linkage analysis

The SimWalk2 parametric linkage analysis results for each of the investigated POAG loci GLC1A-F, including both the high penetrance (0.90) and the alternative lower penetrance (0.75) model are shown in Tables 4.10 to 4.15. The maximum location score for each pedigree within each region is reported, along with the corresponding map position in Haldane centiMorgans. Location scores greater than or equal 1 are highlighted for follow-up consideration while negative location scores are shown in red.

The SimWalk2 parametric analyses revealed three results of interest corresponding to regions identified in the SimWalk2 nonparametric analysis. Family GTas15 produced a maximum location score of 1.12 on chromosome 2 (GLC1B) at 10.8 cM (at marker D2S1892) with the high penetrance model (with similar results for the low penetrance model; Table 4.11). The location score dropped to 0.86 at the previous marker, D2S1897 (data not shown). GTas121 produced a maximum location score of 1.08 at 12.19 cM (at marker D3S1569) with the high penetrance model, which dropped to 1.03 with the alternative model (Table 4.12). The final flagged result from the SimWalk2 location score analysis was for family GTas35 on chromosome 10 (GLC1E), with a peak location score of 1.43 for both models at 12.94 cM (at marker D10S1664; Table 4.14). Neither GTas03 nor GTas11 showed any interesting results in the parametric analyses of chromosome 3 (Table 4.12). GTas37a generated a peak location score of 1.10 on chromosome 7, however the location for this was off the end of the map at -5.0 cM (Table 4.15), hence this result was not highlighted for potential follow-up.

Family ID	Location Score (Penetrance 0.9)	Position (Haldane cM)	Location Score (Penetrance 0.75)	Position (Haldane cM)
GTas03	-0.24	55.7	-0.24	55.7
GTas04	-0.12	55.7	-0.12	55.7
GTas11	0.23	-10.0	0.22	-10.0
GTas15	-0.01	45.7	-0.00	40.7
GTas17	0.07	55.7	0.08	50.7
GTas35	-0.16	-50.0	-0.16	-50.0
GTas37a	-0.02	-50.0	-0.02	-50.0
GTas37b	-0.03	55.7	-0.03	55.7
GTas54	0.08	-30.0	0.09	-30.0
GTas121	-0.17	-50.0	-0.17	-50.0

Table 4.10 - SimWalk2 maximum MCMC based parametric location score results for chromosome 1 (GLC1A)

Red: Negative location scores.

Family ID	Location Score (Penetrance 0.9)	Position (Haldane cM)	Location Score (Penetrance 0.75)	Position (Haldane cM)
GTas03	0.15	-50.0	0.15	-50.0
GTas04	0.78	-10.0	0.77	-10.0
GTas11	-0.04	-50.0	-0.04	-50.0
GTas15	**1.12**	**15.8**	**1.11**	**10.8**
GTas17	0.14	-50.0	0.13	-50.0
GTas35	-0.17	-50.0	-0.17	-50.0
GTas37a	-0.06	60.8	-0.05	60.8
GTas37b	-0.03	60.8	-0.03	60.8
GTas54	-0.12	60.8	-0.12	60.8
GTas121	0.04	-50.0	0.03	-50.0

Table 4.11 - SimWalk2 Maximum MCMC based parametric location score results for chromosome 2 (GLC1B)

Bold: Location scores greater than or equal 1.

Red: Negative location scores.

Family ID	Location Score (Penetrance 0.9)	Position (Haldane cM)	Location Score (Penetrance 0.75)	Position (Haldane cM)
GTas03	0.72	-20.0	0.73	-20.0
GTas04	-0.18	-50.0	-0.18	-50.0
GTas11	0.84	7.4	0.83	7.0
GTas15	-0.12	64.5	-0.11	64.5
GTas17	0.14	-50.0	0.14	-50.0
GTas35	0.48	-10.0	0.47	-10.0
GTas37a	-0.33	64.5	-0.31	64.5
GTas37b	0.01	-50.0	0.01	-50.0
GTas54	0.23	44.5	0.24	39.5
GTas121	**1.03**	**12.4**	**1.08**	**12.2**

Table 4.12 - SimWalk2 maximum MCMC based parametric location score results for chromosome 3 (GLC1C)

Bold: Location scores greater than or equal 1.

Red: Negative location scores.

Family ID	Location Score (Penetrance 0.9)	Position (Haldane cM)	Location Score (Penetrance 0.75)	Position (Haldane cM)
GTas03	0.00	-50.0	0.00	-50.0
GTas04	0.40	22.2	0.39	22.2
GTas11	0.45	22.2	0.44	22.2
GTas15	-0.04	72.2	-0.03	72.2
GTas17	0.16	-50.0	0.16	-50.0
GTas35	-0.00	-50.0	-0.00	-50.0
GTas37a	-0.02	72.2	-0.01	72.2
GTas37b	0.13	42.2	0.13	42.2
GTas54	0.16	37.2	0.15	37.2
GTas121	-0.06	72.2	-0.05	72.2

Table 4.13 - SimWalk2 maximum MCMC based parametric location score results for chromosome 8 (GLC1D)

Red: Negative location scores.

Family ID	Location Score (Penetrance 0.9)	Position (Haldane cM)	Location Score (Penetrance 0.75)	Position (Haldane cM)
GTas03	0.91	22.9	0.93	22.9
GTas04	-0.14	-50.0	-0.13	-50.0
GTas11	-0.07	-50.0	-0.07	-50.0
GTas15	0.01	-50.0	0.01	-50.0
GTas17	0.27	-25.0	0.27	-25.0
GTas35	**1.43**	**12.9**	**1.44**	**12.9**
GTas37a	0.02	57.9	0.02	52.9
GTas37b	0.76	0.0	0.73	0.0
GTas54	-0.09	-50.0	-0.08	-50.0
GTas121	-0.26	-50.0	-0.25	-50.0

Table 4.14 - SimWalk2 maximum MCMC based parametric location score results for chromosome 10 (GLC1E)

Bold: Location scores greater than or equal 1.

Red: Negative location scores.

Family ID	Location Score (Penetrance 0.9)	Position (Haldane cM)	Location Score (Penetrance 0.75)	Position (Haldane cM)
GTas03	-0.08	59.1	-0.08	59.1
GTas04	0.15	-30.0	0.15	-30.0
GTas11	-0.11	-50.0	-0.10	-50.0
GTas15	0.03	-50.0	0.02	-50.0
GTas17	-0.10	-50.0	-0.10	-50.0
GTas35	0.53	8.3	0.56	8.3
GTas37a	**1.10**	**-5.0**	**1.08**	**-5.0**
GTas37b	-0.10	59.1	-0.10	59.1
GTas54	0.50	19.1	0.52	19.1
GTas121	0.09	-50.0	0.09	-45.0

Table 4.15 - SimWalk2 maximum MCMC based parametric location score results for chromosome 7 (GLC1F)

Bold: Location scores greater than or equal 1.

Red: Negative location scores.

4.5.5 Haplotype analysis

Aside from family GTas15 at GLC1B on chromosome 2 and family GTas35 at GLC1E on chromosome 10 (described in Chapter 5), there was little evidence of a shared haplotype across each remaining region of interest. There was also no apparent evidence of common alleles shared across multiple pedigrees that could indicate the presence of a founder effect or common ancestry.

Haplotype analysis revealed that the smallest pedigree, GTas11, shared a 3 marker haplotype across all 5 affected individuals for the first three markers of chromosome 3 (D3S3637 to D3S3694), accounting for the low p-values obtained at these markers in the nonparametric analysis (section 4.5.3). Three unaffected individuals (11-07, 11-09 and 11-10) also shared this haplotype; however, all three of these individuals were under the average age of diagnosis for the pedigree (62 years) and may yet manifest the disease.

Family GTas03 showed evidence of a shared haplotype at the same three markers on chromosome 3 in eight of the 15 affected individuals, however the haplotype did not contain any of the alleles found in the haplotype in family GTas11. The GTas03 chromosome 3 haplotype was also detected in four individuals showing no evidence of POAG (3-01, 3-17, 3-24 and 3-39) and, while one individual (3-17) was 66 at the time of examination and a potential example of non-penetrance, the remaining individuals were less than 50 years old when examined.

In family GTas121, there appeared to be a shared two marker haplotype with the two most distal chromosome 3 markers, D3S1569 and D3S1608, in five of the seven affected individuals. This haplotype was also detected in three unaffected individuals

(121-08, 121-11 and 121-15), all less than 55 years old at the time of examination and well below the average age of onset for this family.

In family GTas11 four of the five affected individuals share a haplotype for all three markers on chromosome 8. This haplotype was not detected in any of the unaffected individuals. However, while the haplotype spans approximately 20 cM, there are so few markers and so few typed individuals in the pedigree that even tentative conclusions could not be drawn without further evidence.

Haplotype generation was routinely repeated three to four times with different random seeds and the results were highly consistent across all pedigrees except family GTas04 on chromosome 2 which did not reach a stable configuration after eight iterations.

4.5.6 Pedigrees selected for follow-up analysis

Three pedigrees satisfied the criteria for further consideration described in 4.3.6: GTas15 on chromosome 2 (GLC1B), GTas121 on chromosome 3 (GLC1C) and GTas35 on chromosome 10 (GLC1E). Families GTas15 and GTas35 were selected for follow up analysis including additional genotyping within the regions of interest (reported in Chapter 5). This selection was eventually based on two factors: firstly that the interesting results generated by the nonparametric analyses of GTas15 and GTas35 extended across three or more markers (Tables 4.5 and 4.8 respectively), whereas the region of interest on chromosome 3 for family GTas121 extended across only 2 markers (Table 4.6); and secondly that, at the point of this decision making process, the GLC1C locus on chromosome 3 had recently been replicated in a published study (Kitsos *et al.* 2001), whereas the *OPTN* gene at GLC1E on chromosome 10 (Rezaie *et al.* 2002) had not yet been identified. Additional genotyping and follow-up analysis of GTas15 at the

GLC1B locus on chromosome 2 and GTas35 at the GLC1E locus on chromosome 10 are therefore described in Chapter 5, and these pedigrees are not included in subsequent analyses described in the remainder of this chapter.

4.5.7 Exact nonparametric linkage analyses of selected pedigrees

Exact nonparametric linkage analyses using GeneHunter-Plus version 1.2 were conducted on a selection of pedigrees that generated 'interesting' results with the estimation based SimWalk2 parametric and nonparametric linkage analyses. A summary of these results is given in Table 4.16. Families GTas03, GTas11 and GTas121 showed some evidence of linkage on chromosome 3 at the GLC1C locus (Table 4.6) and were selected for additional analyses at this locus. Since there was a paucity of other interesting results, several other pedigrees were also selected for additional analyses based on less interesting initial data: the GLC1D region on chromosome 8 in families GTas04 and GTas11 due to weakly positive SimWalk2 parametric results at the last marker, D8S198 (Table 4.13); the GLC1E region on chromosome 10 in family GTas03, due to weakly positive SimWalk2 parametric results 10 cM distal to the last marker, D10S1664 (Table 4.14), and finally the GLC1F region on chromosome 7 in family GTas37a due to a peak in the SimWalk2 parametric results 5 cM proximal to the first marker, D7S2511 (Table 4.15). The final dataset contained 7 regions of interest for additional analyses using exact methods, including 2 pedigrees (GTas03 and GTas11) under investigation at two separate regions.

			Maximum nonparametric result		Maximum parametric result	
Family ID	**Locus**	**Marker**	**p-value (statistic E)**	**Location (Haldane cM)**	**Location score (penetrance 0.9)**	**Location (Haldane cM)**
GTas03	GLC1C	D3S3637	**0.03**	0.0	0.73	-20.0
GTas11	GLC1C	D3S3637	**0.04**	0.0	0.83	7.0
GTas121	GLC1C	D3S1569	**0.04**	12.2	**1.08**	12.2
GTas04	GLC1D	D8S198	0.31	22.2	0.39	22.2
GTas11	GLC1D	D8S198	0.35	22.2	0.44	22.2
GTas03	GLC1E	D10S1664	0.23	12.9	0.93	22.9
GTas37a	GLC1F	D7S2511	0.24	0.0	**1.08**	-5.0

Table 4.16 - A summary of results from the preliminary MCMC based nonparametric and parametric analyses in the pedigrees selected for exact nonparametric analyses

Bold: p-value<0.05 or LOD>1

For the exact nonparametric linkage analyses, pedigrees were manually trimmed to ≤20 bits to include the maximum number of affected individuals without compromising the integrity of the pedigree structure, which in some cases resulted in splitting the original into several smaller pedigrees. The subdivided pedigrees GTas03a and GTas03b were used as the core pedigrees in place of GTas03 since the original pedigree consists of 132 bits. Each of the trimmed pedigrees is described in Table 4.17, including the original and trimmed number of bits, the number of individuals removed and the genotyped individuals retained in the trimmed pedigree.

Family ID	Total	Available	Affected	Original bits	Final bits	Removed*	Genotyped Individuals Remaining
GTas03a	76	39	9	80 (24F 52N)	17	58	3-03, 3-05, 3-07, 3-10, 3-12, 3-18, 3-27, 3-34
GTas03b	41	19	6	42 (13F 28N)	19	22	3-11, 3-13, 3-14, 3-15, 3-55, 3-57, 3-58
GTas04	45	25	9	48 (14F 31N)	20	24	4-04, 4-09, 4-10, 4-14, 4-16, 4-19, 4-24, 4-30, 4-31, 4-32, 4-35
GTas37a	51	29	8	57 (15F 36N)	19	28	37-01, 37-03, 37-05, 37-06, 37-10, 37-17, 37-20, 37-40, 37-41, 37-50
GTas11	15	10	5	15 (5F 10N)	15	nil	11-01, 11-02, 11-03, 11-04, 11-05, 11-06, 11-07, 11-08, 11-09, 11-10
GTas121	45	18	7	42 (16F 29N)	19	22	121-01, 121-03, 121-07, 121-09, 121-11, 121-12, 121-14, 121-19, 121-20

Table 4.17 - Details of the trimming of GIST pedigrees used for analysis with GeneHunter-Plus

*Number of individuals removed from the trimmed pedigree.

The GeneHunter-Plus nonparametric linkage analysis results for each of the selected pedigrees and regions are shown in Table 4.18.

Table 4.18 reveals that only GTas11 and GTas121 produced a result of interest in the nonparametric follow-up analysis. GTas11 generated a nonparametric p-value of 0.031 for the NPL_{all} statistic at the first marker within the GLC1C region on chromosome 3 (D3S3637). This result is similar to the result obtained using the equivalent statistic in SimWalk2 (Statistic E; Sobel and Lange 1996) with a p-value of 0.045 at D3S3637 (Section 4.4.3). GTas121 also generated a p-value of 0.033 on chromosome 3 for the NPL_{all} statistic at the last marker within the GLC1C region (D3S1608). Again, this result is similar to the SimWalk2 Statistic E results (p=0.049 at D3S1608; Section 4.4.3).

Locus	Chromosome	Family ID	p-value	Nearest marker
GLC1C	3	GTas03a	0.316	D3S3637
GLC1C	3	GTas03b	0.073	D3S3637
GLC1C	3	GTas11	**0.031**	D3S3637
GLC1C	3	GTas121	**0.033**	D3S1608
GLC1D	8	GTas04	0.112	D8S198
GLC1D	8	GTas11	0.172	D8S198
GLC1E	10	GTas03a	0.227	D10S1664
GLC1E	10	GTas03b	0.188	D10S1664
GLC1F	7	GTas37a	0.468	D7S2511

Table 4.18 - GeneHunter-Plus exact nonparametric p-values for selected GIST pedigrees and regions

Bold: p-value<0.05

4.5.8 Exact two-point parametric linkage analyses of selected pedigrees

Memory constraints and the presence of loops in some pedigrees prevented multipoint MLINK analyses, even with 3 markers, so two-point analyses were conducted on regions/pedigrees of interest. The dataset described in 4.5.6 was also used for the exact two-point parametric analyses.

The results of the two-point parametric follow-up analyses on selected GIST pedigrees and regions are shown in Table 4.19, including the maximum LOD score for each marker and the value of theta at which is was obtained.

Locus	Family ID	Marker	Max. LOD Pen. 0.9	Location (θ)	Max. LOD Pen. 0.75	Location (θ)
GLC1C	GTas03	D3S3637	**1.080**	0.10	**1.080**	0.10
GLC1C		D3S1301	0.102	0.25	0.100	0.25
GLC1C		D3S3694	0.143	0.20	0.144	0.20
GLC1C		D3S1569	0.081	0.30	0.080	0.30
GLC1C		D3S1608	0.072	0.20	0.068	0.20
GLC1C	*GTas03a*	D3S3637	neg	-	neg	-
GLC1C		D3S1301	neg	-	neg	-
GLC1C		D3S3694	neg	-	neg	-
GLC1C		D3S1569	0.235	0.10	0.242	0.01
GLC1C		D3S1608	neg	-	neg	-
GLC1C	*GTas03b*	D3S3637	**1.130**	0.10	**1.119**	0.10
GLC1C		D3S1301	0.166	0.15	0.167	0.15
GLC1C		D3S3694	0.445	0.10	0.442	0.10
GLC1C		D3S1569	0.001	0.40	neg	-
GLC1C		D3S1608	0.209	0.10	0.210	0.10
GLC1C	GTas11	D3S3637	0.643	0.10	0.642	0.10
GLC1C		D3S1301	0.244	0.10	0.245	0.10
GLC1C		D3S3694	0.680	0.10	0.627	0.10
GLC1C		D3S1569	neg	-	neg	-
GLC1C		D3S1608	0.100	0.10	0.100	0.10
GLC1C	GTas121	D3S3637	0.034	0.40	0.034	0.40
GLC1C		D3S1301	0.287	0.10	0.290	0.10
GLC1C		D3S3694	neg	-	neg	-
GLC1C		D3S1569	0.369	0.10	0.381	0.10
GLC1C		D3S1608	0.323	0.10	0.322	0.10
GLC1D	GTas04	D8S1749	0.053	0.30	0.051	0.30
GLC1D		D8S556	0.210	0.10	0.204	0.10
GLC1D		D8S198	0.415	0.10	0.412	0.10
GLC1D	GTas11	D8S1749	0.340	0.10	0.339	0.10
GLC1D		D8S556	0.050	0.20	0.053	0.20
GLC1D		D8S198	0.580	0.10	0.575	0.10
GLC1E	GTas03	D10S1729	0.031	0.40	0.034	0.40
GLC1E		D10S1713	0.082	0.40	0.081	0.40
GLC1E		D10S1691	0.218	0.10	0.218	0.10
GLC1E		D10S547	0.128	0.10	0.128	0.10
GLC1E		D10S1664	**1.340**	0.10	**1.336**	0.10
GLC1E	*GTas03a*	D10S1729	0.029	0.40	0.025	0.40
GLC1E		D10S1713	0.043	0.40	0.042	0.40
GLC1E		D10S1691	0.751	0.10	0.747	0.10
GLC1E		D10S547	0.030	0.10	0.033	0.01
GLC1E		D10S1664	0.401	0.10	0.397	0.10
GLC1E	*GTas03b*	D10S1729	neg	-	neg	-
GLC1E		D10S1713	neg	-	neg	-
GLC1E		D10S1691	neg	-	neg	-
GLC1E		D10S547	neg	-	neg	-
GLC1E		D10S1664	0.711	0.40	0.706	0.10
GLC1F	GTas37a	D7S2511	0.806	0.10	0.803	0.10
GLC1F		D7S505	neg	-	neg	-
GLC1F		D7S2439	0.298	0.20	0.296	0.20
GLC1F		D7S2546	0.026	0.40	0.025	0.40

Table 4.19 - FASTLINK exact two-point parametric linkage results for select GIST pedigrees and regions

Bold: Maximum LOD scores greater than 1.

There was very little difference between the results obtained using the two different penetrance models, 0.90 and 0.75. The only exact two-point parametric results with LODs>1 were generated by family GTas03 and its sub-pedigree GTas03b. Family GTas03 produced a maximum LOD of 1.08 at the most proximal marker within the GLC1C region on chromosome 3 (D3S3637). When subdivided into two smaller pedigrees, the GTas03b branch produced an even larger LOD (1.34) at this marker, while the other branch (GTas03a) showed no evidence of linkage to this region (Table 4.19). Family GTas03 also produced a LOD of 1.34 at the most distal marker within the GLC1E region on chromosome 10 (D10S1664), but this score was greatly reduced in both sub pedigrees (Table 4.19). Neither of these results extended across more that one marker. There were no other results with LOD>1 identified using this exact two-point parametric approach.

4.6 Discussion

The first stage of the linkage analysis in this dataset was conducted using estimation based parametric and nonparametric analyses using the MCMC algorithm due to the complexity of the disease, the size of the available pedigrees, the number of markers under investigation and the desire for multipoint analyses. These analyses were used to provide first-pass linkage results for follow-up analysis, and since this approach can result in more conservative results than exact methods (Sobel and Lange 1996), low thresholds for follow-up analyses were set. Based on the first pass MCMC based analyses, two pedigrees were selected for additional genotyping and follow-up analyses. Family GTas15 produced p-values of 0.05-0.07 for three markers within the GLC1B region on chromosome 2 (D2S2264 to D2S1892) in the nonparametric analysis described in section 4.5.3. In the parametric analysis, this pedigree produced a maximum location score of 1.12 on chromosome 2 corresponding to marker D2S1892,

as described in section 4.5.4. Family GTas35 produced p-values of 0.05-0.06 for three markers within the GLC1E region on chromosome 10 (D10S1691 to D10S1664) in the nonparametric analysis described in section 4.5.3. The parametric analysis generated a peak location score of 1.43, also on chromosome 10, at marker D10S1664 (section 4.5.4). These two pedigrees were selected for additional genotyping and follow-up analyses, described in Chapter 5.

There were several other moderately suggestive results generated by the first pass analyses. Families GTas03 and GTas11 produced p-values less than 0.05 at the proximal end of the GLC1C locus on chromosome 3 while family GTas121 produced a p-value of 0.04 for marker D3S1569 at the distal end of the GLC1C locus in the initial nonparametric analysis (section 4.5.3). Family GTas121 also generated a location score of 1.08 at marker D3S1569 in the first pass parametric analysis, however neither GTas03 of GTas11 showed any evidence for linkage in the first pass parametric analyses for chromosome 3. Several other pedigrees also showed weakly positive results in the initial SimWalk2 analyses. Since none of these remaining pedigrees were to be followed-up in this investigation, they were used as a basis for an exploration of additional statistical analyses. The rationale behind this approach was partially to extract any additional linkage information, but also to compare the results of some exact statistical methodologies with the performance of the MCMC based analyses. In general, the SimWalk2 and exact GeneHunter nonparametric analyses compared favourably, for example GTas11 produced an exact p-value of 0.031 in GeneHunter compared with 0.04 in SimWalk2, and GTas121 produced a p-value of 0.033 in GeneHunter compared with 0.05 in SimWalk2. Family GTas03, however, was more difficult to compare since GeneHunter was only able to process trimmed versions of each branch of the original pedigree, GTas03a and GTas03b, hence the GeneHunter p-

values did not approach the SimWalk2 result of p=0.03. The exact parametric analyses conducted using FASTLINK did not compare as favourably with the SimWalk2 estimation based results, however it is important to note that due to the capacity of FASTLINK and server memory constraints, the exact parametric analyses were two-point analyses whereas the SimWalk2 analyses were multipoint. The location score of 1.03 obtained in the SimWalk2 analysis for family GTas121 at marker D3S1608 dropped to a LOD of 0.32 in the exact two-point FASTLINK analysis. Similarly, the SimWalk2 location score of 1.10 for family GTas37a at marker D7S2511 dropped to a LOD of 0.81 in the two-point FASTLINK analysis. Conversely, GTas03 and its sub-pedigree GTas03b produced LODs greater than 1 at marker D3S3637 in the two-point FASTLINK analysis compared with a location score of only 0.78 in the SimWalk2 analysis. GTas03 also generated a LOD of 1.34 at marker D10S1664 in the two-point FASTLINK analysis compared with a multipoint location score of 0.91. The differences in these results may be indicative of type 1 error. Of course, taking into account multiple testing would also eradicate the significance of any of the remaining results. However, these findings are useful in the selection of families and methods for further study in future explorations of the GIST.

All statistical calculations in this dissertation were performed using a Sun Microsystems Enterprise 450 server with 4 Ultrasparc-II 480MHz central processing units, 4GB of RAM and 144GB of disk space, running Solaris 8. Server speed and memory constraints were a consideration in the selection of the most appropriate statistical analysis methodology. The simulation analyses were power restricted, due in part to pedigree size, but most significantly to the presence of loops in the pedigree. The smallest of the pedigrees (GTas11) took less that three minutes to complete 1000 replicates, while the largest (GTas03), containing multiple loops, took 1625 hours (68

days) to complete only 500 replicates. While FASTLINK can theoretically analyse several markers in a multipoint parametric analysis, in practice our analyses were restricted to two-point only. Two-point analysis of the largest of the pedigrees analysed in this chapter, GTas03 (including several loops), took an average of 16 minutes to complete. The same analysis model with an additional marker included (two-marker multipoint) showed no signs of nearing completion after 60 days. In comparison, all of the MCMC based SimWalk2 analyses were completed within an acceptable timeframe using this server. For example, multipoint nonparametric analysis of the entire pedigree dataset (all pedigrees including all individuals), with all five markers on chromosome 2, took a total of six hours to complete. This made it possible to easily rerun analyses with different random seeds to reduce the chances of spurious results due to poor mixing (although we found no evidence of poor mixing or spurious results in the SimWalk2 parametric and nonparametric analyses in this study; data not shown). However, analysis processing time is often trivial when compared with the time required for study design and initiation, sample collection, processing and genetic data extraction.

Extended pedigrees may be powerful assets in the detection of disease loci (Wijsman and Amos 1997), however such datasets are also notoriously difficult to analyse, due to the number of possible configurations consistent with the available data, each of which has to be considered for an exact result. The Elston-Stewart algorithm (Elston and Stewart 1971) employed in the analysis programs LINKAGE and FASTLINK is an exact approach that is not affected by pedigree size, but is restricted by the number of markers and the presence of loops and missing data. In this study, a maximum of three markers could be analysed due to server memory restrictions, and less in the presence of loops. The Lander-Green algorithm (Lander and Green 1987), used in the analysis program GeneHunter, is also an exact approach but is restricted by the size of the

pedigree. GeneHunter-Plus can analyse a maximum of 20 bits. In this study, all but family GTas11 had to be manually trimmed prior to exact nonparametric linkage analysis. The analysis program Merlin (Abecasis *et al.* 2002) can analyse larger pedigrees than GeneHunter, using a Lander-Green algorithm with sparse binary trees, however memory constraint on our server restricted Merlin to approximately 23 bits, which was not enough of an improvement to replace GeneHunter for routine analyses. The Markov chain Monte Carlo based analyses employed by SimWalk2 (Sobel and Lange 1996) appear to be the most appropriate solution to the analysis of the selected GIST pedigrees based on pedigree size and complexity, the availability of genetic data, and the increased power of multipoint analyses. SimWalk2 is practically unrestricted by pedigree size or the number of markers. The MCMC algorithm employed by SimWalk2 is able to analyse extended pedigrees because it considers the underlying configurations consistent with the available data in proportion to their likelihood, hence configurations that are theoretically possible but highly unlikely may not be considered. SimWalk2 includes a second speed up by using the MCMC algorithm on the set of genetic descent graphs (inheritance vectors), the paths of gene flow rather than the complete data arrangements, reducing the space of the underlying configurations (Sobel and Lange 1996).

Compared with a collection of independent nuclear families, a single extended pedigree may contain more linkage information, less etiologic heterogeneity, and provide a greater possibility of identifying genotyping errors. While the genotyping error rates in this dataset were low, even small error rates have been shown to have a large impact on linkage results (Douglas *et al.* 2000; Abecasis *et al.* 2001) and can affect trait localisation (Terwilliger *et al.* 1990) if not removed prior to analysis. These effects might be even greater in large pedigrees, particularly with missing inheritance

information such as unrecruited spouses. There appeared to be no fundamental errors in the pedigree structures of the families included in this study since the Mendelian genotyping errors did not cluster in any particular pedigree or individual. Due to the limited availability of genotypic data in this study we were unable to use statistical approaches such as PREST (McPeek and Sun 2000) to check likely pedigree relationships. Genome-wide scan data is required for such approaches to be reliable. The first round of genotyping revealed that some of the selected microsatellite markers were more prone to error due to poor, non-specific or differential allelic amplification. Markers D2S2264, D3S1569, D7S2439 and D10S1713 were subsequently re-optimised and re-genotyped due to the high locus-specific error rates for these markers. Removal of these markers from the initial genotyping dataset reduced the overall Mendelian error rate to approximately 1.4% (an average of three to four errors per marker). Other possible causes of Mendelian error include: interference from dye peaks within the allele size range of interest or interference from a broad peak at approximately 200bp in the blue channel caused by the use of old formamide; interference from stutter peaks caused by polymerase slippage during elongation (especially in the case of adjacent allele heterozygotes) and incorrect peak height (too small or too large) due to variations in sample concentration.

It has been estimated that approximately 40% of genotyping errors are Mendelian consistent (Douglas *et al.* 2002), and that Mendelian consistent error checking is an important part of data cleaning prior to analysis (Sobel *et al.* 2002). In this study the Mendelian consistent error rate was approximately one third of the overall error rate. The majority of Mendelian consistent errors detected by SimWalk2 were the result of false homozygosity due to differential allelic amplification. Proposed causes of this artefact include differences in allele length or GC richness, low template concentration

producing stochastic fluctuations in copy number for each allele, and the existence of polymorphisms interfering with primer binding (Walsh *et al.* 1992). Figure 4.1 displays Genotyper® data that are an example of mistyping due to differential allelic amplification. In these cases, reanalysis of apparently homozygous genotypes revealed the presence of a second, much smaller allele that was missed during the initial typing. In Panel A of Figure 4.1, Individual 1 was initially scored as homozygous for the 275bp allele; there is a small second peak at the 287bp which has not been labelled due to its size (peak height) relative to the 275bp peak. In Panel B of Figure 4.1, re-genotyping of Individual 1 clearly reveals the presence of a second allele at 287bp. During the typing process, recognition of the fact that marker alleles consisting of a large number of repeats are know to amplify less efficiently than alleles of few repeats may have helped to eliminate some of these errors in the initial stages of genotyping. On average, false homozygosity was detected at a rate of 2 occurrences per marker, although due to the unique peak pattern of each marker some were much more likely than others to present with allele dropout.

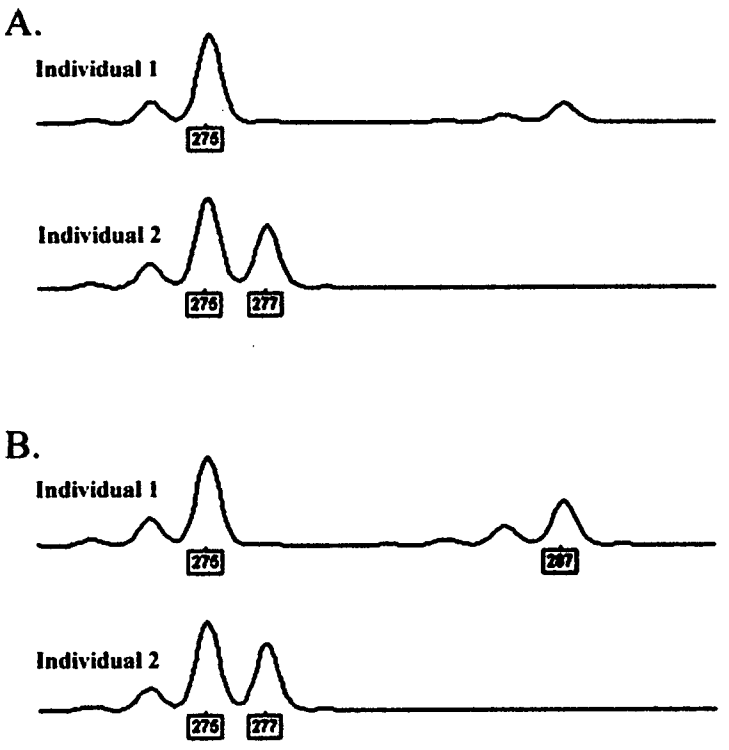

Figure 4.1 - Genotyping error due to false homozygosity (differential allelic amplification)

Genotyper ® data from the HEX-labelled marker D3S1569.

Panel A shows the initial genotyping data for two individuals; Individual 1 (3-60) has been scored as homozygous for the 275bp allele and Individual 2 (3-61) as heterozygous for the 275 and 277bp alleles.

Panel B shows the repeat genotyping data for these individuals, with individual 1 scored as heterozygous for the 275 and 287bp alleles.

POAG is an insidious disease with a late age of onset which often makes ascertaining large, multigenerational families difficult, especially when it comes to collecting relevant clinical data across generations. The GIST pedigrees contained much 'missing' information in the form of individuals in the pedigrees with no clinical or genetic information. A more complex parametric model may have helped to compensate for this lack of information, by utilising liability classes and age dependent penetrances in place of the simplistic model derived from previous studies of POAG. The most critical type of missing data in this study appeared to be due to lack of genetic information from individuals married in to the pedigrees (unaffected spouses), who had neither blood nor clinical data collected during the GIST. The collection of information from married in individuals was not included in the GIST protocols. This missing information increases the number of possible descent state configurations, decreases the power of estimated results and complicates phase determination. A repeat of the simulation process described in 4.4.1, but with spouses of available individuals included (for example individual 18, husband of 3-7 in GTas03; Figure 2.2) was run in order to gain some understanding of the effect the addition of these individuals may create. Only spouses of individuals classed as 'available' were included, as it is more likely that these spouses are also alive and available. An average of four to five individuals were changed from 'unavailable' to 'available' in each pedigree. GTas03 was not included in this simulation due to its size and analysis time, however the subdivided pedigrees GTas03a and GTas03b were included. The simulation results are shown in Table 4.20, including an updated count of the number of 'available' individuals (with the number of spouses added shown in brackets). Across the entire dataset, the maximum simulated LOD score increased by an average of 0.24 ($p=0.28$; not significant) and the average LOD score was unchanged. While this result is not significant, it is nonetheless an increase. What may not have been improved in terms of LOD increases by the addition

of this information might still be gained in terms of more accurate results and phase determination. A more effective way to compensate for missing pedigree information may be to use a denser marker map such as a SNP array (Evans and Cardon 2004; Evans *et al.* 2004). However, it is most important to note that these simulations have limited value in terms of the information they provide to this investigation. The simulation methodology used is intrinsically parametric and only provides two-point information with a theoretical marker, which does not emulate the dominant analysis methodology used in the study; hence these simulations were only used to provide an overall indication of the likely utility of these pedigrees for linkage analysis.

Family ID	Total	Available	Affected	Original Maximum LOD	New Maximum LOD	Average LOD	New Average LOD
GTas03a	76	48 (9)	9	**3.73**	**4.45**	1.42	1.44
GTas03b#	41	23 (4)	6	1.86	2.14	0.66	0.71
GTas04#	45	32 (7)	9	2.59	2.70	0.99	0.95
GTas35	32	18 (3)	6	1.71	2.92	0.73	0.70
GTas37a	51	35 (6)	8	**3.29**	**3.65**	1.22	1.20
GTas37b#	37	26 (2)	15	**4.17**	**4.29**	1.73	1.68
GTas54	35	19 (2)	7	**3.75**	**2.90**	1.13	1.08
GTas11	15	13 (3)	5	1.19	1.18	0.59	0.58
GTas15	31	17 (3)	6	**3.14**	**3.04**	1.12	1.12
GTas17	45	29 (3)	9	**3.34**	**3.99**	1.26	1.21
GTas121	45	23 (5)	7	2.57	2.71	0.98	0.99

Table 4.20 - Maximum LOD simulations for the GIST pedigrees including married-in individuals

# indicates the pedigree has had at least one loop broken prior to simulation.

Bold: LOD>3.

Chapter 5 – Follow-up Analysis and Fine-Mapping of the GLC1B Locus in Family GTas15 and the GLC1E Locus in Family GTas35

5.1 Preface

Sections of this chapter were published in *Ophthalmologica* (Karger) in 2006. The article, entitled 'Confirmation of the adult-onset primary open-angle glaucoma locus GLC1B at 2cen-q13 in an Australian family' (Charlesworth *et al.* 2006), is included in this dissertation as Appendix 3. This chapter also expands on work published in *Human Mutation* (Sale *et al.* 2002).

5.2 Aims

The aims of the work described in this chapter were: to undertake follow-up analysis, including additional genotyping, on the pedigrees and regions of interest identified in Chapter 4.5.6, namely family GTas15 at the GLC1B locus on chromosome 2 and GTas35 at the GLC1E locus on chromosome 10. In particular, the objectives were: to select additional microsatellite markers within the GLC1B region on chromosome 2 and the GLC1E region on chromosome 10 with a final average marker spacing of 1-2 cM within each region; to perform nonparametric multipoint linkage analyses on the new marker datasets, and to generate the most likely haplotypes and search for refined regions of interest.

5.3 Methods

5.3.1 Microsatellite marker selection

Microsatellite markers were selected to fine-map the distal ends of the GLC1B locus on chromosome 2cen-q13 and the GLC1E locus on chromosome 10p15-p14, at a final average marker spacing of 1-2 cM. The primary map source used for marker selection

was the deCODE genetic map (Kong *et al.* 2002), with missing marker locations and distances inferred from the Marshfield genetic map (Broman *et al.* 1998), the Location DataBase integrated maps (Collins *et al.* 1996; Ke *et al.* 2001) and the human genome sequence (Build 34). Heterogeneity information from the Genome Database (http://www.gdb.org/), availability of typed genotyping controls from the Centre d'Etude du Polymorphisme Humain (CEPH; http://www.cephb.fr/cephdb), and marker location and spacing, were used to weight marker choice.

The final set of markers used to fine-map the GLC1B and GLC1E regions are shown in Tables 5.1 and 5.2 respectively. The tables show the POAG loci and chromosomal regions, as well as marker locations and heterozygosities. The addition of 6 markers within the GLC1B region resulted in a final set of 11 microsatellite markers at an average density of 1.6 cM across this 18 cM region (Table 5.1). An additional 7 markers were selected within the GLC1E region, resulting in a total of 12 microsatellite markers at an average density of 1.9 cM across this 22 cM region (Table 5.2).

Marker	Distance from first marker (cM)*	Heterozygosity†
D2S2161	0	0.77
D2S113	3.00	0.77
D2S2187	4.68	0.63
D2S2264	7.32	0.77
D2S373	7.82	0.74
D2S2364	9.97	0.66
D2S1897	10.97	0.89
D2S1890	13.68	0.74
D2S1893	14.68	0.75
D2S1892	16.57	0.80
D2S2269	17.63	0.88

Table 5.1 - The final set of 11 microsatellite markers used to fine-map the GLC1B locus on chromosome 2cen-q13 in family GTas15

Bold: The original markers selected in Chapter 4.

*Location in centiMorgans relative to the first marker, primarily based on the deCODE genetic map (Kong *et al.* 2002).

†Heterozygosity based on CEPH data (http://www.cephb.fr/cephdb).

Marker	Distance from first marker (cM)*	Heterozygosity†
D10S1729	0	0.72
D10S1713	0.59	0.60
D10S189	4.52	0.73
D10S1619	5.75	0.67
D10S1779	7.63	0.82
D10S1649	10.54	0.84
D10S547	12.70	0.74
D10S585	13.58	0.69
D10S570[#]	16.69	0.81
D10S223	19.07	0.66
D10S1664	20.78	0.75
D10S1653	22.88	0.78

Table 5.2 - The final set of 11 microsatellite markers used to fine-map the GLC1B locus on chromosome 10p15-p14 in family GTas35

Bold: The original markers selected in Chapter 4.

*Location in centimorgans relative to the first marker, primarily based on the deCODE genetic map (Kong et al. 2002).

†Heterozygosity based on CEPH data (http://www.cephb.fr/cephdb).

[#]*OPTN* is located on this map between markers D10S570 and D10S223, at approximately 17.1 cM.

5.3.2 Genotyping methods and error checking

The genotyping methodology used is described in Chapter 4.3.2. Genotype error checking was conducted as described in Chapter 4.3.3.

5.3.3 Allele frequency generation

Marker allele frequencies for linkage analysis were derived from a set of 72 elderly glaucoma-free individuals (described in Chapter 2.2.3) genotyped with each of the 13 additional microsatellite markers selected for fine-mapping of GLC1B and GLC1E.

5.3.4 Data storage and file generation

As described in Chapter 4.3.5, all individual, family, genotype, phenotype and genetic map data were stored in a dedicated database program developed by Tim Albion (Menzies Research Institute, unpublished). The linkage utility program MEGA2 (Mukhopadhyay *et al.* 2005b) was used to generate program specific input files for the analysis programs described in this chapter.

5.3.5 **IL1B** *mutation screening in family GTas15*

We screened a synonymous interleukin 1 beta (*IL1B*) exon 5 polymorphism in all available members of GTas15 using the method described by Lin *et al.* (2003). The *IL1B* polymorphism is a T to C transition at base 3953 that disrupts a *TaqI* restriction site. The region of exon 5 containing the polymorphism was PCR amplified according to the methods described in Chapter 3.2, with the primers described by Lin *et al.* (2003), and digested with the *TaqI* enzyme (New England Biolabs). Digest products were electrophoresed on a 1.5% agarose gel containing 0.3ng/ml ethidium bromide and viewed under 100% UV light. The E1 allele consisted of the digested product, visible

as two bands corresponding to 114 and 135bp fragments while the E2 allele was visible as a 249bp undigested fragment.

5.3.6 1410delC PAX6 *mutation screening in family GTas35*

A novel mutation in exon 12 of the *PAX6* gene (1410delC) was identified by Sale *et al.* in 2002. This mutation was investigated in all available members of GTas35 by direct automated sequencing using ABI PRISM BigDye Terminator Cycle Sequencing Kits (Applied Biosystems) and a set of previously published exon 12 primers (Love *et al.* 1998), according to the sequencing methodology described in Chapter 3.5.

5.3.7 MYOC *Phe4Ser polymorphism screening in family GTas35*

The Phe4Ser *MYOC* polymorphism was originally detected by Fingert *et al.* (1999). This change was investigated in all available members of GTas35 by direct automated sequencing using ABI PRISM BigDye Terminator Cycle Sequencing Kits (Applied Biosystems) and a set of previously published *MYOC* exon 1 primers (Alward *et al.* 1998) according to the sequencing methodology described in Chapter 3.5. Was also investigated this polymorphism in 23 available individuals from a Tasmanian family segregating aniridia (MIM#106200) described by Sale *et al.* (2002).

5.4 Statistical methods

5.4.1 Nonparametric linkage analyses

Multipoint MCMC estimation based nonparametric linkage analyses were conducted using SimWalk2 version 2.91 (Sobel and Lange 1996), as described in Chapter 4.4.2 - 4.4.3. Multipoint analyses, utilising information from the entire set of genotyped individuals within the pedigree, were conducted using the set of 11 markers within the

GLC1B region in family GTas15 and the 12 markers within the GLC1E region in family GTas35.

Exact nonparametric linkage analyses were conducted using GeneHunter-Plus version 1.2 (Kruglyak *et al.* 1996; Kong and Cox 1997), as described in Chapter 4.4.7. Family GTas15 was trimmed from its original 29 bits (11 founders and 20 non-founders) to a 16 bit version by removing eight non-founders (18, 19, 15-08, 15-09, 15-10, 15-13, 15-14 and 15-15) and three founders (36, 37 and 44). Family GTas35 was trimmed from 31 bits in its original form to 20 bits for analyses with GeneHunter, by removing seven non-founders (35-01, 35-09, 35-10, 35-12, 35-13, 35-14 and 35-15), and three founders (17, 252 and 452). No affected individuals were removed from either pedigree.

5.4.2 Haplotype generation and analysis

The most likely haplotypes for the GLC1B region in family GTas15 and the GLC1E region in family GTas35, taking account of information from all genotyped individuals, were estimated using the haplotyping component of SimWalk2 version 2.86-2.91 (Sobel and Lange 1996) as described in Chapter 4.4.5.

Haplotypes were displayed using Pedigree/Draw 5.1 (SFBR; http://www.sfbr.org/sfbr/public/software/pedraw/peddrw.html now available from http://www.pedigree-draw.com).

5.5 Results

5.5.1 GTas15 pedigree and clinical data

Family GTas15 contained seven individuals with clinically diagnosed POAG; individuals 15-01, 15-02, 15-03, 15-07, 15-11, 15-12 and 15-16. The clinical features

of family GTas15 are represented in Figure 2.6. One individual (15-04) presented with characteristic visual field loss and could have been considered a glaucoma suspect. However, for our model free, affecteds-only approach it was not necessary to determine whether the remaining family members were glaucoma suspects or truly unaffected; this can be difficult given the late onset and subtleties of POAG. All other individuals were therefore classed as glaucoma status "unknown" for the purposes of the linkage analyses.

The POAG within family GTas15 appears to be transmitted in an autosomal dominant fashion. All affected members of GTas15 and one glaucoma suspect (15-04) presented with characteristic visual field loss. Raised IOP was not present in three of the seven affected individuals, and two of the affected individuals (15-01 and 15-16) had equivocal optic disc appearances in the presence of visual field loss. The monozygotic twins 15-01 and 15-02 differed clinically in the appearance of their optic discs, however as they were genetically identical and both classified as "affected", 15-02 was not included in the genetic analyses. The mean age of diagnosis within the family was 55 years, ranging from 47 to 60 years. Several individuals had their POAG diagnosed as a direct result of the family study.

5.5.2 GTas35 pedigree and clinical data

Family GTas35 contained six individuals with clinically diagnosed POAG; individuals 35-03, 35-04, 35-05, 35-07, 35-08 and 35-11. The clinical features of family GTas35 are represented in Figure 2.8. Two individuals presented with ocular hypertension (raised IOP; 35-06 and 35-10), and two with optic disc abnormalities characteristic of POAG but without other indicators of the disease (35-12 and 35-13). All four of these

individuals could have been considered glaucoma suspects, but were classed as glaucoma status "unknown" for the purposes of the linkage analyses.

All affected members of GTas35 presented with raised IOP. Of the individuals with clinically diagnosed POAG, 35-08 and 35-11 presented with optic disc abnormalities without apparent visual field loss at the time of the investigation. Similarly, clinically diagnosed cases 35-03 and 35-04 had equivocal optic disc appearances in the presence of visual field loss (Figure 2.8). The mean age of diagnosis within the family was 59 years, ranging from 46 to 74 years, with several individuals diagnosed as a direct result of the family study.

During the course of this investigation we determined that family GTas35 is connected to another Tasmanian pedigree with aniridia. Aniridia (MIM#106200) is a rare panocular developmental disorder typically diagnosed postnatally by bilateral absence of the iris, although iris remnants may be observed. About two thirds of cases are familial, with autosomal dominant inheritance, high penetrance and variable expressivity (Hanson and Van Heyningen 1995). Aniridia is caused by mutations of the *PAX6* gene (MIM#607108) (Ton *et al.* 1991; Jordan *et al.* 1992) located on chromosome 11p13. We detected a novel 1410delC *PAX6* mutation in an extended Tasmanian pedigree, as described in Sale *et al.* (2002). The deletion was identified in all 9 aniridia cased in family AN1, and in one individual unavailable for ophthalmological examination (AN1-15), and not detected in seven unaffected individuals (Sale *et al.* 2002). Using genealogical records from the GIST database we determined that family AN1 was connected to family GTas35, as shown in Figure 5.1.

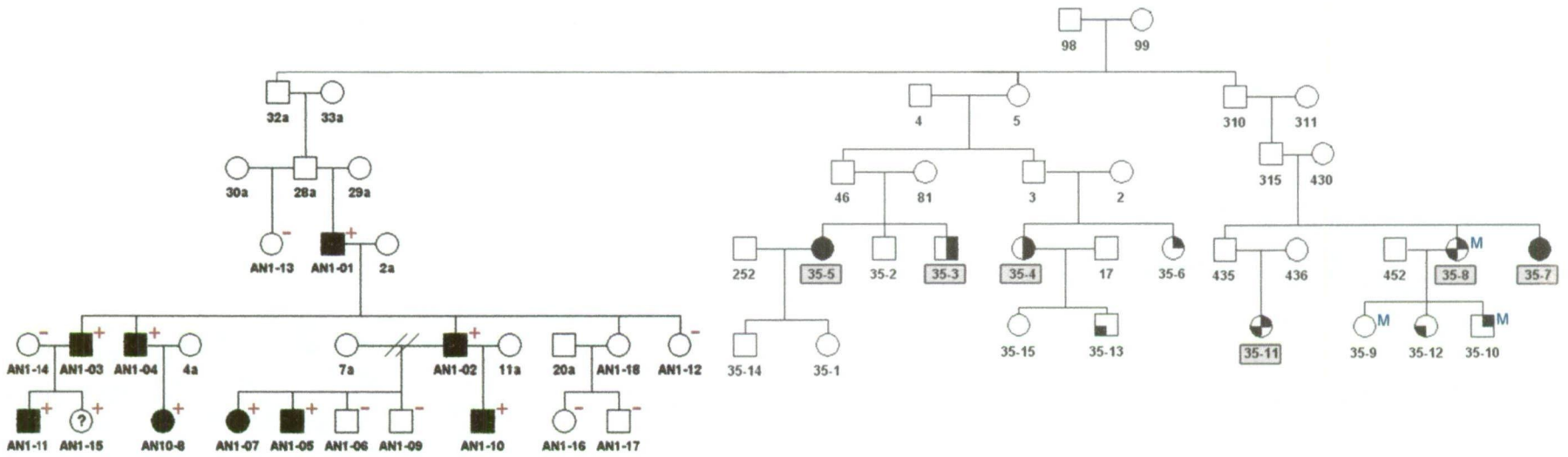

Figure 5.1 - Family GTas35 linked to the aniridia pedigree AN1

The aniridia pedigree AN1 is located to the left of the figure, with affected individuals fully shaded. Available individuals have ID numbers beginning in AN1-. Family GTas35 is located to the right of the image. More information on this family is given in the original Figure 2.8. Individuals 98 and 99 are the common founders linking the two pedigrees.

+ denotes the presence of the 1410decC *PAX6* mutation.

- denotes the absence of the 1410decC *PAX6* mutation.

M denotes the presence of the Phe4Ser *MYOC* polymorphism

5.5.3 Nonparametric linkage analyses of GTas15 at GLC1B

SimWalk2 MCMC based multipoint nonparametric analysis of the 11 markers within the GLC1B region on chromosome 2cen-q13 produced empirical p-values of 0.01 or less at five markers, flanked by D2S1897 and D2S2269, as shown in Table 5.3. The lowest empirical p-value produced by SimWalk2 was 0.009 at marker D2S1897 (Table 5.3).

GeneHunter produced p-values of 0.01 or less at four markers, flanked by D2S1897 and D2S1892 (shown in Table 5.4), with an exact p-value of 0.005 at marker D2S1897, the same marker that generated the lowest p-value in SimWalk2.

Marker	Distance from first marker (cM)	Empirical p-value for Statistic E
D2S2161	0.00	0.34
D2S113	3.00	0.06
D2S2187	4.68	0.06
D2S2264	7.32	0.04
D2S373	7.82	0.03
D2S2364	9.97	0.02
D2S1897	10.97	**0.009**
D2S1890	13.68	**0.01**
D2S1893	14.68	**0.01**
D2S1892	16.57	**0.01**
D2S2269	17.63	**0.01**

Table 5.3 - SimWalk2 empirical p-values for statistic E at the GLC1B locus (2cen-q13) in family GTas15

Bold: The original markers selected in Chapter 4 and p-values≤0.01.

Marker	Distance from first marker (cM)	Exact p-value for the NPL_{all} statistic
D2S2161	0.00	0.35
D2S113	3.00	0.06
D2S2187	4.68	0.06
D2S2264	7.32	0.05
D2S373	7.82	0.05
D2S2364	9.97	0.03
D2S1897	10.97	**0.005**
D2S1890	13.68	**0.01**
D2S1893	14.68	**0.01**
D2S1892	16.57	**0.01**
D2S2269	17.63	0.03

Table 5.4 - GeneHunter-Plus exact p-values for the NPL_{all} statistic at the GLC1B locus (2cen-q13) in family GTas15

Bold: The original markers selected in Chapter 4 and p-values ≤ 0.01.

5.5.4 Nonparametric linkage analyses of GTas35 at GLC1E

SimWalk2 MCMC based multipoint nonparametric analysis of the 12 markers within the GLC1E region on chromosome 10p15-p14 produced non-significant empirical p-values for all markers, as shown in Table 5.5. The smallest empirical p-value produced by SimWalk2 was 0.23 at marker D10S1649 (Table 5.5).

GeneHunter also produced non-significant p-values at all markers on chromosome 10p15-p14 (shown in Table 5.6).

Marker	Distance from first marker (cM)	Empirical p-value for Statistic E
D10S1729	0	0.48
D10S1713	0.59	0.48
D10S189	4.52	0.46
D10S1691	5.75	0.52
D10S1779	7.63	0.30
D10S1649	10.54	0.23
D10S547	12.70	0.36
D10S585	13.58	0.40
D10S570	16.69	0.40
D10S223	19.07	0.45
D10S1664	20.78	0.50
D10S1653	22.88	0.48

Table 5.5 - SimWalk2 empirical p-values for statistic E at the GLC1E locus (10p15-p14) in family GTas35

Bold: The original markers selected in Chapter 4.

Marker	Distance from first marker (cM)	Exact p-value for the NPL_{all} statistic
D10S1729	0	0.40
D10S1713	0.59	0.40
D10S189	4.52	0.40
D10S1691	5.75	0.32
D10S1779	7.63	0.55
D10S1649	10.54	0.55
D10S547	12.70	0.40
D10S585	13.58	0.40
D10S570	16.69	0.40
D10S223	19.07	0.40
D10S1664	20.78	0.32
D10S1653	22.88	0.32

Table 5.6 - GeneHunter-Plus exact p-values for the NPL_{all} statistic at the GLC1E locus (10p15-p14) in family GTas35

Bold: The original markers selected in Chapter 4.

5.5.5 Haplotype analysis of GTas15 at GLC1B

Haplotype reconstruction using SimWalk2, shown in Figure 5.2, revealed a shared haplotype of eight markers (flanked by D2S2264 and D2S2269) in six of the seven affected individuals (including the monozygotic twins), present in both arms of the pedigree. Two of the currently unaffected individuals carry the entire haplotype (15-10 and 15-14) while recombination events in another (15-08) have removed several alleles in the middle of the shared haplotype. Of these currently unaffected individuals, 15-08 and 15-10 were 43 and 45 years of age respectively at examination, below the mean age of diagnosis within the family (55 years; range 47-60 years), however 15-14 was aged 69, carries the full haplotype and showed no sign of glaucoma at the time of examination, indicating likely non-penetrance. Individual 15-04 also carries the full haplotype and although this individual's optic disc ratios were within normal limits, their clinical classification at age 79 years was as a glaucoma suspect based on visual field changes.

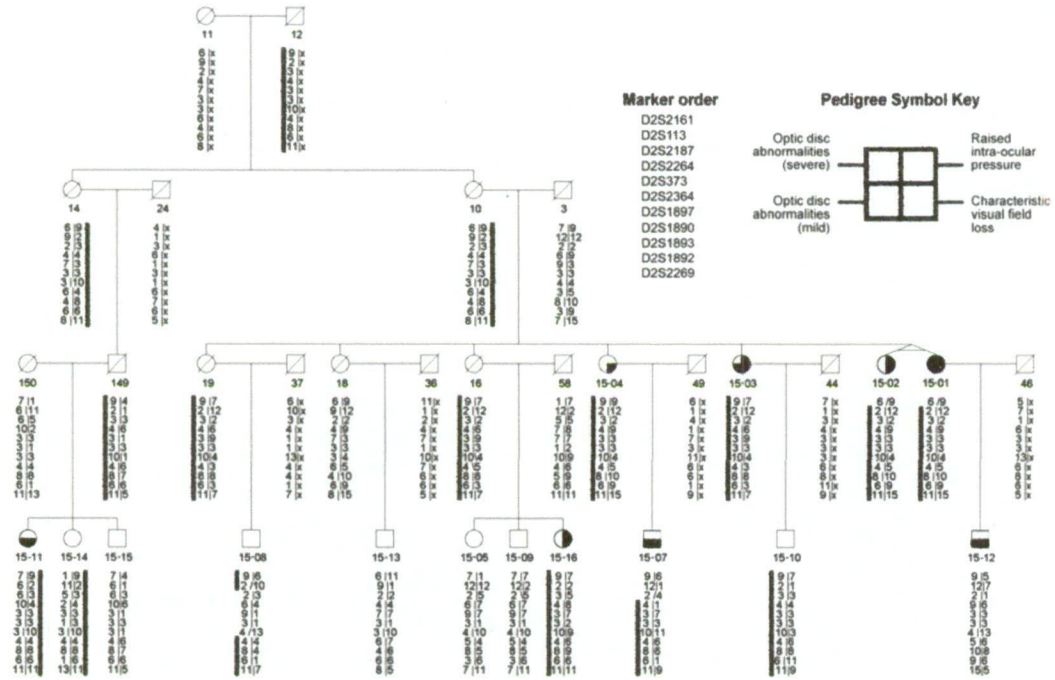

Figure 5.2 - GTas15 pedigree structure, clinical features and haplotype at the GLC1B locus

ID numbers commencing with "15-" indicate individuals who participated in the study. Filled quadrants indicate the clinical characteristics of POAG (Coote *et al.* 1996). A filled upper right quadrant indicates the presence of raised intra-ocular pressure; the bottom right quadrant indicates characteristic visual field loss. The left quadrants indicate optic disc abnormalities characteristic of POAG and are filled from bottom (mild) to top (severe). Individuals with two or more filled quadrants have been classified as affected for the linkage analysis while individuals with only one filled quadrant are glaucoma suspects and classified as unknown for linkage analyses. The haplotype of interest is marked by a vertical black bar. An unknown haplotype is denoted by an 'x'. Forward and backslashes between the haplotypes denote the direction of recombination events. Although confirmed monozygotic twins 15-01 and 15-02 are shown in the figure, individual 15-02 was removed from all linkage analyses.

5.5.6 Haplotype analysis of GTas35 at GLC1E

Haplotype reconstruction of the GLC1E locus in family GTas35 revealed no evidence of a shared haplotype across any of the branches of the family.

5.5.7 IL1B *mutation screening in family GTas15*

Two individuals from family GTas15 were found to carry the synonymous *IL1B* exon 5 polymorphism, determined by the presence of undigested product following the *TaqI* digest. The polymorphism was present in individual 15-07, the affected child of 15-04 (who does not carry the polymorphism) and individual 15-13 who is not affected and does not carry the haplotype of interest. Both individuals were heterozygous for the polymorphism. Figure 5.3 shows the digest results for family GTas15, with individual 15-07 in lane 07 and individual 15-13 in lane 13.

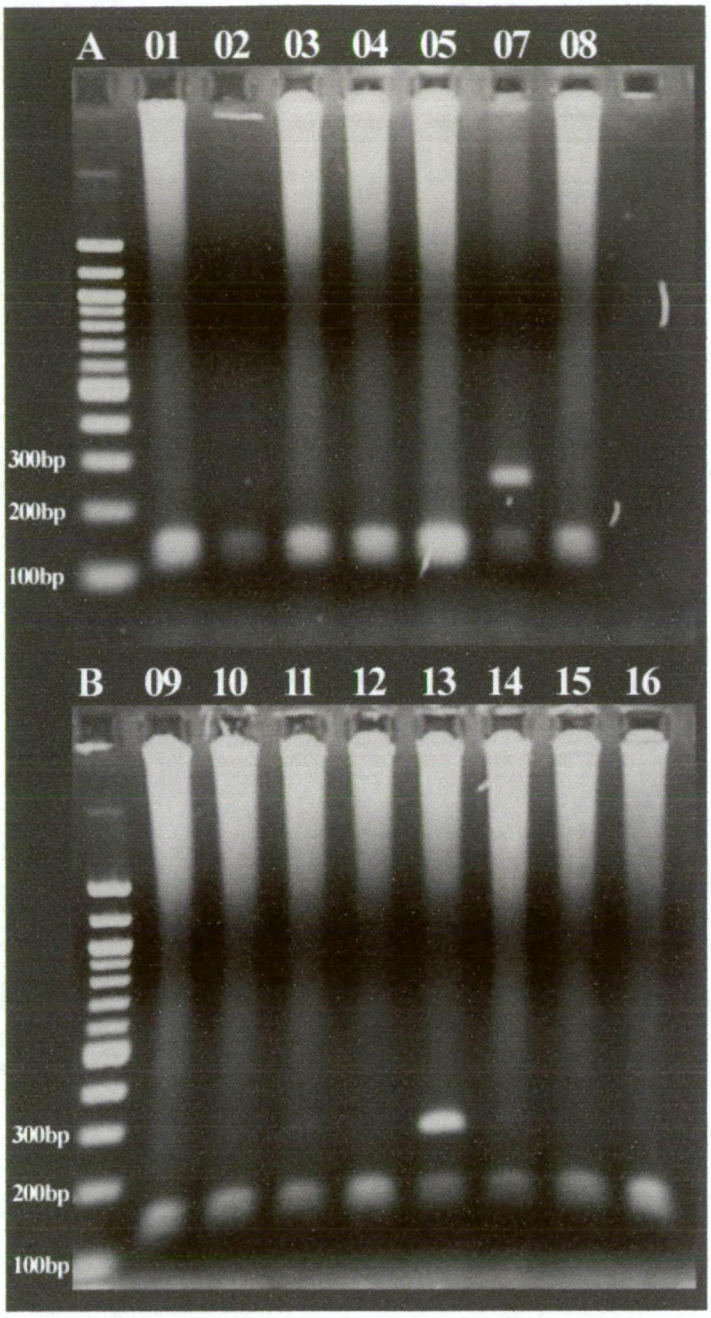

Figure 5.3 – Results of the *IL1B* exon 5 digested with *TaqI* in family GTas15

10µl of the *TaqI* digest products were electrophoresed on 1.5% agarose gel stained with ethidium bromide and photographed under 100% UV light. Lanes A and B contain a 100bp ladder size reference (Promega). All other lanes are labelled with the last two digits of their family ID number; for example, lane 01 denotes individual 15-01. The digested fragments at 114bp and 135bp are inseparable on this gel, and appear as a wide band between 100bp and 200bp. The undigested 249bp fragment is clearly visible in lanes 07 (individual 15-07) and 13 (individual 15-13).

5.5.8 1410delC PAX6 *mutation screening in family GTas35*

The *PAX6* 1410delC mutation was not detected in any of the 15 available individuals from family GTas35.

5.5.9 MYOC *Phe4Ser polymorphism screening in family GTas35*

The *MYOC* Phe4Ser polymorphism was originally detected in individual 35-08 by Fingert *et al.* (1998) when a subset of individual from the GIST were included as part of this multinational search for disease causing variants of the myocilin gene. Individual 35-08 was the only member of family GTas35 included in the original screen, hence in this study we screened all 15 available individuals (including 35-08).

The Phe4Ser *MYOC* polymorphism, was found in three individuals from family GTas35: 35-08 who had mild glaucoma at age 71 years, 35-09, who had no sign of ocular hypertension or glaucoma when last examined at age 45 years, and 35-10 who had ocular hypertension (peak IOP 23mmHg) at age 42 years (clinical features shown in Figure 2.8). The polymorphism was not detected in the remaining individuals from family GTas35 or in any of the 23 individuals from family AN1. An example of the sequence data is shown in Figure 5.4, including the wildtype sequence of individual 35-03 and the heterozygous sequence change from A to G in individual 35-08.

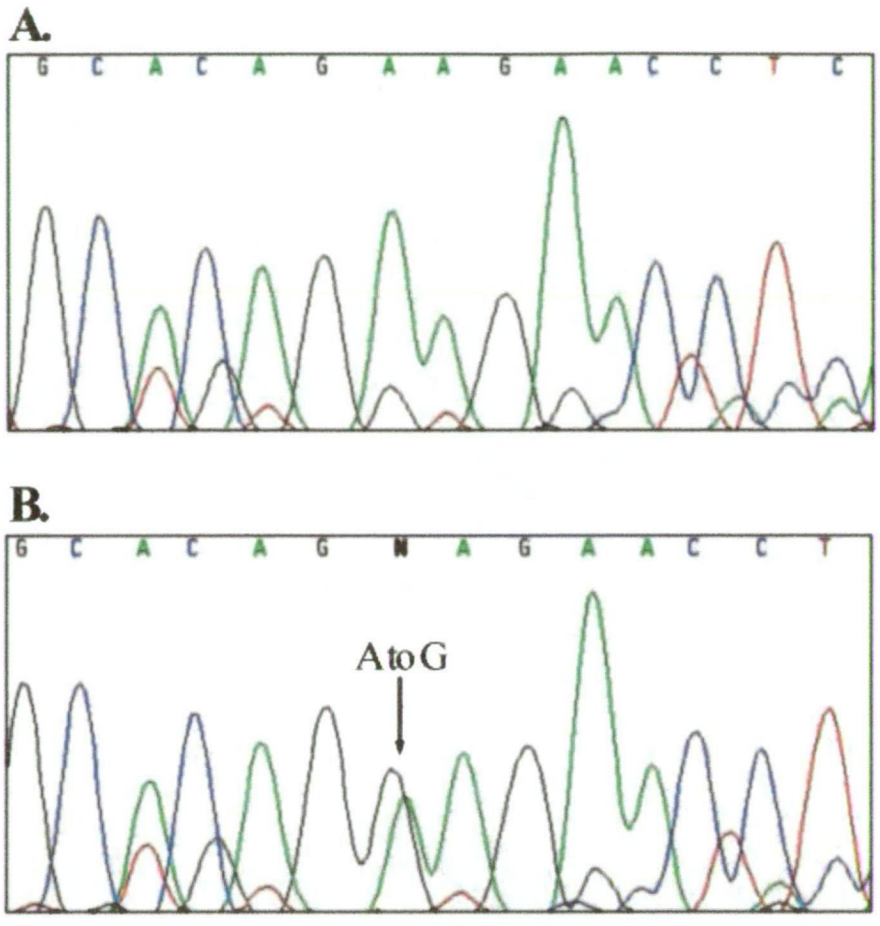

Figure 5.4 –*MYOC* Phe4Ser sequence data from family GTas35

Samples were electrophoresed on an ABI PRISM 310 Genetic Analyzer (Applied Biosystems).

Panel A shows wildtype sequence from individual 35-03.

Panel B shows the A to G change of the Phe4Ser polymorphism from individual 35-08.

5.6 Discussion

5.6.1 Linkage of GTas15 to GLC1B on chromosome 2

In Chapter 4 we found initial evidence for linkage to the GLC1B locus in family GTas15. Fine-mapping of this locus and follow-up analyses strengthened the evidence for linkage. The empirical p-values calculated using SimWalk2 (p=0.01 or less) and exact GeneHunter p-value (p=0.005) at the distal end of the region of interest provide supportive evidence for the existence of a POAG susceptibility locus at 2cen-q13.

The POAG locus GLC1B was originally identified by Stoilova *et al.* (1996) using six Caucasian families, predominantly from the United Kingdom, with three to seven affected individuals per family. Utilizing a penetrance model based approach, the maximum two-point LOD score was 6.48 at marker D2S113 (θ=0). The LOD score calculations were repeated for the affected meioses only to eliminate the effect of potential incomplete penetrance, which shifted the peak LOD distally to marker D2S373 (LOD of 3.40 at θ=0). Both these markers were used in our study, however the region of linkage in family GTas15 is located 2.8 cM distally, with the most significant evidence for linkage at marker D2S1897 (p = 0.005). An American Society of Human Genetics conference abstract of Raymond *et al.* (1999) using a large French-Canadian family identified a peak LOD of 2.97 at marker D2S388 (located between D2S2161 and D2S113), within the proximal portion of the GLC1B region, however no other information relating to the location of their haplotype of interest was provided (Raymond *et al.* 1999).

Fine-mapping and haplotype analysis by Stoilova *et al.* (1996) refined their smallest region of cosegregation to 11.2 cM flanked by D2S2161 and D2S176, however more recent genetic maps suggest a smaller distance of approximately 9.5 cM. A comparison

of the maps and critical regions from Stoilova *et al.* (1996) and our study are shown in Figure 5.5. The 8-marker shared haplotype from our study (flanked by D2S2264 and D2S2269) overlaps the lower portion of the original GLC1B region of interest and is of similar size (9.0 cM). The 8-marker haplotype commences within the critical region of Stoilova *et al.* (1996) at marker D2S2264; however the marker with the lowest p-values in our study (D2S1897) lies outside the overlapping region (Figure 5.5).

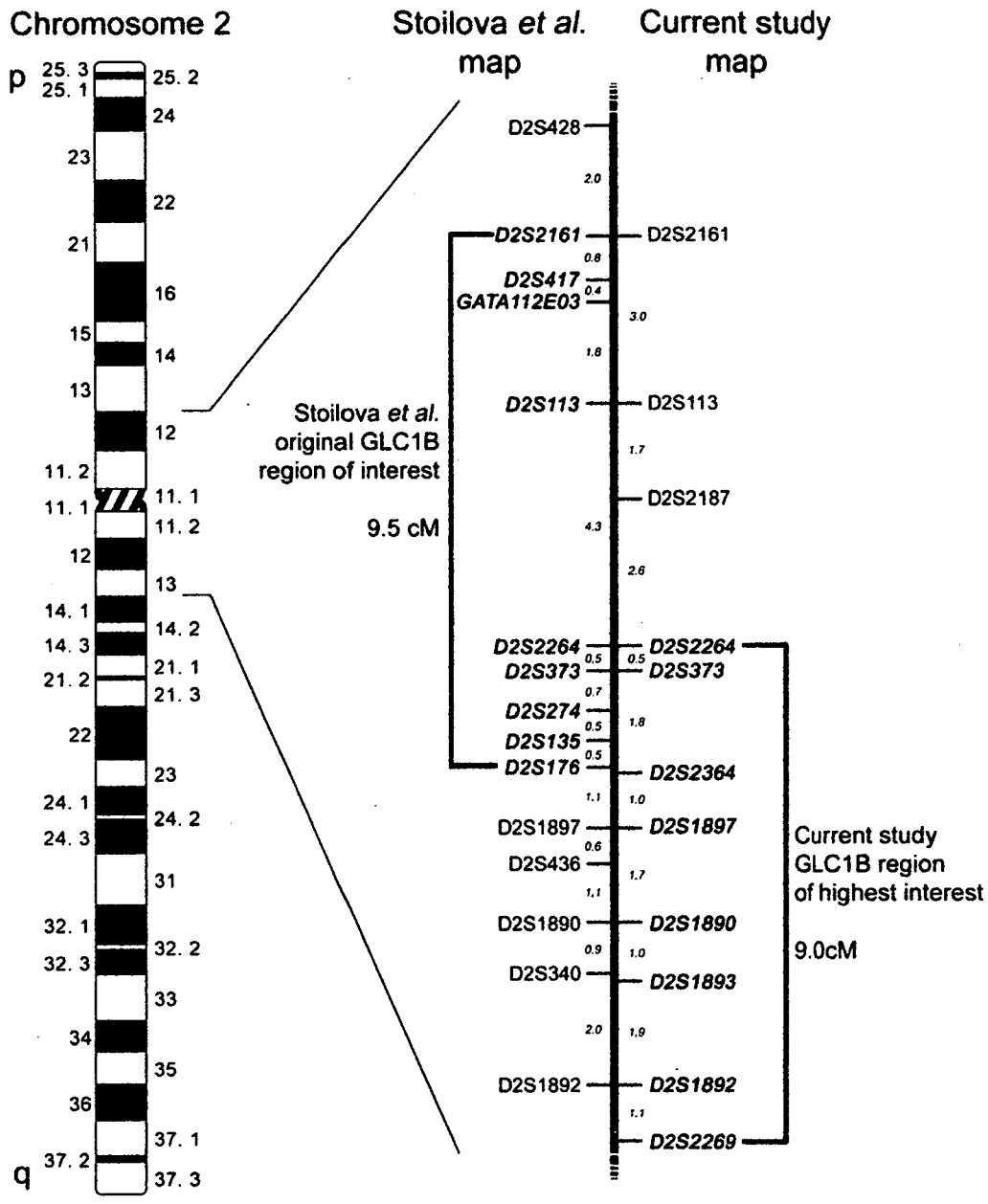

Figure 5.5 - A comparison of the marker map and critical region of the original and current investigations of the GLC1B locus

The ideogram shows the approximate cytogenetic location of the GLC1B locus. The marker map to the left of the expanded region indicates the marker location and haplotype of interest from the original study by Stoilova *et al.* in 1996. The marker map and region of interest from the current study is shown to the right. Numbers in italics indicate centiMorgan distances between adjacent markers.

Key clinical features of the six families originally linked to GLC1B by Stoilova *et al.* were mean age of diagnosis of 47 years and slightly elevated IOP, although half of the affected individuals had IOP within the normal range (<22mmHg) (Stoilova *et al.* 1996). Family GTas15, used in the current study, had similar clinical features, with a slightly higher average age of diagnosis (55 years) and similar IOP distribution. Four of the seven affected individuals had IOP measures over 22mmHg, however only one of these had peak IOP over 28mmHg. The remaining three affected individuals could be considered to have normal-tension glaucoma. These results suggest the susceptibility locus at GLC1B may be involved in POAG pathogenesis through pathways that do not involve IOP in all cases.

The analyses of the unaffected meioses in the six families originally linked to GLC1B revealed an example of incomplete penetrance; a healthy 86-year-old with no evidence of glaucoma who had inherited the entire affected haplotype (Stoilova *et al.* 1996). We similarly saw evidence for non-penetrance in at least one unaffected individual (15-14) aged 69 and carrying the entire haplotype of interest with no clinical sign of glaucoma. We also found evidence of a putative phenocopy, with one affected individual (15-12) who did not share the haplotype of interest.

A candidate gene of interest located within the haplotype overlap is four-and-a-half lim domains 2 (*FHL2*: MIM# 602633), expressed in a wide range of tissues including optic nerve and eye anterior segment. The six member interleukin-1 receptor cluster (Dale and Nicklin 1999) is also located within the haplotype overlap and includes the interleukin-1 receptors type I and II (*IL1R1*: MIM# 147810 and *IL1R2*: MIM# 147811) and also interleukin-1 receptor like 1 (*IL1RL1*: MIM# 601203) expressed in the eye anterior segment. It has been suggested that the immune system, and in particular

interleukin-1, is involved in POAG pathogenesis (Franks *et al.* 1992; Wang *et al.* 2001). In addition, the interleukin-1 gene cluster (Nicklin *et al.* 2002) is located on chromosome 2q13, approximately 0.5 cM beyond the distal end of the GLC1B haplotype identified in this study. The interleukin-1 gene cluster includes interleukin-1α (*IL1A*; 147760) and interleukin-1β (*IL1B*; 147720) as well as the interleukin-1 receptor antagonist (*IL1RN*: 147679) and several other interleukin-1 family members. *IL1B* is expressed in many tissues, including the trabecular meshwork, and a polymorphism within the gene has been associated with sporadic POAG in the Chinese population (Lin *et al.* 2003). The study found significant differences in the distribution of a synonymous *IL1B* exon 5 *TaqI* digest E2 allele between 58 POAG patients and 105 healthy volunteers (p=0.035) from the Chinese population (Lin *et al.* 2003). However, we screened this polymorphism in all available members of GTas15, as described in section 5.5.7, and found no evidence of segregation with the POAG phenotype or haplotype of interest in the pedigree. It is also interesting to note that mer tyrosine kinase protooncogene (*MERTK*: MIM# 604705), a gene associated with retinitis pigmentosa (Gal *et al.* 2000) (a disease that also results in visual field loss) is located near marker D2S2269 at the distal end of the haplotype of interest.

The six smaller pedigrees originally linked to GLC1B (Stoilova *et al.* 1996) when combined with our replication study in an extended POAG pedigree provide support that the 2cen-q13 region contains a POAG susceptibility gene, and increase the likelihood of gene identification. Previous experience with positionally cloned POAG genes *MYOC* and *OPTN* suggests that once identified, the POAG susceptibility gene at GLC1B may also contribute to a significant proportion of sporadic POAG cases.

5.6.2 Lack of evidence for linkage to GLC1E in family GTas35

Suggestive evidence of linkage to the GLC1E region on chromosome 10 in family GTas35 was identified in Chapter 4. Fine-mapping and follow-up analysis of this region, however, revealed the initial linkage signal to be a false positive result, as the final results clearly suggested no evidence for linkage, with p-values greater than 0.2 across all 12 markers in the region.

The initial linkage signal in GTas35, described in Chapter 4, may have been caused by incorrect inference of missing genotypes in SimWalk2, resulting in incorrect reconstruction of shared haplotypes. Several genotypes failed in the original round of typing described in Chapter 4, due to poor DNA sample quality. Isolation of replacement DNA samples from stored blood as described in Chapter 3.1.1, and repeat genotyping of all chromosome 10 markers described in Chapter 4.3.2, were conducted during the follow-up analysis described in this chapter. The resulting complete dataset did not support linkage to the GLC1E region in family GTas35. This is one of the potential limitations of using estimation based analyses; however a false positive result may not be unexpected given the low threshold used to select loci for follow-up analyses (defined in Chapter 4.4.6). Combined with the number of loci investigated and the number of pedigrees analysed independently, the expected rate of false positive results is 60% (higher if the markers at each locus are considered independently).

During the course of this investigation we determined that family GTas35 was connected to family AN1 (figure), a Tasmanian family in which we had previously identified a novel 1410delC *PAX6* mutation (Sale *et al.* 2002). We subsequently screened all of the available members of family GTas35 for the *PAX6* 1410delC mutation according to Sale *et al.* (2002), since glaucoma is part of the phenotype

spectrum of aniridia. However, the *PAX6* mutation was not detected in any of the 15 available individuals in family GTas35.

In addition, the *MYOC* mutation screen conducted by Fingert *et al.* (1999) identified a Phe4Ser polymorphism in individual 35-08 from family GTas35. This polymorphism was also detected in several controls and did not appear to be involved in POAG pathogenesis. We speculated that, if also present in some individuals from family AN1, this polymorphism may have phenotypic modifier effects on the presentation of aniridia in the family, and that this polymorphism may yet have some phenotypic modification effects on the POAG in family GTas35. However, while the polymorphism was detected in three individuals from family GTas35 (shown in Figure 5.1), including individual 35-08, it did not appear to have any obvious influence on POAG in this family (although it is impossible to draw firm conclusions from such a small dataset), nor was it detected in any of the 23 individuals from the aniridia branch.

The effect of an as-yet unidentified 'POAG gene' on the aniridia phenotype could not be evaluated in this dataset, but could, in theory, contribute to the phenotypic spectrum of the disease observed in individuals carrying the *PAX6* mutation. While glaucoma was uncommon in affected individuals from the aniridia branch of this pedigree, optic nerve anomalies were particularly common. The presence of anomalous optic nerves and poor visual acuity in aniridia patients may lead to difficulties in the diagnosis and monitoring of progression of glaucoma.

Chapter 6 - Variance Components Analysis of POAG Phenotype Components Using Genome-Wide Scan Data from an Extended Pedigree

6.1 Preface

Sections of this chapter have been published as the first linkage study to investigate cup-to-disc ratio and second linkage study to investigate IOP and as quantitative traits, using variance components analysis. The article, entitled 'Linkage to 10q22 for maximum intraocular pressure and 1p32 for maximum cup-to-disc ratio in an extended primary open-angle glaucoma pedigree' was published in *IOVS* (Charlesworth *et al.* 2005) and is included in this dissertation as Appendix 4.

6.2 Background

6.2.1 Quantitative traits for POAG

For genetic analyses, the presence of an underlying quantitative trait or traits that may be consistent with the continuous nature of gene action must be considered in the definition of the disease phenotype. For example, type 2 diabetes is defined by exceeding a threshold level of a continuous physiological trait (fasting blood glucose level). POAG is similarly defined by exceeding a threshold level of several continuous or somewhat continuous traits. Intraocular pressure and cup-to-disc ratio are both prime examples of continuous traits underlying a threshold affection status. Visual field loss is likely to be continuous; however its usefulness as a trait is dependent on the method of clinical ascertainment. Visual field loss is generally ascertained as categorical data which are not useful for quantitative trait analysis. Studies of POAG genetics consistently use a combination of these three traits, with a threshold level for each, to generate a dichotomous affection status for the purposes of linkage analysis (Sheffield

et al. 1993; Stoilova *et al.* 1996; Wirtz *et al.* 1997; Sarfarazi *et al.* 1998; Trifan *et al.* 1998; Wirtz *et al.* 1999; Wiggs *et al.* 2000; Nemesure *et al.* 2003).

Given the limited success in identifying glaucoma susceptibility genes so far, one approach that may have greater success is quantitative trait linkage analysis using precursors or phenotype components of glaucoma, such as raised IOP and increased cupping of the optic nerve. Such traits may be more aetiologically homogeneous than an overall diagnosis of glaucoma, with more simple genetic architectures, making it easier to map causative loci (Almasy and Blangero 1998; Amos and de Andrade 2001; Freimer and Sabatti 2004). Furthermore, quantitative trait linkage analysis is inherently more powerful than dichotomous-trait linkage analysis (Duggirala *et al.* 1997; Williams and Blangero 1999a), and is particularly powerful with large families (Wijsman and Amos 1997; Williams and Blangero 1999b).

The heritabilities of IOP and vertical cup-to-disc ratio have been estimated as 0.29-0.36 and 0.48-0.56 respectively (Klein *et al.* 2004; Chang *et al.* 2005), providing evidence for genetic determinants for these components. A recent commingling analysis of IOP and glaucoma suggested the existence of a major gene accounting for 18% of the variance of IOP in the Blue Mountains Eye Study population (Viswanathan *et al.* 2004). Commingling analysis is a form of maximum likelihood model fitting that uses the distribution of quantitative trait values in a population to assesses the likelihood of the trait being influenced by a single biallelic locus of major effect, compared to the null hypothesis of no major trait locus (Maclean *et al.* 1976). A complex segregation and linkage analysis of IOP recently identified two potential regions of linkage, on chromosome 6 and chromosome 13 (Duggal *et al.* 2005). Prior to the study described in this chapter there had been no reported linkage analyses of cup-to-disc ratio.

The inclusion of quantitative phenotype components in the genetic analysis of POAG may offer significant power to identify the genetic basis of glaucoma in the face of limited family and population datasets. The discovery of genes contributing to the variation of maximum IOP and maximum cup-to-disc ratio, components of POAG phenotype, may provide significant insights into glaucoma pathophysiology as a whole.

6.2.2 Variance components analysis for localising quantitative trait loci

Variance component linkage analysis is an approach that enables penetrance model-free multipoint linkage analysis of complex quantitative (or qualitative) traits in extended pedigrees (Blangero and Almasy 1997; Duggirala *et al.* 1997; Almasy and Blangero 1998; Williams *et al.* 1999b; Williams *et al.* 1999a). The superior information content of quantitative traits allows the analysis of quantitative risk factors to serve as a powerful tool for evaluating the genetic mechanisms influencing common disease (Almasy and Blangero 1998). Variance component analysis has been used successfully to localise quantitative trait loci (QTLs) influencing many important disease-related traits, including risk of alcoholism (Williams *et al.* 1999b), serum leptin levels (Comuzzie *et al.* 1997; Martin *et al.* 2002) and resting heart rate (Comuzzie *et al.* 1997).

The variance component linkage method is based on the classical quantitative genetic decomposition of a phenotype, which assumes the phenotype is jointly influenced by genetic and environmental factors. These genetic factors can include specific loci at defined chromosomal locations. Evidence for a locus is obtained by observing trait covariances among different classes of relatives. The linkage analysis utilises both the average IBD probability (the coefficient of relationship) across the genome and the location-specific IBD probabilities estimated from the genetic marker data. Evidence

for a QTL requires that the statistical 'fit' of the observed phenotypic covariances with the expected covariances (given the linkage model under consideration) be significantly better when the locus-specific component is considered than when only the average genomic component is allowed. In practice, this involves testing for the existence of a locus influencing the phenotype at each location in the genome (usually by performing a linkage test at every cM). If the variance component for a specific chromosomal location is significantly greater than zero, there is evidence for a locus influencing the phenotype at that location.

As mentioned above, the variance component method is based on specifying the expected genetic covariances between arbitrary relatives as a function of IBD relationships at a given marker locus (Almasy and Blangero 1998). The total trait phenotypic variance (σ^2_P) is partitioned into components attributable to the effects of a specific QTL (σ^2_q), residual additive genetic effects (σ^2_g), and individual-specific random environmental effects (σ^2_e). The covariance matrix for the pedigree (Ω) is then given by:

$$\Omega = \Pi\sigma^2_q + 2\Phi\sigma^2_g + I\sigma^2_e,$$

where Π is a matrix with elements (π_{qij}) providing the estimated proportion of genes individuals *i* and *j* share IBD at a specific chromosomal location (q); σ^2_q is the variance component corresponding to the additive genetic effects from the major locus; Φ is the matrix of average coefficients of relationship (kinship); σ^2_g is the variance component corresponding to the residual polygenic effects; **I** is the identity matrix; and σ^2_e is the variance component corresponding to the random environmental effects. The test for linkage compares the likelihood of this model, in which the variance due to the n^{th} QTL is estimated, with the likelihood of a null model (no linkage), where the QTL effect size σ^2_q is fixed to be zero. The difference between the two $\log_{10}$ likelihoods produces a

LOD score that can be interpreted in a similar fashion to the classical LOD scores of parametric linkage analysis (Blangero *et al.* 2001).

6.2.3 GTas02 - the family of interest

The family of interest in this investigation is a large, late-onset POAG pedigree identified as part of the GIST. The family originated from British settlers who arrived in Tasmania in the mid 1800s. The pedigree includes more that 1350 individuals, making it one of the largest families identified as part of the GIST.

Segregation of POAG is evident in a core portion of the pedigree, referred to from this point as GTas02, which consists of 246 individuals (including deceased linking members), 139 of whom consented to clinical examination and blood collection for genotyping and mutation analysis. The pedigree extends over six generations and includes 24 available, clinically affected individuals who have elevated IOP and late onset POAG (Figure 6.1). The average age of POAG diagnosis within the pedigree is 69 years.

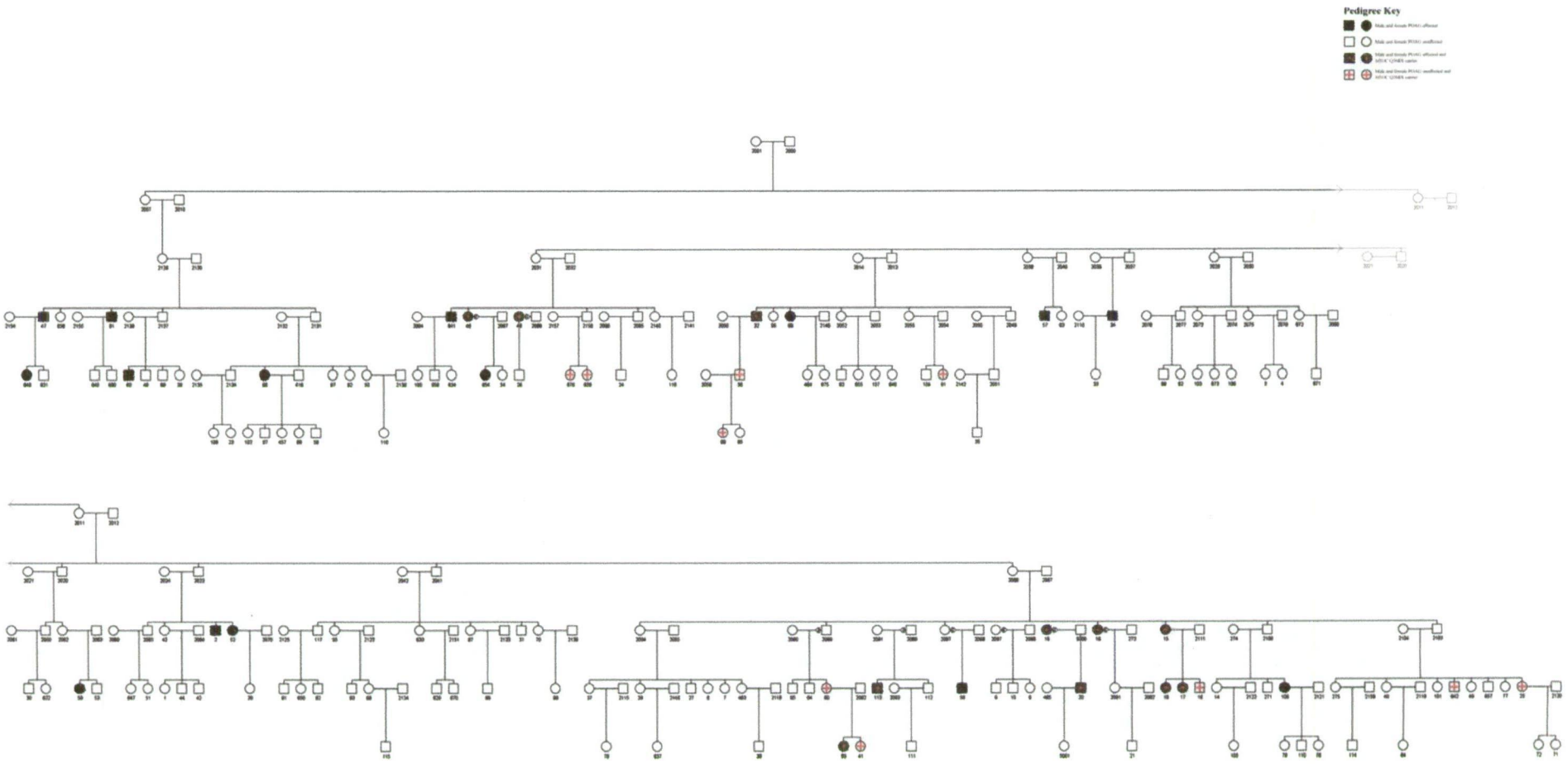

Figure 6.1 Family GTas02 showing clinical diagnosis of POAG and *MYOC* Q368X mutation status

The pedigree in split in half and greyed areas with arrows indicate the reconnection points.

The pedigree includes 246 individuals, 139 of whom were available for clinical examination and mutation screening. A full list of available individuals is given in Appendix 5.

Individuals 19, 46, 2089 and 2097 appear twice due to multiple marriages.

GTas02 had been under investigation by Dr Paul Baird and collaborators at the Walter and Eliza Hall Institute (Victoria) and Royal Victorian Eye and Ear Hospital prior to the inception of this study. These investigations included SSCP screening and sequence analysis of *MYOC* mutations (Craig *et al.* 2001; Baird *et al.* 2003) and a 10 cM genome-wide scan (Baird *et al.* 2005). The resulting genotype data provided an opportunity to apply the method of variance components linkage analysis to the problem of POAG genetics, and were made available to this investigation for that purpose.

MYOC, encoding myocilin, is the glaucoma susceptibility gene at the GLC1A locus on chromosome 1q24.3, described in Chapter 1.8.1. Of the 139 individuals screened for mutations in the *MYOC* gene, 19 were found to carry the glutamine368STOP (Q368X) mutation (Figure 6.1). Q368X is the most common mutation identified in POAG patients, estimated to account for approximately 1.6% of POAG (Fingert *et al.* 1999). The Q368X mutation generally gives rise to a mild phenotype (in contrast to *MYOC* mutations associated with JOAG), with late age of onset and raised IOP (Allingham *et al.* 1998). Allele sharing of Q368X mutation carriers across multiple populations suggests a common origin for this mutation (Fingert *et al.* 1999). Haplotype analysis of Q368X has revealed a founder effect in 15 Tasmanian POAG families, including family GTas02, with a shared four marker haplotype surrounding the Q368X mutation suggesting a common origin prior to European settlement in the early 1800s (Baird *et al.* 2003).

6.3 Aims

The intention of this investigation was to explore the use of quantitative data, collected as a component of routine clinical examination for POAG, as the basis for the genetic linkage analysis. This investigation aimed to identify regions of linkage contributing to

maximum recorded IOP and maximum cup-to-disc ratio, key components of the POAG phenotype; to evaluate the possibility of interaction between these traits and investigate the effect of the myocilin Q368X mutation as a covariate in the analyses of these traits. Analysis of a dichotomous trait based on clinical diagnosis of POAG was also included in the analysis, to provide some comparison between the analysis of discrete and quantitative traits.

6.4 Methods

6.4.1 Clinical examination

Of the 139 available individuals in the pedigree, 24 were diagnosed with POAG. The details of the clinical assessment of this family has been extensively reported (Craig *et al.* 2001) and clinical examination procedures are detailed in Appendix 1. Quantitative measures collected as part of the clinical examination of POAG patients and their relatives included maximum recorded IOP without medication and maximum cup-to-disc ratio from the highest scoring eye (Coote *et al.* 1996; Craig *et al.* 2001) and these were used as quantitative traits in this study. Multiple IOP measures were available for each individual, hence maximum IOP was selected as the trait measure to reduce any bias introduced by using post-medication pressure values. The larger vertical cup-to-disc ratio from either eye was used as the measure for this trait.

6.4.2 Genotyping

A 10 cM genome-wide scan was conducted by the Walter and Eliza Hall Institute (Victoria), using 401 microsatellite markers from the ABI version 2.0 and 2.1 fluorescent marker sets, run on ABI377 Sequenators (Applied Biosystems) and analyzed using the Genescan® and Genotyper® software (Applied Biosystems), as described in Baird *et al.* (2005). The resulting raw genotype, pedigree and phenotype

data were provided by Dr Paul Baird from the Centre for Eye Research Australia (CERA). Inconsistencies in Mendelian inheritance of genotypes were detected using Pedcheck (O'Connell and Weeks 1998). Marker allele frequencies were estimated from 72 elderly glaucoma-free control individuals drawn from the same population (Chapter 2.2.4).

Multipoint identity by descent (IBD) files were created using the Markov chain Monte Carlo (MCMC) based program Loki, version 2.4.7 (Heath 1997; Heath *et al.* 1997) from within SOLAR, version 2.1.1 (Almasy and Blangero 1998). Loki performs similar IBD calculations to SimWalk2, described in chapter 4.4.2. The IBD matrices contain the probability of each pair of individuals sharing 0, 1, or 2 alleles IBD at specified intervals along each chromosome. The IBD matrices were calculated once and stored for all future analyses.

All calculations were performed using a Sun Microsystems Enterprise 450 server with four Ultrasparc-II 480MHz central processing units, 4GB of RAM and 60GB of disk space. All computations were achievable in an acceptable timeframe using this system.

6.4.3 Discrete and quantitative traits

The covariates used for all analyses were age and sex. Age-sex interaction was initially included, but removed after it was found to be not significant in any dataset. POAG affection status (clinical diagnosis of POAG) was analysed as a discrete trait. The quantitative traits analysed were maximum recorded IOP and maximum cup-to-disc ratio. Visual field loss was not used as a trait due to its categorical nature and the incompatibility between the clinical assessment methods of the GIST and the assessment methods used to generate the general population data used in this study.

6.4.4 Population ascertainment correction

Two datasets were created to provide the population ascertainment correction; one for the discrete trait and one for the quantitative traits. The first was an age based distribution of POAG (dichotomous affection based on clinical diagnosis) in 5332 individuals, estimated from Australian population prevalence data provided by the Blue Mountains Eye Study (BMES) (Mitchell *et al.* 1996) and Melbourne Visual Impairment Project (MVIP) (Wensor *et al.* 1998).

The second ascertainment correction data set was taken directly from the MVIP and included 3,905 individuals from the general population with data on age, sex, maximum recorded IOP and maximum cup-to-disc ratio (Wensor *et al.* 1998). This dataset provided a population ascertainment correction for the quantitative traits. The MVIP clinical data used in this study was collected using the same methods as the GIST. Mean values of age and trait variables in the GTas02 sample and the ascertainment correction sample were compared using 2-sided t-tests (or multivariate linear regression when it was necessary to adjust for other variables) to determine the necessity of the ascertainment correction. For example, if the distribution of the trait values between the general population and GTas02 are highly similar, a population based ascertainment correction may not necessarily have been required.

The ascertainment corrections were conducted using SOLAR version 2.1.1 (Almasy and Blangero 1998) and the relevant population based ascertainment correction dataset, by maximising the sporadic model for the population correction dataset alone, including the trait of interest and covariates age and sex. In the sporadic model the variance is not decomposed into genetic and non-genetic components. The mean effects for each trait

were thereby estimated from the population dataset, including the regression coefficients β_{Age} and β_{Sex} which were used to adjust the trait mean for the effect of the covariates age and sex. The resulting values for mean, standard deviation, β_{Age} and β_{Sex}, obtained from the population based dataset, were then employed in the model used to analyse the pedigree data. By constraining these mean effects and the total variance to that of the general population, trait values for individuals in family GTas02 were given the appropriate weight. The standard deviation was not fixed for the dichotomous trait.

6.4.5 Variance components analysis

The heritability of each trait was estimated using genetic variance component modelling as implemented in SOLAR version 2.1.1 (Almasy and Blangero 1998). Variance component linkage analysis was performed to detect and localise quantitative trait loci influencing variation in the traits.

An initial analysis was performed using the discrete trait based on POAG affection status. Of the 139 available individuals in the pedigree, 24 were classified as clinically affected. The continuous traits based on maximum recorded IOP and maximum cup-to-disc ratio were then analysed as individual traits, with age and sex as covariates. A bivariate analysis of these continuous traits was performed to test for potential genetic and/or environmental correlations between the traits (Williams *et al.* 1999b). In this case the original ascertainment correction values for mean, standard deviation, β_{Age} and β_{Sex} for each trait were fixed in the bivariate analysis model.

To test the impact of the *MYOC* Q368X mutation on the linkage results, Q368X status was included as a covariate in a second round of analyses for each quantitative trait, but not in the analysis of the discrete trait. The regression coefficient for Q368X mutation

status (β_{MYOC}), used in the analysis of each trait, was estimated using family GTas02 trait and mutation data and not from the population ascertainment correction dataset. As in previous analyses, age and sex were included in all models, and adjusted LOD scores and empiric p-values were calculated as described below.

6.4.6 Empirical LOD adjustment

Expected LOD scores and empiric locus-specific p-values were determined using the lod adjustment (`lodadj`) command of SOLAR (Blangero *et al.* 2000; Blangero *et al.* 2001). A total of 100,000 replicates were simulated to build up the distribution of LOD scores expected under the null hypothesis of no linkage, using a fully informative, unlinked marker. The observed LOD scores were then regressed on those expected for a multivariate normal trait, with the inverse slope of the regression line providing the LOD correction constant. Final LOD scores were multiplied by the correction constant only if the constant was less than 1. The LOD adjustment is used to account for possible errors introduced by any deviation from normal distribution, such as kurtosis (Blangero *et al.* 2000). Empiric locus-specific p-values were derived from the simulated LOD score distribution.

6.4.7 Genome-wide p-values

In order to control for the overall false positive rate in our linkage screens, we have converted the nominal p-values associated with our peak LOD scores to genome-wide p-values using an approach based on the work of Feingold *et al.* (1993) and implemented in Gauss 5.0.29 (Aptech Systems, Inc). This method takes into account the mean recombination rate in our study population and the marker density of the linkage map utilised in our genome scan.

6.5 Results

6.5.1 Population ascertainment correction

In the first population ascertainment correction dataset, an age based distribution of dichotomous POAG affection, prevalence rose from 0.08% in the initial 10-39 year age block to 9.2% at 90+ years. The prevalence of POAG in individuals >40 years of age was ascertained in 10 year age blocks. The average population prevalence was 3.2%. The distribution of this data is shown in Figure 6.2 and a summary of the data based on POAG affection status is given in Table 6.1.

The fitted coefficients β_{Age} (0.0267) and β_{Sex} (-0.0159) were obtained from the MVIP and BMES population data using SOLAR. A comparison between the ascertainment correction data for the dichotomous trait and family GTas02 is shown in Table 6.2.

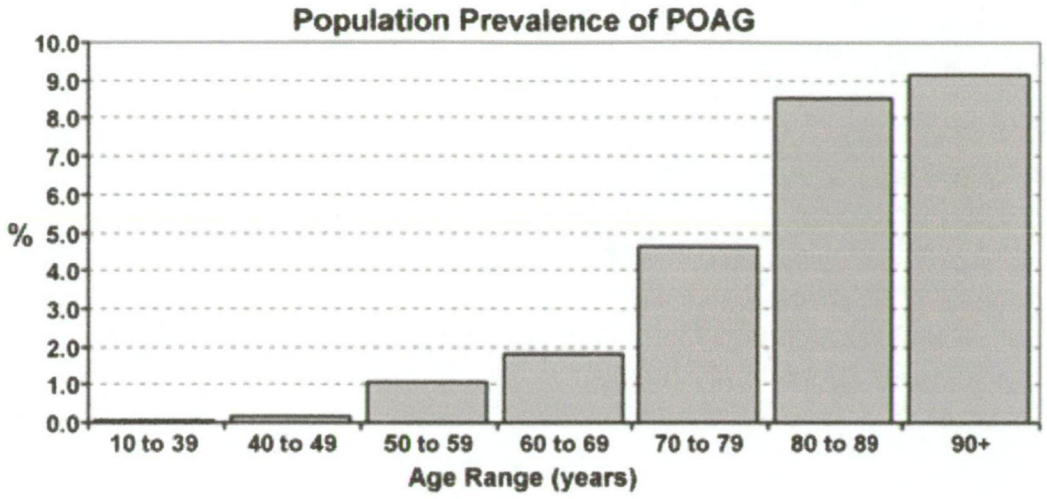

Figure 6.2 - Population prevalence of POAG in Australia

The population prevalence of POAG in Australia, derived from 5332 individuals from the Blue Mountains Eye Study (Mitchell *et al.* 1996) and Melbourne Visual Impairment Project (Wensor *et al.* 1998).

Population	Number of individuals	Mean age (years)	SD age (years)
Entire population	5332	59.5	24.0
Unaffected individuals	5162	58.7	23.9
Affected individuals	170	83.3	12.2

Table 6.1 - Summary of POAG population prevalence data in the first ascertainment correction dataset

	MVIP/BMES	Family GTas02
Age* (N)	5332	139
Age (Mean)	59.5	53.1
Age (SD)	24.0	14.4
POAG prevalence†	3.2%	17.3%

Table 6.2 - Age and trait distribution statistics from the population ascertainment correction datasets for the dichotomous trait and family GTas02

MVIP: Melbourne Visual Impairment Project; BMES: Blue Mountains Eye Study; N: number of observations; SD: standard deviation.

*Age in years.

†Average prevalence.

The second population ascertainment correction dataset was used for the quantitative traits based on maximum recorded IOP and maximum vertical cup-to-disc ratio. The distribution of these traits in the population compared with family GTas02 is shown in Figure 6.3 and a summary of the population trait distributions is shown in Table 6.3.

Although the kurtosis of maximum IOP in the general population appears high (Table 6.3), the empirical LOD adjustment was used to determine whether any correction of the final LOD score was required, before any transformation of the data was considered.

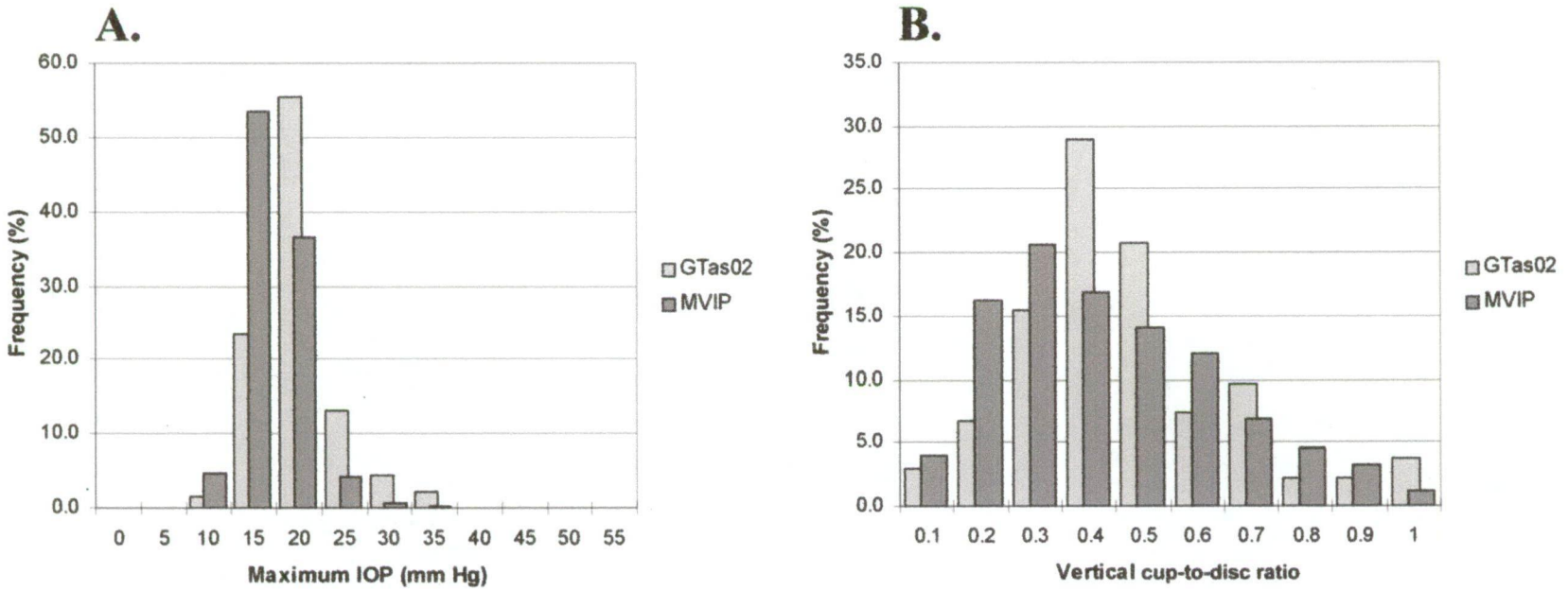

Figure 6.3 - Population distribution of maximum IOP and vertical cup-to-disc ratio

Panel A shows the MVIP population distribution of maximum recorded intraocular pressure compared with family GTas02.

Panel B shows the MVIP population distribution of maximum vertical cup-to-disc ratio compared with family GTas02.

	Mean	SD	Kurtosis	Skew
Age	59.42	11.61	-0.48	0.42
Intraocular pressure	15.20	3.32	7.28	1.31
Cup-to-disc ratio	0.43	0.21	-0.28	0.60

Table 6.3 - Summary of age, maximum IOP and cup-to-disc ratio distribution in the second ascertainment correction dataset

A comparison between the ascertainment correction data for the quantitative traits, maximum recorded IOP and maximum vertical cup-to-disc ratio, and family GTas02 is shown in Table 6.4, including the fitted coefficients β_{Age} and β_{Sex} obtained from the MVIP population data.

The mean age of the 139 subjects in the GTas02 sample (53.1 years, SD=14.4 years) was significantly lower ($p<0.0001$) than the mean age of the 5332 subjects in the ascertainment correction sample used for POAG as a dichotomous trait (59.5 years, SD=24.0 years). The mean age of the 139 GTas02 subjects was also significantly lower ($p<0.0001$) than the mean age of the 3892 subjects in the population ascertainment correction sample used for the quantitative traits maximum IOP and maximum cup-to-disc ratio (59.4 years, SD=11.6 years). The ascertainment correction datasets were not designed to be age matched, however the comparison of age and trait values between the two groups reveals the relative position of family GTas02 within the distributions of these populations.

Trait	MVIP			Family GTas02			Fitted coefficients	
	N	Mean	SD	N	Mean	SD	β_{Age}	β_{Sex}
Age (years)	3892	59.4	11.6	139	53.1	14.4		
Max. Disc	2986	0.43	0.21	135	0.47	0.20	0.0016	-0.032
Max. IOP (mmHg)	3221	15.2	3.32	137	17.9	4.15	0.0033	-0.211

Table 6.4 - Age and trait distribution statistics from the population ascertainment correction datasets for the quantitative traits and family GTas02

MVIP: Melbourne Visual Impairment Project; N: number of observations; SD: standard deviation; β_{Age}: fitted coefficient for age; β_{Sex}: fitted coefficient for sex; Max. Disc: maximum cup-to-disc ratio; Max. IOP: maximum intraocular pressure.

6.5.2 Analysis of the dichotomous trait based on POAG affection status

Based on the population ascertainment correction dataset, the heritability for the dichotomous trait referring to POAG affection status, with covariate age, was 1. Heritabilities of 1 are often returned as incorrect results in the analysis of discrete traits, and this is most likely the result of having to fix parameters from the ascertainment correction model. However, although the heritabilities and resulting LOD score magnitudes may be incorrect, it is still possible to detect the approximate location of genetic loci using the multipoint analysis.

The empirical LOD adjustment coefficient was 0.88 hence the multipoint LOD scores were adjusted down by this factor. The resulting linkage signal was weak, the strongest signals including two peaks on chromosome 10 (near marker D10S547 on 10p and D10S537 on 10q), both with a LOD of 1.9 (p=0.004), and a third peak of LOD 1.8 (p=0.005) on chromosome 1q, near marker D1S249 and the myocilin locus (Figure 6.4).

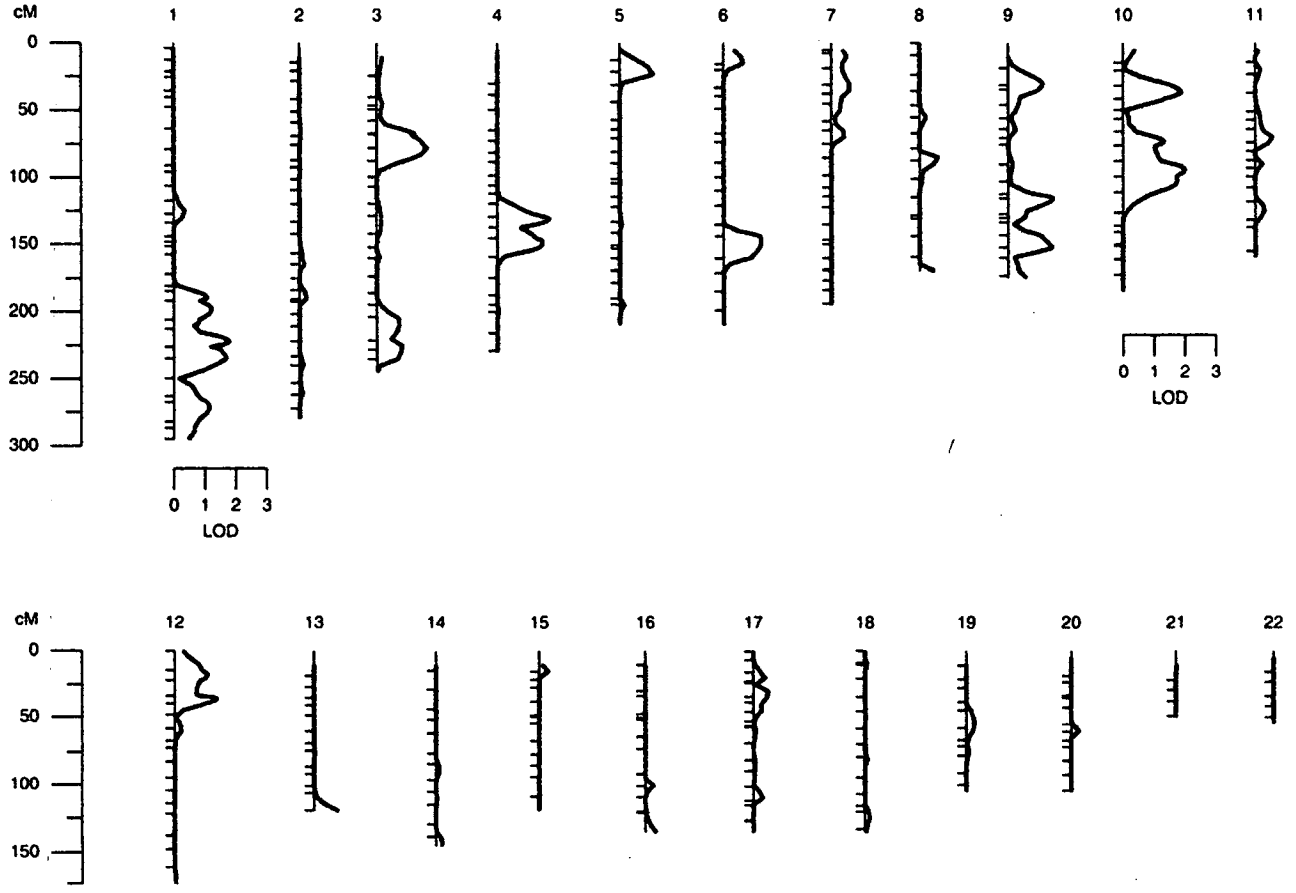

Figure 6.4 - LOD adjusted multipoint linkage results for the discrete trait based on POAG affection status

Chromosome length in centiMorgans is indicated by the left-hand ruler. Marker locations are indicated by dashes on the left side of each stringplot.

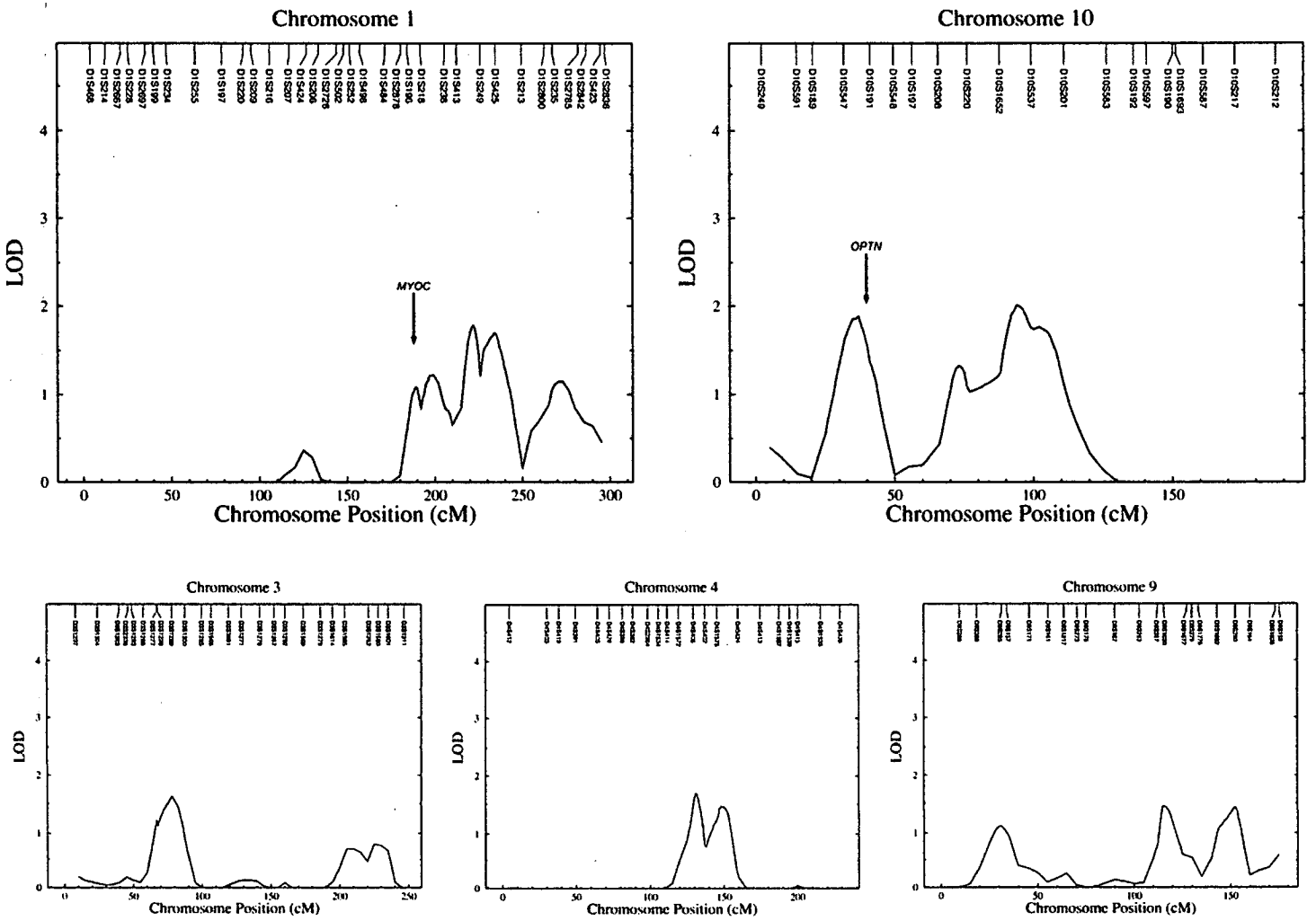

Figure 6.5 - Regions of interest from the linkage analysis of the discrete trait based on POAG diagnosis

The locations of the myocilin (*MYOC*) and optineurin (*OPTN*) genes are indicated (arrow).

6.5.3 Analysis of the quantitative trait based on maximum recorded IOP

Maximum recorded IOP had a heritability of 0.55 for family GTas02. Covariates sex and age were statistically controlled for and included in the analysis, although in the ascertainment correction population neither showed effects that were significant ($p=0.073$ for sex, $p=0.53$ for age), and accounted for only 0.1% of the variance. The mean value for maximum recorded IOP in family GTas02 (17.9mmHg, SD=4.2mmHg) was significantly higher ($p<0.0001$) than the mean IOP in the general population (15.2mmHg, SD=3.3mmHg). The empirical LOD correction constant was greater than 1 (1.05), hence no adjustment was applied to the linkage results. The highest LOD score for IOP in family GTas02 was 3.3 (locus-specific $p=0.00015$) near marker D10S537 (Figure 6.6), with the LOD-1 interval spanning approximately 20 cM on chromosome 10q22 (Figure 6.7). The genome-wide p-value for this result was 0.0165.

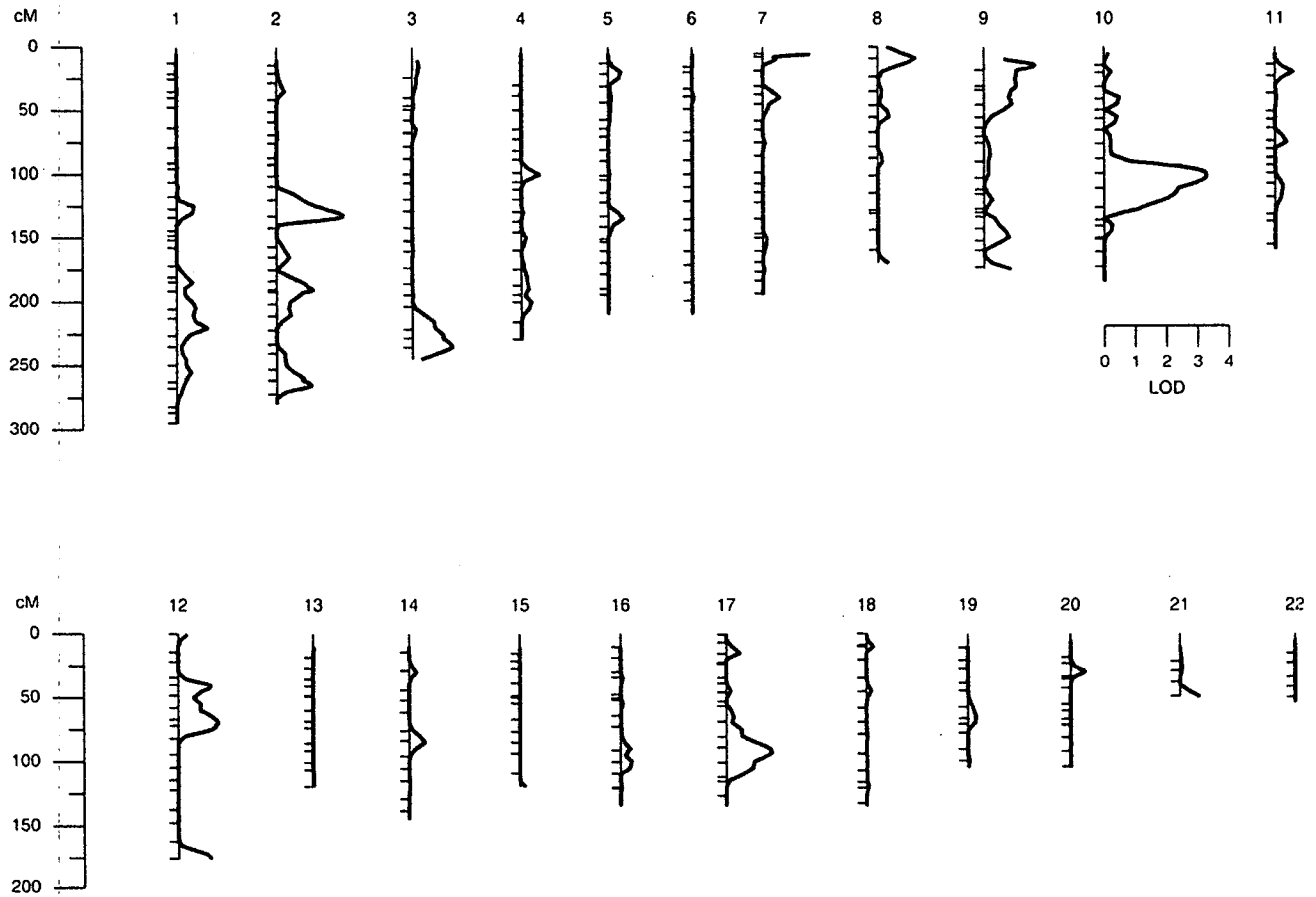

Figure 6.6 - Genome-wide multipoint variance components linkage results for maximum recorded IOP

Chromosome length in centiMorgans is indicated by the left-hand ruler. Marker locations are indicated by dashes on the left side of each stringplot.

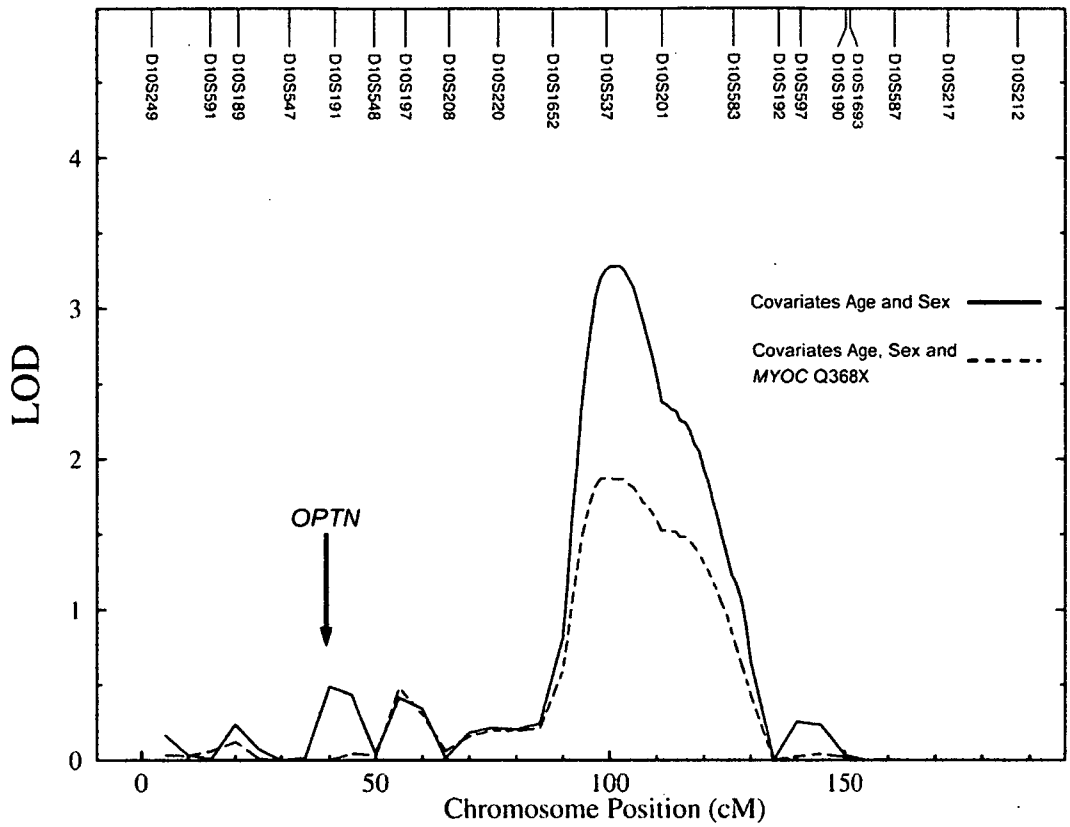

Figure 6.7 - Multipoint variance components linkage results for maximum recorded IOP for chromosome 10 (solid line) and linkage signal following the inclusion of Q368X status as a covariate (dashed line)

Covariates are indicated on the plots. The location of the optineurin (*OPTN*) gene is shown (arrow).

6.5.4 Analysis of the quantitative trait based on maximum cup-to-disc ratio

Maximum vertical cup-to-disc ratio had a heritability of 0.39 for family GTas02. The effect of covariates sex ($p=3.1x10^{-5}$) and age ($p=1.6x10^{-6}$) were highly significant in the ascertainment correction population, accounting for 1.4% of the variance; hence both were statistically controlled for and included in the analysis of family GTas02. After adjustment for age and sex, cup-to-disc ratios were significantly higher in family GTas02 than in the general population ($t=2.59$, $p=0.01$). The empirical LOD correction constant was greater than 1 (1.21), hence no adjustment was applied. The highest LOD score for maximum cup-to-disc ratio in family GTas02 was 2.3 (locus-specific $p=0.00056$) near markers D1S197 and D1S220 (Figure 6.8), with the LOD-1 interval spanning approximately 20 cM on chromosome 1p32 (Figure 6.9). The genome-wide p-value for this LOD score was determined to be 0.208.

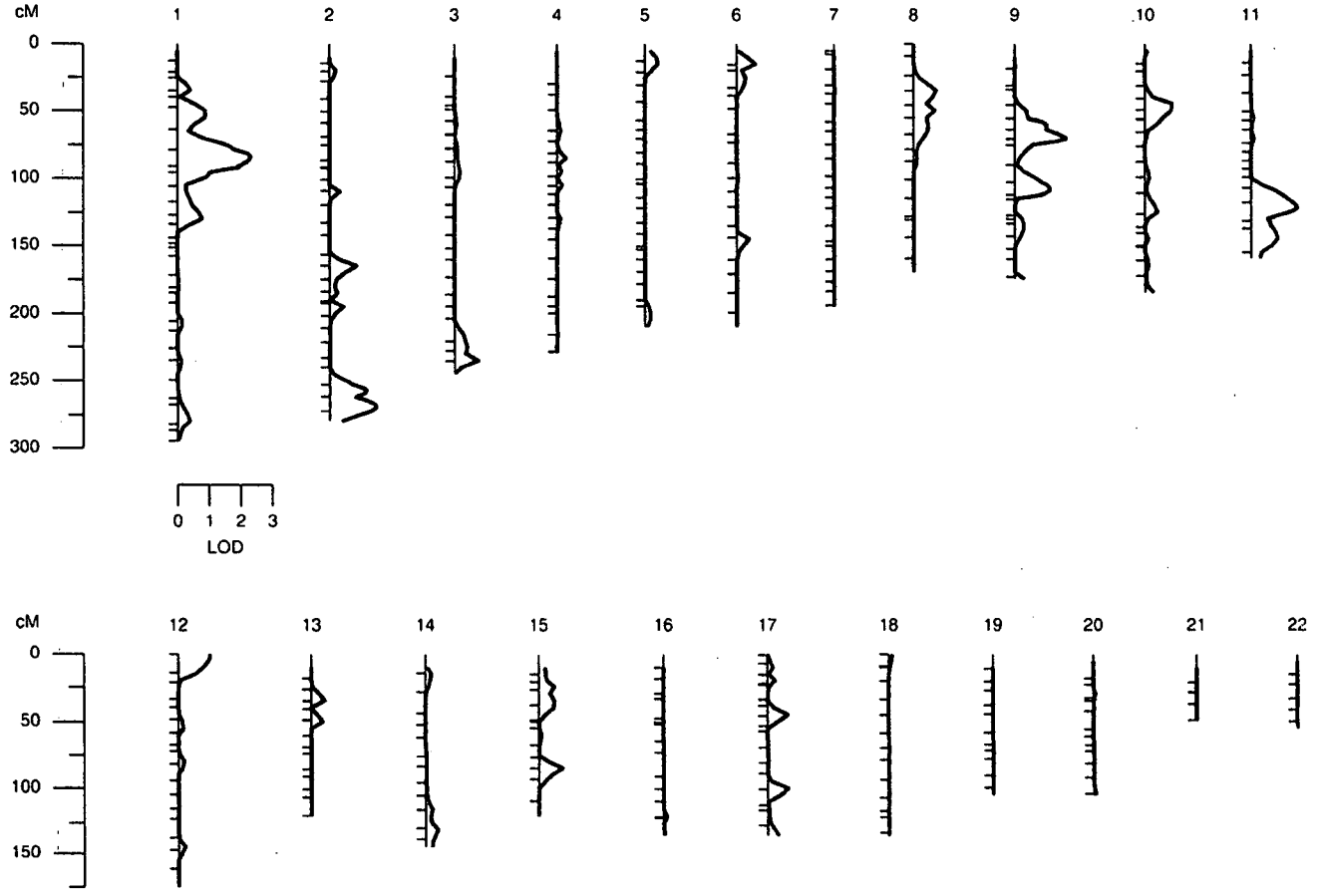

Figure 6.8 - Genome-wide multipoint variance components linkage results for maximum vertical cup-to-disc ratio.

Chromosome length in centimorgans is indicated by the left-hand ruler. Marker locations are indicated by dashes on the left side of each stringplot.

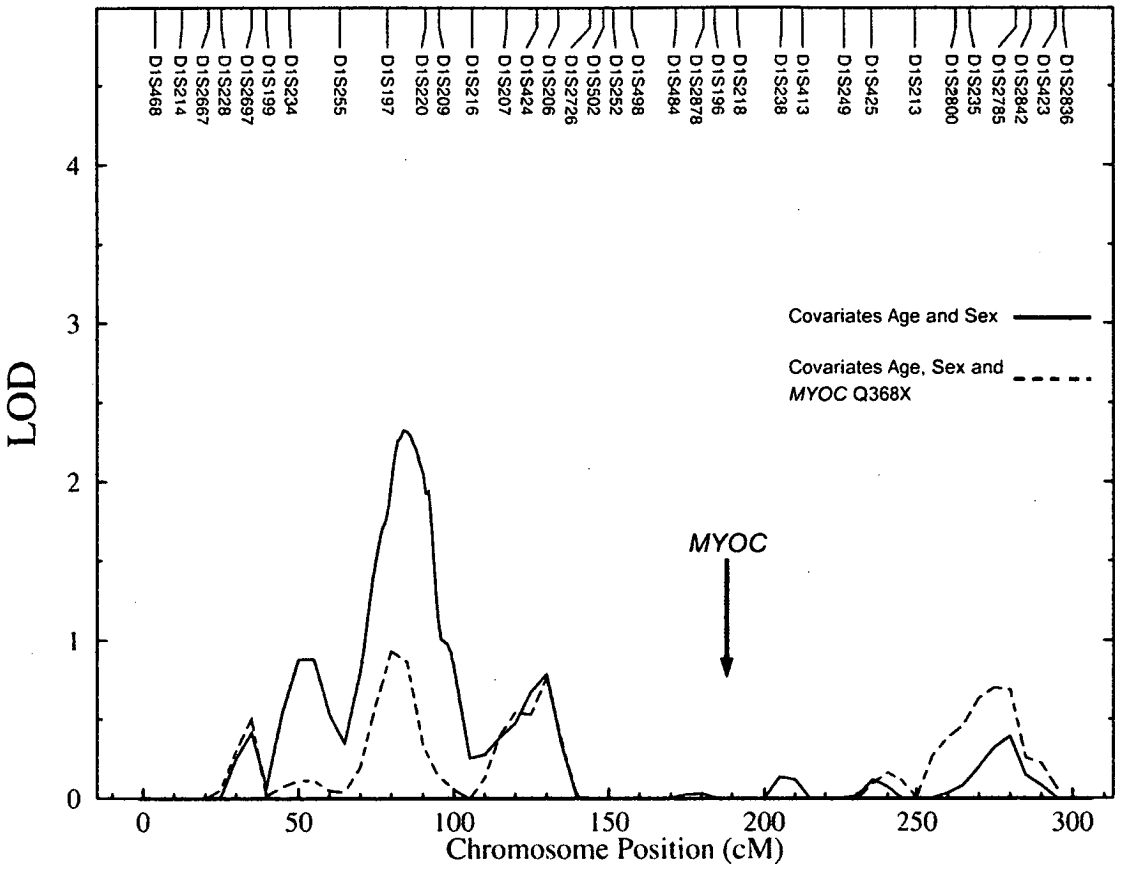

Figure 6.9 - Multipoint variance components linkage results for maximum vertical cup-to-disc ratio for chromosome 1 (solid line), and linkage signal following the inclusion of Q368X status as a covariate (dashed line)

Covariates are indicated on the plots. The location of the myocilin (*MYOC*) gene is shown (arrow).

6.5.5 Inclusion of Q368X mutation status as a covariate

The *MYOC* Q368X mutation was present in nine out of 24 (37.5%) individuals in family GTas02 with diagnosed POAG, and 10 individuals without a diagnosis of POAG at examination. SOLAR was used to compare the trait values of Q368X carriers and non-carriers, accounting for non-independence among relatives and age. *MYOC* Q368X mutation status was included as a covariate in the model used for the multipoint analysis of each trait (described in section 6.4.4). The **`polygenic`** command with covariate screening was used to estimate the β_{MYOC} term (equal to the age-adjusted difference in trait means between Q368X carriers and non-carriers) and calculate a p-value for its significance. While the mean age of individuals carrying the Q368X mutation in family GTas02 was not significantly different from those without the mutation, mean maximum IOP and mean maximum cup-to-disc ratio were significantly higher in Q368X mutation carriers, regardless of POAG affection status (Table 6.5).

	Q368X mutation carriers			Q368X mutation free			
Trait	**N**	**Mean**	**SD**	**N**	**Mean**	**SD**	**p-value***
Age	19	54.32	15.06	120	52.93	14.39	
Max. IOP	19	22.21	5.32	118	17.17	3.48	7.70×10^{-08}
Max. Disc	19	0.64	0.23	116	0.44	0.18	2.26×10^{-4}

Table 6.5 – Age and quantitative trait comparison between myocilin Q368X mutation carriers and mutation-free individuals from family GTas02

N: number of observations; SD: standard deviation (SD); Max. IOP: maximum intraocular pressure; Max. Disc: maximum cup-to-disc ratio.

*p-value obtained by age-adjusted measured genotype analysis accounting for non-independence among relatives.

The regression coefficient for *MYOC* Q368X mutation status used in the analysis of each trait (β_{MYOC}) was derived from family GTas02 trait and mutation data (as described above), and not from the population ascertainment correction dataset. The aim of this process was to use *MYOC* status as a covariate in an attempt to account for the presence of the mutation in family GTas02. The fitted coefficient for myocilin mutation status in the analysis of IOP was 5.065 while β_{MYOC} for the analysis of maximum cup-to-disc ratio was 0.192. Myocilin mutation status was estimated to account for 16% of the genetic variance of maximum IOP (heritability reduced from 0.55 to 0.46) and 49% of the genetic variance of maximum cup-to-disc ratio (heritability reduced from 0.39 to 0.20). Addition of *MYOC* Q368X mutation status as a covariate in the analysis of the quantitative traits resulted in the peak LOD score for maximum recorded IOP (near marker D10S537 on chromosome 10q22) dropping from 3.3 to 1.9 (Figure 6.7), while the peak LOD score for maximum cup-to-disc ratio (near markers D1S197 and D1S220 on chromosome 1p33) was reduced from 2.3 to 0.9 (Figure 6.9).

6.5.6 Bivariate analysis of the quantitative traits

The bivariate analysis of the quantitative traits maximum recorded IOP and maximum cup-to-disc ratio revealed no *apparent* genetic and/or environmental correlation between the traits. Both peaks of interest from the individual analyses were present, however the chromosome 1p (cup-to-disc ratio) peak dropped to a LOD of 1.7 and the chromosome 10q (maximum IOP) peak dropped to a LOD of 2.4 (Figure 6.10). This reduction is most likely due to reduced power in the combined analysis.

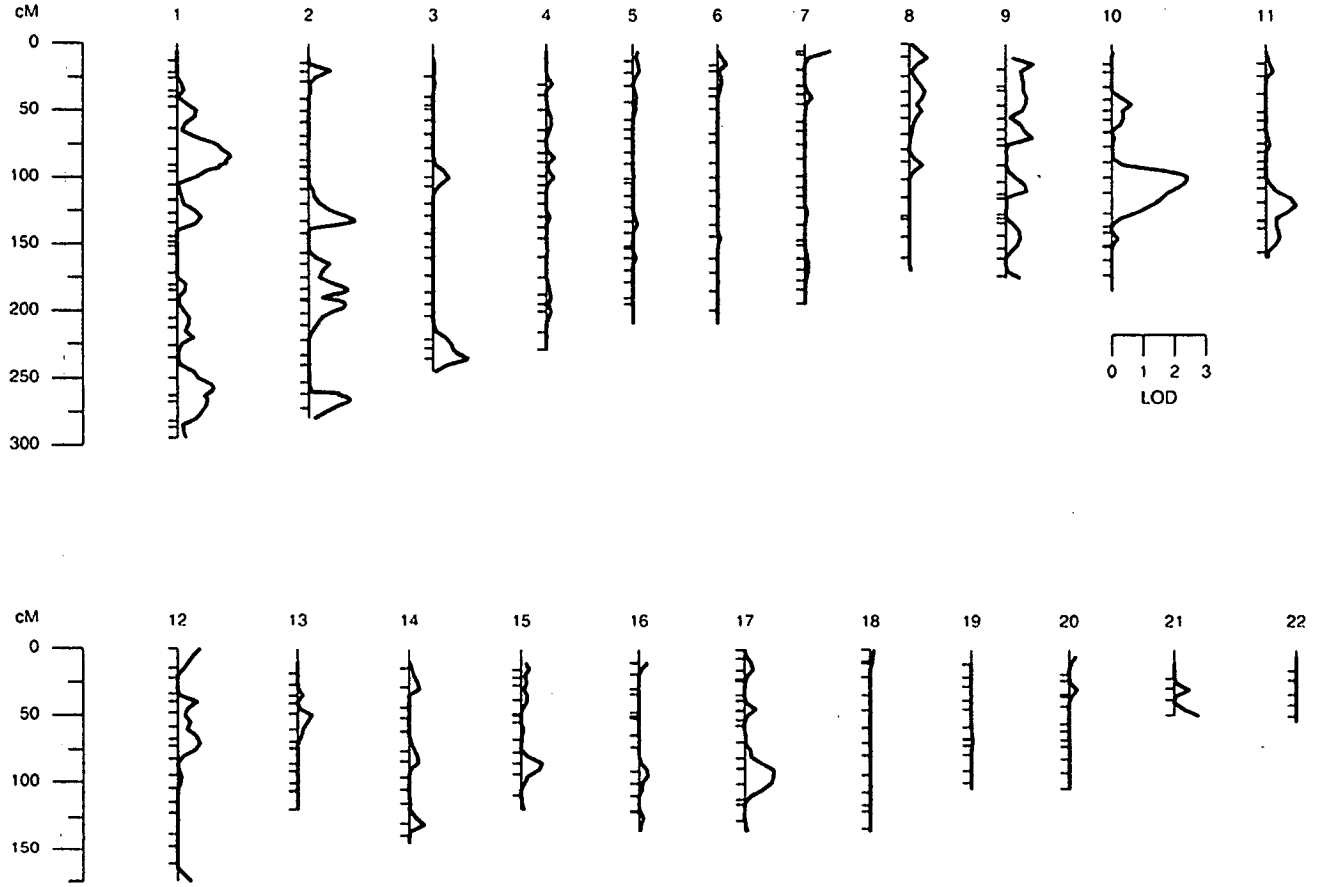

Figure 6.10 - Multipoint linkage results for the bivariate analysis of maximum recorded IOP and maximum vertical cup-to-disc ratio

Chromosome length in centiMorgans is indicated by the left-hand ruler. Marker locations are indicated by dashes on the left side of each stringplot.

6.6 Discussion

The published sections of this chapter represent the one of the first linkage studies to investigate two individual phenotype components of POAG, maximum recorded IOP and maximum vertical cup-to-disc ratio, as quantitative traits using variance components analysis. Genome scan analyses of these traits in an extended pedigree revealed one region of significant or suggestive linkage for each trait. Multipoint linkage analysis of maximum recorded IOP identified a peak LOD of 3.3 (locus-specific p=0.00015) near marker D10S537 on chromosome 10q22; while analysis of maximum cup-to-disc ratio produced a peak LOD score of 2.3 (locus-specific p=0.00056) near markers D1S197 to D1S220 on chromosome 1p32. In comparison, analysis of the dichotomous trait based on POAG diagnosis was seriously underpowered and revealed no significant evidence of linkage. The bivariate analysis of the quantitative traits and analyses involving the inclusion of myocilin mutation status as a covariate suffered similar deficits in power.

The putative trait locus for maximum recorded IOP produced a significant peak LOD of 3.3 on chromosome 10q22 (Figure 6.7). The genome-wide significance level of this result (p=0.0165) strongly suggests that this region contains a gene that contributes to the variance of IOP. We did not see any overlap with the IOP linkage regions on chromosome 6q27 and 13q31 identified by Duggal *et al.* (2005). While our region of interest for IOP on chromosome 10q22 has not been reported previously for IOP, linkage to this region has also been found for systemic hypertension in a Japanese population (Wu *et al.* 2003). The association between systemic blood-pressure (systolic or diastolic) and IOP has been well documented (McLeod *et al.* 1990; Dielemans *et al.* 1995; Tielsch *et al.* 1995b). It is possible that systemic hypertension and IOP share a common QTL in this region on chromosome 10q. This region contains *BMPR1A*

(MIM:601299), a bone morphogenic protein receptor, of interest since *Bmp4* has been implicated in increased IOP in mice (Chang *et al.* 2001). The peak region also contains *RGR* (MIM:600342), an opsin-related gene associated with retinitis pigmentosa (Bernal *et al.* 2003). The *OPTN* gene is located outside our 10p13 linkage peak, approximately 60 cM upstream.

Applanation tomometry measurements of IOP are known to be influenced by central corneal thickness (CCT) (Hansen and Ehlers 1971; Stodtmeister 1998). CCT has a positive and apparently linear correlation with IOP (Wolfs *et al.* 1997), and is strongly genetically determined with an extremely high heritability (Toh *et al.* 2005). There has been a report of familial thick corneas segregating in a family with apparent ocular hypertension (Dohadwala and Damji 2000), which leads to the suggestion that perhaps the variation in IOP in family GTas02 compared with the population is due to CCT. However, there are many individuals in family GTas02 with moderate to advanced visual field loss, which would support the elevated IOP being genuine rather than artefactual in nature. It is possible that measurement of CCT and subsequent adjustment of Goldmann applanation IOP readings for GTas02 may have the effect of strengthening the linkage at the IOP locus on chromosome 10q22, by providing a more accurate approximation of true IOP (as opposed to measured IOP). This approach is worthy of future investigation. However, CCT data is not currently available for this pedigree.

This study identified a putative trait locus for maximum cup-to-disc ratio on chromosome 1p32 – the first reported locus for this trait – with a peak LOD score of 2.3 (p=0.00056; Figure 6.9) and a genome-wide p=0.208. This corresponds to suggestive linkage, since there is a 20% chance of a LOD score of this size or greater occurring by chance in a genome-wide scan. The region covered by the linkage peak includes the

gene *POMGnT1* (MIM:606822), mutant forms of which are responsible for muscle-eye-brain disease (MEB; MIM:253280), a congenital muscular dystrophy based disorder with many additional features including early-onset glaucoma, optic nerve atrophy, severe congenital myopia and retinal hypoplasia. MEB is inherited as a loss-of-function of *POMGnT1* (Manya *et al.* 2003), hence it is possible that more mild, heterozygous mutations of *POMGnT1* may contribute to the optic nerve degeneration in POAG. The peak region also contains *FOXE3* (MIM:601094), known to be associated with anterior segment ocular dysgenesis (Semina *et al.* 2001) and is approximately 25 cM distal to the primary congenital glaucoma locus GLC3B (MIM:600975), on chromosome 1p36 (Akarsu *et al.* 1996).

SOLAR 2.1.1 supports the analysis of a discrete trait that has two possible values, using a liability threshold model. However, the program's authors recommend the use of quantitative traits whenever possible as they provide more information than discrete traits, and the modelling of quantitative traits maximises more quickly and reliably (Williams *et al.* 1999a). The analysis of the discrete trait based on typical POAG affection status (clinical diagnosis) revealed no significant linkage information. There were a set of small peaks on chromosome 1q, including a peak in the region of the myocilin gene (Figure 6.5), but no evidence of overlap with the chromosome 1p locus for maximum cup-to-disc ratio identified in section 6.5.4. The dichotomous trait linkage analysis produced two broad peaks on chromosome 10 (Figure 6.5), one corresponding to the approximate location of *OPTN* and the other corresponding to the maximum IOP locus near marker D10S537 identified in section 6.5.3. Several additional peaks (LOD>1) were identified on chromosomes 3, 4 and 9 (Figure 6.5). One of the peaks on chromosome 9 is of interest, since it overlaps the region on 9q22 that was recently identified as a novel locus for JOAG (Wiggs *et al.* 2004). The peak

region of interest identified by Wiggs *et al.* (2004) lies between markers D9S287 and D9S1690 (see Figure 6.5 for chromosomal locations of these markers). One gene originally identified in JOAG (*MYOC*) had been clearly shown to influence POAG as a whole; hence it is plausible that, if identified, the gene at 9q22 may also be involved POAG pathogenesis. Although the regions are not necessarily the same, the standard of results (many small, somewhat 'noisy' peaks) are typical of other POAG analyses based on a dichotomy of affection (Wiggs *et al.* 2000; Nemesure *et al.* 2003) and are similar to results obtained by other researchers using nonparametric approaches to analyse the GTas02 genome-scan data (Dr Paul Baird 2003, personal communication; data not shown).

The *MYOC* Q368X mutation is the most common mutation identified in POAG patients to date, found to account for approximately 1.6% of POAG (Fingert *et al.* 1999). In comparison to other *MYOC* mutations associated with JOAG, this mutation generally gives rise to a milder phenotype with late age of onset and raised IOP (Allingham *et al.* 1998). Myocilin mutation status and related phenotypic modification effects within family GTas02 have been previously reported (Craig *et al.* 2001; Baird *et al.* 2003). The *MYOC* locus was not apparent in either of the linkage analyses for the two quantitative traits investigated in this study. This mutation is clearly unable to account for the presence of all cases of POAG in the entire family (Baird *et al.* 2003). Despite the absence of a linkage signal at *MYOC*, the Q368X mutation appeared to account for nearly half the genetic variance for the quantitative trait based on maximum cup-to-disc ratio, and nearly 20% of the genetic variance for maximum IOP. The differences between carrier and non-carrier trait values (shown in Table 6.5) were significant, which may indicate epistasis or some other form of interaction between *MYOC* and the putative trait loci for IOP and cup-to-disc ratio. The reduction in peak LOD scores for

both traits following the inclusion of the Q368X mutation as a covariate provides further evidence for the presence of an interaction. However, the sample size of family GTas02 does not provide sufficient power to determine the exact mechanism behind this interaction. Subsequent identification of the genes at these loci is anticipated to aid the investigation into the nature of this interaction.

Baird *et al.* (2005) recently identified linkage of clinical POAG diagnosis to chromosome 3p21-p22 using MCMC based linkage analysis of family GTas02 and the same genome-wide scan data as this study. They generated a maximum two-point LOD score of 1.2 at marker D3S1300, and a minimum locus specific p-value of 0.003 with the S_{pairs} and S_{most} statistics at marker D3S1298 (Baird *et al.* 2005). We did not find any evidence of overlap with this region using the traits maximum IOP and cup-to-disc ratio, however we did identify a modest peak (LOD=1.7; p=0.0058) at the same locus (between markers D3S1298 and D3S1289) in the analysis of the dichotomous trait, which is equivalent to the classification of affection used by Baird *et al.* (2005). There are likely to be many genes contributing to the complex POAG phenotype, beyond those influencing maximum IOP and cup-to-disc ratio, and different analytical approaches will have varying power to detect certain loci. The gene at the 3p locus may contribute to a different POAG trait, such as *progression* from elevated IOP to optic nerve damage and subsequent clinical signs of visual field loss. Finally, as with any genome scan, one must also be mindful that some of these linkage results could represent chance events.

The bivariate multipoint linkage analysis was used to take advantage of any additional information contained in the correlation pattern between two quantitative traits. However the results of the analysis provided no evidence of a common genetic locus

influencing both IOP and vertical cup-to-disc ratio. While both peaks of interest from the individual trait analyses were present, both were reduced in magnitude. This effect is suggestive of a reduction in power for the combined analysis. However, on considering the physiology of each trait, it may be unlikely that a single QTL influencing both intraocular pressure and cup-to-disc ratio exists, or has an influence at a level that could be detected given the power constraints of this study.

The primary aim of this chapter was to explore the use of quantitative data, collected as a component of routine clinical examination for POAG, as the basis for the genetic linkage analysis, in an attempt to identify regions of linkage contributing to maximum recorded IOP and maximum cup-to-disc ratio. Applying this method to a pedigree enriched for POAG should improve the power to map genes related to POAG-correlated traits, since extreme values of IOP and cup-to-disc ratio are likely to be present within an extended POAG pedigree, as we found in family GTas02. When used in combination with population-based ascertainment correction (which provides a comparison between these extreme values and the distribution in the general population), this approach provides greater power to detect linkage to these POAG-correlated traits. Trait selection for this study was based, not only on the data available and the relevance of the chosen trait values to the disease, but also on the quality of the available data. While maximum IOP is not an ideal measure, especially given the occurrence of pressure spikes and diurnal variation, mean IOP or any other measure is likely to be equally problematic, considering the likely inclusion of post-medication pressures. However, these biases in the chosen trait data are also present in the general population data used for the ascertainment correction. Utilising this method, this investigation was able to identify significant or near significant regions of linkage contributing to maximum recorded IOP and maximum cup-to-disc ratio. The discovery

of genes at loci that appear to influence components of the POAG phenotype is anticipated to provide significant insights into glaucoma pathophysiology as a whole.

Chapter 7 – Discussion

POAG is a complex and highly genetically heterogeneous disease. Three genes for adult onset POAG have been identified: *MYOC* (Stone *et al.* 1997), *OPTN* (Rezaie *et al.* 2002) and *WDR36* (Monemi *et al.* 2005), however mutations in these genes account for only a fraction of POAG cases. In addition to these genes, five other loci for adult-onset POAG have been mapped: GLC1B (Stoilova *et al.* 1996), GLC1C (Wirtz *et al.* 1997), GLC1D (Trifan *et al.* 1998), GLC1F (Wirtz *et al.* 1999) and GLC1I (Allingham *et al.* 2005); however, only two of these loci have been replicated in published studies; GLC1B (Raymond *et al.* 1999 [abstract], Charlesworth *et al.* 2006) and GLC1C (Kitsos *et al.* 2001); one of these as a result of this dissertation (Charlesworth *et al.* 2006). Genome-wide scan results suggest several additional chromosomal regions may also be involved in POAG susceptibility (Wiggs *et al.* 2000; Nemesure *et al.* 2003; Wiggs *et al.* 2004; Baird *et al.* 2005).

This dissertation aimed to navigate the complexity of POAG and investigate genetic contributions to the disease in extended pedigrees from the Tasmanian population by applying different analysis methodologies to each of the two distinct datasets used in this investigation. The first investigation was comprised of a set of 10 extended pedigrees with information on disease status and genotypic data restricted to the six POAG loci known at the time, GLC1A-F. This dataset was analysed with exact and MCMC estimation based parametric and nonparametric linkage analyses, as described in Chapters 4 and 5. The second approach included 10 cM genome-wide scan data from a single extended pedigree and analyses of quantitative measures of phenotypic components or correlates of the POAG. For this dataset we were able to utilise multipoint variance components linkage analysis of both dichotomous and quantitative traits, as described in Chapter 6.

There are two common approaches to the exact linkage analysis of dichotomous traits, and these are based on either considering all loci simultaneously or all family members together. The first approach, implemented in programs such as LINKAGE, is based on the Elston-Stewart algorithm (Elston and Stewart 1971) and can be used with extended pedigrees, but with only a limited number of markers. The second, implemented in programs such as GeneHunter, is based on the Lander-Green algorithm (Lander and Green 1987) and can analyse many marker loci, but is restricted in terms of pedigree size. There is no exact likelihood-calculation method for linkage analysis that allows multipoint analysis of extended pedigrees with many markers. However, there are several approximation methods, such as the MCMC based estimation methods employed in SimWalk2, that can utilise extensive marker and genotypic data simultaneously.

Given the size and complexity (the presence of marriage and inbreeding loops) of the pedigree dataset in Chapter 4, the available genetic data (3-5 markers per locus), the computational constraints (discussed in Chapter 4.6) and the available clinical data (dichotomous affection status based on POAG diagnosis), exact parametric analyses using FASTLINK were restricted to two-point analyses (unrestricted by pedigree size) while exact nonparametric analyses using GeneHunter were multipoint but involved trimming all but one of the pedigrees. In anticipation of these restraints, MCMC estimation based parametric and nonparametric linkage analyses (in this case using SimWalk2) were used as a first pass approach in the analysis of the data in Chapter 4. These methods were used to generate multipoint linkage results using all available family information. The lack of phase information from deceased relatives, especially spouses (see Figures 2.2-2.11), reduced our power to detect linkage, thus methods

employing information from all pedigree members, rather than affecteds only or trimmed pedigrees, were preferable. Using these MCMC based analyses as a first pass approach in Chapter 4 we identified two regions of interest that were followed-up in Chapter 5. The evidence for linkage at one of these regions (the GLC1B locus on chromosome 2 in family GTas15) was strengthened following fine mapping and follow-up analysis. The empirical p-values calculated using SimWalk2 (p=0.01 or less) and exact GeneHunter p-value (p=0.005) at the distal end of the region of interest provide supportive evidence for the existence of a POAG susceptibility locus at 2cen-q13 (Charlesworth *et al.* 2006). The success of this result supports the hypothesis that the MCMC estimation based parametric and nonparametric analysis conducted in Chapter 4.5.3-4.5.4 was a suitable first pass approach to search for linkage given the available pedigree and genotypic data.

The results obtained by the initial MCMC based analyses described in Chapter 4.5.3 and 4.5 4 and the duplicate exact analyses described in Chapter 4.5.7 and 4.5.8 are difficult to compare. The results of the two approaches employing nonparametric analyses were similar, supporting the utility of SimWalk2 for estimation based nonparametric linkage analysis. For example, the p-values for GTas11 and GTas121 at the GLC1C locus were similar in both the estimation based nonparametric linkage (NPL) analysis (0.04; Chapter 4.5.3) and the exact analysis (0.03; Chapter 4.5.7). The estimation based and exact parametric analyses are harder to compare, even though the same model constraints were used, because the estimation based analyses were multipoint while the exact were restricted to two-point. However, the results of the two approaches do not appear to compare favourably; for example the LOD of 1.08 at marker D3S1569 in family GTas121 in the estimation based analysis (Chapter 4.5.4) drops to 0.38 in the exact analysis (Chapter 4.5.8). While this may suggest an inherent weakness in the

SimWalk2 estimation based parametric analysis, or a failure of the two-point analysis, it most likely reflects the inability of parametric analyses to appropriately model complex diseases such as POAG. Investigations into the genetic contributions of POAG have traditionally employed some form of exact parametric analysis (Sheffield *et al.* 1993; Stoilova *et al.* 1996; Wirtz *et al.* 1997; Sarfarazi *et al.* 1998; Trifan *et al.* 1998; Wirtz *et al.* 1999; Wiggs *et al.* 2000; Nemesure *et al.* 2003). Parametric analysis is very powerful in situations where the disease model can be accurately described, including the heterogeneity, penetrance functions and disease gene frequency, however it may be less powerful in the case of complex disease where the disease model is not apparent, and where additional complications such as polygenic and epistatic effects may further confound the model. Given the apparent genetic complexity of this disease, the use of parametric models in POAG genetic studies may be a contributing factor to the difficulties of replicating the named POAG susceptibility loci, despite the fact that most of these loci were first reported more than six years ago.

Many complex diseases have quantitative clinical correlates that may be directly related to disease risk. Parametric and nonparametric linkage analyses of complex disease have often involved the dichotomisation of information-rich quantitative phenotype components (Hanis *et al.* 1996; Stoilova *et al.* 1996; Wiggs *et al.* 2000; Wiltshire *et al.* 2001; Angius *et al.* 2002; Nemesure *et al.* 2003). The use of discretised versions of biologically continuous phenotypes for linkage analysis is often unnecessary and can result in marked reductions in power to detect and localise genes influencing these disease phenotypes (Duggirala *et al.* 1997; Wijsman and Amos 1997; Williams *et al.* 1999a). When the observable phenotype is inherently continuous, methods of linkage analysis for quantitative traits are preferable (Duggirala *et al.* 1997). For common diseases in particular, it may be more appropriate to examine the continuum of variation

than to limit analysis to a dichotomy of affected and unaffected individuals (Williams *et al.* 1999a).

In the study by Duggirala *et al.* (1997), using data from the tenth Genetic Analysis Workshop (GAW10), a continuous phenotype was dichotomised using a liability threshold model and both the continuous and discrete traits analysed using variance components analysis in SOLAR. The dichotomisation clearly diminished the power to detect linkage when compared with the direct analysis of the continuous trait (Duggirala *et al.* 1997). The variance-component based method is less model-bound than parametric analyses and therefore more likely to avoid model misspecification problems. The authors of the variance components analysis program SOLAR (Almasy and Blangero 1998) recommend the use of quantitative over discrete traits whenever possible (Williams *et al.* 1999a). It is important to note that there are situations where the analysis of discrete traits may be unavoidable. For example, some phenotypes are classified clinically as qualitative traits (presence or absence of disorder), such as some psychiatric disorders, and even though there may be an underlying continuous phenotype or disease correlate that would be more useful for genetic analysis, such data may not be readily obtainable.

Studies of POAG genetics have consistently used a dichotomous affection status derived from a combination of several clinical characteristics, most notably optic disc degeneration and characteristic visual field loss, and in some cases elevated intraocular pressure, by applying a threshold level to each (Sheffield *et al.* 1993; Stoilova *et al.* 1996; Wirtz *et al.* 1997; Sarfarazi *et al.* 1998; Trifan *et al.* 1998; Wirtz *et al.* 1999; Wiggs *et al.* 2000; Nemesure *et al.* 2003; Allingham *et al.* 2005). There has been little standardisation of this process, which means that the definitions used for affection status

vary between studies (Kahn and Milton 1980; Wolfs *et al.* 2000; Kroese and Burton 2003). The high heterogeneity of the disease also suggests that the set of complex phenotypes that are combined into a clinical diagnosis of the disease may be controlled by a wide range of genetic and environmental factors.

In light of the evidence supporting the likely superior power of quantitative traits over their dichotomous counterparts, we reconsidered the clinical data available from a typical linkage study of POAG and identified quantitative traits corresponding to components of the POAG phenotype. While there are many clinical measures available for this disease, not all are suitable traits for analysis. By selecting maximum recorded IOP and maximum cup-to-disc ratio as quantitative traits for linkage analysis we were attempting to identify loci influencing these particular components of the POAG phenotype, in contrast to the classical approach of identifying 'POAG genes' using clinical diagnosis as the affection status. Applying this method to an extended POAG pedigree should provide an enrichment of extreme values of these traits when compared with the general population, since the hypothesis is that variants at these loci influence traits involved in POAG pathogenesis or progression. The results of Chapter 6 suggest that this approach is appropriate, since one region of significant or suggestive linkage was identified for each trait. Multipoint linkage analysis of maximum recorded IOP (Chapter 6.5.3) identified a peak LOD of 3.3 (p=0.00015; genome-wide p=0.0165) near marker D10S537 on chromosome 10q22; while analysis of maximum cup-to-disc ratio (Chapter 6.5.4) produced a peak LOD score of 2.3 (p=0.00056; genome-wide p=0.208) near markers D1S197 to D1S220 on chromosome 1p32 (Charlesworth *et al.* 2005).

The quantitative trait analyses also appear to out-perform the variance components dichotomous trait analysis based on clinical diagnosis of POAG (equivalent to the

affection status used in previous studies of POAG genetics), both in terms of significance and clarity of the results. The analysis of the discrete trait based on typical clinical diagnosis revealed no significant linkage results (Chapter 6.5.2). However, we did identify a peak (LOD=1.7; p=0.0058) at 3p21-p22 (between markers D3S1298 and D3S1289), a locus also identified by Baird *et al.* (2005) using the same genome-wide scan and phenotype data as this study. The definition of our dichotomous trait was equivalent to the classification of affection used by Baird *et al.* (2005), and the results (a maximum two-point LOD score of 1.2 and a minimum locus specific p-value of 0.003 with the S_{pairs} and S_{most} statistics) were similar to those obtained in our dichotomous trait analysis. Our 3p linkage result may have been more interesting than we initially thought, in view of the fact that Baird *et al.* identified this locus using the same dataset but a completely different analytical approach (MCMC based nonparametric linkage analysis as opposed to variance-components dichotomous trait linkage analysis). However, if multiple testing for linkage to POAG using the same dataset is taken into account, the significance of this finding is further reduced.

Most traditional statistical genetic methods for the analysis of complex phenotypes are not designed to exploit the wealth of linkage information available in extended pedigrees. The results of the GAW10 revealed linkage methods using all available pedigree information were superior to nuclear pedigree approaches (Wijsman and Amos 1997). The extended pedigrees were consistently more informative than their nuclear counterparts in terms of power and accuracy for linkage detection and parameter estimation. However, a surprise result, derived from a variety of contributions, was that more information could be extracted from 23 extended pedigrees analysed with a single, closely linked polymorphic marker than from multipoint analysis of 239 nuclear

pedigrees with as many as 25 equivalent, closely linked markers (Wijsman and Amos 1997).

The computational burden for exact multipoint (IBD) calculations is light in nuclear families but may be prohibitive in extended pedigrees (Almasy and Blangero 1998). Approximate IBD calculations for extended pedigrees can be performed by a range of statistical packages, including the MCMC based programs SimWalk2 (Sobel and Lange 1996) and Loki (Heath 1997; Heath *et al.* 1997). SimWalk2 was utilised for the IBD calculations of the extended pedigree datasets in Chapters 4 and 5, due in part to the ease of use of this program in combination with the utility MEGA2 (Mukhopadhyay *et al.* 2005b), making it easy to perform parametric, nonparametric and haplotyping analyses on this data. Loki was used to calculate IBDs for Family GTas02 in Chapter 6 from within SOLAR version 2.1. SimWalk2 could also have been used to generate the IBD probabilities for use with SOLAR, however Loki was selected due to reports of greater reliability of its mixing algorithm (Dr Thomas Dyer 2003, personal communication).

POAG appears to be highly genetically heterogeneous. Three genes involved in POAG have been identified (Stone *et al.* 1997; Rezaie *et al.* 2002; Monemi *et al.* 2005), along with several named loci (Stoilova *et al.* 1996; Wirtz *et al.* 1997; Sarfarazi *et al.* 1998; Trifan *et al.* 1998; Wirtz *et al.* 1999; Allingham *et al.* 2005). Various other chromosomal regions have also been suggested (Wiggs *et al.* 2000; Nemesure *et al.* 2003; Baird *et al.* 2005). As a result of this genetic heterogeneity, we did not expect to see multiple pedigrees from the GIST dataset analysed in Chapter 4 linked to the same chromosomal region. The ascertainment of the entire pedigree dataset from the same source population, and from a population with demonstrated founder effects (Shepherd

1985; Pridmore 1990; Mackey and Howell 1992; Teh *et al.* 1995; Baird *et al.* 2003) was anticipated to reduce the genetic heterogeneity to some degree. Families GTas03 and GTas11 showed some evidence of linkage to the same region of chromosome 3 (D3S3637 to D3S3694; Chapter 4.5.3), and although no common haplotype or shared alleles could be detected in this investigation, these results would be a worthy avenue for follow-up analyses in future projects of the GIST.

Conclusions

This dissertation explored several different approaches to the analysis of extended POAG pedigrees in an attempt to dissect the genetic aetiology of this phenotypically and genetically heterogeneous disease. The study included two distinct datasets, both derived from the Glaucoma Inheritance Study in Tasmania. Different analysis methodologies were applied to each datasets, determined by the available data.

In Chapter 4 we investigated linkage to markers within the regions of the known POAG loci GLC1A, GLC1B, GLC1C, GLC1D, GLC1E and GLC1F, in a set of 10 extended Tasmanian pedigrees. MCMC estimation based parametric and nonparametric analyses revealed two regions of possible interest. Family GTas15 produced p-values of 0.05-0.07 for three markers within the GLC1B region on chromosome 2 (D2S2264 to D2S1892) in the nonparametric analysis described in Chapter 4.5.3 and a maximum location score of 1.12 on chromosome 2 corresponding to marker D2S1892 in the parametric analysis described in Chapter 4.5.4. Similarly, family GTas35 produced p-values of 0.05-0.06 for three markers within the GLC1E region on chromosome 10 (D10S1691 to D10S1664) in the nonparametric analysis described in Chapter 4.5.3 and a peak location score of 1.43 at marker D10S1664 in the parametric analysis in Chapter 4.5.4. Fine-mapping and follow-up analysis of these two regions, described in Chapter 5, revealed that the initial linkage signal in family GTas35 was most likely a false positive. However, fine-mapping and follow-up analysis of the GLC1B locus in family GTas15, as described in Chapter 5, strengthened the evidence for linkage. The empirical p-values calculated using SimWalk2 (p=0.01 or less) and exact GeneHunter p-value (p=0.005) at the distal end of the region of interest provided supportive evidence for the existence of a POAG susceptibility locus at 2cen-q13 (Charlesworth *et al.* 2006).

In Chapter 6 we utilised multipoint variance components linkage analysis of both dichotomous and quantitative traits using data from an extended POAG pedigree including comprehensive clinical information and genotyping data from a 10 cM genome-wide scan. In this investigation two individual phenotype components of POAG, maximum recorded IOP and maximum vertical cup-to-disc ratio, were analysed as quantitative traits using variance components analysis based on the hypothesis that these traits may have more simple genetic architectures than an overall diagnosis of POAG. Multipoint linkage analysis of maximum recorded IOP identified a peak LOD of 3.3 (locus-specific p=0.00015; genome-wide p=0.0165) near marker D10S537 on chromosome 10q22; while analysis of maximum cup-to-disc ratio produced a peak LOD score of 2.3 (locus-specific p=0.00056; genome-wide p=0.208) near markers D1S197 to D1S220 on chromosome 1p32 (Charlesworth *et al.* 2005). In comparison, however, the analysis of the dichotomous trait based on clinical diagnosis of POAG was underpowered and revealed no significant linkage information. The bivariate analysis of the quantitative traits and analyses involving the inclusion of myocilin mutation status as a covariate suffered similar deficits in power.

The results of this dissertation suggest that the inclusion of quantitative correlates or components of disease in the genetic analysis of POAG may offer significant power to elucidate the genetic basis of glaucoma in the face of limited family and population datasets. The discovery of genes at the loci identified as contributing to the variance of maximum IOP and maximum cup-to-disc ratio in this study may provide significant insights into glaucoma pathophysiology as a whole. As an avenue for future investigation we would recommend that the loci identified in Chapter 6 of this dissertation be followed-up in the dataset of 10 extended POAG families used in

Chapter 4. In combination with the ascertainment correction model created as part of this dissertation, and given that these pedigrees come from the same source population as family GTas02, this dataset may provide significant power for the confirmation of the IOP and cup-to-disc ratio loci.

We would also recommend genotyping the 10 extended Tasmanian POAG pedigrees with either microsatellite markers at a density of at least 10 cM across the entire genome or at least a 10k SNP chip. The combination of the clinical information available from the GIST and comprehensive genome-wide scan data, these 10 POAG pedigrees would form a powerful dataset for the investigation of POAG phenotype components using the methods described in Chapter 6.

Another avenue for additional investigation would be to include CCT as a covariate in the analysis of maximum IOP in family GTas02. CCT is a confounder of IOP measurement, with thick corneas causing artefactual ocular hypertension through measurement error; hence inclusion of CCT as a covariate may benefit the reanalysis of IOP as a quantitative trait by providing trait data that that more accurately models the biological variation.

Another approach for follow-up investigations would be to analyse CCT as a quantitative trait in its own right, given suitable population data to provide the ascertainment correction. CCT is highly heritable (Toh *et al.* 2005) and has been shown to influence the conversion from ocular hypertension to glaucoma (Brandt *et al.* 2001). As an important factor in glaucoma diagnosis and management, determining the genetic contributions to this trait would be of great interest to the wider study of POAG pathogenesis.

This dissertation has contributed to the genetic dissection of POAG through the confirmation of one genetic susceptibility locus (Charlesworth *et al.* 2006) and the identification of one significant and one suggestive quantitative trait locus for components or correlates of POAG (Charlesworth *et al.* 2005). This investigation has also prepared and refined a dataset of 10 extended POAG pedigrees from the Tasmania population that will provide considerable power for future investigations of the genetics of this complex disease. These pedigrees have so far been used for only minimal exploratory linkage analyses and, when combined with genome-wide coverage of a dense marker set, will be a powerful resource for future genetic analyses of POAG.

Appendix 1 - Clinical methodology and definition of POAG in the Glaucoma Inheritance Study in Tasmania

A1.1 Clinical Diagnosis of POAG

Clinical examination and diagnosis of patients involved in the GIST is well documented (Coote *et al.* 1996). In brief, POAG was defined as an optic neuropathy which has present at least two of the following features: (1) optic nerve head excavation with thinning of the neuroretinal rim (generally measured by an enlarged vertical cup-to-disc ratio≥0.7), often but not necessarily including significant focal or generalised loss of retinal nerve fibre layer, notching, pitting, or 'Drance' type nerve fibre layer haemorrhages; (2) elevation of the IOP over a population-based normal range, or over the average of the unaffected individuals within a pedigree (generally IOP>21mmHg or 2 standard deviations from the population mean); and (3) reproducible visual field defects consistent with the disc changes and with common descriptions of glaucomatous field loss (Coote *et al.* 1996). Glaucoma cases secondary to rubeosis, trauma or anterior segment dysgenesis were excluded.

A1.2 Intraocular pressure measurement

IOP measurements were taken using Goldman applanation tonometry and not standardised for the time of day. No corrections were made for corneal thickness since this information was not routinely collected at the time of patient ascertainment. Elevated IOP was generally defined as measured IOP greater than or equal to 22mmHg (two standard deviations above the mean) in either eye at the time of examination or as reported by a reliable third party prior to treatment. Pressure greater than 28mmHg (or four standard deviations from the mean) at the time of examination, or reported by a reliable third party such as a treating clinician, was considered 'extreme'.

A1.3 Optic disc analysis

Optic disc appearance was independently classified by two clinicians at the time of examination using a slit-lamp biomicroscope with a 78D lens for binocular stereovision after pupil dilation. In addition, optic disc stereo photographs (Nidek, Japan) were taken for future reference in all cases. Where a discrepancy existed between the 2 examiners, the stereo disc photos were independently assessed by a third glaucoma specialist. Attention was paid to similarity between eyes, particularly in relation to cup-disc ratio disparity. A category called 'appearance precludes satisfactory assessment' (APSA) was used in situations where the appearance of the optic nerve was unable to be accurately assessed due to media opacity, or was subject to a condition making exclusion of glaucoma impossible. Discs were considered 'normal' if the appearance of both optics discs was normal or consistent with normal variation but not consistent with glaucoma. Optic nerve heads could be classified 'abnormal and consistent with glaucoma' based on observed features such as: a focal notch in the neuroretinal rim but not extending to the margin, a vertical cup-to-disc ratio of 0.7 or greater, or a 0.2 difference in cup-to-disc ratios between two eyes. The appearance of optic discs highly consistent with glaucoma include: an acquired pit in the optic nerve, a notch in the neuroretinal rim extending to the margin or a vertical cup-to-disc ratio of 0.8 or greater.

A1.4 Visual field analysis

Visual field analysis was performed on a Humphrey perimeter using a 24-2 array, a size III target and the full-threshold test system. Both eyes were tested, with a short break between tests. Visual fields were categorised on a scale of A-D. Category A indicates normal field, where all points lie within the age corrected normal values on the pattern deviation plot. Category B indicates a reliable field test with minor depression at one or

two points not consistent with glaucoma on the pattern deviation plot. Category C indicates a reliable test, significant and consistent with glaucoma, where there were 'three or more adjacent or clustered points within a hemifield or within the nasal field with a significantly reduced threshold and a pattern deviation plot consistent with glaucoma' (Coote *et al.* 1996). Category D indicates the visual field was markedly degraded and highly consistent with glaucoma. Normal visual fields were consistent with categories A and B, whereas visual fields allocated to categories C and D were considered glaucomatous. In the case of unreliable performance based on fixation losses, or false positive or false negative rates exceeding 20%, visual fields were repeated on another occasion until reliable fields were obtained enabling definite classification.

Appendix 2 - Microsatellite marker primer information

This appendix includes the primer sequence, pool number, fluorescent label and optimised PCR condition information for primers used in Chapter 4 (Table A2.1 and Table A2.2) and Chapter 5 (Table A2.3).

Primer	Primer Sequence	Heterogeneity	Allele size (min)	Allele size (max)	Label	Pool	Temp °C	Mg^{2+}
D1S2635-F	TAGCAGATCCCCCGTC	0.87	142	160	FAM	2	58	1.5
D1S2635-R	TGAATCCTACCCCTAAGTAGAAT							
D1S2707-F	CCCCTTGGCATAGGGTTCAAGA	0.82	137	159	FAM	1	58	1.5
D1S2707-R	AGCCAGGCATCTGCACCTTC							
D1S2675-F	AGAGGCTGTTCTGAGGTACTGC	0.73	160	174	FAM	3	58	1.0
D1S2675-R	CATGATTGGCTCAAGTCCC							
D2S2161-F	TGTTCACCCCTCAGGC	0.77	176	204	FAM	1	58	1.5
D2S2161-R	ATTACTCCTATTGTCCCTGTCTGC							
D2S113-F	GCTTGTTTCATCTCACCCTG	0.77	206	230	FAM	3	58	1.5
D2S113-R	CTGTTGTTTTTTAGGTGGGAG							
D2S2264-F	CATCTCAAAGGGCATGTC	0.77	241	257	FAM	2	58	1.5
D2S2264-R	TCGAATGAACAGTGCCTC							
D2S1897-F	AGGAATTTGCTGATACTCAACC	0.89	215	237	HEX	3	58	1.5
D2S1897-R	AGGCATTGATATAAGGCTCTCT							
D2S1892-F	TCCTAACTCTGAAATGCTAAAGACA	0.80	211	251	HEX	2	58	1.5
D2S1892-R	AGCTCTGGCAGGGAGA							
D3S3637-F	TGGGAAGCCAGTCAGTCAAT	0.90	178	206	FAM	2	58	1.5
D3S3637-R	TGGCCTGCACATAAAAGGAT							
D3S1301-F	CATAAATATCACAGGGCCAA	0.77	187	197	HEX	2	58	1.5
D3S1301-R	TTCTTATCCGTTCTGCCA							
D3S3694-F	AGTGTCCATCAACATGGG	0.84	138	162	HEX	1	58	1.5
D3S3694-R	TCGCACAAATAACAGGATTC							
D3S1569-F	GCACCTTGGCTTACCTTCTA	0.80	277	297	HEX	3	58	1.5
D3S1569-R	GGACAGTTGAAAGGTTCTTAAAG							
D3S1608-F	AGCAATCATGTGCCCC	0.61	184	206	HEX	4	55	1.0
D3S1608-R	CCCAATGGTAAGTGCAGG							

Table A2.1 – Details of the primers used in the initial investigation of the known POAG loci (Chapter 4) – Table 1 of 2

Primer	Primer Sequence	Heterogeneity	Allele size (min)	Allele size (max)	Label	Pool	Temp °C	Mg^{2+}
D8S1749-F	ACACTTGTGTGCAAGCA	0.74	128	140	HEX	4	55	1.5
D8S1749-R	AGCAATTTGGGCCTGT							
D8S556-F	CTGGTGACTTCCTGCCATATAC	0.80	161	175	HEX	3	58	1.5
D8S556-R	CTTGCTGTGAGGTAAGACGA							
D8S198-F	AACCAGATTAGGGACAAAGA	0.83	155	173	HEX	2	58	1.5
D8S198-R	TAGGGACTACACATGATGGA							
D10S1729-F	AAGGACTGCATTGTTTTTG	0.72	177	183	HEX	1	58	1.5
D10S1729-R	TCAGACACTCTTAGGATTACCTC							
D10S1713-F	GACAGCAACTAACCTCCTGTAAG	0.60	245	255	FAM	4	55	1.5
D10S1713-R	TGTGTTATTCAAGGGTCAGC							
D10S1691-F	TGCTTGCACGAAGGTAATGTTCAG	0.67	247	277	HEX	4	55	1.5
D10S1691-R	TGCCTGCTGAGAAACAGTGATG							
D10S547-F	CTTGAAAGGCGGAGGC	0.74	236	250	HEX	1	58	1.5
D10S547-R	CCCAATAGTCCACAGGGAG							
D10S1664-F	AACCGTAATAACTTAGGTGCTC	0.75	164	198	FAM	4	55	1.5
D10S1664-R	TGCTGAAGACAGGTAAAGAG							
D7S2511-F	CAGAGCAATACCATCAAAAC	0.79	243	265	FAM	3	58	1.0
D7S2511-R	GTACCATAAACTGGGTGGC							
D7S505-F	ACTGGCCTGGCAGAGTCT	0.69	262	278	FAM	1	58	1.0
D7S505-R	CAGCCATTCGAGAGGTGT							
D7S2439-F	CAGCAAAAGGTACAGCAATTTC	0.80	195	211	HEX	1	58	1.5
D7S2439-R	AAAGTCTACGCCGCATTC							
D7S2546-F	GGAGGTTGAACAACTCTGAATAC	0.75	234	242	FAM	1	58	1.5
D7S2546-R	CACGCCAGGGTCTATCTT							

Table A2.2 – Details of the primers used in the initial investigation of the known POAG loci (Chapter 4) – Table 2 of 2

Primer	Primer Sequence	Heterogeneity	Allele size (min)	Allele size (max)	Label	Pool	Temp °C	Mg^{2+}
D2S2187-F	GCTCCAAACCAGCCTC	0.63	149	159	TET	1	55	1.5
D2S2187-R	GAAGCCTCACAATGCAAC							
D2S2364-F	CTCCATGTACCAATTCAGGC	0.66	87	99	FAM	1	55	1.5
D2S2364-R	CCAGGCAGGATGTGTGAGTA							
D2S373-F	ACAGACTTGGCCTGCC	0.74	218	238	FAM	1	55	1.5
D2S373-R	TTGATGATAATGGTGATAGGAAT							
D2S2269-F	AGCCAAACCAAGTCAATGTC	0.88	252	280	FAM	1	55	1.5
D2S2269-R	TGAAAGCATGACACCAATC							
D2S1890-F	TTTCAGATCACCTAATGGGC	0.74	183	220	TET	1	55	1.5
D2S1890-R	AACTGTCTGGTCGGTCATTG							
D2S1893-F	AACAAGGTGAGGCTCTGTC	0.75	244	264	TET	1	55	1.5
D2S1893-R	TCTAAAAATGAAGCAGGATACCA							
D10S189-F	CAAAAGTAACCATTGAGCCC	0.73	180	188	TET	2	55	1.5
D10S189-R	TTGATAGAAGAAGCGATAGATCG							
D10S1649-F	GCTCTTGAAGCATACTTTGG	0.84	120	150	TET	2	58	1.5
D10S1649-R	CTTCTGCCCACTAAACAAAT							
D10S1653-F	CCTTTGGATAAAGCCTCCT	0.78	210	213	FAM	2	58	1.5
D10S1653-R	TATCATTGTCTCATCCGGG							
D10S585-F	TGTTTCCAAAGATAAAGCCC	0.69	233	249	FAM	2	55	1.5
D10S585-R	GTGATAATCCAGATGGTTTCCT							
D10S570-F	GCATTCATCCAACAAGCATA	0.81	287	305	FAM	2	55	1.5
D10S570-R	AATTAGTTCCATGGGCACAG							
D10S223-F	AATTCTGAAGAGGCAAATCTAA	0.66	221	231	TET	2	58	1.5
D10S223-R	AGGAAAATATACACAACCCAAG							
D10S1779-F	TCTGTCTTCAGCACACCC	0.82	265	281	TET	2	55	1.5
D10S1779-R	GCATATCTGTCCCACTCGATAC							

Table A2.3 - Details of the primers used in the follow-up investigation of GLC1B and GLC1E (Chapter 5)

Appendix 3 - Publication of material from Chapter 5

The following article was published in *Ophthalmologica.*

Charlesworth JC, Stankovich JM, Mackey DA, Craig JE, Haybittel M, Westmore RN and Sale MM (2006). Confirmation of the adult-onset primary open angle glaucoma locus GLC1B at 2cen-q13 in an Australian family. *Ophthalmologica* 220(1): 23-30.

Original Paper

Ophthalmologica

Ophthalmologica 2006;220:23–30
DOI: 10.1159/000089271

Received: October 22, 2004
Accepted: December 9, 2004

Confirmation of the Adult-Onset Primary Open Angle Glaucoma Locus GLC1B at 2cen-q13 in an Australian Family

Jac C. Charlesworth[a] James M. Stankovich[a, b] David A. Mackey[a, c–e]
Jamie E. Craig[a, c, e] Michael Haybittel[e] Rodney N. Westmore[f]
Michèle M. Sale[a, g, h]

[a]Menzies Research Institute, Hobart, Tasmania, [b]Walter and Eliza Hall Institute of Medical Research, Melbourne, Victoria, [c]Center for Eye Research Australia, University of Melbourne, Royal Victorian Eye and Ear Hospital, Melbourne, Victoria, [d]Tasmanian Eye Clinics, Launceston, Tasmania, [e]North West Medical Centre, Burnie, Tasmania, and [f]The Eye Hospital, Launceston, Tasmania, Australia; [g]Center for Human Genomics and [h]Department of Internal Medicine, Wake Forest University School of Medicine, Winston-Salem, N.C., USA

Key Words
Glaucoma · Linkage · Genetic susceptibility · Nonparametric statistics · Model-free analysis

Abstract
Primary open-angle glaucoma (POAG) is genetically heterogeneous, with 6 named POAG loci GLC1A-F mapped and genes myocilin *(MYOC)* and optineurin *(OPTN)* identified at 2 of the loci. Using penetrance-model-free methods, we screened the POAG loci GLC1A-F in an extended Australian pedigree, using 3–5 markers within each locus. p values of less than 0.05 were obtained empirically using SimWalk2 and exactly using Genehunter for 2 markers within the GLC1B region on chromosome 2. Fine mapping of this region produced p values of 0.01 or less at 5 markers flanked by D2S1897 and D2S2269. The 9 cM haplotype of interest overlaps the original GLC1B region. These results provide supportive evidence for the GLC1B locus on chromosome 2cen-q13 and verify the existence of POAG susceptibility gene in this region, increasing the likelihood of gene identification.

Introduction

Glaucoma is a term used to describe a heterogeneous group of eye disorders involving damage to the optic nerve and loss of vision, resulting in irreversible blindness if left untreated. Glaucoma is a major cause of visual impairment and blindness in developed countries and is the second leading cause of blindness worldwide [1]. The most common form of glaucoma is adult-onset primary open-angle glaucoma (POAG).

POAG has a strong genetic component, with family history of the disease being an acknowledged risk factor [2–4]. Relatives of POAG patients have been shown to have a ten-fold increase in risk of the disease [3], while studies on the underreporting of family history suggest the genetic component of POAG may be even greater than previously suggested [5].

There is no universally accepted definition of this phenotypically complex and subtle disease [6, 7]. The clinical diagnosis is based on a combination of several main characteristics, including specific changes to the appearance of the optic nerve head, characteristic visual field loss with a slow and progression, and in many cases increased

KARGER
Fax +41 61 306 12 34
E-Mail karger@karger.ch
www.karger.com

0030–3755/06/2201–0023$23.50/0

Accessible online at:
www.karger.com/oph

Michèle M. Sale, PhD
Center for Human Genomics, Wake Forest University School of Medicine
Medical Center Blvd
Winston-Salem NC 27157 USA
Tel. +1 336 713 7510, Fax +1 336 713 7566, E-Mail msale@wfubmc.edu

intraocular pressure (IOP). The complexity of the phenotypic definition of POAG has contributed to the difficulties in identifying genes involved in this disease. Other issues that have hindered mapping of POAG genes include the late age of onset in most cases, unclear mode of inheritance and penetrance in many families, the insidious progression that results in approximately half of cases remaining undiagnosed, and the potential for intrapedigree genetic heterogeneity.

Two genes for adult-onset POAG have been identified [8, 9]; however, mutations in these genes account for only a fraction of familial POAG. The first gene, myocilin *(MYOC)* at the GLC1A locus on chromosome 1q24.3, has been shown to account for approximately 3% of adult-onset POAG [9–12]. The second gene, optineurin *(OPTN)* at the GLC1E locus on chromosome 10p15–14, was identified in a low-tension subset of POAG and shown by Rezaie et al. [8] to be involved in up to 17% of normal-tension glaucoma pedigrees. Mutations in *OPTN* were recently shown to account for up to 1.6–14% of sporadic POAG including high-tension glaucoma, in Chinese subjects [13]. However, recent studies involving Caucasian, African American and Japanese POAG patients and controls have shown little to no association between the 4 previously identified *OPTN* sequence variants and POAG [14, 15].

POAG is clearly genetically heterogeneous. In addition to the 2 genes described above, 4 other loci for POAG have been mapped: GLC1B [16], GLC1C [17], GLC1D [18] and GLC1F [19]; however, the genes at these loci remain to be identified. Although all 4 of these loci were originally mapped between 1996 and 1998, only one (GLC1C) has been replicated in a published study [20]. The results of 2 recent genome-wide scans suggest several additional chromosomal regions may also be involved in POAG susceptibility [21, 22].

Using model-free analysis methods, we screened all 6 named POAG loci, including those containing the *MYOC* and *OPTN* genes, and found evidence for linkage to only the GLC1B locus. This result represents confirmation of the GLC1B locus.

Methods

The Glaucoma Inheritance Study in Tasmania

This investigation was conducted as part of the Glaucoma Inheritance Study in Tasmania [23] (GIST), a large population study of glaucoma genetics based in the island state of Tasmania, Australia. Ethics approval was obtained from the Human Research Ethics Committees of the Royal Children's Hospital, the Royal Victorian Eye and Ear Hospital, the Royal Hobart Hospital, and the University of Tasmania, and this study was conducted in accordance with the tenets of the Declaration of Helsinki. Written informed consent was obtained from all participants.

Through the collaborative involvement of Tasmanian ophthalmologists, the GIST aims to identify all diagnosed glaucoma patients in Tasmania. The study represents almost complete population ascertainment based on population prevalence predictions derived from the Blue Mountains Eye Study [24]. The study identified adult-onset POAG families by first recruiting all diagnosed glaucoma patients and then using genealogical data provided by participants to determine familial relationships between patients. Once apparent pedigrees were identified, each pedigree was expanded and all family members over 40 years of age invited to participate in the study.

The focus of this paper is the GIST family GTas15 which contains 32 individuals across 4 generations (fig. 1), of whom 15 living descendants consented to participate in the study.

Definition of Glaucoma Status

Clinical examination and diagnosis of patients involved in the GIST is documented elsewhere [25]. In brief, POAG was defined as an optic neuropathy which has present at least 2 of the following features: (1) optic nerve head excavation with thinning of the neuroretinal rim, often with 'Drance' type nerve fiber layer hemorrhages, notching, pitting, significant focal loss or general loss of retinal fiber layer; (2) elevation of the IOP over a population-based normal or over the average of the unaffected individuals within a pedigree, and (3) visual field defects consistent with the disc changes and with common descriptions of glaucomatous field loss [25]. Glaucoma cases secondary to trauma or anterior segment dysgenesis are excluded [25].

Family GTas15 contained seven individuals with clinically diagnosed POAG; individuals 15-01, 15-02, 15-03, 15-07, 15-11, 15-12 and 15-16. One individual (15-04) presented with characteristic visual field loss and could have been considered glaucoma suspect. However, for our model-free, affected-only approach it was not necessary to determine whether the remaining family members were glaucoma suspects or truly unaffected; this can be difficult given the late onset and subtleties of POAG. All other individuals were therefore classed as glaucoma status 'unknown' for the purposes of the linkage analyses. Clinical features of GTas15 are indicated in figure 1.

Genotyping

Whole blood was collected in 10-ml EDTA tubes from consenting individuals. DNA was extracted using Nucleon BACC3 kits (Amersham Pharmacia Biotech).

Microsatellite markers were selected from the Genome Database (http://www.gdb.org/) based on location and heterozygosity. Genetic maps used for marker selection and linkage analyses were primarily based on the deCODE genetic map, with missing marker locations and distances estimated from the Marshfield genetic map, the Location DataBase [26, 27] integrated map, and the human genome sequence (Build 34). In the initial targeted screening of the known POAG loci, family GTas15 was genotyped with a total of 25 microsatellite markers from GLC1A, B, C, D, E and F, at an average marker spacing of 4 cM in each region. The microsatellite markers used as well as their genetic distance in centimorgans relative to the deCODE framework map are shown in table 1.

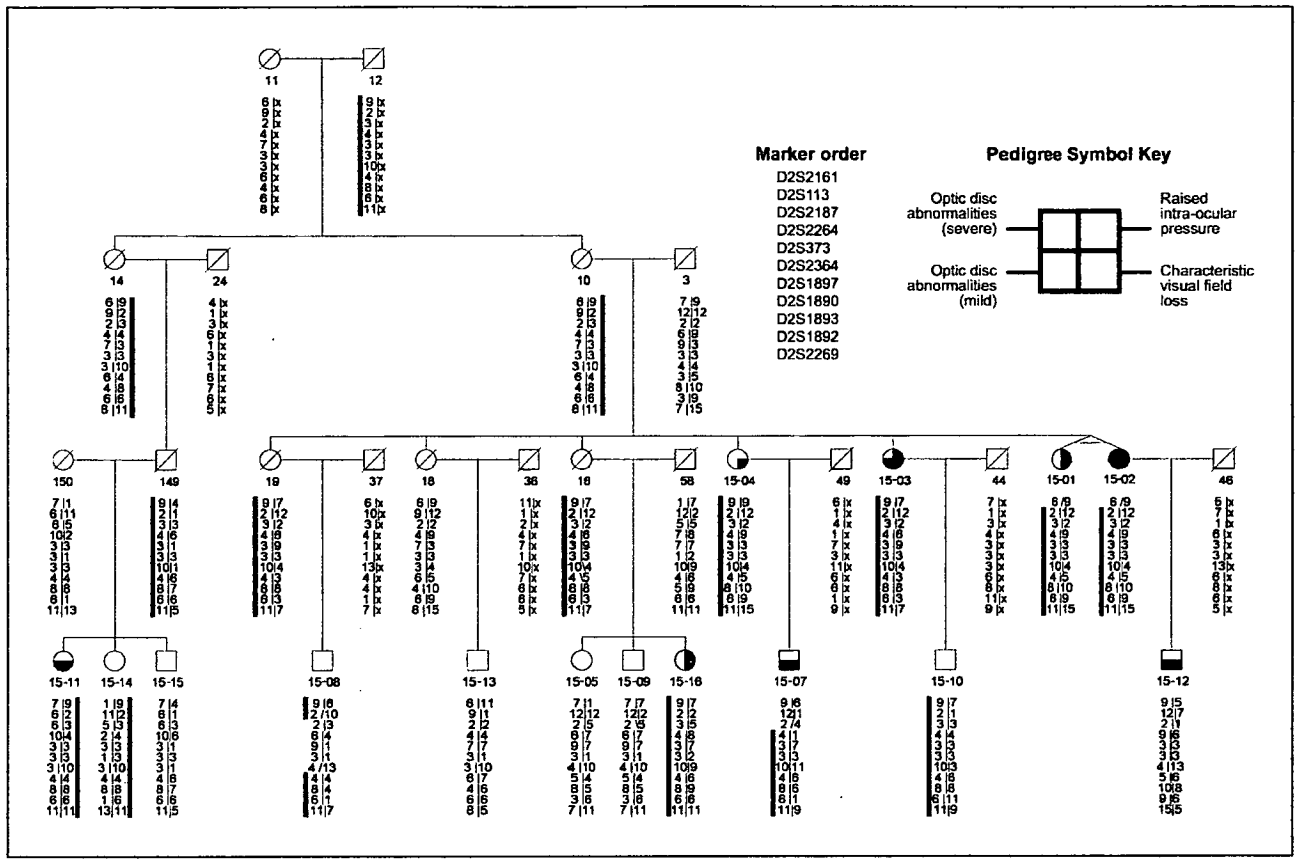

Fig. 1. GTas15 pedigree structure, clinical features and haplotypes at GLC1B. ID numbers commencing with '15-' indicate individuals who participated in the study. Filled quadrants indicate the clinical characteristics of POAG [25]. A filled upper right quadrant indicates the presence of raised intra-ocular pressure; the bottom right quadrant indicates characteristic visual field loss. The left top and bottom quadrants indicate optic disc abnormalities characteristic of POAG and are filled from bottom (mild) to top (severe). Individuals with 2 or more filled quadrants have been classified as affected for the linkage analysis while individuals with only one filled quadrant are glaucoma suspects and classified as unknown for linkage analyses. The haplotype of interest is marked by a vertical black bar. An unknown haplotype is denoted by an 'x'. Forward and backslashes between the haplotypes denote the direction of recombination. Although confirmed monozygotic twins 15-01 and 15-02 are shown in the figure, individual 15-01 was removed for all linkage analyses.

PCR was carried out in a total volume of 10 µl and contained 10 m*M* Tris-HCl, 50 m*M* KCl, 1.5 m*M* Mg^{2+}, 0.2 m*M* dNTP (Promega), 0.8 µ*M* of each primer and 0.005 U/µl *Taq* DNA Polymerase (Qiagen). Reactions underwent 25–35 cycles of 94°C for 30 s, 55°C for 30 s and 72°C for 30 s, followed by a final extension at 72°C for 15 min.

The forward PCR primer for each microsatellite marker was labeled at the 5′ end with either 6-FAM, TET, or HEX (Sigma-Aldrich). Fragments labeled with 6-FAM or TET underwent 25 amplification cycles, while those with HEX underwent 35 cycles. Samples were electrophoresed using an ABI PRISM 310 Genetic Analyzer (Applied Biosystems) with POP4 polymer (Applied Biosystems). Data were analyzed with the Genescan version 3.7 and Genotyper version 3.7 (Applied Biosystems).

Linkage Analyses

Genotyping errors were detected using Pedcheck [28] to identify Mendelian inconsistencies and SimWalk2 [29] to determine unlikely double recombinants [30]. Two of the affected individuals (15-01 and 15-02) were monozygotic twins, confirmed by genotyping at all 31 microsatellite markers. Individual 15-01 was therefore removed from the pedigree prior to all linkage analyses.

Marker allele frequencies were derived from 100 chromosomes from elderly glaucoma-free individuals. SimWalk2 version 2.86b [29] was used to calculate empirical p values for the NPL-all statistic [31], incorporating information from all pedigree members. Model-free linkage analysis was conducted using Genehunter [32] with a trimmed, 20-bit version of the pedigree that included all affected individuals. A disease gene frequency of 0.0001 was used for all analyses.

Table 1. SimWalk2 empirical p values for the NPL-all statistics for microsatellite markers used to evaluate linkage to known POAG loci GLC1A-F

POAG locus and approximate chromosomal location	Marker	Distance from first marker, cM	SimWalk2 p value for NPL-all
GLC1A	D1S2635	0.0	0.20
1q21-31	D1S2707	1.8	0.20
	D1S2675	4.8	0.26
GLC1B	D2S2161	0.0	0.34
2cen-q13	D2S113	3.0	0.06
	D2S2264	7.3	0.04
	D2S1897	11.0	0.03
	D2S1892	16.6	0.08
GLC1C	D3S3637	0.0	0.42
3q21-24	D3S1301	2.0	0.53
	D3S3694	4.0	0.58
	D3S1569	5.8	0.58
	D3S1608	8.0	0.59
GLC1D	D8S1749	0.0	0.50
8q23	D8S556	6.0	0.52
	D8S198	15.0	0.51
GLC1E	D10S1729	0.0	0.33
10p15-14	D10S1713	4.0	0.38
	D10S1691	8.0	0.52
	D10S547	12.4	0.34
	D10S1664	20.3	0.58
GLC1F	D7S2511	0.0	0.80
7q35-36	D7S505	4.0	0.71
	D7S2439	6.0	0.66
	D7S2546	14.0	0.42

The most likely haplotypes for the entire pedigree, including information from individuals classed as POAG status unknown, were estimated in SimWalk2 using a simulated annealing algorithm. These haplotypes were displayed using Pedigree/Draw 5.1 (Southwest Foundation for Biomedical Research http://www.pedigree-draw.com/). Running the algorithm 4 times with different sequences of random numbers produced identical haplotypes each time. For affected individuals, these haplotypes agreed with the most likely set of haplotypes derived using the exact calculations of Genehunter.

Results

Clinical Features

The clinical features of family GTas15 are indicated in figure 1. The POAG within family GTas15 appears to be transmitted in an autosomal dominant fashion. All affected members of GTas15 and 1 glaucoma suspect (15-04) presented with characteristic visual field loss. Raised IOP was not present in 3 of the 7 affected individuals, and 2 of the affected individuals (15-01 and 15-16) had equivocal optic disc appearances in the presence of visual field loss. The monozygotic twins 15-01 and 15-02 differed clinically in the appearance of their optic discs; however, as they were genetically identical and both classified as 'affected', 15-01 was not included in the genetic analyses. The mean age of diagnosis within the family was 55 years, ranging from 47 to 60 years. Several individuals had their POAG diagnosed as a direct result of the family study.

Table 2. SimWalk2 empirical and GeneHunter exact p values for the NPL-all statistics at the microsatellite markers used to evaluate linkage to GLC1B

Marker	Distance from first marker, cM	SimWalk2 empirical p value for NPL-all	GeneHunter exact p value for NPL-all
D2S2161*	0.00	0.34	0.35
D2S113*	3.00	0.06	0.06
D2S2187	4.68	0.06	0.06
D2S2264*	7.32	0.04	0.05
D2S373	7.82	0.03	0.05
D2S2364	9.97	0.02	0.03
D2S1897*	10.97	0.009	0.005
D2S1890	13.68	0.01	0.01
D2S1893	14.68	0.01	0.01
D2S1892*	16.57	0.01	0.01
D2S2269	17.63	0.01	0.03

* Markers used in the original screen of the POAG loci. Remaining markers were added at the fine-mapping stage.

Linkage Analyses of Known POAG Loci

Empirical p values for the NPL-all statistic [31] using complete pedigree information are shown in table 1. A threshold of 0.05 was used to indicate interesting results for follow-up with fine mapping. As 2 markers at GLC1B, D2S2264 and D2S1897, produced p values less than 0.05 (table 1), this locus was targeted for fine-mapping. There was no evidence of linkage of POAG to loci GLC1A, GLC1C, GLC1D, GLC1E, and GLC1F in pedigree GTas15 (p values between 0.20 and 0.80).

Linkage Analyses of GLC1B

An additional 6 microsatellite markers at approximately 1 cM spacing were selected from within the GLC1B region. The SimWalk2 p values at 5 markers, flanked by D2S1897 and D2S2269, were 0.01 or less (ta-

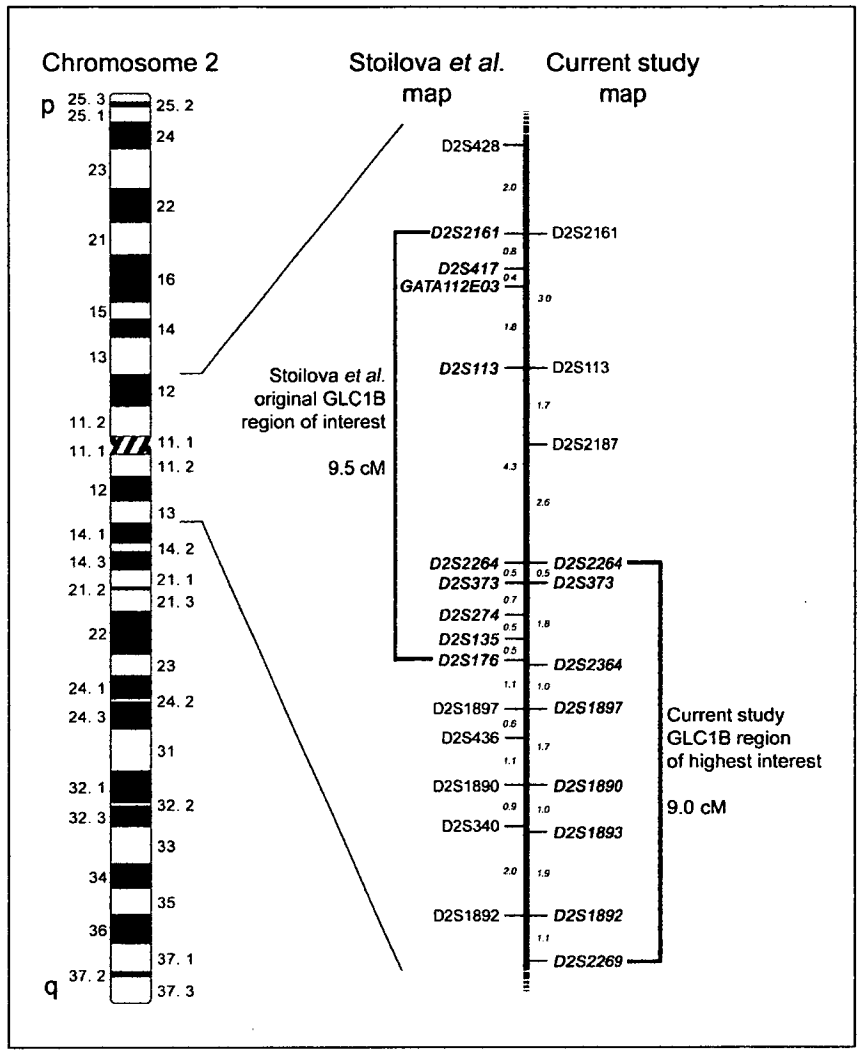

Fig. 2. A comparison of the marker map and critical region of the original and current investigations of the GLC1B locus. The ideogram shows the approximate cytogenetic location of the GLC1B locus. The marker map to the left of the expanded region indicates the marker location and haplotype of interest from the original study by Stoilova et al. [16] in 1996. The marker map and region of interest from the current study is shown to the right. Numbers in italics indicate centimorgan distances between adjacent markers.

ble 2), indicating confirmation of linkage in this region. The lowest empirical p value produced by SimWalk2 was 0.009 at marker D2S1897. GeneHunter produced an exact p value of 0.005 at D2S1897, with p values of 0.01 at 3 additional markers: D2S1890, D2S1893 and D2S1892 (also shown in table 2).

Haplotype Analysis

Haplotype reconstruction using SimWalk2, shown in figure 2, revealed a shared haplotype of 8 markers (flanked by D2S2264 and D2S2269) in 6 of the 7 affected individuals (including the monozygotic twins), present in both arms of the pedigree. Two of the currently unaffected individuals carry the entire haplotype (15-10 and 15-14) while recombination events in another (15-08) have removed several alleles in the middle of the shared haplotype. Of these currently unaffected individuals, 15-08 and 15-10 were 43 and 45 years of age, respectively, at examination, well below the mean age of diagnosis within the family; however, 15-14 was aged 69, carries the full haplotype and showed no sign of glaucoma at the time of examination, indicating likely nonpenetrance at this stage. Individual 15-04 also carries the full haplotype and although this individual's optic disc ratios were within normal limits, their clinical classification at age 79 years was as a glaucoma suspect based on visual field changes.

Discussion

We have investigated all known POAG loci in an extended Australian pedigree using a model-free approach and found evidence for linkage to GLC1B. The empirical p values calculated using SimWalk2 ($p = 0.01$ or less) and exact Genehunter p value ($p = 0.005$) at the GLC1B locus provide supportive evidence for the existence of a POAG susceptibility locus at 2cen-q13.

The POAG susceptibility locus GLC1B was originally identified in 1996 by Stoilova et al. [16] using 6 Caucasian families, predominantly from the United Kingdom, with 3–7 affected individuals per family. Utilizing a penetrance model based approach, the maximum 2-point lod score was 6.48 at marker D2S113 ($\theta = 0$). The lod score calculations were repeated for the affected meioses only, to eliminate the effect of potential incomplete penetrance, which shifted the peak lod distally to marker D2S373 (lod of 3.40 at $\theta = 0$). Both these markers were used in our study; however the region of linkage in family GTas15 is located 2.8 cM distally, with the most significant evidence for linkage at marker D2S1897 ($p = 0.005$). An American Society of Human Genetics conference abstract of Raymond et al. [33] (1999) using a large French-Canadian family identified a peak lod of 2.97 at marker D2S388 (located between D2S2161 and D2S113), within the proximal portion of the GLC1B region; however, no other information relating to the location of their haplotype of interest was provided.

Fine-mapping and haplotype analysis by Stoilova et al. [16] refined their smallest region of cosegregation to 11.2 cM flanked by D2S2161 and D2S176; however, more recent genetic maps suggest a smaller distance of approximately 9.5 cM. A comparison of the maps and critical regions from Stoilova et al. [16] and our study is shown in figure 2. The 8-marker shared haplotype from our study (flanked by D2S2264 and D2S2269) overlaps the lower portion of the original GLC1B region of interest and is of similar size (9.0 cM). The 8-marker haplotype commences within the critical region of Stoilova et al. [16] at marker D2S2264; however, the marker with the lowest p values in our study (D2S1897) lies outside the overlapping region. The smaller 2-marker haplotype (D2S373 and D2S2364) lies almost entirely within the 2.2 cM overlapping region.

Key clinical features of the 6 families originally linked to GLC1B by Stoilova et al. [16] were mean age of diagnosis of 47 years and slightly elevated IOP, although half of the affected individuals had IOP within the normal range (<22 mm Hg). Family GTas15, used in the current study, had similar clinical features, with a slightly higher average age of diagnosis (55 years) and similar IOP distribution. Four of the seven affected individuals had IOP measures over 22 mm Hg; however only 1 of these had peak IOP over 28 mm Hg. The remaining 3 affected individuals could be considered to have normal-tension glaucoma. These results suggest the susceptibility locus at GLC1B may be involved in POAG pathogenesis through pathways that do not involve IOP in all cases.

The analyses of the unaffected meioses in the 6 families originally linked to GLC1B revealed an example of incomplete penetrance: a healthy 86-year-old with no evidence of glaucoma who had inherited the entire affected haplotype [16]. We similarly saw evidence for nonpenetrance in at least 1 unaffected individual (15-14) aged 69 and carrying the entire haplotype of interest with no clinical sign of glaucoma. We also found evidence of a putative phenocopy, with 1 affected individual (15-12) who did not share the haplotype of interest.

A candidate gene of interest located within the haplotype overlap is four-and-a-half lims domain 2 (*FHL2*: MIM# 602633), expressed in a wide range of tissues including optic nerve and eye anterior segment. The 6-member interleukin-1 receptor cluster [34] is also located within the haplotype overlap and includes the interleukin-1 receptors type I and II (*IL1R1*: MIM# 147810 and *IL1R2*: MIM# 147811) and also interleukin-1 receptor-like 1 (*IL1RL1*: MIM# 601203) expressed in the eye anterior segment. It has been suggested that the immune system, and in particular interleukin-1, is involved in POAG pathogenesis [35, 36]. The interleukin-1 gene cluster [37] (including *IL-1B*) lies approximately 0.5 cM beyond the distal end of the GLC1B haplotype identified in this study. A polymorphism within *IL-1B* has recently been associated with sporadic POAG in the Chinese population [38], although investigation of this polymorphism showed no segregation with the POAG phenotype in pedigree GTas15 (data not shown). It is also interesting to note that mer tyrosine kinase protooncogene (*MERTK*: MIM# 604705), a gene associated with retinitis pigmentosa [39] (a disease that also results in visual field loss) is located near marker D2S2269 at the distal end of the haplotype of interest.

The 6 smaller pedigrees originally linked to GLC1B [16] when combined with our replication study in an extended POAG pedigree provides support that the 2cen-q13 region contains a POAG susceptibility gene, and increases the likelihood of gene identification. Previous experience with positionally cloned POAG genes *MYOC* and *OPTN* suggests that once identified, this POAG susceptibility gene at GLC1B may also contribute to a significant proportion of sporadic POAG cases.

Acknowledgements

This study was supported by the Glaucoma Research Foundation. We would like to thank the family for their participation, as well as Dr. Richard L. Cooper, Dr. Gordon M. Wise, genealogist Maree Ring, technician Michele Brown, database administrator Tim Albion for their contribution to GIST and Dr. Eric Sobel (University of California, Los Angeles) for assistance with SimWalk2.

References

1 Quigley HA: Number of people with glaucoma worldwide. Br J Ophthalmol 1996;80:389–393.
2 Weih LM, Nanjan M, McCarty CA, Taylor HR: Prevalence and predictors of open-angle glaucoma: results from the visual impairment project. Ophthalmology 2001;108:1966–1972.
3 Wolfs RC, Klaver CC, Ramrattan RS, van Duijn CM, Hofman A, de Jong PT: Genetic risk of primary open-angle glaucoma. Population-based familial aggregation study. Arch Ophthalmol 1998;116:1640–1645.
4 Rosenthal AR, Perkins ES: Family studies in glaucoma. Br J Ophthalmol 1985;69:664–667.
5 McNaught AI, Allen JG, Healey DL, McCartney PJ, Coote MA, Wong TL, Craig JE, Green CM, Rait JL, Mackey DA: Accuracy and implications of a reported family history of glaucoma: experience from the Glaucoma Inheritance Study in Tasmania. Arch Ophthalmol 2000;118:900–904.
6 Wolfs RC, Borger PH, Ramrattan RS, Klaver CC, Hulsman CA, Hofman A, Vingerling JR, Hitchings RA, de Jong PT: Changing views on open-angle glaucoma: Definitions and prevalences – The Rotterdam Study. Invest Ophthalmol Vis Sci 2000;41:3309–3321.
7 Kahn HA, Milton RC: Alternative definitions of open-angle glaucoma. Effect on prevalence and associations in the Framingham eye study. Arch Ophthalmol 1980;98:2172–2177.
8 Rezaie T, Child A, Hitchings R, Brice G, Miller L, Coca-Prados M, Heon E, Krupin T, Ritch R, Kreutzer D, Crick RP, Sarfarazi M: Adult-onset primary open-angle glaucoma caused by mutations in optineurin. Science 2002;295:1077–1079.
9 Stone EM, Fingert JH, Alward WL, Nguyen TD, Polansky JR, Sunden SL, Nishimura D, Clark AF, Nystuen A, Nichols BE, Mackey DA, Ritch R, Kalenak JW, Craven ER, Sheffield VC: Identification of a gene that causes primary open angle glaucoma. Science 1997;275:668–670.
10 Alward WL, Kwon Y, Khanna C, Johnson AT, Hayreh S, Zimmerman B, Narkiewicz J, Andorf J, Moore P, Fingert J, Sheffield VC, Stone EM: Variations in the myocilin gene in patients with open-angle glaucoma. Arch Ophthalmol 2002;120:1189–1197.
11 Fingert JH, Heon E, Liebmann JM, Yamamoto T, Craig JE, Rait J, Kawase K, Hoh ST, Buys YM, Dickinson J, Hockey RR, Williams-Lyn D, Trope G, Kitazawa Y, Ritch R, Mackey DA, Alward WL, Sheffield VC, Stone EM: Analysis of myocilin mutations in 1,703 glaucoma patients from five different populations. Hum Mol Genet 1999;8:899–905.
12 Alward WL, Fingert JH, Coote MA, Johnson AT, Lerner SF, Junqua D, Durcan FJ, McCartney PJ, Mackey DA, Sheffield VC, Stone EM: Clinical features associated with mutations in the chromosome 1 open-angle glaucoma gene (GLC1A). N Engl J Med 1998;338:1022–1027.
13 Leung YF, Fan BJ, Lam DS, Lee WS, Tam PO, Chua JK, Tham CC, Lai JS, Fan DS, Pang CP: Different optineurin mutation pattern in primary open-angle glaucoma. Invest Ophthalmol Vis Sci 2003;44:3880–3884.
14 Alward WL, Kwon YH, Kawase K, Craig JE, Hayreh SS, Johnson AT, Khanna CL, Yamamoto T, Mackey DA, Roos BR, Affatigato LM, Sheffield VC, Stone EM: Evaluation of optineurin sequence variations in 1,048 patients with open-angle glaucoma. Am J Ophthalmol 2003;136:904–910.
15 Wiggs JL, Auguste J, Allingham RR, Flor JD, Pericak-Vance MA, Rogers K, LaRocque KR, Graham FL, Broomer B, Del Bono E, Haines JL, Hauser M: Lack of association of mutations in optineurin with disease in patients with adult-onset primary open-angle glaucoma. Arch Ophthalmol 2003;121:1181–1183.
16 Stoilova D, Child A, Trifan OC, Crick RP, Coakes RL, Sarfarazi M: Localization of a locus (GLC1B) for adult-onset primary open angle glaucoma to the 2cen-q13 region. Genomics 1996;36:142–150.
17 Wirtz MK, Samples JR, Kramer PL, Rust K, Topinka JR, Yount J, Koler RD, Acott TS: Mapping a gene for adult-onset primary open-angle glaucoma to chromosome 3q. Am J Hum Genet 1997;60:296–304.
18 Trifan OC, Traboulsi EI, Stoilova D, Alozie I, Nguyen R, Raja S, Sarfarazi M: A third locus (GLC1D) for adult-onset primary open-angle glaucoma maps to the 8q23 region. Am J Ophthalmol 1998;126:17–28.
19 Wirtz MK, Samples JR, Rust K, Lie J, Nordling L, Schilling K, Acott TS, Kramer PL: GLC1F, a new primary open-angle glaucoma locus, maps to 7q35-q36. Arch Ophthalmol 1999;117:237–241.
20 Kitsos G, Eiberg H, Economou-Petersen E, Wirtz MK, Kramer PL, Aspiotis M, Tommerup N, Petersen MB, Psilas K: Genetic linkage of autosomal dominant primary open angle glaucoma to chromosome 3q in a Greek pedigree. Eur J Hum Genet 2001;9:452–457.
21 Wiggs JL, Allingham RR, Hossain A, Kern J, Auguste J, DelBono EA, Broomer B, Graham FL, Hauser M, Pericak-Vance M, and Haines JL: Genome-wide scan for adult onset primary open angle glaucoma. Hum Mol Genet 2000;9:1109–1117.
22 Nemesure B, Jiao X, He Q, Leske MC, Wu SY, Hennis A, Mendell N, Redman J, Garchon HJ, Agarwala R, Schaffer AA, Hejtmancik F: A genome-wide scan for primary open-angle glaucoma (POAG): The Barbados Family Study of Open-Angle Glaucoma. Hum Genet 2003;112:600–609.
23 Mackey DA, Craig JE: Glaucoma Inheritance Study in Tasmania: An International Collaboration, in Basic and Clinical Science Course Section 13. American Academy of Ophthalmology, San Francisco, 2002, pp 265–269.
24 Mitchell P, Smith W, Attebo K, Healey PR: Prevalence of open-angle glaucoma in Australia. The Blue Mountains Eye Study. Ophthalmology 1996;103:1661–1669.
25 Coote MA, McCartney PJ, Wilkinson RM, and Mackey DA: The 'GIST' score: Ranking glaucoma for genetic studies. Glaucoma Inheritance Study of Tasmania. Ophthalmic Genet 1996;17:199–208.
26 Collins A, Frezal J, Teague J, Morton NE: A metric map of humans: 23,500 loci in 850 bands. Proc Natl Acad Sci USA 1996;93:14771–14775.
27 Ke X, Tapper W, Collins A: LDB2000: Sequence-based integrated maps of the human genome. Bioinformatics 2001;17:581–586.
28 O'Connell JR, Weeks DE: PedCheck: A program for identification of genotype incompatibilities in linkage analysis. Am J Hum Genet 1998;63:259–266.
29 Sobel E, Lange K: Descent graphs in pedigree analysis: applications to haplotyping, location scores, and marker-sharing statistics. Am J Hum Genet 1996;58:1323–1337.
30 Sobel E, Papp JC, Lange K: Detection and integration of genotyping errors in statistical genetics. Am J Hum Genet 2002;70:496–508.

31 Whittemore AS, Halpern J: A class of tests for linkage using affected pedigree members. Biometrics 1994;50:118–127.
32 Kruglyak L, Daly MJ, Reeve-Daly MP, Lander ES: Parametric and nonparametric linkage analysis: A unified multipoint approach. Am J Hum Genet 1996;58:1347–1363.
33 Raymond VF, Dubois M, Côté S, Anctil G, Morissette JL: Localization of a gene for adult-onset primary open-angle glaucoma to the GLC1B locus at chromosome 2cen-q13 in a French-Canadian family. Abstr American Society of Human Genetics Conference 1999.
34 Dale M, Nicklin MJ: Interleukin-1 receptor cluster: Gene organization of IL1R2, IL1R1, IL1RL2 (IL-1Rrp2), IL1RL1 (T1/ST2), and IL18R1 (IL-1Rrp) on human chromosome 2q. Genomics 1999;57:177–179.
35 Wang N, Chintala SK, Fini ME, Schuman JS: Activation of a tissue-specific stress response in the aqueous outflow pathway of the eye defines the glaucoma disease phenotype. Nat Med 2001;7:304–309.
36 Franks WA, Limb GA, Stanford MR, Ogilvie J, Wolstencroft RA, Chignell AH, Dumonde DC: Cytokines in human intraocular inflammation. Curr Eye Res 1992;11(suppl):187–191.
37 Nicklin MJ, Barton JL, Nguyen M, FitzGerald MG, Duff GW, Kornman K: A sequence-based map of the nine genes of the human interleukin-1 cluster. Genomics 2002;79:718–725.
38 Lin HJ, Tsai SC, Tsai FJ, Chen WC, Tsai JJ, Hsu CD: Association of interleukin 1beta and receptor antagonist gene polymorphisms with primary open-angle glaucoma. Ophthalmologica 2003;217:358–364.
39 Gal A, Li Y, Thompson DA, Weir J, Orth U, Jacobson SG, Apfelstedt-Sylla E, Vollrath D: Mutations in MERTK, the human orthologue of the RCS rat retinal dystrophy gene, cause retinitis pigmentosa. Nat Genet 2000;26:270–271.

Appendix 4 - Publication of material from Chapter 6

The following article was published in *Investigative Ophthalmology and Visual Science.*

Charlesworth JC, Dyer TD, Stankovich JM, Blangero J, Mackey DA, Craig JE, Green CM, Foote SJ, Baird PN and Sale MM (2005). Linkage to 10q22 for Maximum Intraocular Pressure and 1p32 for Maximum Cup-to-Disc Ratio in an Extended Primary Open-Angle Glaucoma Pedigree. *Invest Ophthalmol Vis Sci* 46(10): 3723-9.

Linkage to 10q22 for Maximum Intraocular Pressure and 1p32 for Maximum Cup-to-Disc Ratio in an Extended Primary Open-Angle Glaucoma Pedigree

Jac C. Charlesworth,[1] *Thomas D. Dyer,*[2] *Jim M. Stankovich,*[1,3] *John Blangero,*[2] *David A. Mackey,*[4] *Jamie E. Craig,*[5] *Catherine M. Green,*[4] *Simon J. Foote,*[3] *Paul N. Baird,*[4] *and Michèle M. Sale*[1,6,7]

Purpose. The purpose of this study was to identify genetic contributions to primary open-angle glaucoma (POAG) through investigations of two quantitative components of the POAG phenotype.

Methods. Genome-wide multipoint variance-components linkage analyses of maximum recorded intraocular pressure (IOP) and maximum vertical cup-to-disc ratio were conducted on data from a single, large Australian POAG pedigree that has been found to segregate the myocilin Q368X mutation in some individuals.

Results. Multipoint linkage analysis of maximum recorded IOP produced a peak LOD score of 3.3 ($P = 0.00015$) near marker *D10S537* on 10q22, whereas the maximum cup-to-disc ratio produced a peak LOD score of 2.3 ($P = 0.00056$) near markers *D1S197* to *D1S220* on 1p32. Inclusion of the myocilin Q368X mutation as a covariate provided evidence of an interaction between this mutation and the IOP and cup-to-disc ratio loci.

Conclusions. Significant linkage has been identified for maximum IOP and suggestive linkage for vertical cup-to-disc ratio. Identification of genes contributing to the variance of these traits will enhance understanding of the pathophysiology of POAG as a whole. (*Invest Ophthalmol Vis Sci.* 2005;46: 3723-3729) DOI:10.1167/iovs.05-0312

From the [1]Menzies Research Institute, University of Tasmania, Hobart, Australia; the [2]Department of Genetics, Southwest Foundation for Biomedical Research, San Antonio, Texas; the [3]Genetics and Bioinformatics Division, Walter and Eliza Hall Institute of Medical Research, Melbourne, Australia; the [4]Center for Eye Research Australia, Royal Victorian Eye and Ear Hospital, University of Melbourne, Melbourne, Australia; the [5]Department of Ophthalmology, Flinders University, Adelaide, Australia; and the [6]Center for Human Genomics and the [7]Department of Internal Medicine, Wake Forest University School of Medicine, Winston-Salem, North Carolina.

Supported by National Health and Medical Research Council of Australia Grant 128202, the Glaucoma Research Foundation, the Jack Brockhoff Foundation, SOLAR development Grant MH59490, the Clifford Craig Medical Research Trust, the Ophthalmic Research Institute of Australia, the Dorothy Edols Estate, and Glaucoma Australia.

Submitted for publication March 11, 2005; revised June 10, 2005; accepted August 24, 2005.

Disclosure: **J.C. Charlesworth**, None; **T.D. Dyer**, None; **J.M. Stankovich**, None; **J. Blangero**, None; **D.A. Mackey**, None; **J.E. Craig**, None; **C.M. Green**, None; **S.J. Foote**, None; **P.N. Baird**, None; **M.M. Sale**, None

The publication costs of this article were defrayed in part by page charge payment. This article must therefore be marked "*advertisement*" in accordance with 18 U.S.C. §1734 solely to indicate this fact.

Corresponding author: Michèle M. Sale, Center for Human Genomics, Wake Forest University School of Medicine, Medical Center Boulevard, Winston-Salem, NC 27157; msale@wfubmc.edu.

Glaucoma is a major cause of visual impairment and the second leading cause of blindness worldwide.[1] The most common form is adult-onset primary open-angle glaucoma (POAG), which has a strong genetic component, with family history of the disease an acknowledged risk factor.[2-4] A 10-fold increase in risk of POAG has been documented in first-degree relatives of affected individuals,[3] whereas underreporting of family history suggests that the genetic component of POAG may be even greater than is generally acknowledged.[5]

The clinical diagnosis of glaucoma is based on a combination of several main features, including specific changes to the appearance of the optic nerve head constituting glaucomatous optic neuropathy, characteristic visual field loss with a slow and often asymptomatic progression, and, in most cases, increased intraocular pressure (IOP). The complexity of the phenotypic definition of POAG[6,7] has contributed to the difficulties in identifying genes involved in this disease.

Two genes have been identified for adult-onset POAG[8,9]; however, mutations in these genes account for only a fraction of POAG cases. Myocilin (*MYOC*) on 1q24.3 has been shown to account for approximately 3% of adult-onset POAG.[9-12] Optineurin (*OPTN*) on 10p15-p14 was shown by Rezaie et al.[8] to be involved in up to 17% of low-tension glaucoma pedigrees, although a recent study indicated a low prevalence of *OPTN* mutations (<0.1%) in unselected cases of both POAG and NTG.[13] The WD40-repeat 36 gene (*WDR36*) was recently identified at the GLC1G locus on 5q22.1,[14] although the impact of this gene on the wider POAG population is yet to be determined. In addition to these three genes, four other loci for POAG have been mapped: *GLC1B*,[15] *GLC1C*,[16] *GLC1D*,[17] and *GLC1F*.[18] The results of three genome-wide scans suggest that several additional chromosomal regions may also be involved in susceptibility to POAG[19-21]; however, only *GLC1B*[22] and *GLC1C*[23] have been replicated in published studies.

Given the limited success so far in identifying genes conferring susceptibility to glaucoma, one approach that may have greater success is quantitative trait linkage analysis of precursors of glaucoma, such as raised IOP and increased cupping of the optic nerve. Such traits may have simpler genetic architecture than diagnosis of glaucoma, making it easier to map causative loci.[24-26] Furthermore, quantitative trait linkage analysis is inherently more powerful than dichotomous trait linkage analysis[27,28] and is particularly powerful in large families.[29,30]

The heritabilities of IOP and vertical cup-to-disc ratio were estimated to be 0.36 and 0.48, respectively, in the Beaver Dam Eye Study, providing evidence for genetic determinants for these components.[31] Commingling analysis of IOP and glaucoma by Viswanathan et al.[32] suggested the existence of a major gene accounting for 18% of the variance of IOP in the Blue Mountains Eye Study population.[32] Duggal et al.[33] recently conducted a complex segregation and linkage analysis

TABLE 1. Age and Trait Data Distribution Statistics from the MVIP Dataset and Family GTas02

Trait	MVIP			Family GTas02			Fitted Coefficients	
	n	Mean	SD	*n*	Mean	SD	β_{Age}	β_{Sex}
Age (y)	3892	59.4	11.6	139	53.1	14.4		
Maximum cup-to-disc ratio	2986	0.43	0.21	135	0.47	0.20	0.0016	−0.032
Maximum IOP (mm Hg)	3221	15.2	3.32	137	17.9	4.15	0.0033	−0.21

of IOP, identifying two potential regions of linkage on chromosomes 6 and 13.

The purpose of the present investigation was to identify regions of linkage that contribute to maximum IOP and maximum cup-to-disc ratio, using measures from an extended Australian pedigree. This family already has been analyzed for linkage to glaucoma.[34] The discovery of genes contributing to the variance of maximum IOP and maximum cup-to-disc ratio is expected to provide significant insights into the pathophysiology of glaucoma.

METHODS

The Glaucoma Inheritance Study in Tasmania

This investigation was conducted as part of the Glaucoma Inheritance Study in Tasmania[35] (GIST), a large population study of glaucoma-affected families in Tasmania, Australia. Ethics approval was obtained from the Human Research Ethics Committees of the Royal Children's Hospital, the Royal Victorian Eye and Ear Hospital, the Royal Hobart Hospital, and the University of Tasmania, and the study was conducted in accordance with the tenets of the Declaration of Helsinki. Written informed consent was obtained from all participants.

GTas02, the family of interest in this investigation, is one of the largest pedigrees identified as part of the GIST. It consists of more than 1350 members, and ancestry can be traced back to a founder couple six generations ago. The "core" pedigree containing the POAG cases consists of 246 individuals when deceased linking members are included. One hundred thirty-nine family members consented to clinical examination and blood collection for genotyping and mutation analysis. The structure, clinical diagnosis, and *MYOC* mutation status of this family have been published.[36]

Clinical Examination

Clinical examination and diagnosis of patients involved in the GIST are documented elsewhere.[37] In brief, POAG was clinically defined as an optic neuropathy that had at least two of the following features: (1) optic nerve head excavation with thinning of the neuroretinal rim, often with Drance-type nerve fiber layer hemorrhages, notching, pitting, significant focal loss or general loss of the retinal nerve fiber layer (generally measured by an enlarged vertical cup-to-disc ratio ≥ 0.7); (2) elevated IOP above a population-based normal range or above the average of the unaffected individuals within a pedigree (generally IOP >21 mm Hg or two standard deviations from the population mean); and (3) visual field defects consistent with the disc changes and with common descriptions of glaucomatous field loss.[37] Glaucoma cases secondary to trauma or anterior segment dysgenesis were excluded. Of the 139 individuals available for examination, 24 had a diagnosis of POAG. The details of the clinical diagnoses for this family have been extensively reported.[36]

IOP was measured with a calibrated Goldmann applanation tonometer. Multiple IOP measures were available for each individual; hence, maximum IOP was selected, to reduce any bias introduced by using postmedication pressure values. No corrections were made for corneal thickness, because this information was not routinely collected at the time of patient ascertainment. Optic disc appearance was classified by two clinicians at the time of examination, with a slit lamp biomicroscope after pupil dilation. In addition, optic disc stereo photographs (Nidek, Gamagori, Japan) were obtained for future reference in all cases. When there was a discrepancy between the two examiners, the stereo disc photographs were independently assessed by a glaucoma specialist. The highest vertical cup-to-disc ratio in either eye at any clinical examination was used as the trait measure.

Quantitative measures collected as part of the clinical examination of patients with POAG and their relatives included maximum recorded intraocular pressure (IOP) without medication and maximum vertical cup-to-disc ratio from the highest-scoring eye.[36]

Myocilin mutation detection in this family has been reported.[36,38] Of the 139 individuals from GTas02 screened for mutations in the *MYOC* gene, 19 were known to carry the Q368X mutation.

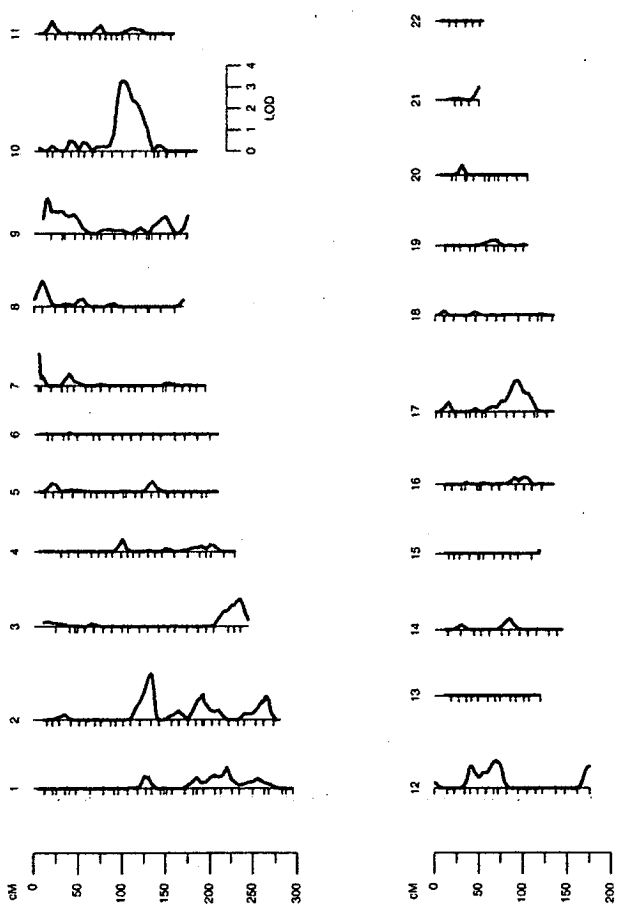

FIGURE 1. Genome-wide multipoint variance components linkage results for maximum recorded IOP.

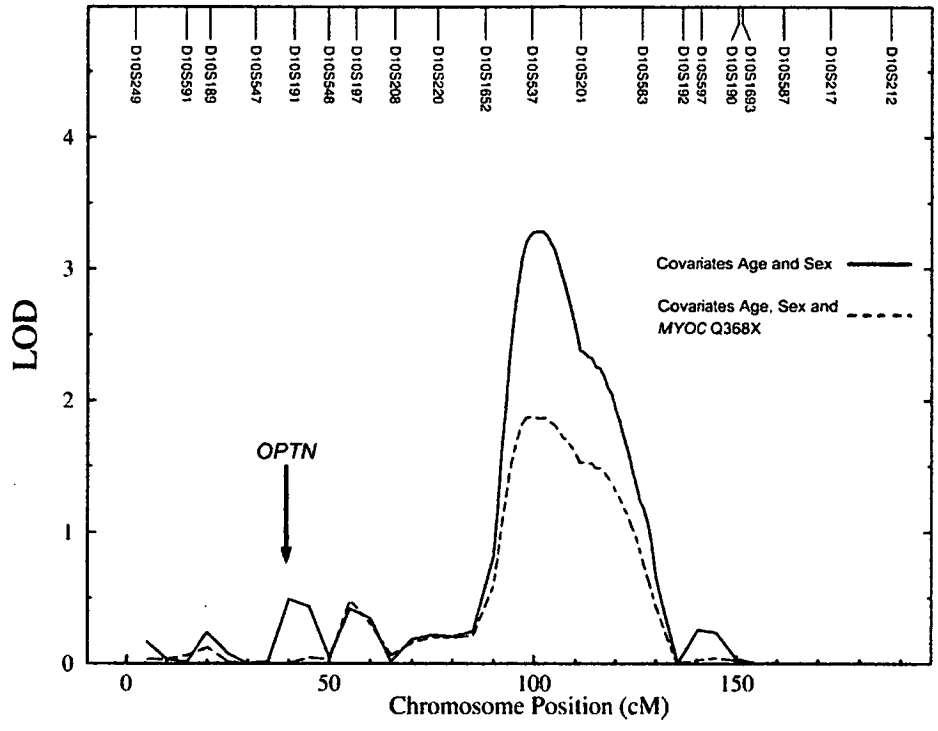

FIGURE 2. Multipoint variance-components linkage results for maximum recorded IOP for chromosome 10 (*solid line*) and linkage signal after the inclusion of Q368X status as a covariate (*dashed line*). Covariates are indicated on the plots. The location of the optineurin (*OPTN*) gene is indicated.

Genotyping

A 10-cM genome-wide scan was conducted with 401 microsatellite markers from fluorescence marker sets (vers. 1 and 2; Applied Biosystems, Inc. [ABI], Foster City, CA), run on sequencers (model 377; ABI) and analyzed (GeneScan and GenoTyper software; ABI).[34] Inconsistencies in Mendelian inheritance of genotypes were detected with Pedcheck.[39] Marker allele frequencies were estimated from 72 elderly glaucoma-free control individuals drawn from the same population.[40]

Multipoint identity by descent (IBD) files were created with the Markov chain Monte Carlo (MCMC)-based program Loki (ver. 2.4.7)[41,42] from within SOLAR (Sequential Oligogenic Linkage Analysis Routines, ver. 2.1.1; http//:www.sfbr.org/ provided in the public domain by the Southwest Foundation for Biomedical Research, San Antonio, TX).[25]

Ascertainment Correction

The population ascertainment correction data set was taken from the Melbourne Visual Impairment Project (MVIP) and included 3905 individuals from the general population with data on age, sex, maximum recorded IOP, and maximum cup-to-disc ratio.[43] The MVIP clinical data were collected by the same methods as were used in the GIST. A comparison between the MVIP and family GTas02 data is shown in Table 1. Mean age and trait variables in family GTas02 and the ascertainment correction sample were compared by two-tailed *t*-tests. The ascertainment correction dataset was not intended to be age matched; however, comparison of age and trait between the two groups revealed the relative position of family GTas02 within the distribution of the general population.

The ascertainment correction was conducted with SOLAR (ver. 2.1.1)[25] and the population-based ascertainment correction dataset. The mean effects for each trait were estimated from this dataset, including the regression coefficients β_{Age} and β_{Sex}, which were used to adjust the trait mean for the effect of the covariates age and sex. The resultant mean, SD, β_{Age}, and β_{Sex} obtained from the population-based dataset were then used in the model to analyze the pedigree data. By constraining these mean effects and the total variance to that of the general population, trait values for individuals in family GTas02 were given the appropriate weight.

Variance Components Analysis

Heritability for each trait was estimated with genetic variance component modeling as implemented in SOLAR (ver. 2.1.1).[25] The covariates were selected among age, sex, age-sex interaction; however, age-sex interaction was not significant in any dataset and was thus removed. Variance component linkage analysis was performed to detect and localize quantitative trait loci (QTLs) influencing variation in maximum IOP and maximum cup-to-disc ratio, by using SOLAR.[25]

The variance-component linkage method is based on specifying the expected genetic covariances between arbitrary relatives as a function of IBD relationships at a given marker locus.[25] The method involves partitioning the total trait phenotypic variance (σ^2_P) into components attributable to covariate effects, effects of a specific QTL (QTL (σ^2_q), and residual additive genetic effects (σ^2_{h2r}). The test for linkage compares the likelihood of this model with the likelihood of a null model (no linkage), where the QTL effect size σ_q^2 is fixed to be zero. The difference between the two $\log_{10}$ likelihoods produces a LOD score that can be interpreted in a fashion similar to that of the classic LOD scores of parametric linkage analysis.[44] The variance component quantitative genetic approach enables penetrance model-free multipoint linkage analysis of complex quantitative traits in pedigrees of arbitrary size and complexity[25,28,45–47] and has been used successfully to localize QTLs that influence many important disease-related traits, including risk of alcoholism,[47] serum leptin levels,[48,49] and resting heart rate.[49]

Expected LOD scores and empiric locus-specific probabilities were determined with the "lodadj" command of SOLAR.[44,50] A total of 100,000 replicates were simulated to build up the distribution of LOD scores expected under the null hypothesis of no linkage, using a fully informative, unlinked marker. The observed LOD scores were then regressed on those expected for a multivariate normal trait, with the inverse slope of the regression line providing the LOD correction constant. Final LOD scores were multiplied by the correction constant only if the constant was <1.

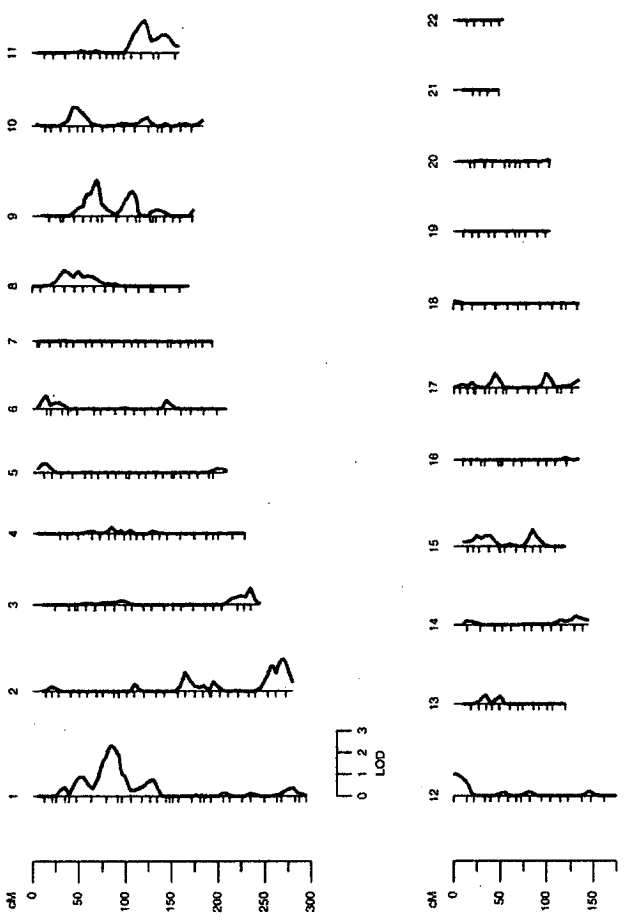

FIGURE 3. Genome-wide multipoint variance components linkage results for maximum vertical cup-to-disc ratio.

To test the impact of the *MYOC* Q368X mutation on the linkage results, Q368X status was included as a covariate in a second round of analyses for each trait. The regression coefficient for Q368X mutation status (β_{MYOC}), used in the analysis of each trait, was estimated from the family GTas02 trait and mutation data and not from the population ascertainment correction dataset. As in previous analyses, age and sex were included in all models, and adjusted LOD scores and empiric probabilities were calculated as described earlier. The fitted coefficient for *MYOC* mutation status (β_{MYOC}) in the analysis of IOP was 5.065, whereas β_{MYOC} for the analysis of maximum cup-to-disc ratio was 0.192.

To control for the overall false-positive rate in our linkage screens, we converted the nominal probabilities associated with our peak LOD scores to genome-wide probabilities, using an approach developed by Feingold et al.[51] This method takes into account the mean recombination rate in our study population and the marker density of the linkage map used in our genome scan.

RESULTS

Maximum recorded IOP had a heritability of 0.55 for family GTas02. The covariates sex and age were statistically controlled for and included in the analysis, although in the ascertainment correction population, neither showed effects that were substantial ($P = 0.073$ for sex, $P = 0.53$ for age), and accounted for only 0.1% of the variance. The mean value for maximum recorded IOP in family GTas02 (17.9 ± 4.2 mm Hg [SD]) was significantly higher ($P < 0.0001$) than the mean IOP in the general population (15.2 ± 3.3 mm Hg). The empiric LOD correction constant was greater than 1; hence, no adjustment was applied to the linkage results. The highest LOD score for IOP in family GTas02 was 3.3 (locus-specific $P = 0.00015$) near marker *D10S537* (Fig. 1), with the LOD-1 interval spanning approximately 20 cM on 10q22 (Fig. 2). The genome-wide probability for this result was 0.0165.

Maximum cup-to-disc ratio had a heritability of 0.39 for family GTas02. The effect of the covariates sex ($P = 3.1 \times 10^{-5}$) and age ($P = 1.6 \times 10^{-6}$) were highly significant in the ascertainment correction population, accounting for 1.4% of the variance; hence, both were statistically controlled for and included in the analysis of family GTas02. The mean ± SD cup-to-disc ratio in family GTas02 (0.47 ± 0.20) was not significantly different ($P > 0.05$) from the mean cup-to-disc ratio in the general population (0.43 ± 0.21). The empiric LOD correction constant was greater than 1; hence, no adjustment was applied. The highest LOD score for maximum cup-to-disc ratio in family GTas02 was 2.3 (locus-specific $P = 0.00,056$) near markers *D1S197* and *D1S220* (Fig. 3), with the LOD-1 interval spanning approximately 20 cM on 1p32 (Fig. 4). The genome-wide probability for this LOD score was determined to be 0.208.

The *MYOC* Q368X mutation was present in 9 (37.5%) of 24 individuals in family GTas02 with diagnosed POAG and in 10 individuals without a diagnosis of POAG at examination. Whereas the mean age of individuals with the Q368X mutation in family GTas02 was not significantly different from those without the mutation, mean maximum IOP and mean maximum cup-to-disc ratio were significantly higher in Q368X mutation carriers, regardless of POAG affection status (Table 2). *MYOC* Q368X mutation status (β_{MYOC}) accounted for 16% of the genetic variance of the maximum IOP (heritability reduced from 0.55 to 0.46) and 49% of the genetic variance of the maximum cup-to-disc ratio (heritability reduced from 0.39 to 0.20). Addition of *MYOC* Q368X mutation status as a covariate in the analysis of the quantitative traits resulted in the peak LOD score for maximum recorded IOP (near marker *D10S537* on 10q22) decreasing from 3.3 to 1.9 (Fig. 2), and the peak LOD score for maximum cup-to-disc ratio (near markers *D1S197* and *D1S220* on 1p32) was reduced from 2.3 to 0.9 (Fig. 4).

DISCUSSION

In this study, we investigated two individual disease components of POAG—maximum recorded IOP and maximum vertical cup-to-disc ratio—as quantitative traits using variance components linkage analysis. Genome scan analyses of these traits in an extended pedigree revealed one region of significant or suggestive linkage for each trait. Multipoint linkage analysis of maximum recorded IOP identified a peak LOD of 3.3 (locus-specific $P = 0.00015$) near marker *D10S537* on 10q22, whereas analysis of the maximum cup-to-disc ratio produced a peak LOD score of 2.3 (locus-specific $P = 0.00056$) near markers *D1S197* to *D1S220* on 1p32.

The putative trait locus for maximum recorded IOP produced a significant peak LOD of 3.3 on 10q22. The genome-wide significance level of this result ($P = 0.0165$) strongly suggests that this region contains a gene that contributes to the variance of IOP. We did not see any overlap with the IOP linkage regions identified by Duggal et al.[33] Although our region of interest for IOP on 10q22 has not been reported previously for IOP, linkage to this region has also been found for systemic hypertension in a Japanese population.[52] The association between systemic blood-pressure (systolic or diastolic) and IOP has been well documented.[53–55] It is possible

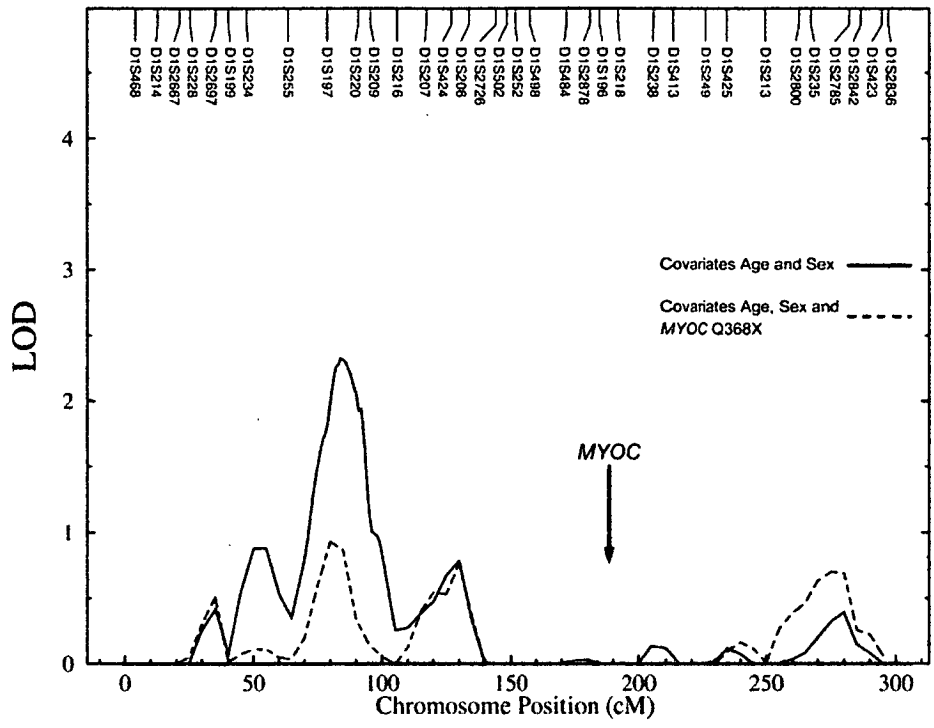

FIGURE 4. Multipoint variance components linkage results for maximum vertical cup-to-disc ratio for chromosome 1 (*solid line*), and linkage signal after the inclusion of Q368X status as a covariate (*dashed line*). Covariates are indicated on the plots. The location of the myocilin (*MYOC*) gene is indicated.

that systemic hypertension and IOP share a common QTL in this region on the long arm of chromosome 10. The region contains *BMPR1A* (MIM: 601299), a bone morphogenic protein receptor—interesting because *Bmp4* has been implicated in increased IOP in mice.[56] The peak region also contains *RGR* (MIM: 600342), an opsin-related gene associated with retinitis pigmentosa.[57] The *OPTN* gene is located outside our 10p13 linkage peak, approximately 60 cM upstream.

Applanation tonometry measurements of IOP are known to be influenced by central corneal thickness (CCT).[58,59] CCT has a positive and apparently linear correlation with IOP[60] and is strongly genetically determined (Toh TY, et al. *IOVS* 2005;46: ARVO E-Abstract 1093). There has been a report of thick corneas segregating in a family with apparent ocular hypertension,[61] which leads to the suggestion that perhaps the variation in IOP in family GTas02 compared with the population is due to CCT. However, there are many individuals in family GTas02 with moderate to advanced visual field loss, which would support the elevated IOP's being genuine rather than artifactual in nature. It is possible that measurement of CCT and subsequent adjustment of Goldmann applanation IOP readings for GTas02 may have the effect of strengthening the linkage at the IOP locus on 10q22 by providing a more accurate approximation of true IOP (as opposed to measured IOP). This approach is worthy of future investigation.

This study identified a putative trait locus for maximum cup-to-disc ratio on 1p32—the first reported locus for this trait—with a peak LOD score of 2.3. This corresponds to suggestive linkage, because there is a 20% chance of a LOD score of this size or greater occurring by chance in a genome-wide scan. The region covered by the linkage peak includes the gene *POMGnT1* (MIM: 606822), mutant forms of which are responsible for muscle-eye-brain disease (MEB; MIM: 253280), a congenital muscular dystrophy–based disorder with many additional features, including early-onset glaucoma, optic nerve atrophy, severe congenital myopia and retinal hypoplasia. MEB is inherited as a loss of function of *POMGnT1*.[62] The peak region also contains *FOXE3* (MIM: 601094), known to be associated with anterior segment ocular dysgenesis[63] and is approximately 25 cM distal to the primary congenital glaucoma locus GLC3B (MIM: 600975), on 1p36.[64]

The *MYOC* Q368X mutation is the most common mutation identified in patients with POAG to date, found to account for approximately 1.6% of POAG.[11] In comparison to other *MYOC* mutations associated with the juvenile-onset form of POAG (JOAG), this mutation generally gives rise to a milder phenotype with late age of onset and increased IOP.[65] Myocilin mutation status and related phenotype modification effects within family GTas02 have been reported.[36,38] The *MYOC* locus was not apparent in either of the linkage analyses for the

TABLE 2. Comparison between Myocilin Q368X Mutation Carriers and Mutation-Free Individuals from Family GTas02

	Q368X Mutation Carriers			Q368X Mutation Free			
Trait	***n***	**Mean**	**SD**	***n***	**Mean**	**SD**	***P****
Maximum IOP	19	22.21	5.32	118	17.17	3.48	7.70×10^{-8}
Maximum cup-to-disc ratio	19	0.64	0.23	116	0.44	0.18	2.26×10^{-4}

* Obtained by age-adjusted measured genotype analysis accounting for nonindependence among relatives.

two quantitative traits investigated in this study. Because only 9 of the 19 Q368X mutation carriers in this family were clinically diagnosed with POAG, this mutation is unable to account for the presence of all cases of POAG in the entire family.[38] Despite the absence of a linkage signal at *MYOC*, the Q368X mutation appeared to account for nearly half the genetic variance for the quantitative trait based on maximum cup-to-disc ratio, and nearly 20% of the genetic variance for maximum IOP. The differences between carrier and non-carrier-trait values (shown in Table 2) were significant, which may indicate epistasis or some other form of interaction between *MYOC* and the putative trait loci for IOP and cup-to-disc ratio. The reduction in peak LOD scores for both traits after the inclusion of the Q368X mutation as a covariate provides further evidence for the presence of an interaction. However, the sample size of family GTas02 does not provide sufficient power to determine the exact mechanism behind this interaction. Subsequent identification of the genes at these loci is anticipated to aid investigation into the nature of this interaction.

Baird et al.[34] recently identified linkage of clinical POAG diagnosis to 3p21-p22 in this family, using MCMC-based linkage analysis. We did not find any evidence of overlap with this region using the traits maximum IOP and cup-to-disc ratio. There are likely to be many genes contributing to the complex POAG phenotype, and different analytical approaches will have variable power to detect certain loci. It is also possible that the gene at the 3p locus may contribute to a different POAG trait, such as *progression* from elevated IOP to optic nerve damage and subsequent clinical signs of visual field loss. Although we are unaware of any systemic biases in pedigree or family member ascertainment, genotyping methodology, or trait measurements, if any such biases exist they would impact both linkage studies and any subsequent analyses of this dataset. Finally, as with any genome scan, one must also be mindful that some of these linkage results could represent chance events.

The loci identified in this study are believed to contribute to the variance of IOP and cup-to-disc ratio in the general population. However, since more extreme values are present in a POAG pedigree, when combined with population-based ascertainment correction, the approach used in this investigation is expected to provide greater power to map genes for these traits. Maximum IOP and maximum vertical cup-to-disc ratio may not be ideal measures, given the influence of pressure spikes and diurnal variation on IOP, for example, however other traits such as mean IOP are likely to be equally problematic considering the probable inclusion of postmedication levels. In addition, any measurement error in IOP and cup-to-disc ratio would also be present in the population data used for ascertainment correction.

In this investigation, we were able to identify regions of linkage contributing to maximum recorded IOP and maximum cup-to-disc ratio, quantitative clinical contributors to POAG diagnosis that are collected as a routine part of clinical practice. The discovery of the genes involved in these components of POAG at these loci is anticipated to provide significant insights into glaucoma pathophysiology as a whole.

Acknowledgments

The authors thank the GTas02 family members, the population control subjects, and the MVIP participants for their participation; Hien Vu (Population Health Division of the University of Melbourne) for providing the MVIP population data; and Danielle Healy, Susan Stanwix, Tiffany Wong, Maree Ring, Julie Barbour, Robin Wilkinson, Colleen Wilkinson, Robert Buttery, Andrew McNaught, Michael Coote, and Julian Rait for assistance with examination and data collection.

References

1. Quigley HA. Number of people with glaucoma worldwide. *Br J Ophthalmol.* 1996;80:389-93.
2. Weih LM, Nanjan M, McCarty CA, Taylor HR. Prevalence and predictors of open-angle glaucoma: results from the visual impairment project. *Ophthalmology.* 2001;108:1966-1972.
3. Wolfs RC, Klaver CC, Ramrattan RS, van Duijn CM, Hofman A, de Jong PT. Genetic risk of primary open-angle glaucoma. Population-based familial aggregation study. *Arch Ophthalmol.* 1998;116:1640-1645.
4. Rosenthal AR, Perkins ES. Family studies in glaucoma. *Br J Ophthalmol.* 1985;69:664-667.
5. McNaught AI, Allen JG, Healey DL, et al. Accuracy and implications of a reported family history of glaucoma: experience from the Glaucoma Inheritance Study in Tasmania. *Arch Ophthalmol.* 2000;118:900-904.
6. Wolfs RC, Borger PH, Ramrattan RS, et al. Changing views on open-angle glaucoma: definitions and prevalences–The Rotterdam Study. *Invest Ophthalmol Vis Sci.* 2000;41:3309-3321.
7. Kahn HA, Milton RC. Alternative definitions of open-angle glaucoma. Effect on prevalence and associations in the Framingham eye study. *Arch Ophthalmol.* 1980;98:2172-21777.
8. Rezaie T, Child A, Hitchings R, et al. Adult-onset primary open-angle glaucoma caused by mutations in optineurin. *Science.* 2002;295:1077-1079.
9. Stone EM, Fingert JH, Alward WL, et al. Identification of a gene that causes primary open angle glaucoma. *Science.* 1997;275:668-670.
10. Alward WL, Kwon Y, Khanna C, et al. Variations in the myocilin gene in patients with open-angle glaucoma. *Arch Ophthalmol.* 2002;120:1189-1197.
11. Fingert JH, Heon E, Liebmann JM, et al. Analysis of myocilin mutations in 1703 glaucoma patients from five different populations. *Hum Mol Genet.* 1999;8:899-905.
12. Alward WL, Fingert JH, Coote MA, et al. Clinical features associated with mutations in the chromosome 1 open- angle glaucoma gene (GLC1A). *N Engl J Med.* 1998;338:1022-1027.
13. Alward WL, Kwon YH, Kawase K, et al. Evaluation of optineurin sequence variations in 1,048 patients with open-angle glaucoma. *Am J Ophthalmol.* 2003;136:904-910.
14. Monemi S, Spaeth G, Dasilva A, et al. Identification of a novel adult-onset primary open angle glaucoma (POAG) gene on 5q22.1. *Hum Mol Genet.* 2005;14:725-733.
15. Stoilova D, Child A, Trifan OC, Crick RP, Coakes RL, Sarfarazi M. Localization of a locus (GLC1B) for adult-onset primary open angle glaucoma to the 2cen-q13 region. *Genomics.* 1996;36:142-150.
16. Wirtz MK, Samples JR, Kramer PL, et al. Mapping a gene for adult-onset primary open-angle glaucoma to chromosome 3q. *Am J Hum Genet.* 1997;60:296-304.
17. Trifan OC, Traboulsi EI, Stoilova D, et al. A third locus (GLC1D) for adult-onset primary open-angle glaucoma maps to the 8q23 region. *Am J Ophthalmol.* 1998;126:17-28.
18. Wirtz MK, Samples JR, Rust K, et al. GLC1F, a new primary open-angle glaucoma locus, maps to 7q35-q36. *Arch Ophthalmol.* 1999;117:237-241.
19. Wiggs JL, Allingham RR, Hossain A, et al. Genome-wide scan for adult onset primary open angle glaucoma. *Hum Mol Genet.* 2000;9:1109-1117.
20. Nemesure B, Jiao X, He Q, et al. A genome-wide scan for primary open-angle glaucoma (POAG): the Barbados Family Study of Open-Angle Glaucoma. *Hum Genet.* 2003;112:600-609.
21. Wiggs JL, Lynch S, Ynagi G, et al. A genomewide scan identifies novel early-onset primary open-angle glaucoma loci on 9q22 and 20p12. *Am J Hum Genet.* 2004;74:1314-1320.
22. Charlesworth JC, Stankovich JM, Mackey DA, et al. Confirmation of the adult-onset primary open angle glaucoma locus GLC1B at 2cen-q13 in an Australian family. *Ophthalmologica.* In press.
23. Kitsos G, Eiberg H, Economou-Petersen E, et al. Genetic linkage of autosomal dominant primary open angle glaucoma to chromosome 3q in a Greek pedigree. *Eur J Hum Genet.* 2001;9:452-457.
24. Freimer N, Sabatti C. The use of pedigree, sib-pair and association studies of common diseases for genetic mapping and epidemiology. *Nat Genet.* 2004;36:1045-1051.

25. Almasy L, Blangero J. Multipoint quantitative-trait linkage analysis in general pedigrees. *Am J Hum Genet.* 1998;62:1198-211.
26. Amos CI, de Andrade M. Genetic linkage methods for quantitative traits. *Stat Methods Med Res.* 2001;10:3-25.
27. Williams JT, Blangero J. Comparison of variance components and sibpair-based approaches to quantitative trait linkage analysis in unselected samples. *Genet Epidemiol.* 1999;16:113-34.
28. Duggirala R, Williams JT, Williams-Blangero S, Blangero J. A variance component approach to dichotomous trait linkage analysis using a threshold model. *Genet Epidemiol.* 1997;14:987-992.
29. Williams JT, Blangero J. Power of variance component linkage analysis to detect quantitative trait loci. *Ann Hum Genet.* 1999; 63:545-563.
30. Wijsman EM, Amos CI. Genetic analysis of simulated oligogenic traits in nuclear and extended pedigrees: summary of GAW10 contributions. *Genet Epidemiol.* 1997;14:719-735.
31. Klein BE, Klein R, Lee KE. Heritability of risk factors for primary open-angle glaucoma: the Beaver Dam Eye Study. *Invest Ophthalmol Vis Sci.* 2004;45:59-62.
32. Viswanathan AC, Hitchings RA, Indar A, et al. Commingling analysis of intraocular pressure and glaucoma in an older Australian population. *Ann Hum Genet.* 2004;68:489-497.
33. Duggal P, Klein AP, Lee KE, et al. A genetic contribution to intraocular pressure: the Beaver Dam Eye Study. *Invest Ophthalmol Vis Sci.* 2005;46:555-560.
34. Baird PN, Foote SJ, Mackey DA, Craig JE, Speed TP, Bureau A. Evidence for a novel glaucoma locus at chromosome 3p21-22. *Hum Genet.* 2005;117:249-257.
35. Mackey DA, Craig JE. Glaucoma Inheritance Study in Tasmania: An International Collaboration. In: *Basic and Clinical Science Course Section 13.* San Francisco: American Academy of Ophthalmology; 2002:265-269.
36. Craig JE, Baird PN, Healey DL, et al. Evidence for genetic heterogeneity within eight glaucoma families, with the GLC1A Gln368STOP mutation being an important phenotypic modifier. *Ophthalmology.* 2001;108:1607-1620.
37. Coote MA, McCartney PJ, Wilkinson RM, Mackey DA. The 'GIST' score: ranking glaucoma for genetic studies. Glaucoma Inheritance Study of Tasmania. *Ophthalmic Genet.* 1996;17:199-208.
38. Baird PN, Craig JE, Richardson AJ, et al. Analysis of 15 primary open-angle glaucoma families from Australia identifies a founder effect for the Q368STOP mutation of myocilin. *Hum Genet.* 2003; 112:110-116.
39. O'Connell JR, Weeks DE. PedCheck: a program for identification of genotype incompatibilities in linkage analysis. *Am J Hum Genet.* 1998;63:259-266.
40. Vickers JC, Craig JE, Stankovich J, et al. The apolipoprotein epsilon4 gene is associated with elevated risk of normal tension glaucoma. *Mol Vis.* 2002;8:389-393.
41. Heath SC. Markov chain Monte Carlo segregation and linkage analysis for oligogenic models. *Am J Hum Genet.* 1997;61:748-760.
42. Heath SC, Snow GL, Thompson EA, Tseng C, Wijsman EM. MCMC segregation and linkage analysis. *Genet Epidemiol.* 1997;14:1011-1016.
43. Wensor MD, McCarty CA, Stanislavsky YL, Livingston PM, Taylor HR. The prevalence of glaucoma in the Melbourne Visual Impairment Project. *Ophthalmology.* 1998;105:733-739.
44. Blangero J, Williams JT, Almasy L. Variance component methods for detecting complex trait loci. *Adv Genet.* 2001;42:151-181.
45. Blangero J, Almasy L. Multipoint oligogenic linkage analysis of quantitative traits. *Genet Epidemiol.* 1997;14:959-964.
46. Williams JT, Van Eerdewegh P, Almasy L, Blangero J. Joint multipoint linkage analysis of multivariate qualitative and quantitative traits. I. Likelihood formulation and simulation results. *Am J Hum Genet.* 1999;65:1134-1147.
47. Williams JT, Begleiter H, Porjesz B, et al. Joint multipoint linkage analysis of multivariate qualitative and quantitative traits. II. Alcoholism and event-related potentials. *Am J Hum Genet.* 1999;65: 1148-1160.
48. Martin LJ, Mahaney MC, Almasy L, et al. A quantitative trait locus on chromosome 22 for serum leptin levels adjusted for serum testosterone. *Obes Res.* 2002;10:602-607.
49. Comuzzie AG, Hixson JE, Almasy L, et al. A major quantitative trait locus determining serum leptin levels and fat mass is located on human chromosome 2. *Nat Genet.* 1997;15:273-276.
50. Blangero J, Williams JT, Almasy L. Robust LOD scores for variance component-based linkage analysis. *Genet Epidemiol.* 2000;19 (suppl 1):S8-S14.
51. Feingold E, Brown PO, Siegmund D. Gaussian models for genetic linkage analysis using complete high-resolution maps of identity by descent. *Am J Hum Genet.* 1993;53:234-251.
52. Wu Z, Nakura J, Abe M, et al. Genome-wide linkage disequilibrium mapping of hypertension in Japan. *Hypertens Res.* 2003;26:533-540.
53. Dielemans I, Vingerling JR, Algra D, Hofman A, Grobbee DE, de Jong PT. Primary open-angle glaucoma, intraocular pressure, and systemic blood pressure in the general elderly population. The Rotterdam Study. *Ophthalmology.* 1995;102:54-60.
54. Tielsch JM, Katz J, Sommer A, Quigley HA, Javitt JC. Hypertension, perfusion pressure, and primary open-angle glaucoma: a population-based assessment. *Arch Ophthalmol.* 1995;113:216-221.
55. McLeod SD, West SK, Quigley HA, Fozard JL. A longitudinal study of the relationship between intraocular and blood pressures. *Invest Ophthalmol Vis Sci.* 1990;31:2361-2366.
56. Chang B, Smith RS, Peters M, et al. Haploinsufficient Bmp4 ocular phenotypes include anterior segment dysgenesis with elevated intraocular pressure. *BMC Genet.* 2001;2:18.
57. Bernal S, Calaf M, Garcia-Hoyos M, et al. Study of the involvement of the RGR, CRPB1, and CRB1 genes in the pathogenesis of autosomal recessive retinitis pigmentosa. *J Med Genet.* 2003;40: E89.
58. Hansen FK, Ehlers N. Elevated tonometer readings caused by a thick cornea. *Acta Ophthalmol (Copenh).* 1971;49:775-778.
59. Stodtmeister R. Applanation tonometry and correction according to corneal thickness. *Acta Ophthalmol Scand.* 1998;76:319-324.
60. Wolfs RC, Klaver CC, Vingerling JR, Grobbee DE, Hofman A, de Jong PT. Distribution of central corneal thickness and its association with intraocular pressure: The Rotterdam Study. *Am J Ophthalmol.* 1997;123:767-772.
61. Dohadwala AA, Damji KF. Familial occurrence of artefactual ocular hypertension from thick corneas and of primary open angle glaucoma in a French Canadian kindred. *Ophthalmic Genet.* 2000;21: 1-7.
62. Manya H, Sakai K, Kobayashi K, et al. Loss-of-function of an N-acetylglucosaminyltransferase, POMGnT1, in muscle-eye-brain disease. *Biochem Biophys Res Commun.* 2003;306:93-97.
63. Semina EV, Brownell I, Mintz-Hittner HA, Murray JC, Jamrich M. Mutations in the human forkhead transcription factor FOXE3 associated with anterior segment ocular dysgenesis and cataracts. *Hum Mol Genet.* 2001;10:231-236.
64. Akarsu AN, Turacli ME, Aktan SG, et al. A second locus (GLC3B) for primary congenital glaucoma (Buphthalmos) maps to the 1p36 region. *Hum Mol Genet.* 1996;5:1199-1203.
65. Allingham RR, Wiggs JL, De La Paz MA, et al. Gln368STOP myocilin mutation in families with late-onset primary open- angle glaucoma. *Invest Ophthalmol Vis Sci.* 1998;39:2288-2295.

Appendix 5 - Complete list of individuals genotyped in family GTas02

Individual ID	Individual ID	Individual ID	Individual ID	Individual ID
1	35	66	99	634
2	36	67	100	636
3	37	68	101	637
4	38	69	102	638
6	39	70	103	640
7	40	71	104	641
8	41	72	105	642
9	42	76	106	647
10	44	77	107	648
14	46	78	108	649
15	47	79	109	650
16	48	80	110	654
17	49	81	111	655
18	50	82	112	657
19	51	83	113	659
20	52	84	114	660
21	53	85	115	670
23	54	86	116	671
24	55	87	117	672
25	56	88	271	673
26	57	89	273	675
27	58	90	416	676
28	59	91	457	2081
29	60	92	463	
30	61	93	464	
31	62	95	629	
32	63	96	631	
33	64	97	632	
34	65	98	633	

Table A5.1 - A complete list of the individuals genotyped in family GTas02

Numbers listed are individual ID numbers. Data from these individuals, including the 10 cM genome-wide scan, clinical information and mutation analysis, were used in Chapter 6.

References

Abecasis GR, Cherny SS and Cardon LR (2001). The impact of genotyping error on family-based analysis of quantitative traits. *Eur J Hum Genet* 9(2): 130-4.

Abecasis GR, Cherny SS, Cookson WO and Cardon LR (2002). Merlin--rapid analysis of dense genetic maps using sparse gene flow trees. *Nat Genet* 30(1): 97-101.

Akarsu AN, Turacli ME, Aktan SG, Barsoum-Homsy M, Chevrette L, Sayli BS and Sarfarazi M (1996). A second locus (GLC3B) for primary congenital glaucoma (Buphthalmos) maps to the 1p36 region. *Hum Mol Genet* 5(8): 1199-203.

Allingham RR, Wiggs JL, De La Paz MA, Vollrath D, Tallett DA, Broomer B, Jones KH, Del Bono EA, Kern J, Patterson K, Haines JL and Pericak-Vance MA (1998). Gln368STOP myocilin mutation in families with late-onset primary open- angle glaucoma. *Invest Ophthalmol Vis Sci* 39(12): 2288-95.

Allingham RR, Wiggs JL, Hauser ER, Larocque-Abramson KR, Santiago-Turla C, Broomer B, Del Bono EA, Graham FL, Haines JL, Pericak-Vance MA and Hauser MA (2005). Early adult-onset POAG linked to 15q11-13 using ordered subset analysis. *Invest Ophthalmol Vis Sci* 46(6): 2002-5.

Almasy L and Blangero J (1998). Multipoint quantitative-trait linkage analysis in general pedigrees. *Am J Hum Genet* 62(5): 1198-211.

Alward WL, Fingert JH, Coote MA, Johnson AT, Lerner SF, Junqua D, Durcan FJ, McCartney PJ, Mackey DA, Sheffield VC and Stone EM (1998). Clinical features associated with mutations in the chromosome 1 open- angle glaucoma gene (GLC1A). *N Engl J Med* 338(15): 1022-7.

Alward WL, Kwon Y, Khanna C, Johnson AT, Hayreh S, Zimmerman B, Narkiewicz J, Andorf J, Moore P, Fingert J, Sheffield VC and Stone EM (2002). Variations in the myocilin gene in patients with open-angle glaucoma. *Arch Ophthalmol* 120: 1189-1197.

Alward WL, Kwon YH, Kawase K, Craig JE, Hayreh SS, Johnson AT, Khanna CL, Yamamoto T, Mackey DA, Roos BR, Affatigato LM, Sheffield VC and Stone EM (2003). Evaluation of optineurin sequence variations in 1,048 patients with open-angle glaucoma. *Am J Ophthalmol* 136(5): 904-10.

American Academy of Ophthalmology Preferred Practice Patterns: Primary Open-Angle Glaucoma (Limited Revision) (2003) http://www.aao.org/aao/education/library/ppp/index.cfm

Amos CI and de Andrade M (2001). Genetic linkage methods for quantitative traits. *Stat Methods Med Res* 10(1): 3-25.

Anderson DR, Drance SM and Group. TCN-TGS (1998). Comparison of glaucomatous progression between untreated patients with normal-tension glaucoma and patients with therapeutically reduced intraocular pressures. Collaborative Normal-Tension Glaucoma Study Group. *Am J Ophthalmol* 126(4): 487-97.

Angius A, Spinelli P, Ghilotti G, Casu G, Sole G, Loi A, Totaro A, Zelante L, Gasparini P, Orzalesi N, Pirastu M and Bonomi L (2000). Myocilin Gln368stop mutation and advanced age as risk factors for late- onset primary open-angle glaucoma. *Arch Ophthalmol* 118(5): 674-9.

Angius A, Petretto E, Maestrale GB, Forabosco P, Casu G, Piras D, Fanciulli M, Falchi M, Melis PM, Palermo M and Pirastu M (2002). A new essential hypertension susceptibility locus on chromosome 2p24-p25, detected by genomewide search. *Am J Hum Genet* 71(4): 893-905.

Asrani S, Zeimer R, Wilensky J, Gieser D, Vitale S and Lindenmuth K (2000). Large diurnal fluctuations in intraocular pressure are an independent risk factor in patients with glaucoma. *J Glaucoma* 9(2): 134-42.

Australian Bureau of Statistics (2001). Australian Bureau of Statistics: Census Data for Tasmania.

Australian Bureau of Statistics (2002) http://www.abs.gov.au

Baird PN, Craig JE, Richardson AJ, Ring MA, Sim P, Stanwix S, Foote SJ and Mackey DA (2003). Analysis of 15 primary open-angle glaucoma families from Australia identifies a founder effect for the Q368STOP mutation of myocilin. *Hum Genet* 112(2): 110-6.

Baird PN, Richardson AJ, Craig JE, Mackey DA, Rochtchina E and Mitchell P (2004). Analysis of optineurin (*OPTN*) gene mutations in subjects with and without glaucoma: the Blue Mountains Eye Study. *Clin Experiment Ophthalmol* 32(5): 518-22.

Baird PN, Foote SJ, Mackey DA, Craig J, Speed TP and Bureau A (2005). Evidence for a novel glaucoma locus at chromosome 3p21-22. *Hum Genet* 117(2-3): 249-57.

Bathija R, Gupta N, Zangwill L and Weinreb RN (1998). Changing definition of glaucoma. *J Glaucoma* 7(3): 165-9.

Bayer AU, Keller ON, Ferrari F and Maag KP (2002). Association of glaucoma with neurodegenerative diseases with apoptotic cell death: Alzheimer's disease and Parkinson's disease. *Am J Ophthalmol* 133(1): 135-7.

Bengtsson BO (1989). Incidence of manifest glaucoma. *Br J Ophthalmol* 73(7): 483-7.

Bernal S, Calaf M, Garcia-Hoyos M, Garcia-Sandoval B, Rosell J, Adan A, Ayuso C and Baiget M (2003). Study of the involvement of the *RGR*, *CRPB1*, and *CRB1* genes in the pathogenesis of autosomal recessive retinitis pigmentosa. *J Med Genet* 40(7): e89.

Blangero J and Almasy L (1997). Multipoint oligogenic linkage analysis of quantitative traits. *Genet Epidemiol* 14(6): 959-64.

Blangero J, Williams JT and Almasy L (2000). Robust LOD scores for variance component-based linkage analysis. *Genet Epidemiol* 19 Suppl 1: S8-14.

Blangero J, Williams JT and Almasy L (2001). Variance component methods for detecting complex trait loci. *Adv Genet* 42: 151-81.

Bonomi L, Marchini G, Marraffa M, Bernardi P, Morbio R and Varotto A (2000). Vascular risk factors for primary open angle glaucoma: the Egna-Neumarkt Study. *Ophthalmology* 107(7): 1287-93.

Bourne RR, Sukudom P, Foster PJ, Tantisevi V, Jitapunkul S, Lee PS, Johnson GJ and Rojanapongpun P (2003). Prevalence of glaucoma in Thailand: a population based survey in Rom Klao District, Bangkok. *Br J Ophthalmol* 87(9): 1069-74.

Brandt JD, Beiser JA, Kass MA and Gordon MO (2001). Central corneal thickness in the Ocular Hypertension Treatment Study (OHTS). *Ophthalmology* 108(10): 1779-88.

Broadway DC and Drance SM (1998). Glaucoma and vasospasm. *Br J Ophthalmol* 82(8): 862-70.

Broman KW, Murray JC, Sheffield VC, White RL and Weber JL (1998). Comprehensive human genetic maps: individual and sex-specific variation in recombination. *Am J Hum Genet* 63(3): 861-9.

Budde WM and Jonas JB (1999). Family history of glaucoma in the primary and secondary open-angle glaucomas. *Graefes Arch Clin Exp Ophthalmol* 237(7): 554-7.

Buhrmann RR, Quigley HA, Barron Y, West SK, Oliva MS and Mmbaga BB (2000). Prevalence of glaucoma in a rural East African population. *Invest Ophthalmol Vis Sci* 41(1): 40-8.

Bullido MJ, Artiga MJ, Recuero M, Sastre I, Garcia MA, Aldudo J, Lendon C, Han SW, Morris JC, Frank A, Vazquez J, Goate A and Valdivieso F (1998). A polymorphism in the regulatory region of *APOE* associated with risk for Alzheimer's dementia. *Nat Genet* 18(1): 69-71.

Bunce C, Hitchings RA, Bhattacharya SS and Lehmann OJ (2003). Single-nucleotide polymorphisms and glaucoma severity. *Am J Hum Genet* 72(6): 1593-4; author reply 1594-5.

Carel RS, Korczyn AD, Rock M and Goya I (1984). Association between ocular pressure and certain health parameters. *Ophthalmology* 91(4): 311-4.

The Centre d'Etude du Polymorphisme Humain (CEPH) Genotype Database http://www.cephb.fr/cephdb/

Chang B, Smith RS, Peters M, Savinova OV, Hawes NL, Zabaleta A, Nusinowitz S, Martin JE, Davisson ML, Cepko CL, Hogan BL and John SW (2001). Haploinsufficient *Bmp4* ocular phenotypes include anterior segment dysgenesis with elevated intraocular pressure. *BMC Genet* 2(1): 18.

Chang TC, Congdon NG, Wojciechowski R, Munoz B, Gilbert D, Chen P, Friedman DS and West SK (2005). Determinants and heritability of intraocular pressure and cup-to-disc ratio in a defined older population. *Ophthalmology* 112(7): 1186-91.

Charlesworth JC, Dyer TD, Stankovich JM, Blangero J, Mackey DA, Craig JE, Green CM, Foote SJ, Baird PN and Sale MM (2005). Linkage to 10q22 for maximum intraocular pressure and 1p32 for maximum cup-to-disc ratio in an extended primary open-angle glaucoma pedigree. *Invest Ophthalmol Vis Sci* 46(10): 3723-9.

Charlesworth JC, Stankovich JM, Mackey DA, Craig JE, Haybittel M, Westmore RN and Sale MM (2006). Confirmation of the adult-onset primary open angle glaucoma locus GLC1B at 2cen-q13 in an Australian family. *Ophthalmologica* 220(1): 23-30.

Cheng AC, Pang CP, Leung AT, Chua JK, Fan DS and Lam DS (2000). The association between cigarette smoking and ocular diseases. *Hong Kong Med J* 6(2): 195-202.

Coffey M, Reidy A, Wormald R, Xian WX, Wright L and Courtney P (1993). Prevalence of glaucoma in the west of Ireland. *Br J Ophthalmol* 77(1): 17-21.

Coleman AL, Gordon MO, Beiser JA and Kass MA (2004). Baseline risk factors for the development of primary open-angle glaucoma in the Ocular Hypertension Treatment Study. *Am J Ophthalmol* 138(4): 684-5.

Collins A, Frezal J, Teague J and Morton NE (1996). A metric map of humans: 23,500 loci in 850 bands. *Proc Natl Acad Sci U S A* 93(25): 14771-5.

Comuzzie AG, Hixson JE, Almasy L, Mitchell BD, Mahaney MC, Dyer TD, Stern MP, MacCluer JW and Blangero J (1997). A major quantitative trait locus determining serum leptin levels and fat mass is located on human chromosome 2. *Nat Genet* 15(3): 273-6.

Coote MA, McCartney PJ, Wilkinson RM and Mackey DA (1996). The 'GIST' score: ranking glaucoma for genetic studies. Glaucoma Inheritance Study of Tasmania. *Ophthalmic Genet* 17(4): 199-208.

Copin B, Brezin AP, Valtot F, Dascotte JC, Bechetoille A and Garchon HJ (2002). Apolipoprotein E-promoter single-nucleotide polymorphisms affect the phenotype of primary open-angle glaucoma and demonstrate interaction with the myocilin gene. *Am J Hum Genet* 70(6): 1575-81.

Cottingham RW, Jr., Idury RM and Schaffer AA (1993). Faster sequential genetic linkage computations. *Am J Hum Genet* 53(1): 252-63.

Craig JE and Mackey DA (1999). Glaucoma genetics: where are we? Where will we go? *Curr Opin Ophthalmol* 10(2): 126-34.

Craig JE, Baird PN, Healey DL, McNaught AI, McCartney PJ, Rait JL, Dickinson JL, Roe L, Fingert JH, Stone EM and Mackey DA (2001). Evidence for genetic heterogeneity within eight glaucoma families, with the GLC1A Gln368STOP mutation being an important phenotypic modifier. *Ophthalmology* 108(9): 1607-20.

Dale M and Nicklin MJ (1999). Interleukin-1 receptor cluster: gene organization of *IL1R2*, *IL1R1*, *IL1RL2* (*IL-1Rrp2*), *IL1RL1* (T1/ST2), and *IL18R1* (*IL-1Rrp*) on human chromosome 2q. *Genomics* 57(1): 177-9.

Dielemans I, Vingerling JR, Wolfs RC, Hofman A, Grobbee DE and de Jong PT (1994). The prevalence of primary open-angle glaucoma in a population-based study in The Netherlands. The Rotterdam Study. *Ophthalmology* 101(11): 1851-5.

Dielemans I, Vingerling JR, Algra D, Hofman A, Grobbee DE and de Jong PT (1995). Primary open-angle glaucoma, intraocular pressure, and systemic blood pressure in the general elderly population. The Rotterdam Study. *Ophthalmology* 102(1): 54-60.

Dielemans I, de Jong PT, Stolk R, Vingerling JR, Grobbee DE and Hofman A (1996). Primary open-angle glaucoma, intraocular pressure, and diabetes mellitus in the general elderly population. The Rotterdam Study. *Ophthalmology* 103(8): 1271-5.

Dohadwala AA and Damji KF (2000). Familial occurrence of artefactual ocular hypertension from thick corneas and of primary open angle glaucoma in a French Canadian kindred. *Ophthalmic Genet* 21(1): 1-7.

Douglas JA, Boehnke M and Lange K (2000). A multipoint method for detecting genotyping errors and mutations in sibling-pair linkage data. *Am J Hum Genet* 66(4): 1287-97.

Douglas JA, Skol AD and Boehnke M (2002). Probability of detection of genotyping errors and mutations as inheritance inconsistencies in nuclear-family data. *Am J Hum Genet* 70(2): 487-95.

Drance SM (1963). Diurnal Variation of Intraocular Pressure in Treated Glaucoma. Significance in Patients with Chronic Simple Glaucoma. *Arch Ophthalmol* 70: 302-11.

Duggal P, Klein AP, Lee KE, Iyengar SK, Klein R, Bailey-Wilson JE and Klein BE (2005). A genetic contribution to intraocular pressure: the beaver dam eye study. *Invest Ophthalmol Vis Sci* 46(2): 555-60.

Duggirala R, Williams JT, Williams-Blangero S and Blangero J (1997). A variance component approach to dichotomous trait linkage analysis using a threshold model. *Genet Epidemiol* 14(6): 987-92.

Ellis JD, Evans JM, Ruta DA, Baines PS, Leese G, MacDonald TM and Morris AD (2000). Glaucoma incidence in an unselected cohort of diabetic patients: is diabetes mellitus a risk factor for glaucoma? DARTS/MEMO collaboration. Diabetes Audit and Research in Tayside Study. Medicines Monitoring Unit. *Br J Ophthalmol* 84(11): 1218-24.

Elston RC and Stewart J (1971). A general model for the genetic analysis of pedigree data. *Hum Hered* 21(6): 523-42.

European Glaucoma Society: Terminology and Guidelines for Glaucoma (1998) http://www.eugs.org

Evans DM, Cardon LR and Morris AP (2004). Genotype prediction using a dense map of SNPs. *Genet Epidemiol* 27(4): 375-84.

Evans DM and Cardon LR (2004). Guidelines for genotyping in genomewide linkage studies: single-nucleotide-polymorphism maps versus microsatellite maps. *Am J Hum Genet* 75(4): 687-92.

Faber PW, Barnes GT, Srinidhi J, Chen J, Gusella JF and MacDonald ME (1998). Huntingtin interacts with a family of WW domain proteins. *Hum Mol Genet* 7(9): 1463-74.

Fan BJ, Leung YF, Wang N, Lam SC, Liu Y, Tam OS and Pang CP (2004). Genetic and environmental risk factors for primary open-angle glaucoma. *Chin Med J (Engl)* 117(5): 706-10.

Feingold E, Brown PO and Siegmund D (1993). Gaussian models for genetic linkage analysis using complete high-resolution maps of identity by descent. *Am J Hum Genet* 53(1): 234-51.

Fautsch MP and Johnson DH (2001). Characterization of myocilin-myocilin interactions. *Invest Ophthalmol Vis Sci* 42(10): 2324-31.

Fingert JH, Ying L and Swinderski RE (1998). Characterization and comparison of the human and mouse GLC1A glaucoma genes. *Genome Res.* 8: 377-384.

Fingert JH, Heon E, Liebmann JM, Yamamoto T, Craig JE, Rait J, Kawase K, Hoh ST, Buys YM, Dickinson J, Hockey RR, Williams-Lyn D, Trope G, Kitazawa Y, Ritch R, Mackey DA, Alward WL, Sheffield VC and Stone EM (1999). Analysis of myocilin mutations in 1703 glaucoma patients from five different populations. *Hum Mol Genet* 8(5): 899-905.

Fingert JH, Stone EM, Sheffield VC and Alward WL (2002). Myocilin glaucoma. *Surv Ophthalmol* 47(6): 547-61.

Forsman E, Lemmela S, Varilo T, Kristo P, Forsius H, Sankila EM and Jarvela I (2003). The role of *TIGR* and *OPTN* in Finnish glaucoma families: a clinical and molecular genetic study. *Mol Vis* 9: 217-22.

Foster PJ, Buhrmann R, Quigley HA and Johnson GJ (2002). The definition and classification of glaucoma in prevalence surveys. *Br J Ophthalmol* 86(2): 238-42.

Franks WA, Limb GA, Stanford MR, Ogilvie J, Wolstencroft RA, Chignell AH and Dumonde DC (1992). Cytokines in human intraocular inflammation. *Curr Eye Res* 11 Suppl: 187-91.

Freimer N and Sabatti C (2004). The use of pedigree, sib-pair and association studies of common diseases for genetic mapping and epidemiology. *Nat Genet* 36(10): 1045-51.

Funayama T, Ishikawa K, Ohtake Y, Tanino T, Kurosaka D, Kimura I, Suzuki K, Ideta H, Nakamoto K, Yasuda N, Fujimaki T, Murakami A, Asaoka R, Hotta Y, Tanihara H, Kanamoto T, Mishima H, Fukuchi T, Abe H, Iwata T, *et al.* (2004). Variants in optineurin gene and their association with tumor necrosis factor-alpha polymorphisms in Japanese patients with glaucoma. *Invest Ophthalmol Vis Sci* 45(12): 4359-67.

Gal A, Li Y, Thompson DA, Weir J, Orth U, Jacobson SG, Apfelstedt-Sylla E and Vollrath D (2000). Mutations in MERTK, the human orthologue of the RCS rat retinal dystrophy gene, cause retinitis pigmentosa. *Nat Genet* 26(3): 270-1.

Goldberg I, Graham SL and Healey PR (2002). Primary open-angle glaucoma. *Med J Aust* 177(10): 535-6.

Gordon MO, Beiser JA, Brandt JD, Heuer DK, Higginbotham EJ, Johnson CA, Keltner JL, Miller JP, Parrish RK, 2nd, Wilson MR and Kass MA (2002). The Ocular Hypertension Treatment Study: baseline factors that predict the onset of primary open-angle glaucoma. *Arch Ophthalmol* 120(6): 714-20; discussion 829-30.

Gottfredsdottir MS, Sverrisson T, Musch DC and Stefansson E (1999). Chronic open-angle glaucoma and associated ophthalmic findings in monozygotic twins and their spouses in Iceland. *J Glaucoma* 8(2): 134-9.

Graff (1995). Confirmation of linkage to 1q21-31 in a Danish autosomal dominant juvenile-onset glaucoma family. *Human Genetics* 96: 285-289.

Hanis CL, Boerwinkle E, Chakraborty R, Ellsworth DL, Concannon P, Stirling B, Morrison VA, Wapelhorst B, Spielman RS, Gogolin-Ewens KJ, Shepard JM, Williams SR, Risch N, Hinds D, Iwasaki N, Ogata M, Omori Y, Petzold C, Rietzch H, Schroder HE, *et al.* (1996). A genome-wide search for human non-insulin-dependent (type 2) diabetes genes reveals a major susceptibility locus on chromosome 2. *Nat Genet* 13(2): 161-6.

Hansen FK and Ehlers N (1971). Elevated tonometer readings caused by a thick cornea. *Acta Ophthalmol (Copenh)* 49(5): 775-8.

Hanson I and Van Heyningen V (1995). Pax6: more than meets the eye. *Trends Genet* 11(7): 268-72.

Hattula K and Peranen J (2000). FIP-2, a coiled-coil protein, links Huntingtin to Rab8 and modulates cellular morphogenesis. *Curr Biol* 10(24): 1603-6.

Hauser ER, Watanabe RM, Duren WL, Bass MP, Langefeld CD and Boehnke M (2004). Ordered subset analysis in genetic linkage mapping of complex traits. *Genet Epidemiol* 27(1): 53-63.

Heath SC (1997). Markov chain Monte Carlo segregation and linkage analysis for oligogenic models. *Am J Hum Genet* 61(3): 748-60.

Heath SC, Snow GL, Thompson EA, Tseng C and Wijsman EM (1997). MCMC segregation and linkage analysis. *Genet Epidemiol* 14(6): 1011-6.

Hughes E, Spry P and Diamond J (2003). 24-hour monitoring of intraocular pressure in glaucoma management: a retrospective review. *J Glaucoma* 12(3): 232-6.

Jansson M, Wadelius C, Rezaie T and Sarfarazi M (2005). Analysis of rare variants and common haplotypes in the optineurin gene in Swedish glaucoma cases. *Ophthalmic Genet* 26(2): 85-9.

Jonas JB, Gusek GC and Naumann GO (1988a). Optic disc morphometry in chronic primary open-angle glaucoma. I. Morphometric intrapapillary characteristics. *Graefes Arch Clin Exp Ophthalmol* 226(6): 522-30.

Jonas JB, Gusek GC and Naumann GO (1988b). Optic disc, cup and neuroretinal rim size, configuration and correlations in normal eyes. *Invest Ophthalmol Vis Sci* 29(7): 1151-8.

Jonas JB, Muller-Bergh JA, Schlotzer-Schrehardt UM and Naumann GO (1990). Histomorphometry of the human optic nerve. *Invest Ophthalmol Vis Sci* 31(4): 736-44.

Jonas JB, Budde WM and Panda-Jonas S (1999). Ophthalmoscopic evaluation of the optic nerve head. *Surv Ophthalmol* 43(4): 293-320.

Jordan T, Hanson I, Zaletayev D, Hodgson S, Prosser J, Seawright A, Hastie N and van Heyningen V (1992). The human *PAX6* gene is mutated in two patients with aniridia. *Nat Genet* 1(5): 328-32.

Kahn HA and Milton RC (1980). Alternative definitions of open-angle glaucoma. Effect on prevalence and associations in the Framingham eye study. *Arch Ophthalmol* 98(12): 2172-7.

Kamal D and Hitchings R (1998). Normal tension glaucoma--a practical approach. *Br J Ophthalmol* 82(7): 835-40.

Kang JH, Pasquale LR, Rosner BA, Willett WC, Egan KM, Faberowski N and Hankinson SE (2003). Prospective study of cigarette smoking and the risk of primary open-angle glaucoma. *Arch Ophthalmol* 121(12): 1762-8.

Kass MA, Heuer DK, Higginbotham EJ, Johnson CA, Keltner JL, Miller JP, Parrish RK, 2nd, Wilson MR and Gordon MO (2002). The Ocular Hypertension Treatment Study: a randomized trial determines that topical ocular hypotensive medication delays or prevents the onset of primary open-angle glaucoma. *Arch Ophthalmol* 120(6): 701-13; discussion 829-30.

Ke X, Tapper W and Collins A (2001). LDB2000: sequence-based integrated maps of the human genome. *Bioinformatics* 17(7): 581-6.

Khaw PT, Shah P and Elkington AR (2004). Glaucoma--1: diagnosis. *Bmj* 328(7431): 97-9.

Kirstein L, Cvekl A, Chauhan BK and Tamm ER (2000). Regulation of human myocilin/TIGR gene transcription in trabecular meshwork cells and astrocytes: role of upstream stimulatory factor. *Genes Cells* 5(8): 661-76.

Kitsos G, Eiberg H, Economou-Petersen E, Wirtz MK, Kramer PL, Aspiotis M, Tommerup N, Petersen MB and Psilas K (2001). Genetic linkage of autosomal dominant primary open angle glaucoma to chromosome 3q in a Greek pedigree. *Eur J Hum Genet* 9(6): 452-7.

Klein BE, Klein R, Sponsel WE, Franke T, Cantor LB, Martone J and Menage MJ (1992). Prevalence of glaucoma. The Beaver Dam Eye Study. *Ophthalmology* 99(10): 1499-504.

Klein BE, Klein R and Ritter LL (1993). Relationship of drinking alcohol and smoking to prevalence of open-angle glaucoma. The Beaver Dam Eye Study. *Ophthalmology* 100(11): 1609-13.

Klein BE, Klein R and Jensen SC (1994). Open-angle glaucoma and older-onset diabetes. The Beaver Dam Eye Study. *Ophthalmology* 101(7): 1173-7.

Klein BE, Klein R and Lee KE (2004). Heritability of risk factors for primary open-angle glaucoma: the Beaver Dam Eye Study. *Invest Ophthalmol Vis Sci* 45(1): 59-62.

Kong A and Cox NJ (1997). Allele-sharing models: LOD scores and accurate linkage tests. *Am J Hum Genet* 61(5): 1179-88.

Kong A, Gudbjartsson DF, Sainz J, Jonsdottir GM, Gudjonsson SA, Richardsson B, Sigurdardottir S, Barnard J, Hallbeck B, Masson G, Shlien A, Palsson ST, Frigge ML, Thorgeirsson TE, Gulcher JR and Stefansson K (2002). A high-resolution recombination map of the human genome. *Nat Genet* 31(3): 241-7.

Kramer PL, Samples JR, Schilling K, Sykes RL, Man J, Rust K and Wirtz MK (2004). [Abstract] Mapping the GLC1G locus for Primary Open-Angle Glaucoma (POAG) in an Oregon family of Dutch origin. *Am J Hum Genet* 75: Abstract# 1914.

Kroese M and Burton H (2003). Primary open angle glaucoma. The need for a consensus case definition. *J Epidemiol Community Health* 57(9): 752-4.

Kruglyak L, Daly MJ, Reeve-Daly MP and Lander ES (1996). Parametric and nonparametric linkage analysis: a unified multipoint approach. *Am J Hum Genet* 58(6): 1347-63.

Kubota R, Noda S, Wang Y, Minoshima S, Asakawa S, Kudoh J, Mashima Y, Oguchi Y and Shimizu N (1997). A novel myosin-like protein (Myocilin) expressed in the connecting cilium of the photoreceptor: Molecular cloning, tissue expression and chromosomal mapping. *Genomics* 41: 360-369.

Lafranchi M, Mitchell RJ and Kosten M (1988). Mating structure, isonymy and social class in late nineteenth century Tasmania. *Ann Hum Biol* 15(5): 325-36.

Lambert JC, Berr C, Pasquier F, Delacourte A, Frigard B, Cottel D, Perez-Tur J, Mouroux V, Mohr M, Cecyre D, Galasko D, Lendon C, Poirier J, Hardy J, Mann D, Amouyel P and Chartier-Harlin MC (1998). Pronounced impact of Th1/E47cs mutation compared with -491 AT mutation on neural *APOE* gene expression and risk of developing Alzheimer's disease. *Hum Mol Genet* 7(9): 1511-6.

Lambert JC, Brousseau T, Defosse V, Evans A, Arveiler D, Ruidavets JB, Haas B, Cambou JP, Luc G, Ducimetiere P, Cambien F, Chartier-Harlin MC and Amouyel P (2000). Independent association of an *APOE* gene promoter polymorphism with increased risk of myocardial infarction and decreased APOE plasma concentrations-the ECTIM study. *Hum Mol Genet* 9(1): 57-61.

Lander E and Kruglyak L (1995). Genetic dissection of complex traits: guidelines for interpreting and reporting linkage results. *Nat Genet* 11(3): 241-7.

Lander ES and Green P (1987). Construction of multilocus genetic linkage maps in humans. *Proc Natl Acad Sci U S A* 84(8): 2363-7.

Lander ES, Linton LM, Birren B, Nusbaum C, Zody MC, Baldwin J, Devon K, Dewar K, Doyle M, FitzHugh W, Funke R, Gage D, Harris K, Heaford A, Howland J, Kann L, Lehoczky J, LeVine R, McEwan P, McKernan K, *et al.* (2001). Initial sequencing and analysis of the human genome. *Nature* 409(6822): 860-921.

Landers J, Goldberg I and Graham SL (2002). Analysis of risk factors that may be associated with progression from ocular hypertension to primary open angle glaucoma. *Clin Experiment Ophthalmol* 30(4): 242-7.

Lathrop GM and Lalouel JM (1984). Easy calculations of lod scores and genetic risks on small computers. *Am J Hum Genet* 36(2): 460-5.

Lathrop GM, Lalouel JM, Julier C and Ott J (1984). Strategies for multilocus linkage analysis in humans. *Proc Natl Acad Sci U S A* 81(11): 3443-6.

Lathrop GM, Lalouel JM and White RL (1986). Construction of human linkage maps: likelihood calculations for multilocus linkage analysis. *Genet Epidemiol* 3(1): 39-52.

Le A, Mukesh BN, McCarty CA and Taylor HR (2003). Risk factors associated with the incidence of open-angle glaucoma: the visual impairment project. *Invest Ophthalmol Vis Sci* 44(9): 3783-9.

Leske MC and Rosenthal J (1979). Epidemiologic aspects of open-angle glaucoma. *Am J Epidemiol* 109(3): 250-72.

Leske MC, Connell AM, Schachat AP and Hyman L (1994). The Barbados Eye Study. Prevalence of open angle glaucoma. *Arch Ophthalmol* 112(6): 821-9.

Leske MC, Connell AM, Wu SY, Hyman LG and Schachat AP (1995). Risk factors for open-angle glaucoma. The Barbados Eye Study. *Arch Ophthalmol* 113(7): 918-24.

Leske MC, Connell AM, Wu SY, Nemesure B, Li X, Schachat A and Hennis A (2001). Incidence of open-angle glaucoma: the Barbados Eye Studies. The Barbados Eye Studies Group. *Arch Ophthalmol* 119(1): 89-95.

Leske MC, Heijl A, Hussein M, Bengtsson B, Hyman L and Komaroff E (2003). Factors for glaucoma progression and the effect of treatment: the early manifest glaucoma trial. *Arch Ophthalmol* 121(1): 48-56.

Leske MC, Heijl A, Hyman L, Bengtsson B and Komaroff E (2004). Factors for progression and glaucoma treatment: the Early Manifest Glaucoma Trial. *Curr Opin Ophthalmol* 15(2): 102-6.

Leung YF, Fan BJ, Lam DS, Lee WS, Tam PO, Chua JK, Tham CC, Lai JS, Fan DS and Pang CP (2003). Different optineurin mutation pattern in primary open-angle glaucoma. *Invest Ophthalmol Vis Sci* 44(9): 3880-4.

Li Y, Kang J and Horwitz MS (1998). Interaction of an adenovirus E3 14.7-kilodalton protein with a novel tumor necrosis factor alpha-inducible cellular protein containing leucine zipper domains. *Mol Cell Biol* 18(3): 1601-10.

Lichter PR, Richards JE, Boehnke M, Othman M, Cameron BD, Stringham HM, Downs CA, Lewis SB and Boyd BF (1996). Juvenile glaucoma linked to GLCIA in a Panamanian family. *Trans Am Ophthalmol Soc* 94: 335-46.

Lin HJ, Tsai SC, Tsai FJ, Chen WC, Tsai JJ and Hsu CD (2003). Association of interleukin 1beta and receptor antagonist gene polymorphisms with primary open-angle glaucoma. *Ophthalmologica* 217(5): 358-64.

Liu JH (2001). Diurnal measurement of intraocular pressure. *J Glaucoma* 10(5 Suppl 1): S39-41.

Liu JH, Zhang X, Kripke DF and Weinreb RN (2003). Twenty-four-hour intraocular pressure pattern associated with early glaucomatous changes. *Invest Ophthalmol Vis Sci* 44(4): 1586-90.

Love J, Axton R, Churchill A, van Heyningen V and Hanson I (1998). A new set of primers for mutation analysis of the human *PAX6* gene. *Hum Mutat* 12(2): 128-34.

Mackey D and Howell N (1992). A variant of Leber hereditary optic neuropathy characterized by recovery of vision and by an unusual mitochondrial genetic etiology. *Am J Hum Genet* 51(6): 1218-28.

Mackey DA and Craig JE (2002). Glaucoma Inheritance Study in Tasmania: An International Collaboration. Basic and Clinical Science Course Section 13. San Francisco, American Academy of Ophthalmology. International Ophthalmology: 265-269.

Mackey DA and Craig JE (2003). Predictive DNA testing for glaucoma: reality in 2003. *Ophthalmol Clin North Am* 16(4): 639-45.

Maclean CJ, Morton NE, Elston RC and Yee S (1976). Skewness in commingled distributions. *Biometrics* 32(3): 695-9.

Mahley RW and Huang Y (1999). Apolipoprotein E: from atherosclerosis to Alzheimer's disease and beyond. *Curr Opin Lipidol* 10(3): 207-17.

Manya H, Sakai K, Kobayashi K, Taniguchi K, Kawakita M, Toda T and Endo T (2003). Loss-of-function of an N-acetylglucosaminyltransferase, *POMGnT1*, in muscle-eye-brain disease. *Biochem Biophys Res Commun* 306(1): 93-7.

Mao M, Biery MC, Kobayashi SV, Ward T, Schimmack G, Burchard J, Schelter JM, Dai H, He YD and Linsley PS (2004). T lymphocyte activation gene identification by coregulated expression on DNA microarrays. *Genomics* 83(6): 989-99.

Martin LJ, Mahaney MC, Almasy L, Hixson JE, Cole SA, MacCluer JW, Jaquish CE, Blangero J and Comuzzie AG (2002). A quantitative trait locus on chromosome 22 for serum leptin levels adjusted for serum testosterone. *Obes Res* 10(7): 602-7.

Mason RP, Kosoko O, Wilson MR, Martone JF, Cowan CL, Jr., Gear JC and Ross-Degnan D (1989). National survey of the prevalence and risk factors of glaucoma in St. Lucia, West Indies. Part I. Prevalence findings. *Ophthalmology* 96(9): 1363-8.

McLeod SD, West SK, Quigley HA and Fozard JL (1990). A longitudinal study of the relationship between intraocular and blood pressures. *Invest Ophthalmol Vis Sci* 31(11): 2361-6.

McNaught AI, Allen JG, Healey DL, McCartney PJ, Coote MA, Wong TL, Craig JE, Green CM, Rait JL and Mackey DA (2000). Accuracy and implications of a reported family history of glaucoma: experience from the Glaucoma Inheritance Study in Tasmania. *Arch Ophthalmol* 118(7): 900-4.

McPeek MS and Sun L (2000). Statistical tests for detection of misspecified relationships by use of genome-screen data. *Am J Hum Genet* 66(3): 1076-94.

Metropolis N, Rosenbluth A, Rosenbluth M, Teller M and Teller E (1953). Equations of state calculations by fast computing machines. *J Chem Phys* 21: 1087-1092.

Meyer A, Bechetoille A, Valtot F, Dupont de Dinechin S, Adam MF, Belmouden A, Brezin AP, Gomez L, Bach JF and Garchon HJ (1996). Age-dependent penetrance and mapping of the locus for juvenile and early-onset open-angle glaucoma on chromosome 1q (GLC1A) in a French family. *Hum Genet* 98(5): 567-71.

Mitchell P, Smith W, Attebo K and Healey PR (1996). Prevalence of open-angle glaucoma in Australia. The Blue Mountains Eye Study. *Ophthalmology* 103(10): 1661-9.

Mitchell P, Rochtchina E, Lee AJ and Wang JJ (2002). Bias in self-reported family history and relationship to glaucoma: the Blue Mountains Eye Study. *Ophthalmic Epidemiol* 9(5): 333-45.

Mitchell P, Lee AJ, Rochtchina E and Wang JJ (2004). Open-angle glaucoma and systemic hypertension: the blue mountains eye study. *J Glaucoma* 13(4): 319-26.

Mitchell R, Rochtchina E, Lee A, Wang JJ and Mitchell P (2003). Iris color and intraocular pressure: the Blue Mountains Eye Study. *Am J Ophthalmol* 135(3): 384-6.

Miyata M and Smith JD (1996). Apolipoprotein E allele-specific antioxidant activity and effects on cytotoxicity by oxidative insults and beta-amyloid peptides. *Nat Genet* 14(1): 55-61.

Monemi S, Child A, Lehmann O, Spaeth GL, Crick RP and Sarfarazi M (2003). [Abstract] Genome scan of two large families with adult-onset primary open angle glaucoma (POAG) suggests a probable locus on 5q33-q35. *The Association for Research in Vision and Ophthalmology (ARVO) Annual Meeting* Fort Lauderdale, FL: Abstract# 1128.

Monemi S, Spaeth G, Dasilva A, Popinchalk S, Ilitchev E, Liebmann J, Ritch R, Heon E, Crick RP, Child A and Sarfarazi M (2005). Identification of a novel adult-onset primary open angle glaucoma (POAG) gene on 5q22.1. *Hum Mol Genet.*

Moreland RJ, Dresser ME, Rodgers JS, Roe BA, Conaway JW, Conaway RC and Hanas JS (2000). Identification of a transcription factor IIIA-interacting protein. *Nucleic Acids Res* 28(9): 1986-93.

Morissette J, Cote G, Anctil JL, Plante M, Amyot M, Heon E, Trope GE, Weissenbach J and Raymond V (1995). A common gene for juvenile and adult-onset primary open-angle glaucomas confined on chromosome 1q. *Am J Hum Genet* 56(6): 1431-42.

Mukesh BN, McCarty CA, Rait JL and Taylor HR (2002). Five-year incidence of open-angle glaucoma: the visual impairment project. *Ophthalmology* 109(6): 1047-51.

Mukhopadhyay A, Komatireddy S, Acharya M, Bhattacharjee A, Mandal AK, Thakur SK, Chandrasekhar G, Banerjee A, Thomas R, Chakrabarti S and Ray K (2005a). Evaluation of Optineurin as a candidate gene in Indian patients with primary open angle glaucoma. *Mol Vis* 11: 792-7.

Mukhopadhyay N, Almasy L, Schroeder M, Mulvihill WP and Weeks DE (2005b). Mega2: data-handling for facilitating genetic linkage and association analyses. *Bioinformatics* 21(10): 2556-7.

Nemesure B, Leske MC, He Q and Mendell N (1996). Analyses of reported family history of glaucoma: a preliminary investigation. The Barbados Eye Study Group. *Ophthalmic Epidemiol* 3(3): 135-41.

Nemesure B, He Q, Mendell N, Wu SY, Hejtmancik JF, Hennis A and Leske MC (2001). Inheritance of open-angle glaucoma in the Barbados family study. *Am J Med Genet* 103(1): 36-43.

Nemesure B, Jiao X, He Q, Leske MC, Wu SY, Hennis A, Mendell N, Redman J, Garchon HJ, Agarwala R, Schaffer AA and Hejtmancik F (2003). A genome-wide scan for primary open-angle glaucoma (POAG): the Barbados Family Study of Open-Angle Glaucoma. *Hum Genet* 112(5-6): 600-9.

Nguyen TD, Chen P, Huang WD, Chen H, Johnson D and Polansky JR (1998). Gene structure and properties of *TIGR*, an olfactomedin-related glycoprotein cloned from glucocorticoid-induced trabecular meshwork cells. *J Biol Chem* 273(11): 6341-50.

NHMRC (1999). National Statement on Ethical Conduct in Research Involving Humans. http://www.nhmrc.gov.au/publications/pdf/e35.pdf.

Nicklin MJ, Barton JL, Nguyen M, FitzGerald MG, Duff GW and Komman K (2002). A sequence-based map of the nine genes of the human interleukin-1 cluster. *Genomics* 79(5): 718-25.

Ntim-Amponsah CT, Amoaku WM, Ofosu-Amaah S, Ewusi RK, Idirisuriya-Khair R, Nyatepe-Coo E and Adu-Darko M (2004). Prevalence of glaucoma in an African population. *Eye* 18(5): 491-7.

O'Connell JR and Weeks DE (1998). PedCheck: a program for identification of genotype incompatibilities in linkage analysis. *Am J Hum Genet* 63(1): 259-66.

Ott J (1989). Computer-simulation methods in human linkage analysis. *Proc Natl Acad Sci U S A* 86(11): 4175-8.

Polansky JR, Fauss DJ, Chen P, Chen H, Lutjen-Drecoll E, Johnson D, Kurtz RM, Ma ZD, Bloom E and Nguyen TD (1997). Cellular pharmacology and molecular biology of the trabecular meshwork inducible glucocorticoid response gene product. *Ophthalmologica* 211(3): 126-39.

Pridmore SA (1990). The large Huntington's disease family of Tasmania. *Med J Aust* 153(10): 593-5.

Quigley HA, Brown AE, Morrison JD and Drance SM (1990). The size and shape of the optic disc in normal human eyes. *Arch Ophthalmol* 108(1): 51-7.

Quigley HA, Katz J, Derick RJ, Gilbert D and Sommer A (1992). An evaluation of optic disc and nerve fiber layer examinations in monitoring progression of early glaucoma damage. *Ophthalmology* 99(1): 19-28.

Quigley HA (1993). Open-angle glaucoma. *N Engl J Med* 328(15): 1097-106.

Quigley HA (1996). Number of people with glaucoma worldwide. *Br J Ophthalmol* 80(5): 389-93.

Raymond V, Faucher M, Dubois S, CÔté G, Anctil JL and Morissette J (1999). [Abstract] Localization of a gene for adult-onset primary open-angle glaucoma to the GLC1B locus at chromosome 2cen-q13 in a French-Canadian family. *American Society of Human Genetics Conference 1999*: Abstract# 2503.

Resnikoff S, Pascolini D, Etya'ale D, Kocur I, Pararajasegaram R, Pokharel GP and Mariotti SP (2004). Global data on visual impairment in the year 2002. *Bull World Health Organ* 82(11): 844-51.

Ressiniotis T, Griffiths PG, Birch M, Keers S and Chinnery PF (2004). The role of apolipoprotein E gene polymorphisms in primary open-angle glaucoma. *Arch Ophthalmol* 122(2): 258-61.

Rezaie T, Child A, Hitchings R, Brice G, Miller L, Coca-Prados M, Heon E, Krupin T, Ritch R, Kreutzer D, Crick RP and Sarfarazi M (2002). Adult-onset primary open-angle glaucoma caused by mutations in optineurin. *Science* 295(5557): 1077-9.

Richards JE, Lichter PR, Boehnke M, Uro JL, Torrez D, Wong D and Johnson AT (1994). Mapping of a gene for autosomal dominant juvenile-onset open-angle glaucoma to chromosome Iq. *Am J Hum Genet* 54(1): 62-70.

Rochtchina E and Mitchell P (2000). Projected number of Australians with glaucoma in 2000 and 2030. *Clin Experiment Ophthalmol* 28(3): 146-8.

Rosenthal AR and Perkins ES (1985). Family studies in glaucoma. *Br J Ophthalmol* 69(9): 664-7.

Roses AD (1996). Apolipoprotein E alleles as risk factors in Alzheimer's disease. *Annu Rev Med* 47: 387-400.

Sacca SC, Rolando M, Marletta A, Macri A, Cerqueti P and Ciurlo G (1998). Fluctuations of intraocular pressure during the day in open-angle glaucoma, normal-tension glaucoma and normal subjects. *Ophthalmologica* 212(2): 115-9.

Sale MM, Craig JE, Charlesworth JC, FitzGerald LM, Hanson IM, Dickinson JL, Matthews SJ, Heyningen Vv V, Fingert JH and Mackey DA (2002). Broad phenotypic variability in a single pedigree with a novel 1410delC mutation in the PST domain of the *PAX6* gene. *Hum Mutat* 20(4): 322.

Samples JR, Sykes R, Man J, Rust K, Kramer PL and Wirtz MK (2004). [Abstract] Mapping a new POAG locus on chromosome 5. *The Association for Research in Vision and Ophthalmology (ARVO) Annual Meeting* Fort Lauderdale, FL: Abstract# 4622.

Sarfarazi M (1997). Recent advances in molecular genetics of glaucomas. *Hum Mol Genet* 6(10): 1667-77.

Sarfarazi M, Child A, Stoilova D, Brice G, Desai T, Trifan OC, Poinoosawmy D and Crick RP (1998). Localization of the fourth locus (GLC1E) for adult-onset primary open-angle glaucoma to the 10p15-p14 region. *Am J Hum Genet* 62(3): 641-52.

Schaffer AA, Gupta SK, Shriram K and Cottingham RW, Jr. (1994). Avoiding recomputation in linkage analysis. *Hum Hered* 44(4): 225-37.

Schwamborn K, Weil R, Courtois G, Whiteside ST and Israel A (2000). Phorbol esters and cytokines regulate the expression of the NEMO-related protein, a molecule involved in a NF-kappa B-independent pathway. *J Biol Chem* 275(30): 22780-9.

Semina EV, Brownell I, Mintz-Hittner HA, Murray JC and Jamrich M (2001). Mutations in the human forkhead transcription factor *FOXE3* associated with anterior segment ocular dysgenesis and cataracts. *Hum Mol Genet* 10(3): 231-6.

Pedigree/Draw version 5.1. Southwest Foundation for Biomedical Research, SFBR; http://www.sfbr.org/sfbr/public/software/pedraw/peddrw.html now available from http://www.pedigree-draw.com.

Sheffield VC, Stone EM, Alward WL, Drack AV, Johnson AT, Streb LM and Nichols BE (1993). Genetic linkage of familial open angle glaucoma to chromosome 1q21-q31. *Nat Genet* 4(1): 47-50.

Shepherd JJ (1985). Latent familial multiple endocrine neoplasia in Tasmania. *Med J Aust* 142(7): 395-7.

Shimizu S, Lichter PR, Johnson AT, Zhou Z, Higashi M, Gottfredsdottir M, Othman M, Moroi SE, Rozsa FW, Schertzer RM, Clarke MS, Schwartz AL, Downs CA, Vollrath D and Richards JE (2000). Age-dependent prevalence of mutations at the GLC1A locus in primary open-angle glaucoma. *Am J Ophthalmol* 130(2): 165-77.

Sobel E and Lange K (1996). Descent graphs in pedigree analysis: applications to haplotyping, location scores, and marker-sharing statistics. *Am J Hum Genet* 58(6): 1323-37.

Sobel E, Papp JC and Lange K (2002). Detection and integration of genotyping errors in statistical genetics. *Am J Hum Genet* 70(2): 496-508.

Sommer A, Tielsch JM, Katz J, Quigley HA, Gottsch JD, Javitt J and Singh K (1991). Relationship between intraocular pressure and primary open angle glaucoma among white and black Americans. The Baltimore Eye Survey. *Arch Ophthalmol* 109(8): 1090-5.

Stodtmeister R (1998). Applanation tonometry and correction according to corneal thickness. *Acta Ophthalmol Scand* 76(3): 319-24.

Stoilov I, Akarsu AN and Sarfarazi M (1997). Identification of three different truncating mutations in cytochrome P4501B1 (*CYP1B1*) as the principal cause of primary congenital glaucoma (Buphthalmos) in families linked to the GLC3A locus on chromosome 2p21. *Hum Mol Genet* 6(4): 641-7.

Stoilova D, Child A, Trifan OC, Crick RP, Coakes RL and Sarfarazi M (1996). Localization of a locus (GLC1B) for adult-onset primary open angle glaucoma to the 2cen-q13 region. *Genomics* 36(1): 142-50.

Stone EM, Fingert JH, Alward WL, Nguyen TD, Polansky JR, Sunden SL, Nishimura D, Clark AF, Nystuen A, Nichols BE, Mackey DA, Ritch R, Kalenak JW, Craven ER and Sheffield VC (1997). Identification of a gene that causes primary open angle glaucoma. *Science* 275(5300): 668-70.

Suzuki Y, Shirato S, Taniguchi F, Ohara K, Nishimaki K and Ohta S (1997). Mutations in the TIGR gene in familial primary open-angle glaucoma in Japan. *Am J Hum Genet* 61(5): 1202-4.

Tamm ER (2002). Myocilin and glaucoma: facts and ideas. *Prog Retin Eye Res* 21(4): 395-428.

Teh BT, Cardinal J, Shepherd J, Hayward NK, Weber G, Cameron D and Larsson C (1995). Genetic mapping of the multiple endocrine neoplasia type 1 locus at 11q13. *J Intern Med* 238(3): 249-53.

Teikari JM (1987). Genetic factors in open-angle (simple and capsular) glaucoma. A population-based twin study. *Acta Ophthalmol (Copenh)* 65(6): 715-20.

Teikari JM, Airaksinen PJ, Kaprio J and Koskenvuo M (1987). Primary open-angle glaucoma in 2 monozygotic twin pairs. *Acta Ophthalmol (Copenh)* 65(5): 607-11.

Terwilliger JD, Weeks DE and Ott J (1990). [Abstract] Laboratory errors in the reading of marker alleles cause massive reductions in lod score and lead to gross overestimates of the recombination fraction. *Am J Hum Genet Suppl* 47: A201.

Tielsch JM, Katz J, Singh K, Quigley HA, Gottsch JD, Javitt J and Sommer A (1991a). A population-based evaluation of glaucoma screening: the Baltimore Eye Survey. *Am J Epidemiol* 134(10): 1102-10.

Tielsch JM, Sommer A, Katz J, Royall RM, Quigley HA and Javitt J (1991b). Racial variations in the prevalence of primary open-angle glaucoma. The Baltimore Eye Survey. *Jama* 266(3): 369-74.

Tielsch JM, Katz J, Sommer A, Quigley HA and Javitt JC (1994). Family history and risk of primary open angle glaucoma. The Baltimore Eye Survey. *Arch Ophthalmol* 112(1): 69-73.

Tielsch JM, Katz J, Quigley HA, Javitt JC and Sommer A (1995a). Diabetes, intraocular pressure, and primary open-angle glaucoma in the Baltimore Eye Survey. *Ophthalmology* 102(1): 48-53.

Tielsch JM, Katz J, Sommer A, Quigley HA and Javitt JC (1995b). Hypertension, perfusion pressure, and primary open-angle glaucoma. A population-based assessment. *Arch Ophthalmol* 113(2): 216-21.

Toda Y, Tang S, Kashiwagi K, Mabuchi F, Iijima H, Tsukahara S and Yamagata Z (2004). Mutations in the optineurin gene in Japanese patients with primary open-angle glaucoma and normal tension glaucoma. *Am J Med Genet* 125A(1): 1-4.

Toh T, Liew SH, MacKinnon JR, Hewitt AW, Poulsen JL, Spector TD, Gilbert CE, Craig JE, Hammond CJ and Mackey DA (2005). Central corneal thickness is highly heritable: the twin eye studies. *Invest Ophthalmol Vis Sci* 46(10): 3718-22.

Tomita G (2000). The optic nerve head in normal-tension glaucoma. *Curr Opin Ophthalmol* 11(2): 116-20.

Ton CC, Hirvonen H, Miwa H, Weil MM, Monaghan P, Jordan T, van Heyningen V, Hastie ND, Meijers-Heijboer H, Drechsler M and et al. (1991). Positional cloning and characterization of a paired box- and homeobox-containing gene from the aniridia region. *Cell* 67(6): 1059-74.

Trifan OC, Traboulsi EI, Stoilova D, Alozie I, Nguyen R, Raja S and Sarfarazi M (1998). A third locus (GLC1D) for adult-onset primary open-angle glaucoma maps to the 8q23 region. *Am J Ophthalmol* 126(1): 17-28.

Van Veldhuisen PC, Ederer F, Gaasterland DE, Sullivan EK, Beck A, Prum BE, Cyrlin MN, Weiss H and investigators. TA (2000). The Advanced Glaucoma Intervention Study (AGIS): 7. The relationship between control of intraocular pressure and visual field deterioration.The AGIS Investigators. *Am J Ophthalmol* 130(4): 429-40.

Varma R, Tielsch JM, Quigley HA, Hilton SC, Katz J, Spaeth GL and Sommer A (1994). Race-, age-, gender-, and refractive error-related differences in the normal optic disc. *Arch Ophthalmol* 112(8): 1068-76.

Varma R, Heuer DK, Lundy DC, Baerveldt G, Lee PP and Minckler DS (1995). Pars plana Baerveldt tube insertion with vitrectomy in glaucomas associated with pseudophakia and aphakia. *Am J Ophthalmol* 119(4): 401-7.

Vickers JC, Craig JE, Stankovich J, McCormack GH, West AK, Dickinson JL, McCartney PJ, Coote MA, Healey DL and Mackey DA (2002). The apolipoprotein epsilon4 gene is associated with elevated risk of normal tension glaucoma. *Mol Vis* 8: 389-93.

Viggosson G, Bjornsson G and Ingvason JG (1986). The prevalence of open-angle glaucoma in Iceland. *Acta Ophthalmol (Copenh)* 64(2): 138-41.

Vincent AL, Billingsley G, Buys Y, Levin AV, Priston M, Trope G, Williams-Lyn D and Heon E (2002). Digenic inheritance of early-onset glaucoma: *CYP1B1*, a potential modifier gene. *Am J Hum Genet* 70(2): 448-60.

Viswanathan AC, Hitchings RA, Indar A, Mitchell P, Healey PR, McGuffin P and Sham PC (2004). Commingling analysis of intraocular pressure and glaucoma in an older Australian population. *Ann Hum Genet* 68(Pt 5): 489-97.

Vittitow J and Borras T (2002). Expression of optineurin, a glaucoma-linked gene, is influenced by elevated intraocular pressure. *Biochem Biophys Res Commun* 298(1): 67-74.

Voogd SD, Ikram MK, Wolfs RC, Jansonius NM, Hofman A and de Jong PT (2005). Incidence of Open-Angle Glaucoma in a General Elderly Population The Rotterdam Study. *Ophthalmology*.

Wain HM, Bruford EA, Lovering RC, Lush MJ, Wright MW and Povey S (2002). Guidelines for human gene nomenclature. *Genomics* 79(4): 464-70.

Walsh PS, Erlich HA and Higuchi R (1992). Preferential PCR amplification of alleles: mechanisms and solutions. *PCR Methods Appl* 1(4): 241-50.

Wang N, Chintala SK, Fini ME and Schuman JS (2001). Activation of a tissue-specific stress response in the aqueous outflow pathway of the eye defines the glaucoma disease phenotype. *Nat Med* 7(3): 304-9.

Weeks DE, Ott J and Lathrop GM (1990). [Abstract] SLINK: a general simulation program for linkage analysis. *Am J Hum Genet* 47: Abstract# A204.

Weih LM, Mukesh BN, McCarty CA and Taylor HR (2001a). Association of demographic, familial, medical, and ocular factors with intraocular pressure. *Arch Ophthalmol* 119(6): 875-80.

Weih LM, Nanjan M, McCarty CA and Taylor HR (2001b). Prevalence and predictors of open-angle glaucoma: results from the visual impairment project. *Ophthalmology* 108(11): 1966-72.

Weisschuh N, Neumann D, Wolf C, Wissinger B and Gramer E (2005). Prevalence of myocilin and optineurin sequence variants in German normal tension glaucoma patients. *Mol Vis* 11: 284-7.

Wensor MD, McCarty CA, Stanislavsky YL, Livingston PM and Taylor HR (1998). The prevalence of glaucoma in the Melbourne Visual Impairment Project. *Ophthalmology* 105(4): 733-9.

Werner E (1996). Progressive normal-tension glaucoma. I. Analysis. *J Glaucoma* 5(6): 422-6.

Whittemore AS and Halpern J (1994). A class of tests for linkage using affected pedigree members. *Biometrics* 50(1): 118-27.

Wiggs JL, Haines JL, Paglinauan C, Fine A, Sporn C and Lou D (1994). Genetic linkage of autosomal dominant juvenile glaucoma to 1q21-q31 in three affected pedigrees. *Genomics* 21(2): 299-303.

Wiggs JL, Del Bono EA, Schuman JS, Hutchinson BT and Walton DS (1995). Clinical features of five pedigrees genetically linked to the juvenile glaucoma locus on chromosome 1q21-q31. *Ophthalmology* 102(12): 1782-9.

Wiggs JL, Allingham RR, Vollrath D, Jones KH, De La Paz M, Kern J, Patterson K, Babb VL, Del Bono EA, Broomer BW, Pericak-Vance MA and Haines JL (1998). Prevalence of mutations in *TIGR*/Myocilin in patients with adult and juvenile primary open-angle glaucoma. *Am J Hum Genet* 63(5): 1549-52.

Wiggs JL, Allingham RR, Hossain A, Kern J, Auguste J, DelBono EA, Broomer B, Graham FL, Hauser M, Pericak-Vance M and Haines JL (2000). Genome-wide scan for adult onset primary open angle glaucoma. *Hum Mol Genet* 9(7): 1109-17.

Wiggs JL, Auguste J, Allingham RR, Flor JD, Pericak-Vance MA, Rogers K, LaRocque KR, Graham FL, Broomer B, Del Bono E, Haines JL and Hauser M (2003). Lack of association of mutations in optineurin with disease in patients with adult-onset primary open-angle glaucoma. *Arch Ophthalmol* 121(8): 1181-3.

Wiggs JL, Lynch S, Ynagi G, Maselli M, Auguste J, Del Bono EA, Olson LM and Haines JL (2004). A genomewide scan identifies novel early-onset primary open-angle glaucoma loci on 9q22 and 20p12. *Am J Hum Genet* 74(6): 1314-20.

Wijsman EM and Amos CI (1997). Genetic analysis of simulated oligogenic traits in nuclear and extended pedigrees: summary of GAW10 contributions. *Genet Epidemiol* 14(6): 719-35.

Williams JT and Blangero J (1999a). Comparison of variance components and sibpair-based approaches to quantitative trait linkage analysis in unselected samples. *Genet Epidemiol* 16(2): 113-34.

Williams JT, Van Eerdewegh P, Almasy L and Blangero J (1999a). Joint multipoint linkage analysis of multivariate qualitative and quantitative traits. I. Likelihood formulation and simulation results. *Am J Hum Genet* 65(4): 1134-47.

Williams JT, Begleiter H, Porjesz B, Edenberg HJ, Foroud T, Reich T, Goate A, Van Eerdewegh P, Almasy L and Blangero J (1999b). Joint multipoint linkage analysis of multivariate qualitative and quantitative traits. II. Alcoholism and event-related potentials. *Am J Hum Genet* 65(4): 1148-60.

Williams JT and Blangero J (1999b). Power of variance component linkage analysis to detect quantitative trait loci. *Ann Hum Genet* 63(Pt 6): 545-63.

Wiltshire S, Hattersley AT, Hitman GA, Walker M, Levy JC, Sampson M, O'Rahilly S, Frayling TM, Bell JI, Lathrop GM, Bennett A, Dhillon R, Fletcher C, Groves CJ, Jones E, Prestwich P, Simecek N, Rao PV, Wishart M, Bottazzo GF, *et al.* (2001). A genomewide scan for loci predisposing to type 2 diabetes in a U.K. population (the Diabetes UK Warren 2 Repository): analysis of 573 pedigrees provides independent replication of a susceptibility locus on chromosome 1q. *Am J Hum Genet* 69(3): 553-69.

Wirtz MK, Samples JR, Kramer PL, Rust K, Topinka JR, Yount J, Koler RD and Acott TS (1997). Mapping a gene for adult-onset primary open-angle glaucoma to chromosome 3q. *Am J Hum Genet* 60(2): 296-304.

Wirtz MK, Samples JR, Rust K, Lie J, Nordling L, Schilling K, Acott TS and Kramer PL (1999). GLC1F, a new primary open-angle glaucoma locus, maps to 7q35-q36. *Arch Ophthalmol* 117(2): 237-41.

Wolfs RC, Klaver CC, Vingerling JR, Grobbee DE, Hofman A and de Jong PT (1997). Distribution of central corneal thickness and its association with intraocular pressure: The Rotterdam Study. *Am J Ophthalmol* 123(6): 767-72.

Wolfs RC, Klaver CC, Ramrattan RS, van Duijn CM, Hofman A and de Jong PT (1998). Genetic risk of primary open-angle glaucoma. Population-based familial aggregation study. *Arch Ophthalmol* 116(12): 1640-5.

Wolfs RC, Borger PH, Ramrattan RS, Klaver CC, Hulsman CA, Hofman A, Vingerling JR, Hitchings RA and de Jong PT (2000). Changing views on open-angle glaucoma: definitions and prevalences--The Rotterdam Study. *Invest Ophthalmol Vis Sci* 41(11): 3309-21.

Wormald RP, Basauri E, Wright LA and Evans JR (1994). The African Caribbean Eye Survey: risk factors for glaucoma in a sample of African Caribbean people living in London. *Eye* 8 (Pt 3): 315-20.

Wu SY and Leske MC (1997). Associations with intraocular pressure in the Barbados Eye Study. *Arch Ophthalmol* 115(12): 1572-6.

Wu Z, Nakura J, Abe M, Jin JJ, Yamamoto M, Chen Y, Tabara Y, Yamamoto Y, Igase M, Bo X, Kohara K and Miki T (2003). Genome-wide linkage disequilibrium mapping of hypertension in Japan. *Hypertens Res* 26(7): 533-40.

Yan X, Tezel G, Wax MB and Edward DP (2000). Matrix metalloproteinases and tumor necrosis factor alpha in glaucomatous optic nerve head. *Arch Ophthalmol* 118(5): 666-73.

Yuan L and Neufeld AH (2000). Tumor necrosis factor-alpha: a potentially neurodestructive cytokine produced by glia in the human glaucomatous optic nerve head. *Glia* 32(1): 42-50.

Zhang L, Cui X, Schmitt K, Hubert R, Navidi W and Arnheim N (1992). Whole genome amplification from a single cell: implications for genetic analysis. *Proc Natl Acad Sci U S A* 89(13): 5847-51.